THE PETROLOGY AND GEOCHEMISTRY OF THE GRANITIC ROCKS OF THE TAK BATHOLITH, THAILAND.

by

CHAMRAT MAHAWAT

Thesis submitted in accordance with the requirements of the University of Liverpool for the degree of Doctor in Philosophy

1982

Abstract

A detailed petrological and geochemical study has been made of the complex Tak Granitic Batholith in Northern Thailand. The batholith is composed of four separate plutons, intruded at different times and showing distinctive variable character. One pluton is of a classic 'normal' inward zoning, with a wide range of silica content and having a basic margin and an acidic core. The other three plutons all exhibit unusual outward zoning, having an acidic outer part and a less acidic core; they also have a restricted compositional range at a high silica content.

Samples from these plutons have been examined for mineralogical make-up and analysed by a variety of methods for major, minor and trace elements. This information has been used to attempt to come to conclusions about the mechanisms which might have been responsible for the observed differentiation and zonation.

Major element modelling suggests that a plagioclase - hornblende fractionation process is appropriate for two of the plutons, including one which is highly acidic. Two plutons appear to require a model of extraction of a quartz-feldspar phase. Most of the trace element data do not conflict with this too strongly, but the rare earth element data is sometimes at variance with this. Further work is necessary to establish the precise nature of the processes causing zonation.

Deductions about the type of granite and possible mode of emplacement strongly indicate that the granites are of I-(Caledonian) type and were emplaced by block-like intrustion at a high level.

Abnormally high lead, thorium and uranium contents were observed in these granites.

ACKNOWLEDGEMENTS

I would first like to thank my joint supervisor during my first year, Professor W.S. Pitcher, now Emeritus Professor, for accepting me into the Department of Geology, University of Liverpool to study for a Doctorate of Philosophy. Also to my other joint supervisor, Dr. M.P. Atherton, who on taking over full responsibility as my supervisor upon the retirement of Professor Pitcher, has given me a great deal of help, guidance and encouragement during all stages of my study and preparation of this thesis.

Grateful thanks are extended to Professor Pitcher, whose world-wide knowledge of granites has greatly increased my understanding of granite geology, during several fruitful and enjoyable trips to the granites of Donegal, Eire and Cornwall, U.K.

Many thanks go to fellow students, friends and colleagues in the Department of Geology, University of Liverpool and elsewhere for much time and help - Dr. Geoff Mason, Vanita Warden and especially to Dr. John Cobbing, Institute of Geological Sciences; to all those at Liverpool who have assisted me in their various ways; Dave Oates for preparation of thin sections, Dave Smart for photographic assistance, Joe Lynch for cartographic skill, Hilda Longworth and Helen Farrall for typing the script, Dee Stewart for extensive help with the X-ray analysis; finally to Mike Brotherton for much help and encouragement, both with the laboratory and activation work, the use of the microcomputer and during the traumatic final stages of compilation of the thesis.

Thanks also to the present Head of Department, Professor D. Flinn for continued support and use of departmental facilities and to countless other individuals in Liverpool, who may have got forgotten, but whose help is much appreciated.

I wish to express my thanks to Dr. Pisoot Sudasna, former Director-General of the Department of Mineral Resources, Bangkok, Thailand, now Deputy-Secretary to the Ministry of Industry, for granting permission to study for a Ph.D. degree, and for making available financial support from the Department of Mineral Resources. Thanks to Dr. Sanarm Suensilpong of the Geological Survey Division, Department of Mineral Resources, for initiation of the project, much encouragement and support; also to many geological colleagues in Bangkok, particularly Nopadon Mantajit, Pinya Puthapiban and Nikom Jungusuk, who held many valuable discussions in the field, both before leaving for the United Kingdom and during my return visit in 1980. Thanks are extended to several field assistants and staff at the Chemistry Section of the Geological Survey Division.

CONTENTS

LIST OF FIGURES

LIST OF TABLES

LIST OF PLATES

CHAPTER 1

General Introduction

1.1 Regional geological setting

1.1.1 General geology

Figure 1.1 shows some of the principal geological features of S.E. Asia as given by Ridd (1980). He suggested that the present features of S.E. Asia have been formed by fusion of more than one small platelet or micro-continents. One of these is the Thai-Malay Peninsula Block which includes the western part of Thailand and the western part of Malaysia as well as Indonesia. The Thai-Malay Peninsula Block rifted away from the edge of Gondwanaland during the mid-Palaeozoic, drifted northwards in the late-Palaeozoic and collided with the S. China Block and Indochina Block of Asia in the late Triassic.

Ridd (op. cit.) showed that the rifting of the Thai-Malay Peninsula Block away from the Gondwanaland super-continent during the Devonian-Permian led to the opening of the Neo-Tethys and the closing of the Palaeo-Tethys which lay to the north, between the Thai-Malay Peninsula Block and a small micro-continent called the Indochina Block. The Palaeo-Tethys closed and ceased to exist in the late Triassic to mid-Jurassic because of its collision with the Eurasia, whereas the Neo-Tethys continued to open.

Ridd (op. cit.) considers that the Thai-Malay Peninsula Block was part of Gondwanaland from the occurrence of detrital diamonds and a fragmentary Gloseopteris fauna in Thailand. Furthermore, Lower Palaeozoic rocks show a derivation from a western landmass which has now disappeared. Widespread deposits of turbidites, slumped beds and pebbly mudstones of Carboniferous-Devonian age are considered to be rift-infill facies which

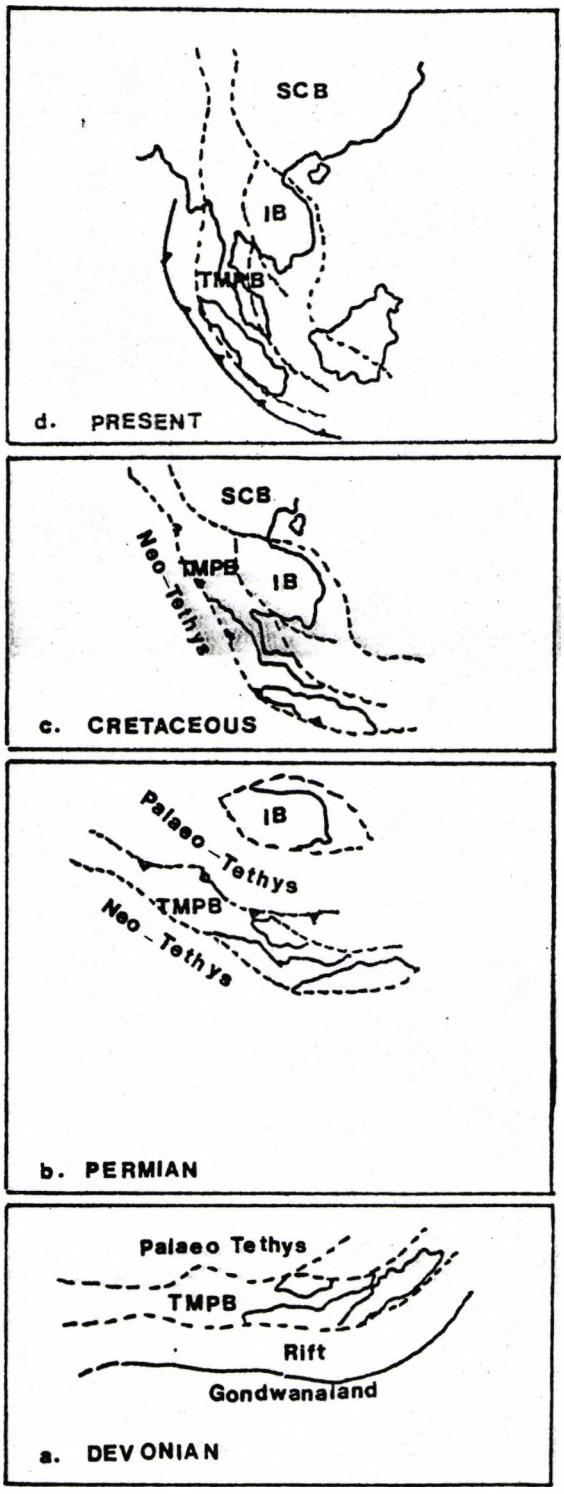

Figure 1.1 Sketch maps showing the present regional geology and suggested origin of the S.E. Asia peninsula (after Ridd, 1980).
SCB = South China Block; IB = Indo-China Block; TMPB = Thai-Malay Peninsula Block.

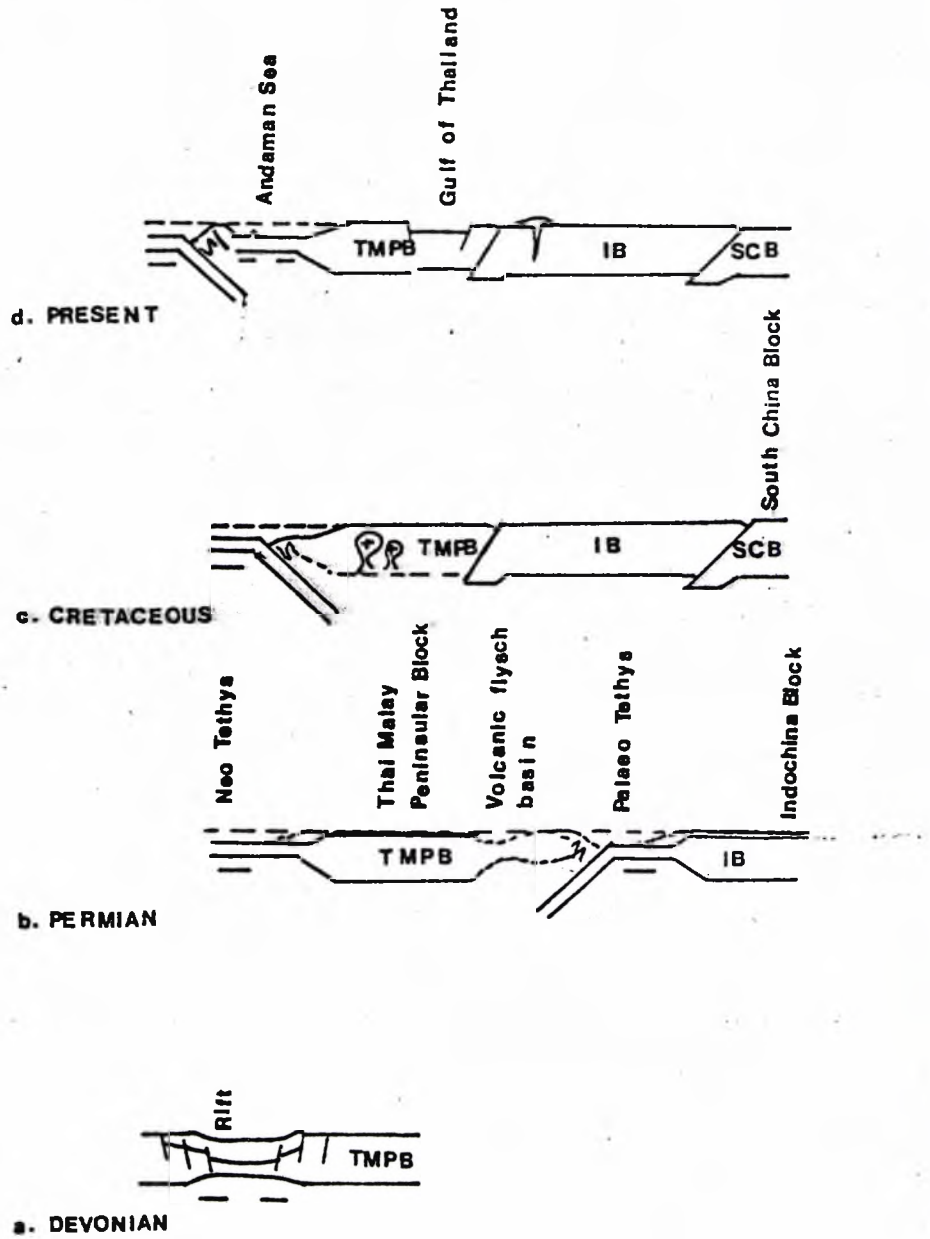

Figure 1.1 continued

represents deposits of the continental rise transported by mass gravity processes (Mitchell et al., 1970; Ridd, 1971b).

By the Permian, the Thai-Malay Peninsula Block was in low latitudes moving northwards towards the Indochina and S. China Blocks. Warm water Tethyan faunas characterised the shelf carbonate which was deposited over much of the Block. However, a terrigenous clastic facies with intercalated volcanic rocks in the eastern part of W. Malaysia and eastern Thailand provides some evidences of volcanic arc close to its leading edge (Ridd, 1971a; Hutchison, 1975; Stauffer, 1974; Mitchell, 1975). A westward dip of the subduction zone may be indicated by westward variation of volcanic rocks from tholeiitic to alkaline (Hutchison, 1973). A W-E facies change from shelf carbonates to basinal chert and volcanic clastic flysch in Thailand and W. Malaysia has been documented (Burton, 1973; Ridd, 1978).

The collision and fusion of the Thai-Malay Peninsual Block with the S. China Block and the Indochina Block is believed to have taken place during the Middle or Late Triassic, resulting in the main orogenesis of the region, as the Indosinian orogeny (Gubler, 1935) or Cimmerian orogenic belt (Klompe, 1962).

As a result of subduction, there was a widespread intrusion of Middle to Late Triassic granites, as well as extrusion of rhyolite, andesite and acid tuffs, extending from east Thailand to West Malaysia along the line of the plate boundaries.

Erosion of the orogen resulted in a widespread cover of late Jurassic to Cretaceous molasse on the eastern part of Thailand, and this has been called the Khorat Group in Thailand (Ridd, 1978), Gre's Superieurs in Indochina (Gubler, 1935) and the Gagau Formation in W. Malaysia (Burton, 1973).

Therefore, the S.E. Asia Peninsula is believed to have been cratonised by the Triassic collision, and the subduction of Palaeo-Tethys oceanic crust ceased. However, sea-floor spreading in the Neo-Tethys continued and a new westerly-dipping subduction zone developed on the western margins of the S.E. Asian Peninsula (Ridd, op. cit.). In the late Tertiary and Quaternary a marginal basin developed in the Andaman Sea (Rodolfo, 1969).

On the craton, extensional tectonics prevailed, resulting in block-faulting and down-warping of the Gulf of Thailand and extrusion of olivine basalts (Ridd, 1971c). The developement of the "Andaman Rhombochasm" was due to the movement between the dextral Sumatra fault zone and the sinistral fault zones in Thailand, (Ridd, 1971c).

1.1.2 General geology of Thailand

The early syntheses of the geology of Thailand are given by Brown et al., (1951), Kobayashi (1960) and Klompe (1962). They provide a useful background for stratigraphic correlation, however, the timing of the emplacement of the granites remains uncertain. The recent reviews on the geology of Thailand have been done by Bunopas (1976) and Suensilpong et al., (1978). The geological map of Thailand and its stratigraphic sequences are shown in figure 1.1.2. and table 1.1.2. respectively. The stratigraphic sequences are briefly described as follows:

The oldest rocks, which presumably are of Precambrian age and consist of paragneiss, mica schist, quartzite, marble and calc-silicate which are mainly exposed in the core of the large anticlinorium fold-belt of Palaeozoic metasediments on the northwestern part of Thailand (Baum et al., 1970). Campbell (1974) gives a review of these rocks which he describes as basement complexes. There is no conformable

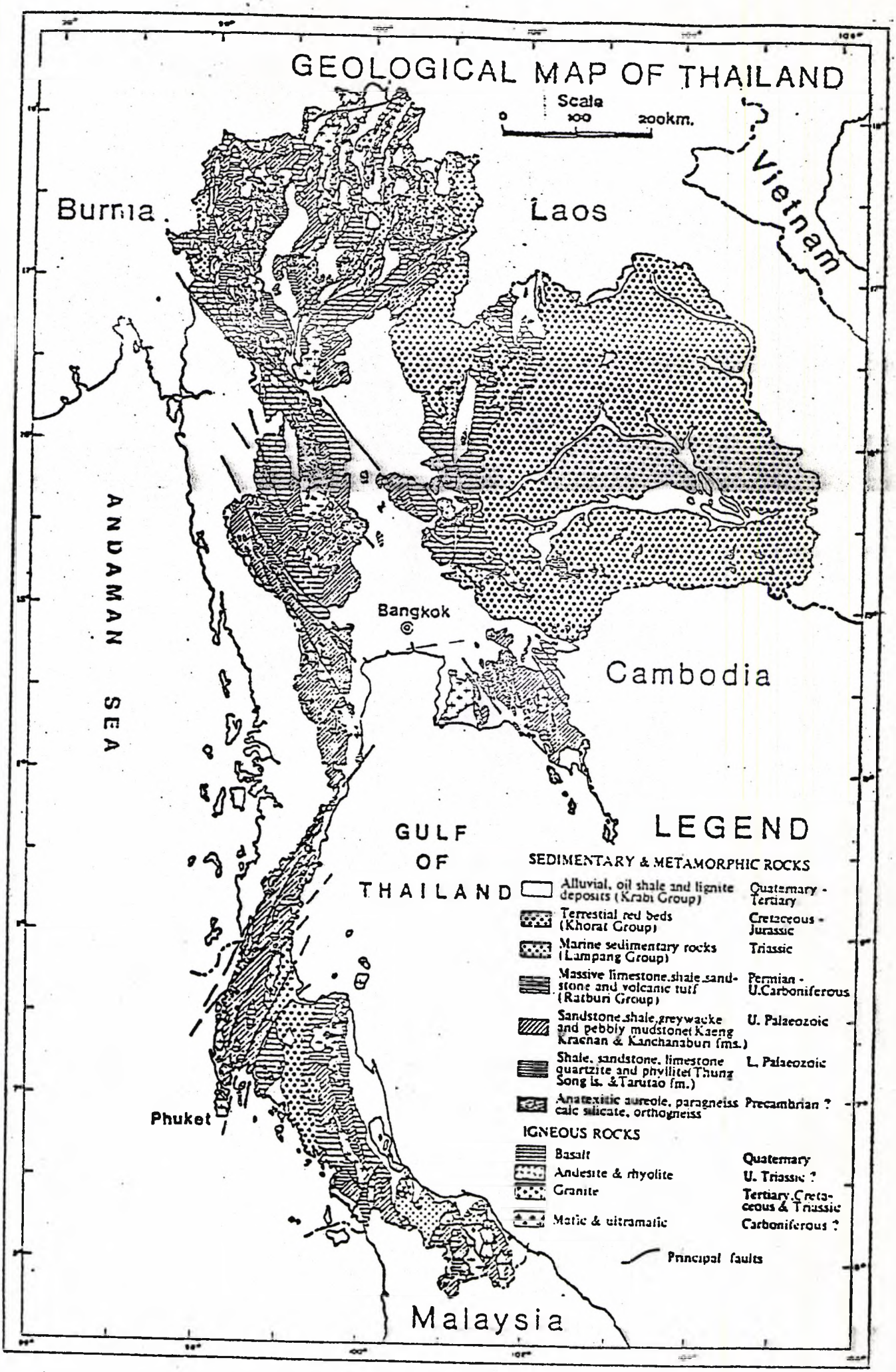

Figure 1.1.2 Geological Map of Thailand (from Suensilpong, 1978)

Table 1.1.2 Stratigraphy of Thailand (from Suensilpong et. al., 1978)

ERA	Period	Stratigraphic Units: Group	Stratigraphic Units: Formation	Lithology	Igneous Activity		Orogenic Cycle
TERTIARY	Recent	Krabi Group		Alluvium, colluvium, gravel, silt & clay	Basalt		
	Pleistocene		Mae Taeng Fm.	Gravel beds & terrace deposits			
	Pleiocene		Mae Mo Fm.	Sandstone, conglomerate with interbedded lignite & oil shale			
	Miocene	?	Li Fm.	do			
	Oligocene						
	Eocene						
	Palaeocene		Salt Fm.	Rock salt, gypsum & conglomerate		Granite (50-70 m.y.)	*Tertiary Orogeny*
MESOZOIC	Cretaceous	Khorat Group	Ban Na Yo Fm.	Sst.,siltst.,congl. & ls		Granite (110-135 m.y.)	
	Jurassic		Phu Phan Fm.	Sst.,sh.,conglomeratic sst. & congl.			
			Phra Wihan Fm.				
			Phu Kradung Fm.	Congl.with ls and rhyolite pebbles, gray sh/sst, ls. &congl.	Andesite, rhyolite, agglo.	Granite (190-210 m.y.	*Mesozoic Orogeny (Indosinian)*
	Triassic	Lampang Gp.	Nam Phong Fm.				
			Marine Fm.	Marine sh/sst., red sst/sh.,ls & volc.	Andesite & rhyolite	Granite (235-240 m.y.	
PALAEOZOIC	Permian	Rat Buri Gp.	Sara Buri lm. / Matsi fm.	Massive ls., sh., slaty sh., sst., rhyolite and andesite, tuff, agglo. & chert	Interm.-acid volc.rks.,tuff		
	Carboniferous	Phuket Gp.	Kaeng Krachan fm.	Pebbly mudstone, turbidites and Laminated mudstone and sst.	Basic-Interm. volc. rks.	Granite ?	*Carboniferous Orogeny*
	Devonian	Satun Gp.	Kanchanaburi fm.	Black sh., slate, sst., qzite., green schist & phyllite			
	Silurian						
	Ordovician		Thung Song Ls.	Massive and bedded ls., slate, slaty phyllite, bedded ls & sh			
	Cambrian	Tarutao Gp.	Nai Tak Fm. / Tarutao Fm.	Marine red sst., micaceous sst. & sh., qzite & phyllite			
	Precambrian			Paragneiss, amphibolite schist,qzite, marble & calc silicate		Granite ?	*Precambrian Orogeny*

succession from the Precambrian basement complexes to the Cambrian. The contacts between the Precambrian and the Palaeozoic sequences occur as a plane of detachment.

The entire Palaeozoic sequences are a product of marine sedimentation. The Cambrian and Ordovician systems are represented by shallow water facies followed in the Silurian-Devonian by geosynclinal deposits. A major orogenic episode occurred in Upper Devonian - Lower Carboniferous which resulted in N.S. folding and granite intrusion (Baum et al., 1970). The early Carboniferous shows a distinct flysch facies followed by a volcanic sequence. The Upper Carboniferous to Permian is represented by extensive deposits of limestone with abundant fusulinids and brachiopods. The Permo-Carboniferous sequences are present extensively in the central part of Thailand.

The early Triassic sedimentation consists largely of flysch facies in the northern part of Thailand. Marine sedimentation also plays an important role in the middle Triassic. The major Mesozoic folding and emplacement of granites occurred in the upper Triassic.

The Jurassic and Cretaceous are almost entirely periods of continental sedimentation, which extended eastward to the Korat Plateau in north-east Thailand. There is also evidence of Cretaceous and Teriary granitic intrusions.

1.2 The study area

1.2.1 Location

The study area is located in northern Thailand, between latitudes 16^{o} 45' N - 17^{o} 30' N and longitudes 90^{o} 00' E - 99^{o} 00'E as shown in the 1:50,000 topographic maps with sheet numbers 4842 III, 4842 IV, 4843 I, 4843 II, 4843 III and 4843 IV.

It covers an area of approximately 2700 sq. km., with the Tak township located at the southeastern part of the area. The study area is situated about 450 km. north of Bangkok and can be reached within five hours by car. The accessibility to the investigated area is by cart tracks and dirt roads.

1.2.2 Geology

Figure 1.2.1 shows the geological map of the study area, the Tak Batholith. The Tak Batholith comprises four composite plutons, called the Tak Pluton, the Mae-Salit Pluton, the Western Main Range Pluton and the Eastern Pluton.

The Tak Batholith is emplaced into lower Palaeozoic sediments ranging from schist, phyllite, volcanic tuff up to the limestone volcanic tuff and agglomerate of the Permo-Triassic age (Piyasin, 1974; Bunopas, 1974). The contacts of the Tak Batholith with the stratified country rocks are mostly sharp, and there is a lack of xenoliths of sedimentary rocks in the granites. The contacts are mostly vertical or subvertical. In several places the contact planes are fault contacts with shearing and brecciation features along the contact planes. Most of the contacts between the Batholith and the country rocks are covered by alluvium deposits.

The Eastern Pluton is located in the eastern part of the Tak Batholith. The pluton comprises mainly of quartzdiorite, granodiorite and monzogranite. The Eastern Pluton is the only pluton in this area that shows a roof contact with volcanic tuffs and schists of the Silurian-Devonian ages (Bunopas, 1974). Chilled marginal rocks are also locally formed along the roof contact.

The Western Main Range Pluton is located in the western part of the Tak Batholith. The Western Main Range Pluton is intruded along the

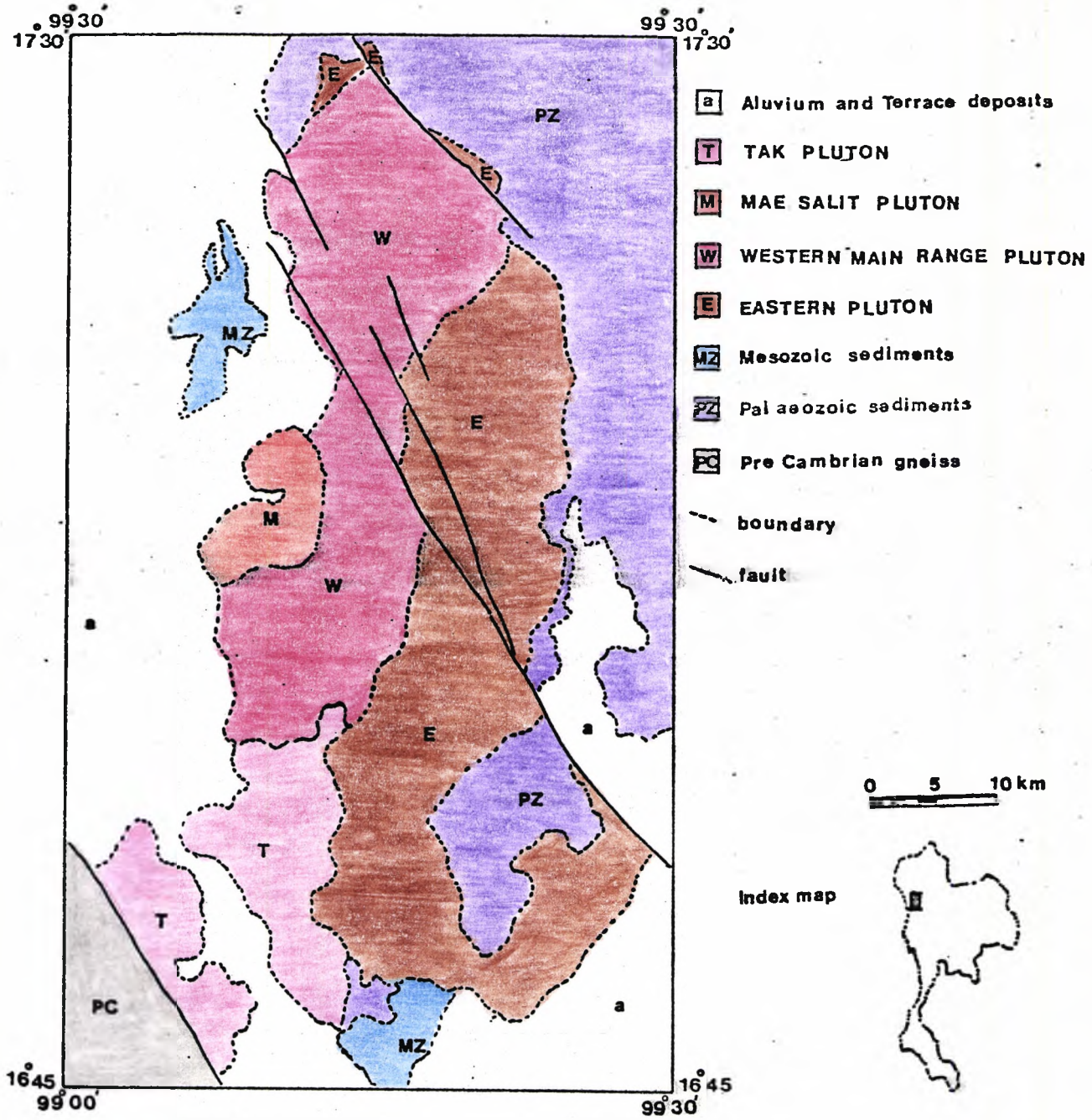

Figure 1.2.1 Geological map of the Tak Batholith, North Thailand.

western side of the Eastern Pluton and also cuts through the northern end of the Eastern Pluton. The Western Main Range Pluton is composed mainly of pinkish hornblende-biotite monzonitic granites and commonly is associated with appinitic rocks. Basic xenoliths of appinitic composition are common in the rock of this pluton.

The Mae-Salit Pluton is the smallest pluton in the study area and is located on the eastern side of the Tak Batholith. The Mae-Salit Pluton also comprises mainly of pinkish hornblende-biotite monzogranitic rocks and is intruded into the eastern side of the Western Main Range Pluton. Basic xenoliths are also common in the rock of the Mae-Salit Pluton.

The Tak Pluton is located in the southwestern part of the Tak Batholith. The Tak Pluton cuts through the southeastern side of the Eastern Pluton and the southern end of the Western Main Range Pluton. The Tak Pluton is composed mainly of pinkish hornblende-biotite monzogranitic rocks.

Leucogranite, microgranite, aplite, granite porphyry and acid dykes mostly occur as minor intrusive phases at the peripheries of the Tak Pluton, Mae-Salit Pluton and Western Main Range Pluton, whereas these late minor acid intrusive rocks usually occur elsewhere in the Eastern Pluton.

Faulting in the Tak Batholith is prominent. The late faulting indicates sinistral movement and off-sets the northern part of the Tak Batholith. Note that the evidence of the sinistral transcurrent faults in the study area are probably related to the large sinistral transcurrent fault which extends from Burma to the north western part of Thailand (Ridd, 1971c).

1.2.3 Previous work

During the period between 1969-1970 the southern part of the Tak Batholith has been mapped on a scale of 1:50,000 by Mahawat and Joungusook (1971). This reconnaissance geological survey has been conducted under the programme of compiling the geological map of Thailand on a scale of 1:250,000, sheet NE 47-15, (Bunopas , 1974).

The boundary of the northern part of the Tak Batholith has been mapped on a scale of 1:250,000 on the geological map of Thailand, sheet NE 47-11 (Piyasin, 1974).

Teggin (1975), has studied the granitic rocks in the southwestern part of the Tak Batholith and reported the ages of the "white granite" and the "pink granite" as 213 ± 10 and 219 ± 12 Ma respectively.

Further geological study of the Tak Batholith during the period 1973-1977 by the author revealed that it is a composite of two series of granitic instructions, namely, the quartzdiorite-granodiorite series on the eastern part and the monzogranite-granite series on the western part of the batholith (Pongsapich and Mahawat, 1977).

During the period between 1977-1979, the author attempted to define the intrabatholithic contacts on a map scale of 1:50,000 and recognised that the Tak Batholith is a composite of four plutons, namely, the Tak Pluton, the Mae-Salit Pluton, the Western Main Range Pluton and the Eastern Pluton

1.2.4 Methods of Investigation

The field mapping has been carried out by using a topographic map scale 1:50,000 (2 cm to 1 km) as a base map. The samples collected in the field were studied in detail by means of binocular microscope, polarizing microscope, X-ray fluorescence, wet chemical analysis, electron micro-

probe and Neutron Activation Analysis. Staining techniques for rocks slabs and thin section have been employed to facilitate the modal analysis. Some details of these techniques are described in the appendix.

1.2.5 Rock sampling

Due to poor exposure and the strong weathering of these rocks, fresh samples for chemical anlysis can only be obtained by the use of explosives. This requires a field party of at least four, and consumes a tremendous amount of time, expense and effort. Therefore, the number of rock samples has been limited to serve the main objective of the research.

However, prior to the selection of the locations for sampling, thorough field observation has been carried out to establish the boundaries of the individual plutons.

Two samples, each of approximately 5 kg, were collected at each locality. One sample was retained and provided a rock slab, about 10 cm square and 2 cm thick, for petrographic study. The other sample was crushed for chemical analysis as described in Appendix 1.

1.3 Aims of research

The overall aims of the research embodied in this thesis are to investigate the petrological, mineralogical and geochemical characteristics of the granitic Tak Batholith. In particular, it was considered important to examine each of the four separate plutons, comprising the Tak Batholith, as initial indications were that there might be significant differences in their individual make-up. This research should provide useful information on the processes

involving crystallisation of certain minerals, differentiation and fractionation of granitic magmas. These investigations will help to enhance the geological and geochemical knowledge of the rocks of Thailand and could have implications in the understanding of the overall geology of South East Asia - an area which has important known, or possibly hidden, mineral deposits.

CHAPTER 2

THE TAK PLUTON

2.1 Introduction

The Tak Pluton is situated on the southwestern flank of the Tak Batholith and covers an area of approximately 300 sq. km. The pluton is roughly elongated along a NS axis (Fig. 1.2.1). Only the eastern part of the pluton is well exposed, the western part is concealed by alluvium, river terraces and the Tak province town site.

The Tak Pluton is the only pluton in the area studied that was looked at in some detail by Teggin (1975). He recognised that the Tak Pluton consists principally of "pink granite" and "white granite" in which the latter cuts through the former; he obtained radioactive dates of 219 ± 12 Ma and 213 ± 10 Ma respectively. This Pluton has been mapped in more detail than the other plutons which are included in this thesis.

2.2 Components of the Pluton

The Tak Pluton is a roughly zoned pluton consisting principally of pinkish monzogranite in the central part, which is surrounded by pinkish syenogranite, especially on the eastern and outhern periphery of the pluton (Fig. 2.2.1). These rocks were subsequently extensively surrounded by microgranite, several minor acid intrusives, granite porphyry as well as large feldspar pegmatite dykes and quartz feldspathic dykes.

The terms inner facies and outer facies will be used to refer to the monzogranite in the central part of the pluton and the syenogranite in the outer part, in order to understand the structure of the pluton in accordance with petrological and chemical characteristics resulting from these studies. The boundary between the monzogranite and the syenogranite is gradational. The microgranite which crops out marginally has intrusive contacts with the monzogranite and the syenogranite and the country rocks and will be referred to as the "late intrusive border zone".

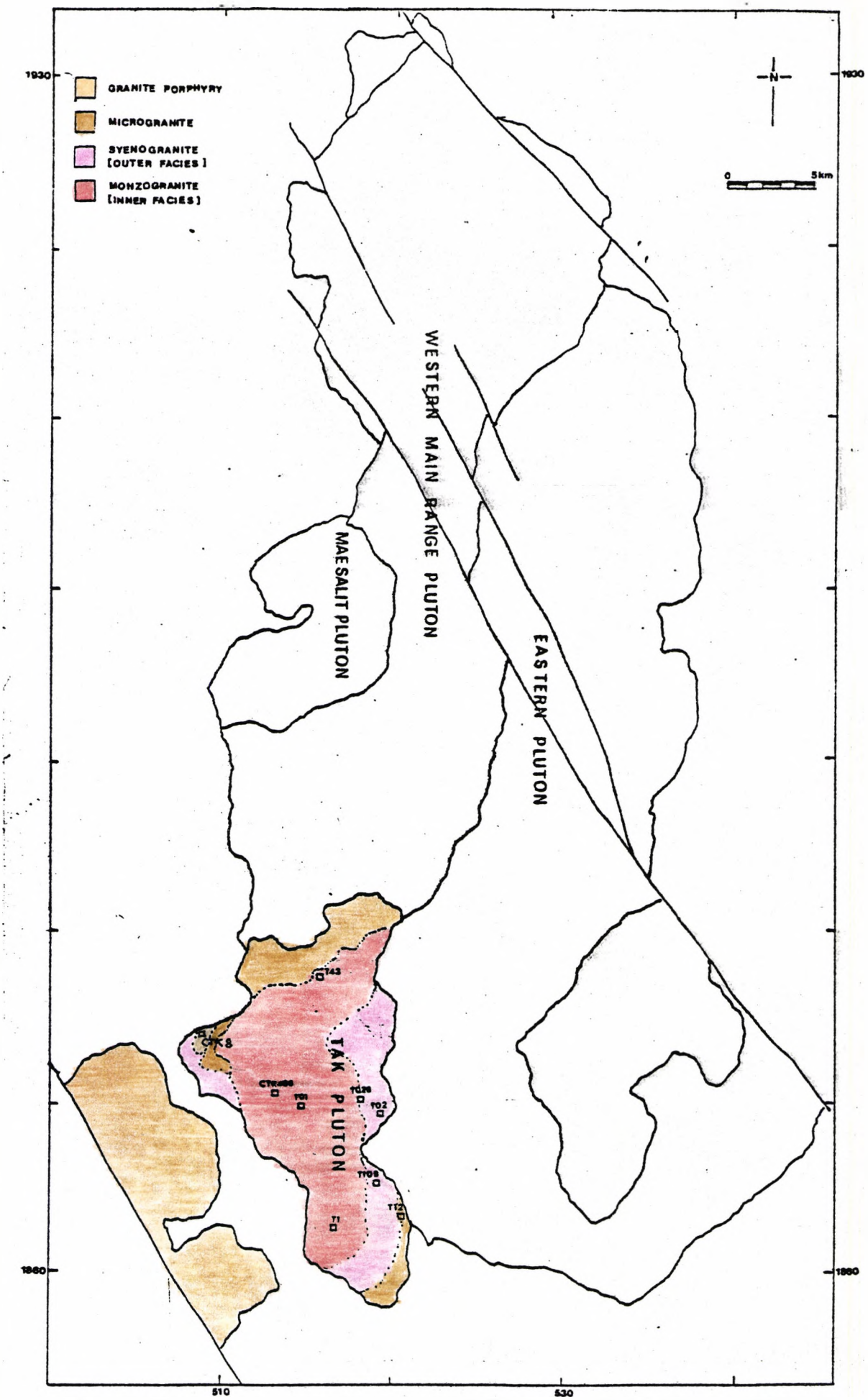

Figure 2.2.1 Outcrop map of the Tak Batholith, showing the different facies and the sample localities of the Tak Pluton.

This microgranite is considered to be the same rock as the "white granite" recognised by Teggin (1975), with an age of 213±10 Ma. Teggin (op. cit.) grouped the monzogranite and the syenogranite as the "pink granite" (age, 219±12 Ma).

The granite poropyry crops out as small dykes cutting the monzogranite of the inner facies. Pegmatite dykes occur only where the Tak Pluton is in contact with the wall rocks and they cut both the wall rocks and the Tak Pluton. These pegmatite dykes are mostly feldspar pegmatite and quartz-feldspar-tourmaline pegmatite. Some feldspar pegmatites occur as pockets about 5 metres long. Feldspar crystals up to 15 metres long are the main source of widespread feldspar mining in this area.

2.3 Field Relationships

Relation with the Eastern Pluton and the Western Main Range Pluton

The Tak Pluton is located at the southern end of the Western Main Range Pluton and the western flank of the eastern pluton. The exact mode of contact of the monzogranite or the syenogranite of the Tak Pluton with the Western Main Range Pluton or with the Eastern Pluton is not clear because most of the contact boundary is obscured by the intrusions of pegmatite, microgranite and other late minor acid rocks. These minor bodies are considered to be a part of the border of the Tak Pluton and make up "the late intrusive border zone" (see section 2.2). This zone cuts through the rocks of the Eastern and the Western Main Range Plutons. Enclaves of the rocks of the Eastern Pluton are found in the microgranite in several places along the contact zone.

Relation with the country rocks

The contact of the Tak Pluton with the Lower Palaeozoic metasediments along the rim of the pluton is a faulted one. The rocks along the faults contact are strongly sheared and cataclasites are well developed. Teggin

(1975) observed that the granitic rocks in this part of the pluton are mostly contaminated.

The southern part of the Tak Pluton is intruded into volcanics of Triassic-Jurassic age (Bunopas, 1974).

2.4 Petrography

The monzogranite of the inner facies is a pinkish medium-grained rock with predominant K-feldspar and quartz, subordinate plagioclase and some hornblende and biotite. A triangular plot showing the relative proportions of quartz, alkali-feldspar and plagioclase is shown in Fig. 2.4.1. Plagioclase (An_{8-15}) forms clusters of subhedral to anhedral twinned and zoned crystals and oscillatory zoning is weakly developed. Most of the zoned plagioclase crystals have an intensely saussuritized core. Small plagioclase crystals are commonly enclosed by K-feldspar which is perthitic and occurs as large subhedral to anhedral twinned plates. Quartz occurs both as large patches and as aggregates of small grains intersitital to plagioclase and K-feldspar. Hornblende (x = deep green, y = z = yellow green) occurs as euhedral to subhedral twinned crystals often replaced by biotite and altered to chlorite. Biotite (x = yellow brown, y = z = brown) occurs as clusters of small flakes in association with hornblende and is intensely chloritised. Accessory sphene, allanite, magnetite, zircon and apatite commonly occur in association with biotite and hornblende (Plate 2.4.1).

The syenogranite (outer facies) is also a medium grained equigranular pinkish rock consisting prominently of quartz and K-feldspar with subordinate plagioclase and some biotite and hornblende. A plot showing the relative proportions of modal quartz, alkali-feldspar, plagioclase is shown in Fig. 2.4.1. Plagioclase (An_{5-12}) usually occurs as subhedral twinned crystals and has weakly developed zoning. The small discrete crystals are usually poikilitically enclosed by K-feldspar which occurs

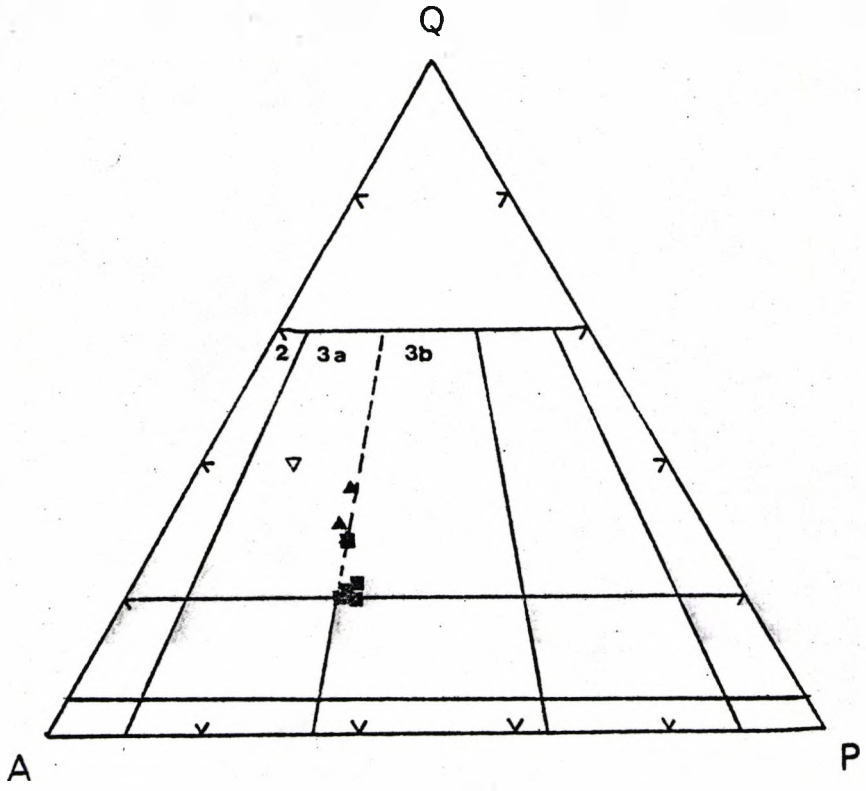

Figure 2.4.1 Classification of the plutonic rocks of the Tak Pluton (following Streckeisen, 1976). Symbols as follows:-
solid squares - inner facies - monzogranite
solid triangle - outer facies - syenogranite
open triangle - microgranite
(calculated from modes in Table 2.4.1)

Table 2.4.1 Modes of the rocks from the Tak Pluton

	inner facies				
	T01	T1	CTK48-B	T43	T02B
plagioclase	29.63	27.81	27.44	26.19	21.25
k-feldspar	48.69	48.21	47.06	49.81	47.13
quartz	16.88	18.50	20.19	17.56	30.62
hornblende	1.80	1.88	1.43	2.21	0.38
biotite	2.56	2.81	3.19	2.50	0.50
others	0.44	0.69	0.69	1.73	0.12

	outer facies		micro-granite
	T10B	T02	T12
plagioclase	23.45	21.19	12.50
k-feldspar	45.56	42.63	45.50
quartz	28.70	35.56	40.80
hornblende	0.00	0.00	0.00
biotite	1.26	0.56	0.90
others	1.03	0.06	0.30

*Granite porphyry (CTK8) contains phenocrysts of 16.20% plagioclase, 5.00% k-feldspar, 5.40% quartz, 0.50% hornblende, 2.70% biotite, 0.02% accessory minerals and 70.00% groundmass.

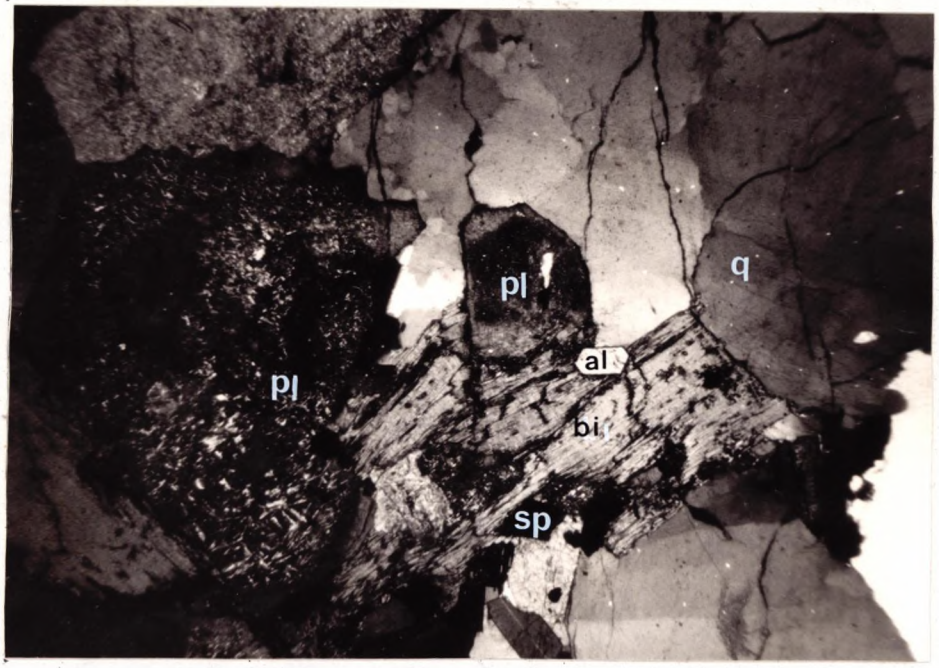

Plate 2.4.1. Photomicrograph of the monzogranite (inner facies) of the Tak Pluton, showing allanite (al), sphene (sp) in association with biotite (bi). Weakly zoned plagioclase (pl) is intensely altered. Quartz (q) occurs as large anhedral patches. (Sample CTK 48B, X nicol, 2.5 x 8 x).

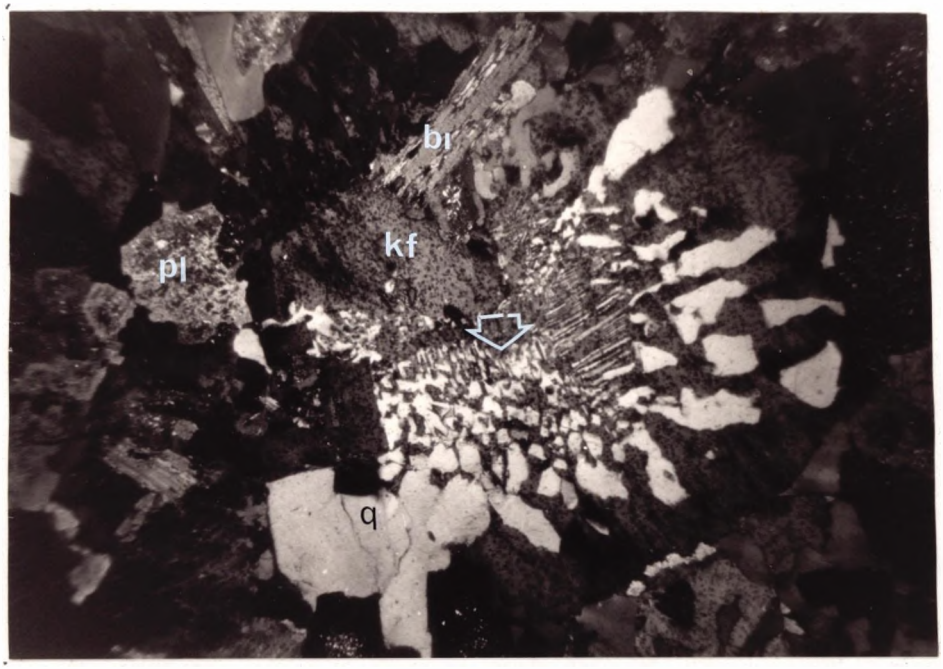

Plate 2.4.2. Photomicrograph of the syenogranite (outer facies) of the Tak Pluton, showing granophyric intergrowth (pointed arrow) at the contact of quartz (q) and K-feldspar (Kf). Plagioclase (pl) and biotite (bi) are enclosed by K-feldspar. (Sample T02, X nicol, 2.5 x 8 x).

as large subhedral to anhedral twinned perthitic grains, commonly showing myrmekitic veins when in contact with plagioclase and granophyric intergrowth when in contact with quartz (Plate 2.4.2). Most of the K-feldspar is very turbid and tiny albite crystals are developed along the K-feldspar twinning plane. Quartz forms both large anhedral patches and aggregates of small grains interstitial to plagioclase and K-feldspar. Biotite (x = brown, y = z = yellow brown) occurs as clusters of flakes and is commonly altered to chlorite. Hornblende (x = green, y = z = greenish brown) occurs as subhedral prismatic twinned crystals, and is commonly replaced by biotite and altered to chlorite. Accessory sphene, allanite, magnetite, zircon and apatite occur in association with biotite.

The microgranite is a leucocratic medium- to fine-grained rock and is composed mainly of quartz and feldspar with accessory ferromagnesian minerals. A plot showing the relative proportion of modal quartz, alkali-feldspar and plagioclase is shown in Fig. 2.4.1. Plagioclase (An_{5-8}) occurs as subhedral twinned crystals. Zoning in plagioclase is weakly developed. Small plagioclase crystals are enclosed by K-feldspar which occurs as large subhedral to anhedral twinned patches (Plate 2.4.3). K-feldspar is perthitic and commonly shows cross-hatched twinning. Granophyric intergrowths are commonly developed when in contact with quartz. Quartz commonly occurs as large aggregates of small anhedral grains and is interstitial to plagioclase and K-feldspar. Biotite occurs as small flakes and is partially or wholly altered to chlorite. Small granules of magnetite occur as an accessory mineral.

The granite porphyry is a porphyritic rock with phenocrysts of plagioclase and subordinate mafic minerals set in a fine-grained matrix of quartz and feldspar. Plagioclase phenocrysts (An_{5-10}) occur as twinned and weakly zoned subhedral crystals. Plagioclase phenocrysts commonly show corroded rims when in contact with the groundmass.

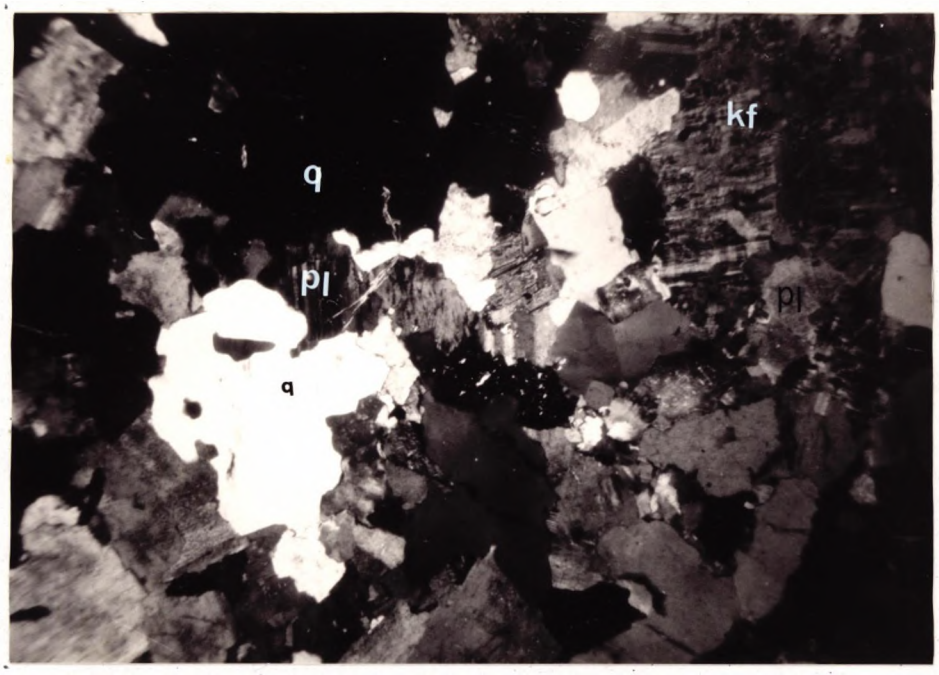

Plate 2.4.3. Photomicrograph of the microgranite of the Tak Pluton, showing small anhedral twinned and weakly zoned plagioclase (pl) enclosed by large anhedral patches of K-feldspar (kf) and quartz (q). (Sample T12, X nicol, 2.5 x 8 x).

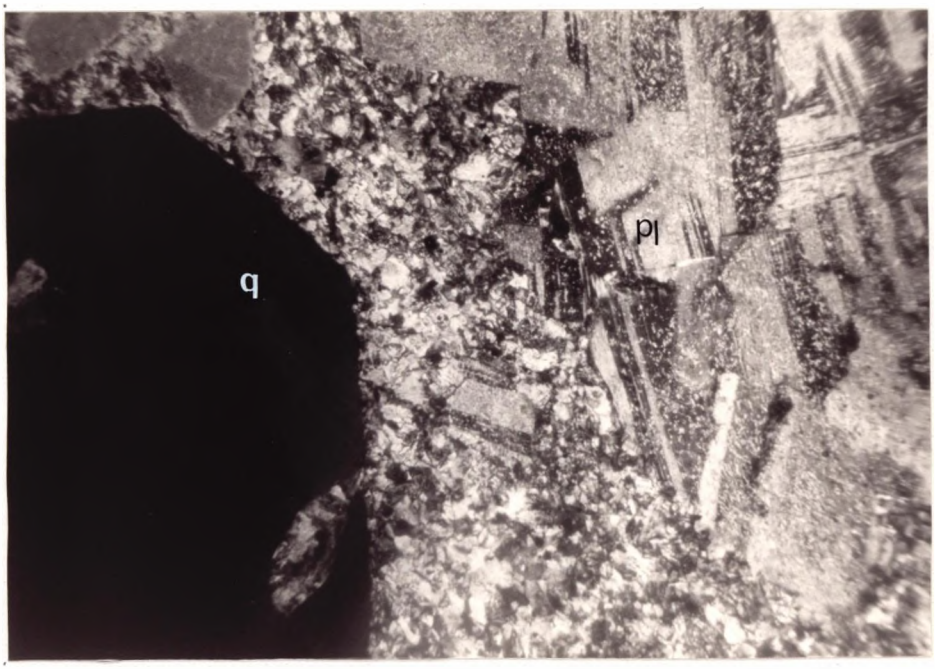

Plate 2.4.4. Photomicrograph of the granite porphyry of the Tak Pluton, showing quartz (q) and clusters of plagioclase (pl) phenocrysts set in a fine-grained quartz and feldspar groundmass. (Sample CTK8, X nicol, 2.5 x 8 x).

Quartz phenocrysts occur as euhedral bipyramidal crystals, showing resorbed rims and granophyric intergrowth when in contact with the groundmass (Plate 2.4.4). Phenocrysts of hornblende (x = greenish brown, y = z = green) occur as discrete subhedral twinned crystals and are partially replaced by biotite and altered to chlorite. Biotite (x = y = z = yellow brown) occurs as small flakes scattered in the groundmass which is composed of fine-grained quartz and feldspar, showing microgranophyric intergrowths.

Summary

The important point gained from the petrographic studies of the Tak Pluton are as follows:

1. Hornblende is a subordinate mafic mineral to biotite in the monzogranite of the inner facies and becomes very rare or absent in the syenogranite of the outer facies.
2. Plagioclase in both the monzogranite and the syenogranite occurs as subhedral to anhedral weakly zoned and twinned crystals and is intensively altered.

Clusters of large plagioclase crystals commonly occur in the monzogranite. The plagioclase crystals in the syenogranite occur mostly as clusters of small crystals and are commonly enclosed in K-feldspar.

3. K-feldspar in both the monzogranite and the syenogranite occurs distinctively as large subhedral to anhedral twinned patches and develops erratic patterns of perthite. In the syenogranite, aggregates of small quartz granules and tiny ablite grains are well developed along K-feldspar twinning planes. Albite is also developed along the rims of plagioclase when in contact with K-feldspar. Granophyric intergrowth is also a common feature in the outer facies when K-feldspar is in contact with quartz.
4. Accessory sphene, allanite, zircon, magnetite and apatite are more

abundant in the monzogranite than in the syenogranite. These accessory minerals occur in association with biotite.

2.5 Chemical characteristics

2.5.1 Major elements

The analysed samples from the Tak Pluton show a range of SiO_2 values from 68-76 wt% (Table 2.5.1).

Consideration of the analysed samples plotted on the Fe-(Na+K)-Mg, and Ca-Na-K ternary diagrams (Fig. 2.5.1a), shows that Mg, Fe and Ca decrease while Na and K increase from the monzogranite of the inner facies to the syenogranite of the outer facies. The plot for the granite porphyry falls close to the syenogranite whereas the plot for the microgranite falls at the end of the trend.

Consideration of the ternary plot of Q-An-Or and An-Ab-Or (Fig. 2.5.1b) for the analysed samples of the monzogranite of the inner facies, the syenogranite of the outer facies and the microgranite, shows that normative quartz increases and albite increases at the expense of orthoclase (Fig. 2.5.1b-i), and anorthite decreases simultaneously with the increase of albite while orthoclase is not increased. The increase of normative albite coincides with the petrographic observation of the development of albitic plagioclase between the twinning plane of K-feldspar, and along plagioclase rims which is poikilitically enclosed in K-feldspar (see section 2.4). The same diagrams (Fig. 2.5.1b) show that the microgranite has higher normative quartz, albite, less orthoclase and little else.

2.5.2 Trace elements

Cobalt, Nickel and Chromium

Co in the Tak Pluton varies from 58 ppm to 163 ppm in the monzogranite to syenogranite. The granite porphyry and the microgranite have much the

TABLE 2.5.1

Analyses of the rocks from the Tak Pluton

	inner facies				outer facies			micro-granite	por-phyry
Sample	T01	T1	CTK48-B	T43	T02B	T10B	T02	T12	CTK8
SiO2	67.87	70.73	72.50	72.99	73.80	74.42	74.19	75.61	73.98
TiO2	0.31	0.23	0.23	0.18	0.16	0.17	0.12	0.08	0.12
Al_2O_3	15.89	14.70	13.83	13.99	13.48	13.31	13.57	13.09	13.79
Fe_2O_3	1.07	1.11	1.05	0.94	0.57	0.68	0.70	0.95	0.94
FeO	1.59	0.97	0.93	0.65	1.12	0.96	0.79	0.39	0.42
MnO	0.08	0.06	0.06	0.20	0.05	0.06	0.07	0.06	0.05
MgO	0.53	0.41	0.42	0.63	0.39	0.42	0.17	0.09	0.12
CaO	1.63	1.38	1.16	1.43	1.06	0.91	0.84	0.52	0.99
Na_2O	3.77	3.68	3.67	3.80	3.70	3.78	3.77	3.94	4.19
K_2O	5.90	5.70	5.25	5.16	5.51	5.15	5.04	4.77	4.70
P_2O_5	0.09	0.05	0.05	0.06	0.03	0.04	0.01	0	0.01
Ba	624	525	475	553	722	247	108	52	213
Ce	199	119	98	82	84	90	65	53	58
Co	99	106	101	58	87	163	123	154	206
Cr	2	10	6	7	7	2	7	7	9
La	115	69	62	54	51	52	29	29	27
Nd	83	40	44	36	39	45	34	27	36
Ni	5	5	4	7	3	1	4	0	0
Pb	89	246	63	105	53	67	97	324	219
Rb	241	253	248	387	252	253	338	459	218
Sc	6	2	0	1	1	0	1	0	1
Sr	150	127	130	217	106	76	44	23	61
Th	76	93	77	84	65	88	52	56	158
Ti	1797	1230	1333	1243	1000	964	668	408	699
U	16	16	19	-	14	-	11	23	-
V	16	9	13	17	3	8	6	2	6
Y	22	21	20	27	21	19	19	55	13
Zn	43	31	31	43	28	31	32	36	24
Zr	305	227	219	177	150	167	116	88	173

TABLE 2.5.2.

C.I.P.W. norms of the rocks from the Tak Pluton

	inner facies				outer facies			micro-granite	por-phyry
Sample	T01	T1	CTK48-B	T43	T02B	T10B	T02	T12	CTK8
Q	18.64	23.81	28.83	27.07	28.03	29.85	30.78	33.02	29.04
Or	34.87	33.69	31.02	30.32	32.56	30.43	29.79	28.19	28.31
Ab	31.90	31.13	31.05	31.98	31.31	31.98	31.90	33.59	35.45
An	7.50	6.52	5.43	5.87	3.92	4.14	4.10	2.58	4.68
Le	-	-	-	-	-	-	-	-	-
Ne	-	-	-	-	-	-	-	-	-
C	0.56	0.09	0.12	-	-	-	0.41	0.45	-
Ac	-	-	-	-	-	-	-	-	-
DiCa	-	-	-	0.33	0.48	0.05	-	-	0.07
DiMg	-	-	-	0.23	0.20	0.02	-	-	0.06
DiFe	-	-	-	0.07	0.28	0.02	-	-	-
Wo	-	-	-	-	-	-	-	-	-
HyMg	1.32	1.02	1.05	1.34	0.77	1.02	0.17	0.22	0.24
HyFe	1.52	0.60	0.57	0.43	1.12	1.00	0.69		
OlMg	-	-	-	-	-	-	-	-	-
OlFe	-	-	-	-	-	-	-	-	-
Mt	1.81	1.61	1.52	1.38	0.83	0.99	1.22	1.22	1.17
He	-	-	-	-	-	-	-	0.11	0.13
Il	0.21	0.44	0.44	0.38	0.30	0.32	0.23	0.15	0.23
Ap	-	0.12	0.11	0.14	0.06	0.09	0.02	-	0.02

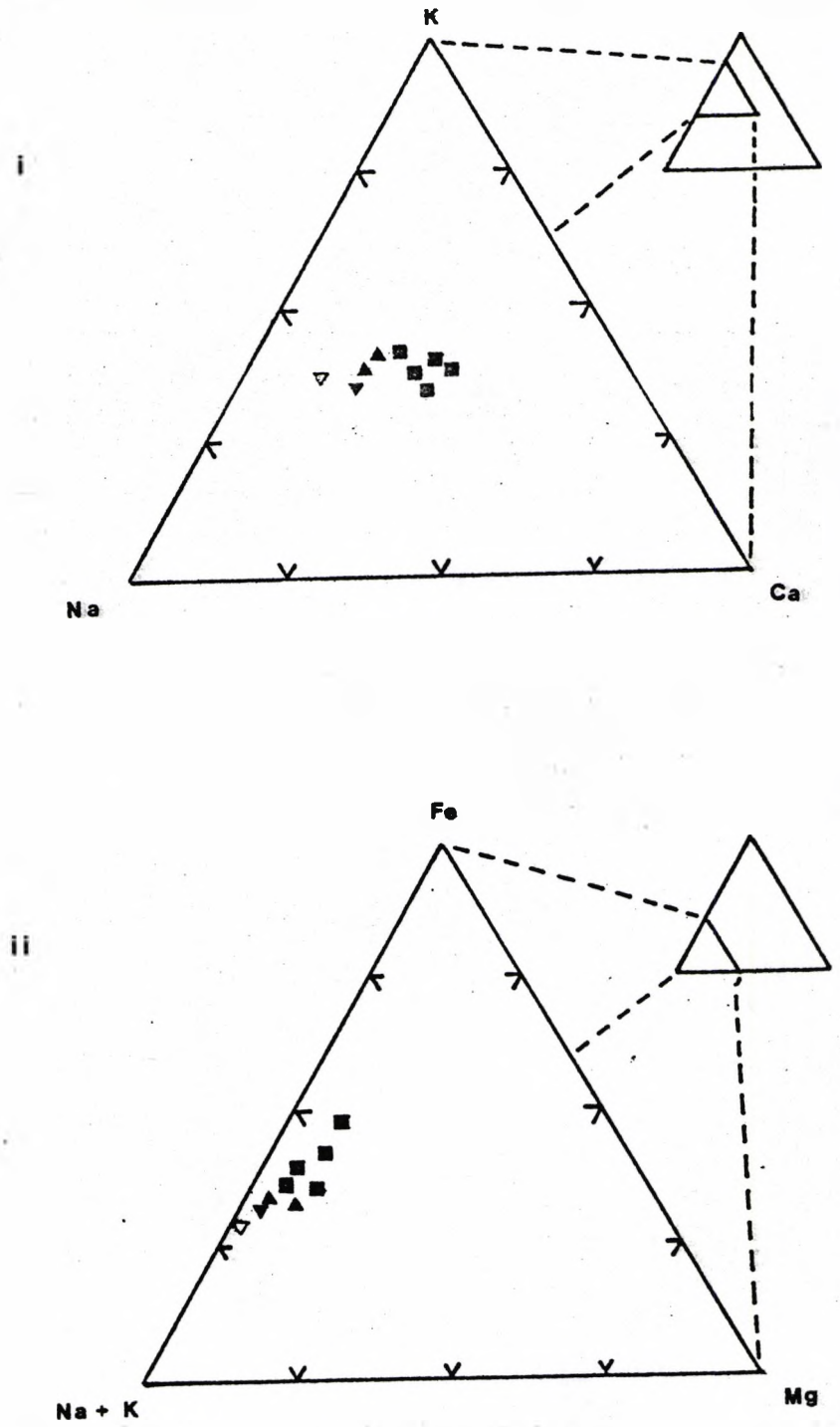

Figure 2.5.1a Triangular plots of the plutonic rocks of the Tak Pluton
solid squares - inner facies - monzogranite
solid triangle, point up - outer facies - syenogranite
solid triangle, point down - porphyry
open triangle - microgranite

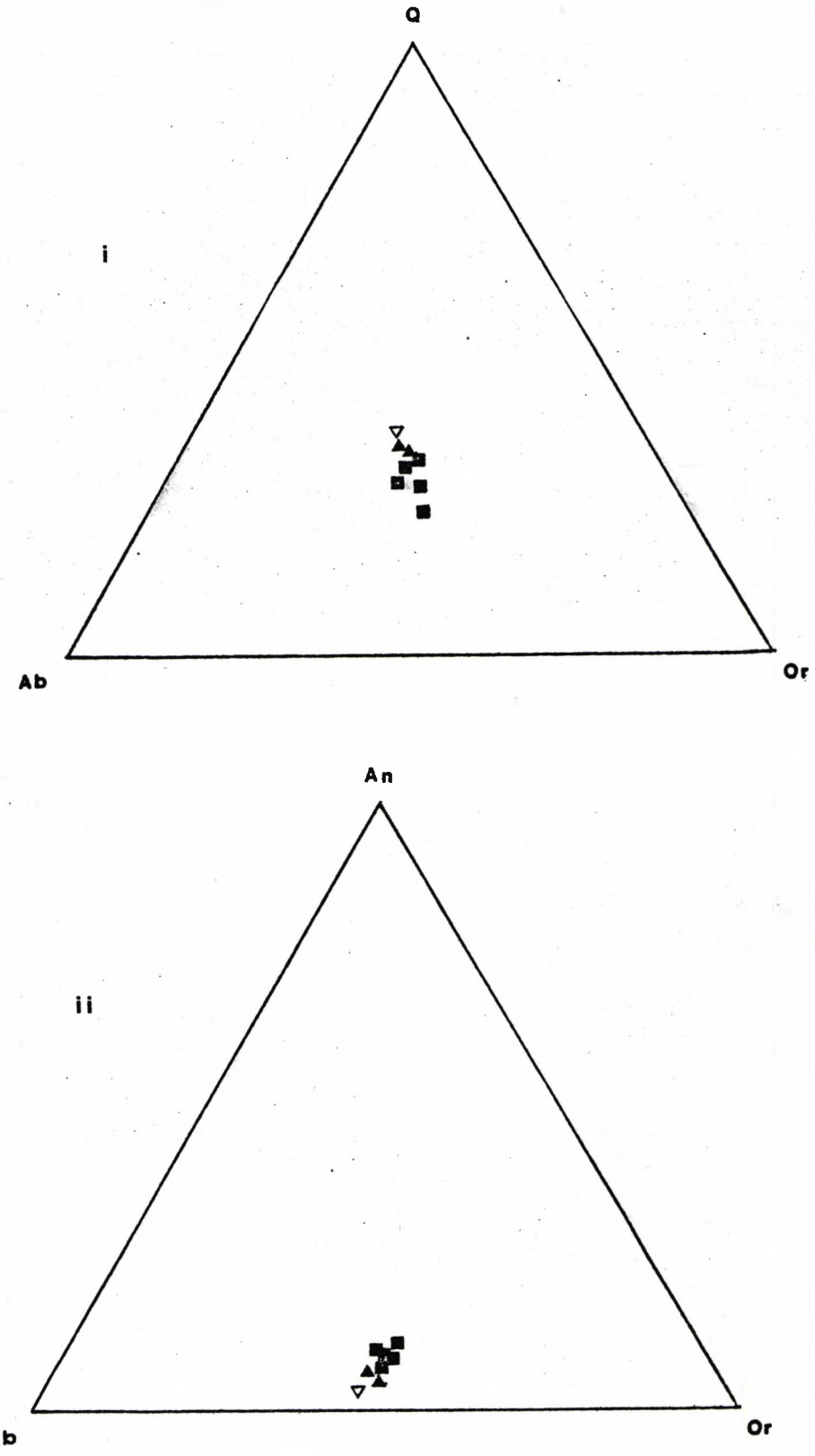

Figure 2.5.1b Triangular plots of the plutonic rocks of the Tak Pluton
solid squares - inner facies - monzogranite
solid triangle - outer facies - syenogranite
open triangle - microgranite
(calculated from C.I.P.W. norms in Table 2.5.2).

same concentration as the syenogranite. The variation of Co (Fig. 2.5.2a) shows a positive correlation with DI. This variation is different from that expected. Co should decrease as differentiation increases and the behaviour could be due to the anomalous behaviour of Co^{+2}, Ni^{+2} and Cr^{+3} which may be concentrated in residual magmas during the later stages of crystallisation of a volatile-rich magma (Ringwood, 1955b). The rocks in the Tak Pluton commonly show granophyric textures, especially in the syenogranite of the outer facies (section 2.4), indicating crystallisation in a volatile-rich acid magma.

Cr in the Tak Pluton varies between 2 ppm and 10 ppm, and is distributed erratically in the monzogranite of the inner facies and in the syenogranite of the outer facies (Fig. 2.5.2a). The granite porphyry and the microgranite have concentrations of Cr similar to the syenogranite. The variation of Cr in the Tak Pluton which contradicts the expected trend of decreasing Cr content as the differentiation increases, may be the same volatile situation as seen for Co.

Ni in the Tak Pluton varies from 7 ppm to 1 ppm in the monzogranite of the inner facies to syenogranite of the outer facies, and shows negative correlation with DI (Fig. 2.5.2a). The analyses for the granite porphyry and the microgranite show that there is no detectable Ni in these rocks. Ni^{+2} (radius = 0.69Å) can substitute for both Fe^{+2} (radius = 0.74Å) and Mg^{+2} (radius = 0.65Å) in hornblende, biotite and other ferromagnesian minerals. In the case of the Tak Pluton, the decrease of Ni content from the monzogranite of the inner facies to syenogranite of the outer facies coincides with the decrease in abundance of hornblende and biotite from the inner facies toward the outer facies as indicated in modal analyses (see table 2.4.1). Thus Ni shows compatible character in this Pluton.

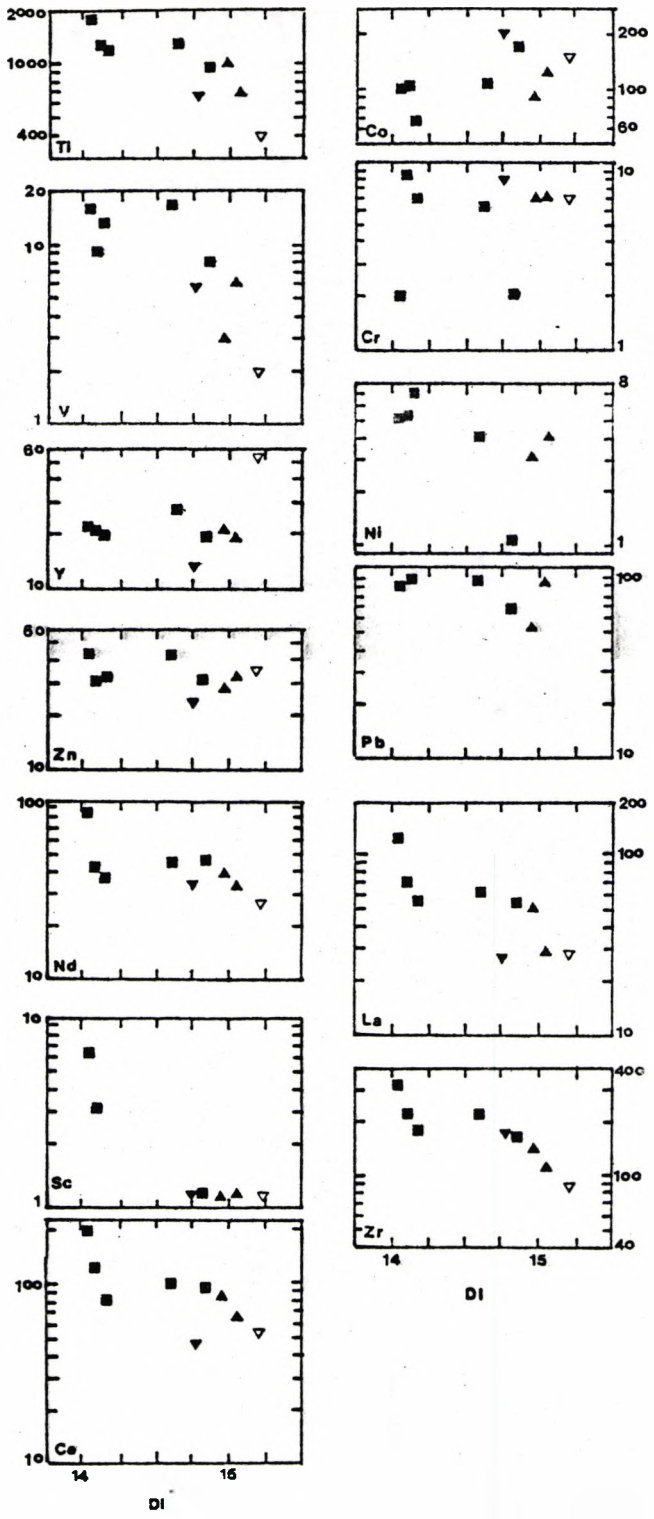

Figure 2.5.2a Plots of trace element content vs. Differentiation Index for the plutonic rocks of the Tak Pluton.
solid squares - inner facies - monzogranite
solid triangle, point up - outer facies - syenogranite
solid triangle, point down - porphyry
open triangle - microgranite

Scandium and Vanadium

Sc varies from 6 ppm to 1 ppm in the monzogranite of the inner facies to the syenogranite of the outer facies and shows a negative correlation with DI (Fig. 2.5.2a). The granite porphyry and the microgranite have low concentrations of Sc cf. syenogranite.

V varies from 17 ppm to 3 ppm in the monzogranite to syenogranite and shows negative correlation with DI (Fig. 2.5.2a). The granite porphyry has much the same concentration of V as the syenogranite whereas the microgranite has lower concentrations than the syenogranite.

Both Sc^{+3} (radius = 0.81Å) and V^{+3} (radius = 0.74Å) are strongly concentrated in ferromagnesian minerals, and the highest concentrations occur in hornblende (Ewart and Taylor 1969).

In the Tak Pluton, the decrease of Sc and V as the DI increases from the monzogranite to syenogranite coincides with the decrease in hornblende and other mafic minerals. Therefore, Sc and V behave compatibly with the extraction of hornblende or other mafic minerals in this pluton.

Lanthanum, Cerium and Neodynium

La varies from 115 ppm to 29 ppm, Ce varies from 199 ppm to 65 ppm and Nd varies from 83 ppm to 34 ppm from the monzogranite of the inner facies to the syenogranite of the outer facies. These variations show negative correlations with DI (Fig. 2.5.2a). The granite porphyry and the microgranite have much the same concentrations of these trace elements as the syenogranite.

Accessory sphene, allanite, xenotime and monzonite are the main sources of LREE in granitic rocks (Condie 1978). Sphene and allanite are the common accessory minerals in the rock of the Tak Pluton and are associated with mafic minerals (see section 2.4). The decrease in LREE concentration with the increase of DI from the monzogranite of the inner facies to the syenogranite of the outer facies may be related to a

crystallisation of LREE-bearing accessory minerals. Therefore, the LREE's behave compatibly in this pluton.

Lead

Most of Pb content in the Tak Pluton varies between 53 - 100 ppm and the distribution is erratic and independent of DI. It is extremely high compared with Turekian and Wedepohl's (1961) value of 19 ppm for "low-calcium" granites. From detailed investigations Wedepohl (1956) concluded that Pb replaces K - principally in K-feldspars (in Siedner, 1965). Ringwood (1955a), explained that the high charge and smaller size of Pb^{+2} (electronegativity 1.8 and radius 1.2Å) compared to K^{+1} (electronegativity 0.8 and radius 1.33Å) causes Pb to be concentrated in residual magmas rather than in K-bearing minerals.

Zinc

Zn varies from 43 ppm to 28 ppm in the monzogranite of the inner facies to the syenogranite of the outer facies and shows negative correlation with DI (Fig. 2.5.2a). The granite porphyry and the micro-granite have much the same concentration of Zn as the syenogranite.

The ionic radii of Zn^{+2} and Fe^{+2} are similar (0.74Å), consequently Zn is camouflaged in minerals containing ferrous iron (Ringwood, 1955a). The decrease of Zn as DI increases from monzogranite to syenogranite in the Tak Pluton may be related to the decrease in mafic minerals (section 2.4). Thus, Zn behaves comaptibly in this pluton.

Thorium

Th varies from 93 ppm to 52 ppm in the monzogranite of the inner facies to the syenogranite of the outer facies and shows a negative correlation with DI (Fig. 2.5.2b). The microgranite has a Th concentration much the same as the syenogranite. The distinctively high concentration of Th in the Tak Pluton is similar to the recorded Th values by Rogers

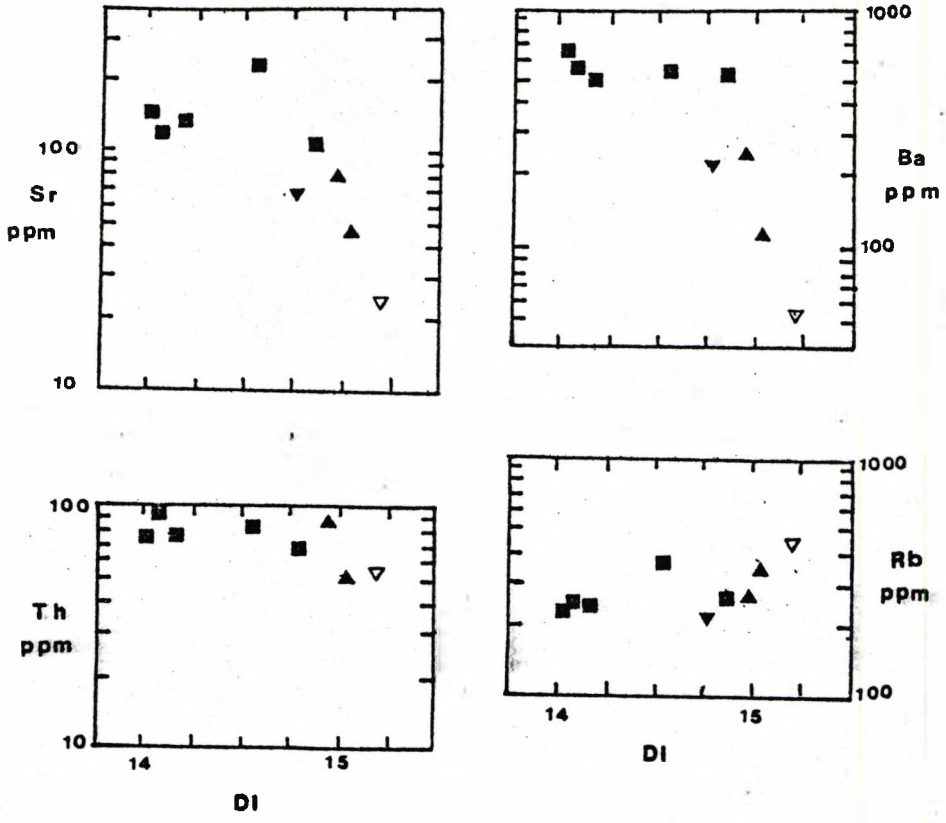

Figure 2.5.2b Plots of trace element content vs. Differentiation Index for the plutonic rocks of the Tak Pluton.
solid squares - inner facies - monzogranite
solid triangle, point up - outer facies - syenogranite
solid triangle, point down - porphyry
open triangle - microgranite

Ragland (1961) for biotite granite (Conway) of the White Mt. Series, North America which have Th contents of 53 - 98 ppm, for rocks with K content greater than 4 wt.%. Rogers and Ragland (op. cit.) noted the possibility that Th has been added to the Conway granite and may be related to the exceptionally rich allanite content. They also showed that Th has a tendency to increase when K content in the rock increases. The Tak Pluton contains allanite, and the K wt.% is high and decreases from 5.90 to 5.04%. The decrease of Th content therefore may be related to the decrease of K content. However, the associated very high Pb contents suggest the Th content may be due to the allanite in these rocks.

Titanium and Zirconium

Ti varies from 1797 ppm to 668 ppm in the mongranite of the inner facies to the syenogranite of the outer facies and shows a negative correlation with DI (Fig. 2.5.2a). The granite porphyry has Ti concentrations (699 ppm) much the same as the syenogranite whereas the microgranite has lower Ti (408 ppm) than the syenogranite.

Zr varies from 305 ppm to 116 ppm in the monzogranite to the syenogranite and shows a negative correlation with DI (Fig. 2.5.2a). The granite porphyry has much the same concentration of Zr as the syenogranite whereas the microgranite has a Zr content lower than the syenogranite.

The plot of Ti-Zr (Fig. 2.5.2c) shows a trend due to the fractionation of a combination of zircon, biotite, hornblende and possibly magnetite (Pearce and Norry, 1979). Hornblende and biotite commonly contain Ti and zircon is the main sources of Zr.

The decrease of Ti coincides with the decrease of hornblende and biotite from the monzogranite to syenogranite (see modal data table 2.4).

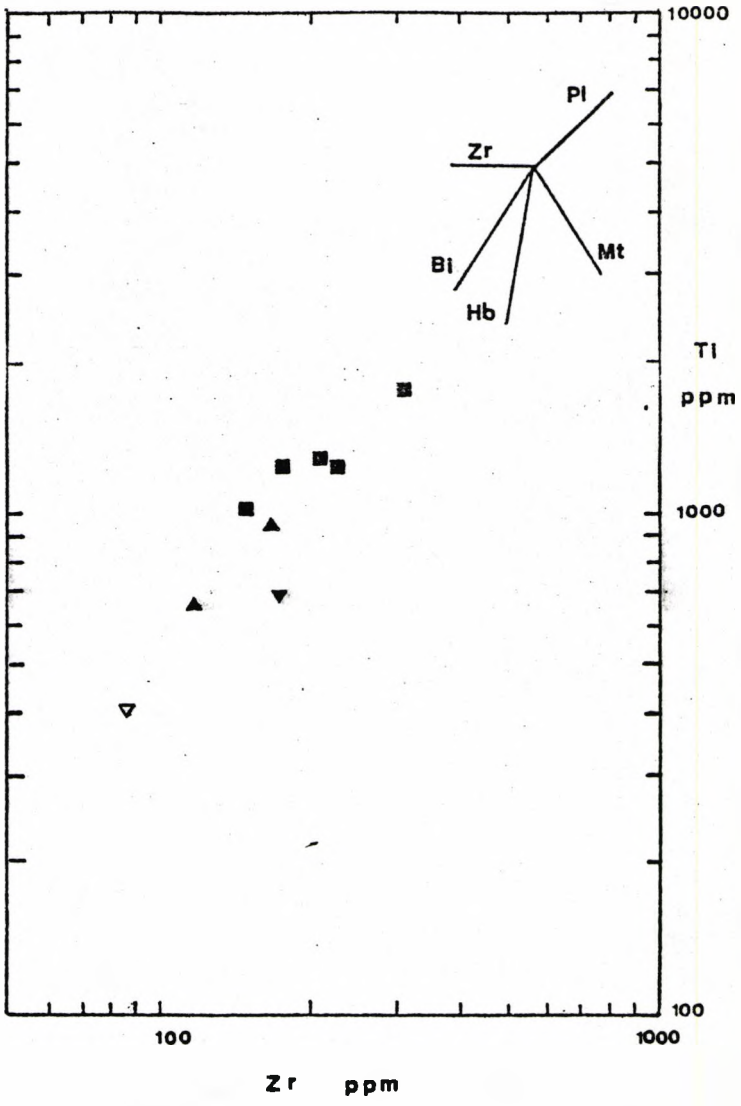

Figure 2.5.2c Plot of Ti vs. Zr for the plutonic rocks of the Tak Pluton
solid squares - inner facies - monzogranite
solid triangle, point up - outer facies - syenogranite
solid triangle, point down - porphyry
open triangle - microgranite
The mineral vectors shown are taken from Pearce and Narry (1979) and indicate the relative change in these elements upon extraction of each mineral. Bi = biotite; hb = hornblende; Mt = magnetite; Pl = plagioclase; Zr = zircon.

Zircon occurs mostly as inclusions in biotite as noted in the petrographic observation and probably decreases as biotite decreases, although some Zr may be removed by hornblende + biotite.

In brief, the decrease of Ti and Zr in this pluton shows the compatible character of these elements. Note that the Zr concentration of the Tak Pluton is between the average low and high Zr values in quartz-monzonites and granites (50 - 700 ppm) recorded by Chao and Fleischer (1960).

Yttrium

Y varies from 27 ppm to 19 ppm from the monzogranite of the inner facies to the syenogranite of the outer facies and shows a very slight decrease as the DI increases (Fig. 2.5.2a). The granite porphyry has a Y content (13 ppm) lower than the syenogranite whereas the microgranite has an abnormally high value (55 ppm), for a very low CaO (0.52 wt.%) in the rock, compared to the other rocks in this pluton. This may be due to the fractionation of Ca-poor phases, viz. K-feldspar, mica or sodic plagioclase as suggested by Lambert and Holland (1974).

The plot of Y versus CaO (Fig. 2.5.2d) shows a trend of slightly decreasing Y as CaO decreases. The work of Lambert and Holland (1974) shows that this trend may be due to the fractionation of hornblende, sphene and apatite. The slight decrease of Y from the inner facies to the outer facies of the Tak Pluton coincides with the decrease in hornblende (see section 2.4). Therefore Y shows compatible characteristics in this pluton.

Rubidium, Strontium and Barium

Rb varies from 241 ppm to 338 ppm, whereas Sr varies from 217 ppm to 44 ppm and Ba varies from 722 ppm to 108 ppm in the monzogranite of

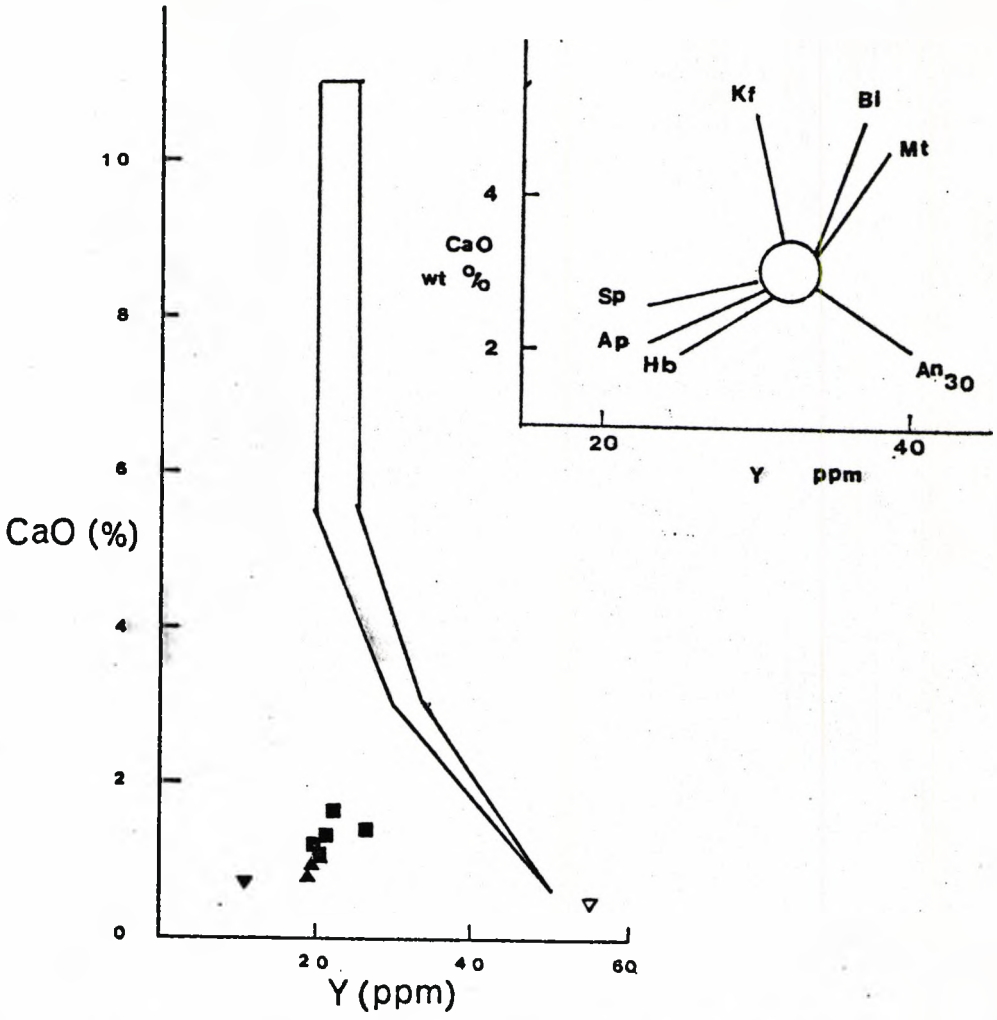

Figure 2.5.2d Plot of CaO vs. Y for the plutonic rocks of the Tak Pluton.
solid squares - inner facies - monzogranite
solid triangle, point up - outer facies - syenogranite
solid triangle , point down - porphyry
open triangle - microgranite
Enclosed area represents "standard calc-alkali trend"; inset shows "liquid fractionation trends" for minerals (after Lambert and Holland, 1974). Sp = sphene; Ap = apatite; Hb = hornblende; An_{30} = plagioclase of anorthite 30%; Mt = magnetite; Bi = biotite; Kf - K-feldspar.

the outer facies to the syenogranite of the inner facies of the Tak Pluton. The Rb contents in these rocks show positive correlation with DI, while Sr and Ba decrease with increasing DI (Fig. 2.5.2b). The granite porphyry has Rb, Sr and Ba concentrations much the same as the syenogranite whereas the microgranite has lower Sr and Ba contents and a higher Rb content than the syenogranite (Fig. 2.5.2b). The possibility of a chemical relationship of these rocks will be discussed later. The decrease of Ba and Sr contents from the inner facies to the outer facies as well as the increase of Rb will be discussed in the Ba-Sr, Ba-Rb and Rb-Sr diagrams.

Ba-Sr diagram

The plot of Ba-Sr content (Fig. 2.5.2e), shows from the mineral vectors that plagioclase ($\pm$ hornblende) and biotite ($\pm$ feldspar) can cause Ba and Sr to decrease in the liquid during fractionation. Due to the similarity in size of Ba^{+2} (radius = 1.34Å) and K^{+2} (radius = 1.33Å).

Ba is incorporated in biotite and K-feldspar by substitution for K and becomes depleted in the liquid during fractionation. Sr^{+2} (radius = 1.18Å) is preferentially incorporated into plagioclase (and hornblende) by substitution for Ca^{+2} (radius = 1.02Å) and becomes depleted in the liquid during fractionation.

The decreasing trend of Ba-Sr is in agreement with the decrease of plagioclase, biotite and K-feldspar as quartz increases from the rocks in the inner facies towards the outer facies (see modal data table 2.4). Thus Ba and Sr behave compatibly in this pluton. The granite porphyry plots close to the syenogranite whereas the microgranite falls at the end of the trend and may imply that the granite porphyry may be chemically related to the rocks of the outer facies as it occurs as a rapidly chilled

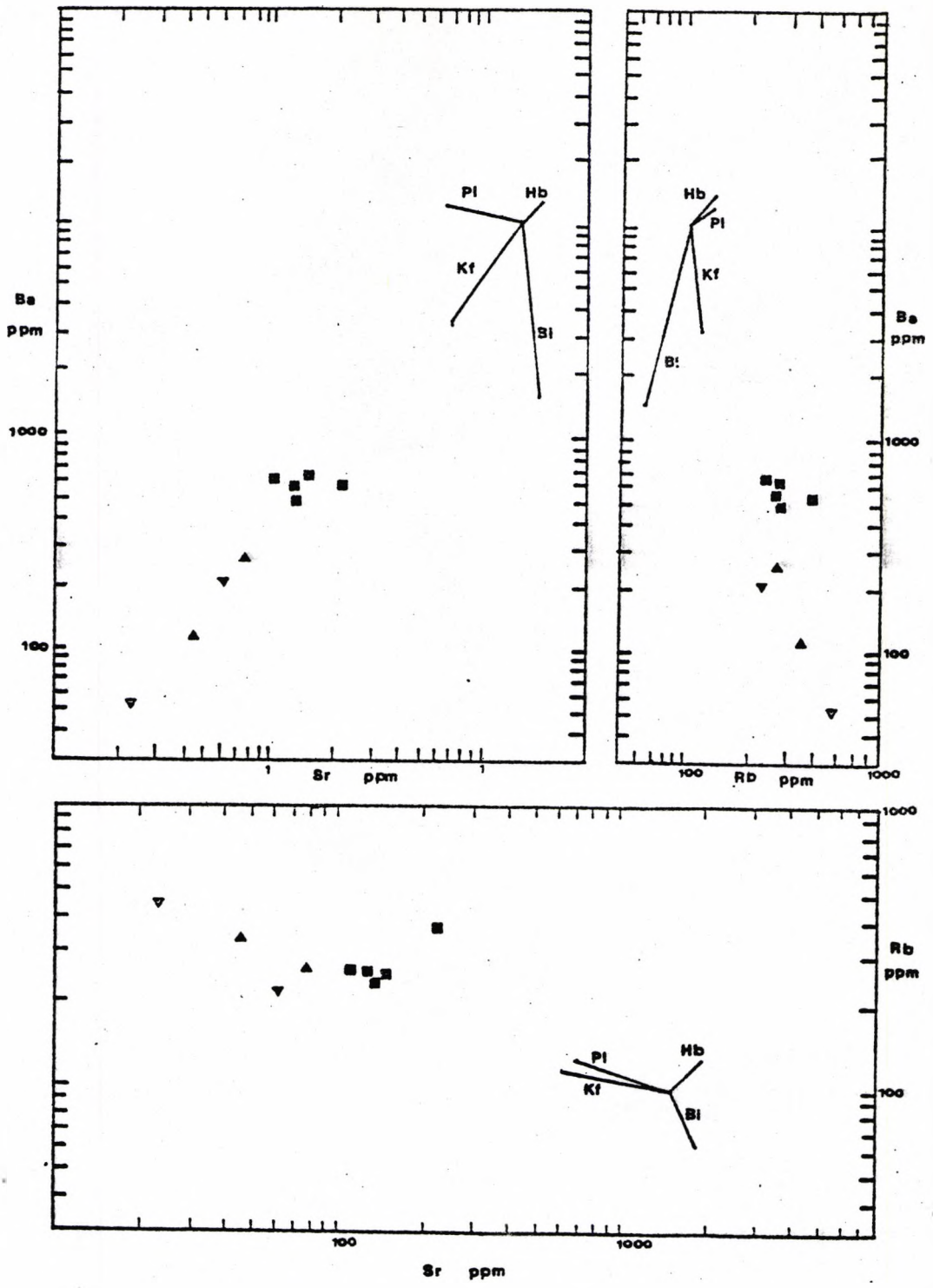

Figure 2.5.2e Plots of Rb, Sr, Ba for the plutonic rocks of the Tak Pluton.
solid squares - inner facies - monzogranite
solid triangles, point up - outer facies - syenogranite
solid triangles - point down - porphyry
open triangles - microgranite
Mineral vectors calculated from the distribution coefficients for acid plutonic rocks (Table 14.1 from Cox et al. 1979). Length of vector indicates 20% fractionation of mineral. Kf = K-feldspar; Bi = biotite; Hb = hornblende; Pl = plagioclase.

intrusive dyke, whereas the microgranite may be differentiated from the syenogranite.

Rb-Sr diagram

The plot of Rb versus Sr (Fig. 2.5.2e) shows that Sr decreases as Rb increases from the monzogranite of the inner facies to the syenogranite of the outer facies and the plotted point for the granite porphyry falls close to the outer facies, whereas the plotted point for the microgranite falls at the end of the trend. The mineral fractionation vectors indicate that the fractionation of plagioclase and possibly K-feldspar (mechanism unclear) can cause the depletion of Sr and enrichment of Rb in the liquid. Due to the close resemblance in size of Sr^{+2} (radius = 1.18Å) and Ca^{+2} (radius = 1.02Å), Sr is incorporated into plagioclase and hornblende by substitution for Ca and becomes depleted in the liquid during fractionation. The larger size of Rb^{+1} (Radius = 1.47Å) compared to Ca^{+2} (radius = 1.02Å) and K^{+1} (radius = 1.33Å) makes it difficult for Rb to substitute for Ca and K (less so) in plagioclase, hornblende or K-feldspar, therefore, it becomes enriched in the liquid. Thus, Sr shows compatible characteristics but Rb does not, in this pluton.

The relationship of the granite porphyry and the microgranite on this diagram are compatible with the interpretation given earlier (Ba-Sr diagram).

Ba-Rb diagram

The plot of Ba versus Rb (Fig. 2.5.2e), shows as expected, similar features to the previous diagrams. The mineral vectors indicate that the fractionation is some combination of plagioclase, hornblende, biotite and K-feldspar which causes the depletion of Ba and enrichment of Rb in

the liquid. The closely similar size of Ba^{+2} (radius = 1.34Å) and K^{+1} (radius = 1.33Å) enables Ba to substitute for K in biotite, and possibly in K-feldspar during fractionation and so it is depleted in liquid. The larger in size of $Rb^{=1}$ (radius = 1.47Å) compared to Ca^{+2} (radius = 1.02Å) and K makes it difficult for Rb to be incorporated in plagioclase, hornblende biotite or K-feldspar by substitution for Ca and K and so it becomes enriched in the liquid during the fractionation. The decrease in mineral proportions of plagioclase, hornblende, biotite and K-feldspar as quartz increases from the monzogranite of the inner facies to the syenogranite of the outer facies (see table 2.4.1) is in agreement with this diagram. Thus Ba shows compatible characteristics but Rb does not.

The relationship of the granite porphyry and the microgranite to the syenogranite of the outer facies, and general trend is compatible with the earlier interpretation.

Summary

The important chemical characteristics of the rocks in the Tak Pluton are as follows:

1. The decreasing content of Y and Sr is compatible with precipitation of Ca-bearing minerals; and the decrease of Ba is compatible with K-bearing mineral precipitation.

The increase of Rb which is incompatible with Ca-bearing and to a lesser extent K-bearing minerals, reflects the fractionation of plagioclase, hornblende, ($\pm$ apatite, $\pm$ sphene), biotite and possibly K-feldspar (see section 2.5.2d and 2.5.2e).

2. The decreasing content of the trace elements Ni, V, Sc are compatible with ferromagnesian minerals from the monzogranite of the inner facies to the syenogranite of the outer facies, i.e. with DI increasing, is coincident with the trend of decreasing Fe and Mg in the Fe-(Na + K)-Mg diagram (Fig. 2.5.1a), and compatible with the extraction of these elements

from the liquid by hornblende, biotite and magnetite which are the common ferromagnesian minerals.

It is noteworthy that the abnormal behaviour of Co which increases with differentiation may be related to the crystallisation of an acid magma with a high volatile residual liquid (Ringwood, 1955b). The common granophyric texture in the rocks, especially in the outer facies, plus the turbid K-feldspar and the numerous feldspar and quartz feldspar pegmatite dykes at the periphery of the pluton, is also indicative of high volatiles. The erratic distribution of Cr may also be related to the conditions mentioned above.

3. The decrease of Ti and Zr in these rocks of the inner facies to the outer facies (as DI increases) indicates the fractionation of hornblende, biotite and possibly magnetite which can deplete Ti content, plus fractionation of zircon which can deplete Zr content.

4. The decrease of LREE contents from the monzogranite to the syenogranite as differentiation increases, reflects the fractionation of sphene and allanite and the silicates such as hornblende and plagioclase.

5. The Tak Pluton has a relatively high Th content (52 - 93 ppm) compared to the average granite (17 - 36 ppm) of Heier and Rogers (1963), but similar to the high K and allanite bearing granite of the White Mountain Series, North America, recorded by Rogers and Ragland (1961). The high associated Pb also suggests Th occurs in the accessory minerals.

6. The granite porphyry have chemical characteristics close to those of the syenogranite of the outer facies and the microgranite shows chemical characteristics of a differential member of the syenogranite

7. These data plus the other trace element variation (Ni, V, Sc, Ti and Zr) also indicate a very crude chemical zoning from the inner part of the pluton to the outer part of the pluton which will be discussed later.

CHAPTER 3

THE MAE-SALIT PLUTON

3.1 Introduction

The Mae-Salit Pluton is situated on the western side of the Tak Batholith and covers an area of approximately 50 sq. km. (Fig. 1.2.1). It is a roughly rounded body and cuts the western part of the Western Main Range Pluton. The western rim of the Mae-Salit Pluton is covered by terraces and alluvium deposits.

Detailed studies of the rocks in this pluton have not previously been made.

3.2 Components of the pluton

The Mae-Salit Pluton is made up mainly of pinkish coarse-grained monzogranite and medium- to fine-grained monzogranite. The coarse-grained monzogranite mostly crops out in the central part of the pluton whereas the medium- to fine-grained monzogranite mostly crops out marginally.

The terms "inner facies" and "outer facies" will be used to refer to the coarse-grained monzogranite in the central part of the pluton and the medium- to fine-grained monzogranite on the outer part of the pluton, respectively (Fig. 3.2.1).

The contact between the two facies is gradational and the boundary between these two facies is based on the different grain size of these rocks.

3.3 Field Relationship

The Mae-Salit Pluton shows a field relationship only with the Western Main Range Pluton because the western side of the Mae-Salit Pluton is concealed by alluvium and river terraces. The eastern part of the Mae-Salit intrudes the western edge of the Western Main Range Pluton. A sharp contact

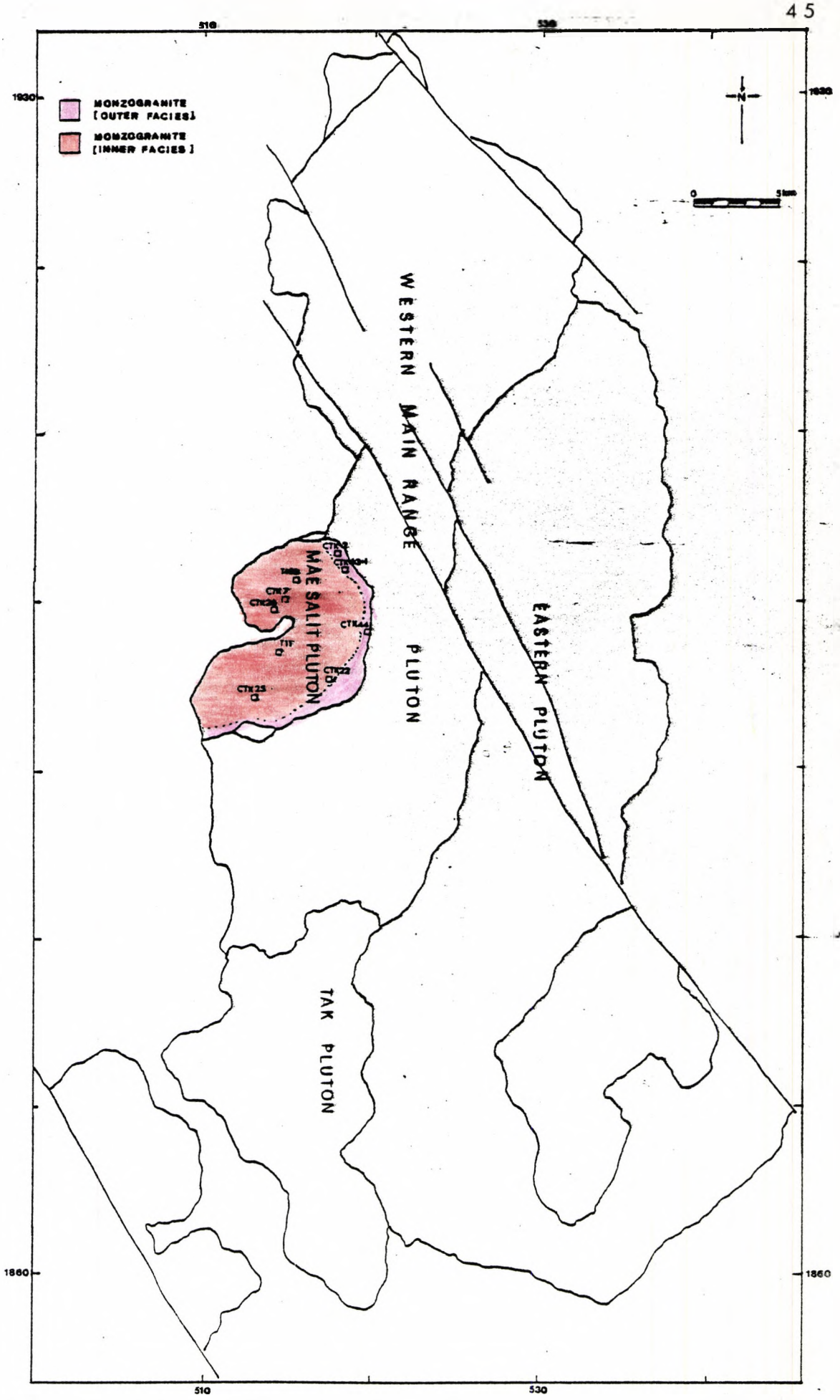

Figure 3.2.1 Outcrop map of the Tak Batholith, showing the different facies and samples localities of the Mae-Salit Pluton.

of a medium- to fine-grained monzogranite of the outer facies of the Mae-Salit pluton cuts a coarse-grained monzonite of the inner facies of the Western Main Range Pluton and is well observed at the sample location CTK 44, (Fig. 3.2.1).

3.4 Petrography

The monzogranite of the inner facies is a pinkish equigranular coarse-grained rock consisting of pink K-feldspar (0.5 - 1 cm in length), plagioclase and quartz with hornblende and biotite. A plot showing the relative proportions of modal quartz - alkali feldspar - plagioclase is shown in Fig. 3.4.1.

Plagioclase (An_{12-28}) forms clusters of subhedral laths 3-5 mm in length and small discrete plagioclase laths are often embayed by K-feldspar. Twinning is well developed in the large plagioclase laths, and normal and oscillatory zoning are common with intensively saussuritized cores. Myrmekitic intergrowths are locally developed where in contact with K-feldspar. The K-feldspar occurs as large subhedral, twinned, microcline perthite plates, some of which show zoning. Aggregates of tiny quartz grains are locally developed along the K-feldspar twin planes or between the contacts of K-feldspar crystals. K-feldspar encloses other minerals, even quartz, which occurs as patches of large subhedral grains.

Hornblende (x = green, y = z = greenish brown) forms twinned prismatic crystals and is commonly replaced by biotite. Biotite (x = greenish brown, y = z = yellow brown) occurs as clusters of flakes and is partially altered to chlorite. Inclusions in biotite are apatite, sphene, zircon and magnetite. Large well-formed wedge-shaped sphene commonly forms clusters with magnetite (plate 3.4.1).

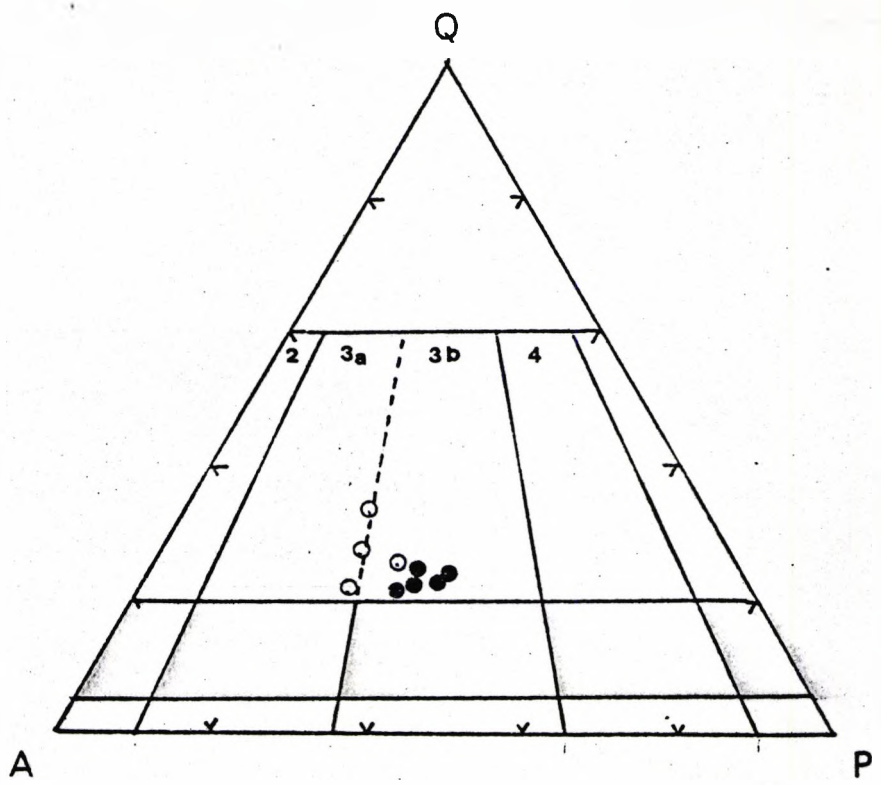

Figure 3.4.1 Classification of the plutonic rocks of the Mae-Salit Pluton (following Streckeisen, 1976). Symbols as follows:
solid circles - inner facies - monzogranite
open circles - outer facies - monzogranite
(calculated from modes in Table 3.4.1).

TABLE 3.4.1

Modes of the rocks from the Mae-Salit Pluton

	inner facies				
	T11	CTK7	T48A	CTK25	CTK26
Plagioclase	34.34	33.85	32.55	34.45	34.85
K-feldspar	28.01	45.25	39.75	40.45	38.40
Quartz	21.63	19.75	22.45	20.20	20.87
Hornblende	2.72	2.45	2.25	1.50	2.52
Biotite	3.14	2.90	2.35	2.05	2.34
Others	0.16	0.80	0.65	0.35	1.02

	outer facies			
	CTK22	CTK63	CTK2	CTK44
Plagioclase	28.35	25.47	27.53	21.87
K-feldspar	45.33	48.41	45.37	42.05
Quartz	22.96	23.46	24.11	35.05
Hornblende	1.42	1.00	1.43	0.08
Biotite	1.23	1.06	1.01	0.50
Others	0.71	0.60	0.55	0.45

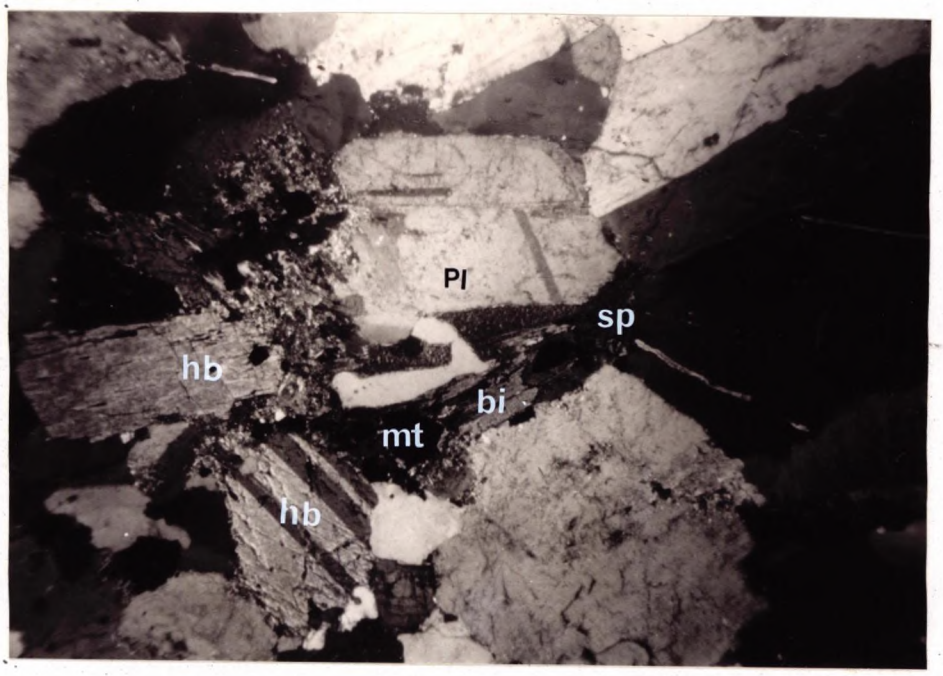

Plate 3.4.1. Photomicrograph of the monzonite (inner facies) of the Mae-Salit Pluton, showing clusters of plagioclase (pl) hornblende (hb), biotite (bi) in association with magnetite (mt) and sphene (sp). (Sample T48B, X nicol, 2.5 x 8 x).

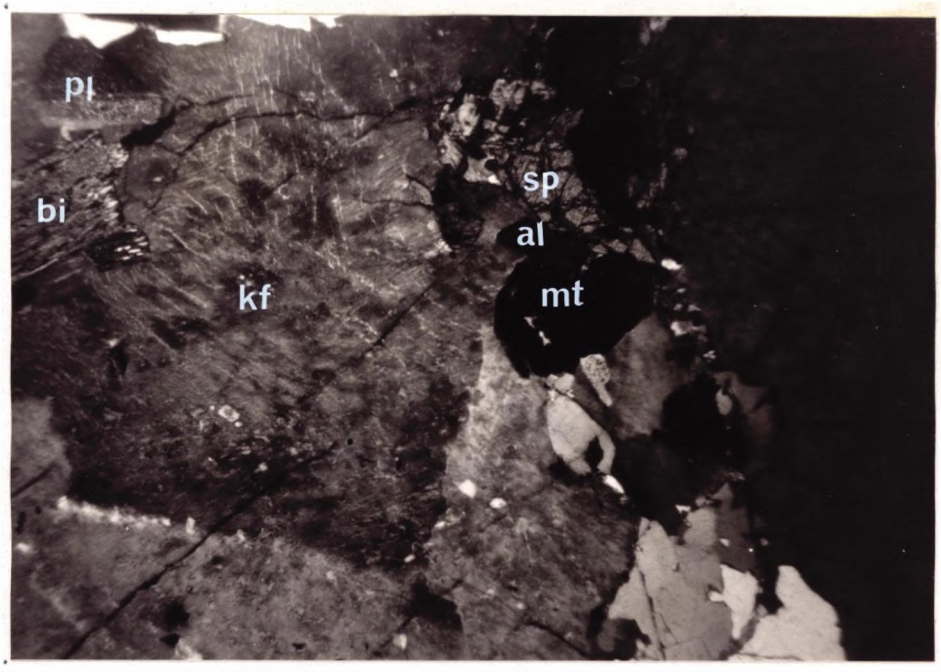

Plate 3.4.2 Photomicrograph of the monzogranite (outer facies) of the Mae-Salit Pluton, showing large K-feldspar (kf) enclosing plagioclase (pl) and biotite (bi). Sphene (sp), allanite (al) and magnetite (mt) occur in clusters. (Sample CTK44, X nicol, 2.5 x 8 x).

The monzogranite of the outer facies is a medium-grained pinkish rock with a grain size of 2-5 mm diameter. It consists of pink K-feldspar, plagioclase and quartz with some hornblende and biotite. A plot showing the relative proportions of modal quartz - alkali feldspar - plagioclase is shown in Fig. 3.4.1.

Plagioclase (An_{8-12}) occurs as subhedral twinned and weakly zoned crystals. Small plagioclase crystals with poorly developed twinning are poikilitically enclosed in K-feldspar, which occurs as large anhedral to subhedral twinned plates enclosing the other minerals. Granophyric intergrowths of quartz and K-feldspar are locally developed along the contacts of these minerals. Tiny albite crystals with aggregates of small quartz grains are commonly developed along the contact of K-feldspar plates or along the K-feldspar twin planes. Clouding in K-feldspar is intensively developed. Hornblende (x = yellow green, y = z = greenish brown) forms subhedral twinned crystals partially or wholly replaced by biotite. Biotite (x = greenish brown, y = z = yellow brown) forms clusters of flakes and is often altered to chlorite. Sphene, apatite, allanite, zircon and magnetite are common accessory minerals and occur in association with biotite (plate 3.4.2).

Summary

The important petrographic features of these rocks are as follows:-

1. The clusters of large zoned and well twinned plagioclase crystals are common in the monzogranite of the inner facies, whereas small discrete weakly zoned plagioclase crystals which are poikilitically enclosed by K-feldspar are common in the monzogranite of the outer facies.
2. K-feldspar in the monzogranite of the inner facies occurs as large twinned patches, slightly turbid, with locally developed zoning, whereas K-feldspar in the monzogranite lacks zoning, is usually turbid, often has developed tiny albite crystals and small quartz grains along the twin

plane or along the contact of K-feldspar crystals, and locally develop granophyric intergrowth when in contact with quartz.

3. Biotite is the predominant mafic mineral in both facies and forms large clusters of flakes in the rocks of the inner facies but occurs as small intensively chloritized flakes in the rocks of the outer facies.

4. Among the common accessory minerals, sphene, allanite, apatite, zircon, and magnetite occur in the rocks of both facies. Sphene often forms clusters of large wedge-shaped crystals in the inner facies but occurs as small discrete crystals in the rocks of the outer facies. All of these accessory minerals are associated with biotite.

3.5 Chemical characteristics

3.5.1 Major elements

The analysed samples from the Mae-Salit Pluton show a range of SiO_2 values varying from 69-75 wt.% when plotted on Fe-(Na + K)-Mg and Ca-Na-K ternary diagrams (Fig. 3.5.1a). They show that Fe, Mg and Ca decrease while (Na + K) increases from the rocks of the inner facies towards the outer facies (see also Table 3.5.1).

Consideration of the ternary plots of Q-Ab-Or and An-Ab-Or (Fig. 3.5.1b) show that normative quartz and orthoclase increase at the expense of albite (Fig. 3.5.1b-i) and anorthite decreases as orthoclase increases (Fig. 3.5.1b-ii), from the rocks of the inner facies towards the outer facies (see petrographic section 3.4). In brief, all the diagrams show good trends in major elements which indicate progressive changes in chemical characteristics from the inner part of the pluton towards the outer part of the pluton.

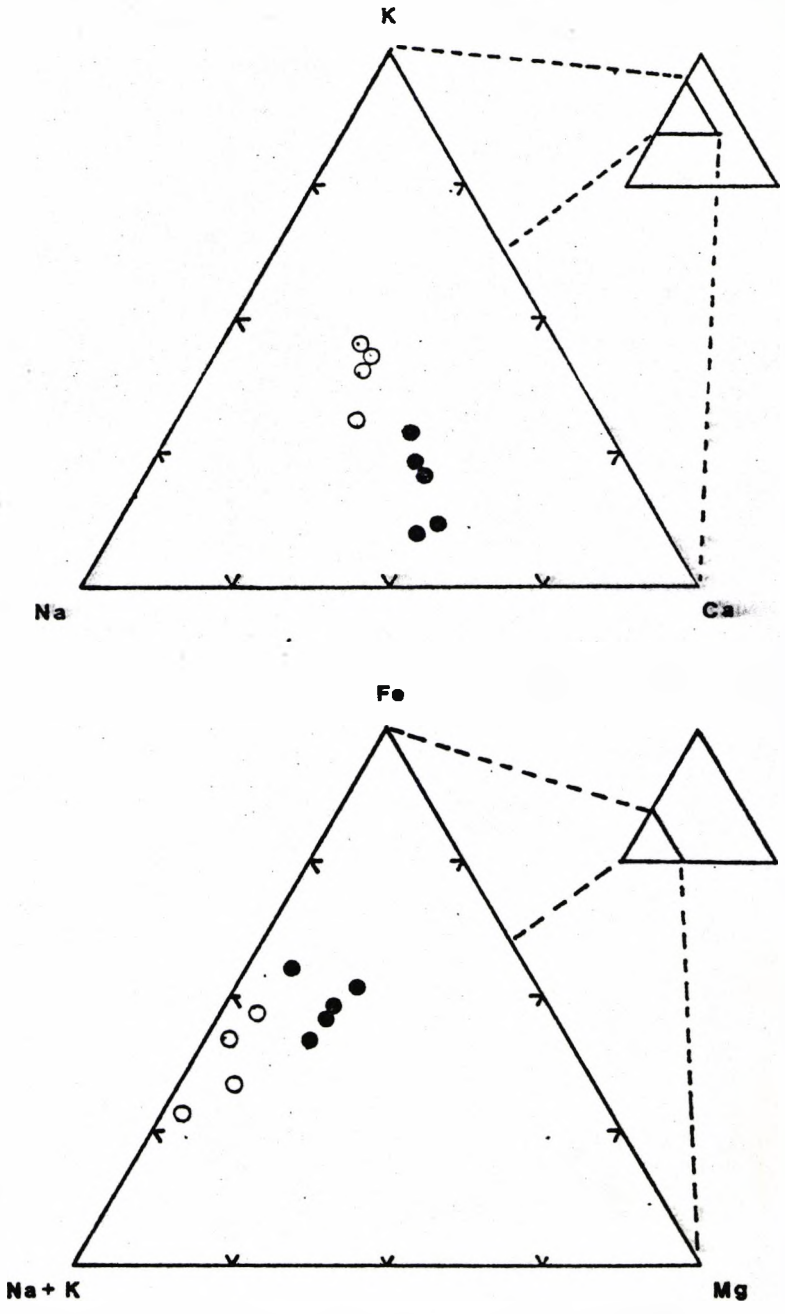

Figure 3.5.1a Triangular plots of the plutonic rocks of the Mae-Salit Pluton.
solid circles - inner facies - monzogranite
open circles - outer facies - monzogranite

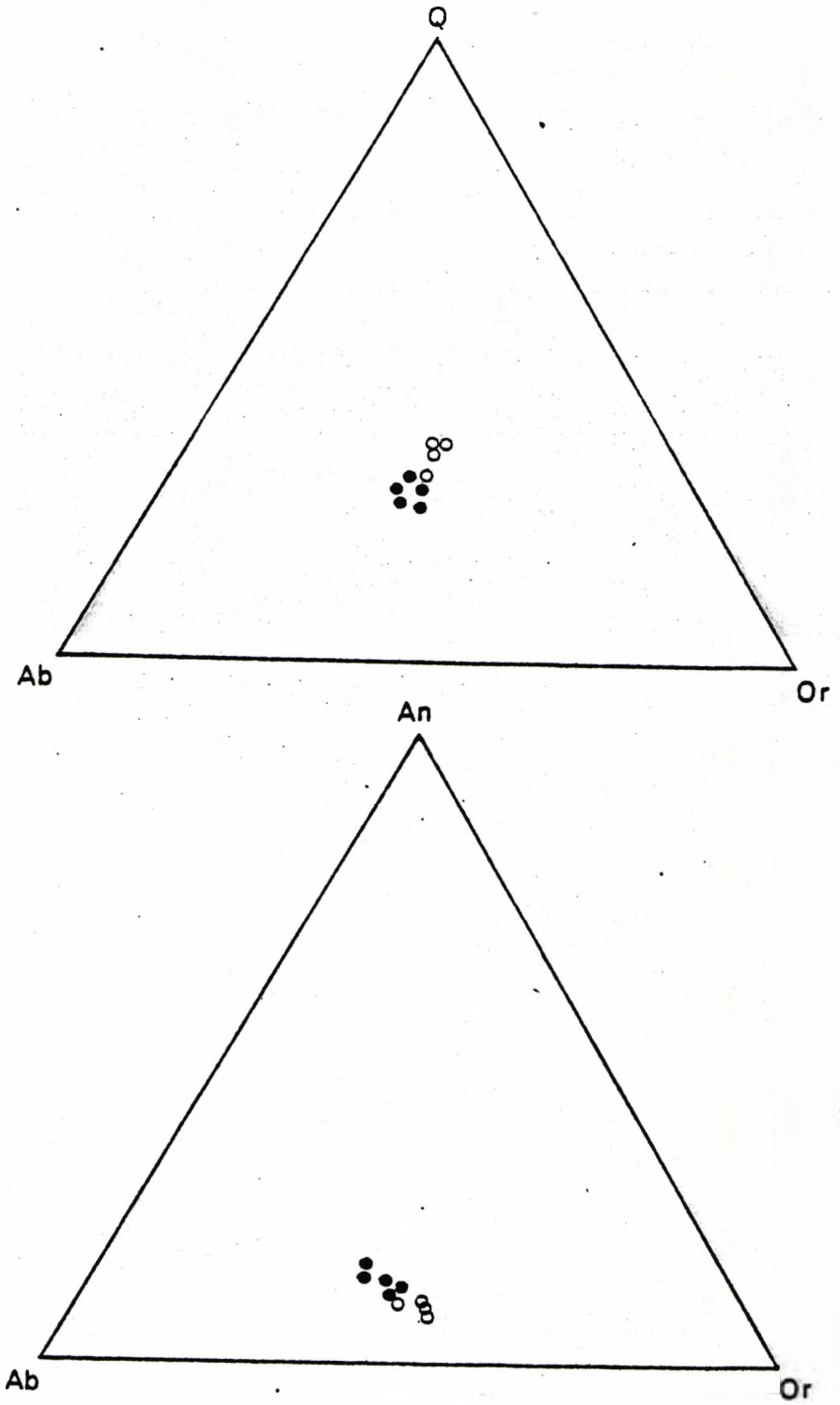

Figure 3.5.1b Triangular plots of the plutonic rocks of the Mae-Salit Pluton.
solid circles - inner facies - monzogranite
open circles - outer facies - monzogranite
(calculated from C.I.P.W. norms in Table 3.5.2)

TABLE 3.5.1

Analyses of the rocks from the Mae-Salit Pluton

	inner facies				
Sample	T11	CTK7	T48A	CTK25	CTK26
SiO_2	68.75	69.55	69.92	68.59	69.41
TiO_2	0.36	0.35	0.31	0.35	0.34
Al_2O_3	15.39	15.11	14.92	15.21	15.41
Fe_2O_3	1.15	1.20	0.95	0.93	1.33
FeO	1.05	1.14	1.11	1.93	0.85
MnO	0.07	0.07	0.07	0.08	0.07
MgO	1.05	0.97	0.89	0.47	0.95
CaO	2.36	2.04	2.00	1.86	2.29
Na_2O	4.09	3.70	3.81	3.83	4.05
K_2O	4.39	4.70	4.80	5.38	4.35
P_2O_5	0.12	0.13	0.10	0.12	0.12
Ba	1392	1218	1262	1145	1270
Ce	84	92	79	100	70
Co	135	58	59	91	136
Cr	9	11	9	4	7
La	57	59	54	67	46
Nb	33	37	48	17	40
Ni	6	0	0	0	0
Pb	193	57	206	219	198
Rb	178	221	205	249	187
Sc	3	3	2	4	0
Sr	320	284	282	205	315
Th	228	49	243	263	74
Ti	2250	2302	1931	2070	2096
U	-	-	-	-	-
V	32	31	27	12	27
Y	26	22	27	25	25
Zn	30	29	29	45	36
Zr	204	178	185	241	213

TABLE 3.5.1
(continued)

	outer facies			
Sample	CTK22	CTK63	CTK2	CTK44
SiO_2	70.51	73.83	74.39	74.97
TiO_2	0.24	0.18	0.12	0.12
Al_2O_3	14.75	13.20	13.70	13.08
Fe_2O_3	1.23	0.81	0.39	0.81
FeO	1.06	1.12	0.74	0.32
MnO	0.22	0.05	0.03	0.05
MgO	0.38	0.22	0.20	0.28
CaO	1.45	1.11	1.11	1.07
Na_2O	3.97	3.56	3.48	3.40
K_2O	5.22	5.15	5.24	5.37
P_2O_5	0.06	0.04	0.02	0.02
Ba	362	618	426	145
Ce	114	81	37	37
Co	114	106	162	128
Cr	8	8	8	12
La	68	47	16	25
Nb	51	34	22	17
Ni	5	4	6	5
Pb	61	55	60	103
Rb	237	236	234	412
Sc	1	1	2	1
Sr	137	107	138	100
Th	102	67	54	54
Ti	1331	1052	664	652
U	15	-	-	-
V	11	6	5	8
Y	20	20	14	8
Zn	29	28	7	14
Zr	237	163	57	117

TABLE 3.5.2

C.I.P.W. norms of the rocks from the Mae-Salit Pluton

	inner facies				
Sample	T11	CTK7	T48A	CTK25	CTK26
Q	21.70	24.80	23.95	20.31	22.95
Or	25.94	27.78	28.22	31.80	25.71
Ab	34.60	31.30	32.24	32.40	34.26
An	10.67	8.10	9.27	8.43	10.58
Le	-	-	-	-	-
Ne	-	-	-	-	-
C	-	0.98	0.06	-	0.16
Ac	-	-	-	-	-
DiCa	0.10	-	-	0.01	-
DiMg	0.08	-	-	-	-
DiFe	0.02	-	-	0.01	-
Wo	-	-	-	-	-
HyMg	2.54	2.42	2.22	1.17	2.34
HyFe	0.50	0.65	0.23	2.34	0.03
OlMg	-	-	-	-	-
OlFe	-	-	-	-	-
Mt	1.67	1.74	1.76	1.35	1.93
He	-	-	-	-	-
Il	0.68	0.66	0.59	0.66	0.65
Ap	0.28	0.22	0.23	0.28	0.28

TABLE 3.5.2

(continued)

	outer facies			
Sample	CTK22	CTK63	CTK2	CTK44
Q	23.73	31.70	31.32	32.24
Or	31.15	30.61	31.15	31.91
Ab	33.84	28.60	29.53	28.93
An	6.85	5.25	5.33	4.56
Le	-	-	-	-
Ne	-	-	-	-
C	0.09	0.19	0.37	-
Ac	-	-	-	-
DiCa	-	-	-	0.28
DiMg	-	-	-	0.24
DiFe	-	-	-	-
Wo	-	-	-	-
HyMg	0.95	0.57	0.50	0.46
HyFe	1.01	1.09	0.83	-
OlMg	-	-	-	-
OlFe	-	-	-	-
Mt	1.78	1.38	0.68	0.85
He	-	-	-	0.27
Il	0.46	0.34	0.23	0.23
Ap	0.14	0.09	0.05	0.05

3.5.2 Trace elements

Cobalt, Chromium and Nickel

The Co, Cr and Ni contents in the rocks of the Mae-Salit Pluton show erratic variation with little or no change with DI (Fig. 3.5.2a). Co varies between 58 ppm and 162 ppm, Cr varies between 4 ppm and 12 ppm and Ni varies between 4 ppm and 6 ppm, (three analysed samples for the rocks of the inner facies have Ni contents below detection limit). These variations are contradictory to the normal trends of Co, Cr and Ni, which usually decrease as differentiation increases. This abnormal behaviour of Co, Cr, Ni has been explained by Ringwood (1955b).

Thus acid magmas, rich in volatiles can cause the enrichment of these elements in the late differentiated rocks. This is due to the electron characteristics of Co, Cr and Ni which have ionic potentials intermediate between those of "network formers" and "network modifiers" (see Ringwood, 1955) and have a tendency to form tetrahedral complexes with anions ($OH^{-1} + O^{-2} + F^{-1}$) in volatile rich magmas. The large size of these tetrahedral complexes are not accepted into silicate minerals and are therefore concentrated in the residual magma. This seems to be the case in the Mae-Salit Pluton as indicated by the granophyric texture in the rocks of the outer facies (see section 3.4). Since Co, Cr and Ni contents in the rocks of the Mae-Salit Pluton do not show sympathetic relations with the decrease of mafic minerals from the rocks in the inner facies to the outer facies (see modal data table 3.4.1), these elements behave incompatibly in this pluton.

Lanthanum, Cerium and Neodymium

La varies between 68 ppm and 16 ppm, Ce varies between 114 ppm and 37 ppm and Nd varies between 51 ppm and 17 ppm in the rocks of the Mae-Salit Pluton; all elements show a negative correlation with DI in the outer facies rocks only. The inner facies shows slight positive correlations with DI (Fig. 3.5.2a).

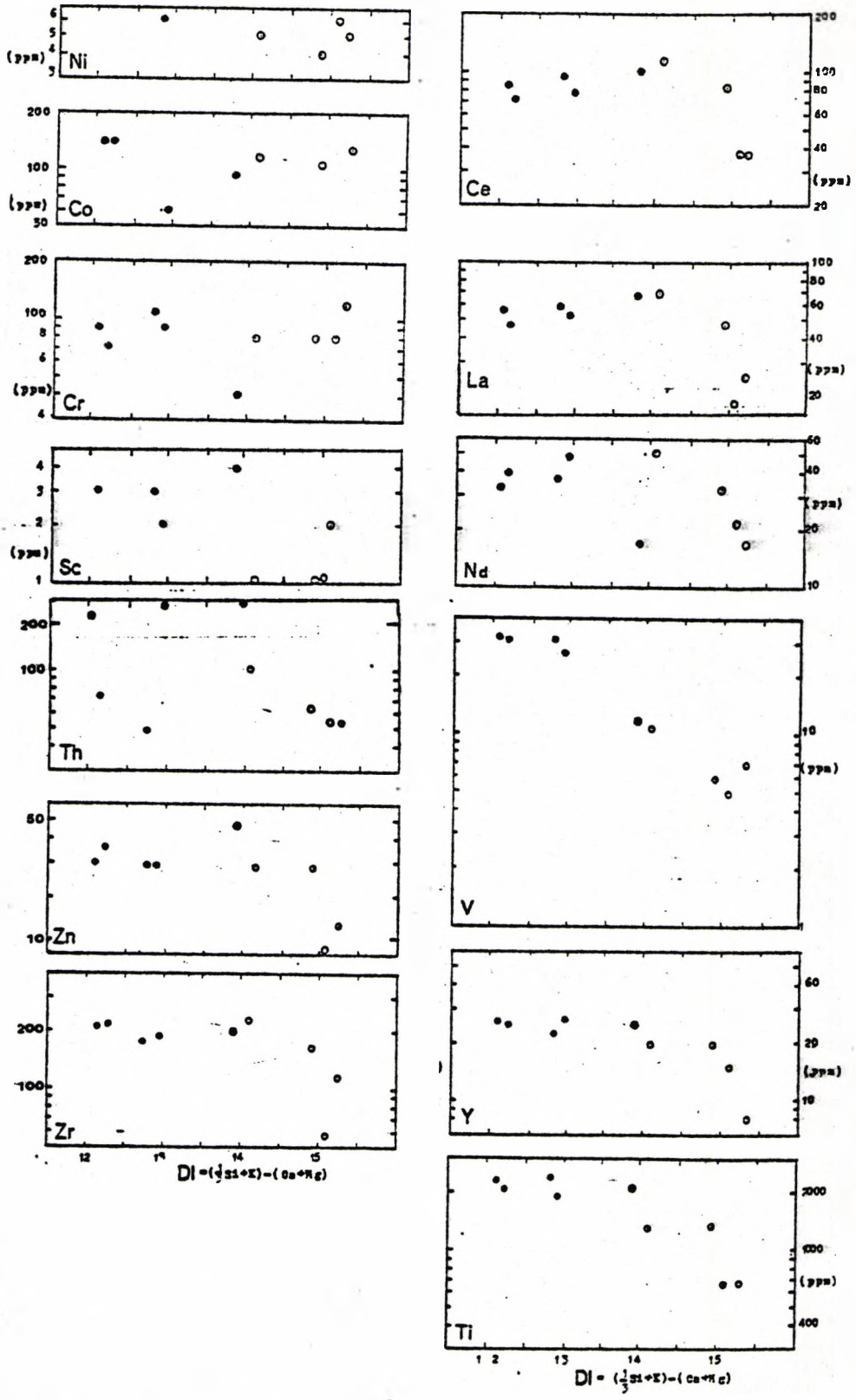

Figure 3.5.2a Plots of trace element content vs. Differentian Index for the plutonic rocks of the Mae-Salit Pluton.
solid circles - inner facies - monzogranite
open circles - outer facies - monzogranite

Accessory minerals, viz. sphene, allanite xenotime, monazite, zircon and apatite are the main sources of La, Ce and Nd in granitic rocks (Condie, 1978). The fractionation of these accessory minerals will deplete these LREE in the liquid. Sphene, allanite, apatite and zircon are distinctively abundant in the rocks of the Mae-Salit Pluton and are usually associated with mafic minerals (see section 3.4). The decrease of LREE concentration with the increasing DI from the rocks in the inner facies to the outer facies may be related to the crystallization of LREE-bearing accessory minerals, particularly in the outer facies. It may also relate to the crystallisation of hornblende which in acid rocks has K_D values greater than 1.0 (Hanson, 1980). Thus, in this pluton, the LREE behave compatibly in the outer facies, but may show slight incompatibility during crystallization of the inner facies.

Lead

The Pb content in the Mae-Salit Pluton varies from 219 to 57 ppm in the inner facies and from 103 to 55 ppm in the outer facies and shows an overall tendency to decrease as the differentiation increases (Fig. 3.5.2b). These values are distinctively higher than those reported by Turekian and Wedepohl (1961) for low calcium granites (19 ppm) and correlate with the high values of Th.

Zinc

Zn varies from 45 ppm to 7 ppm in the rocks of the inner facies to the rocks of the outer facies and shows negative correlation with DI (Fig. 3.5.2a), again the decrease occurs mainly in the outer facies.

The ionic radii of Zn^{+2} and Fe^{+2} are similar (0.74Å), and thus Zn has a tendency to be incorporated in minerals containing ferrous iron. The decrease of Zn with the increase of DI from the rocks in the inner facies to the outer facies may be related to the decrease of mafic minerals

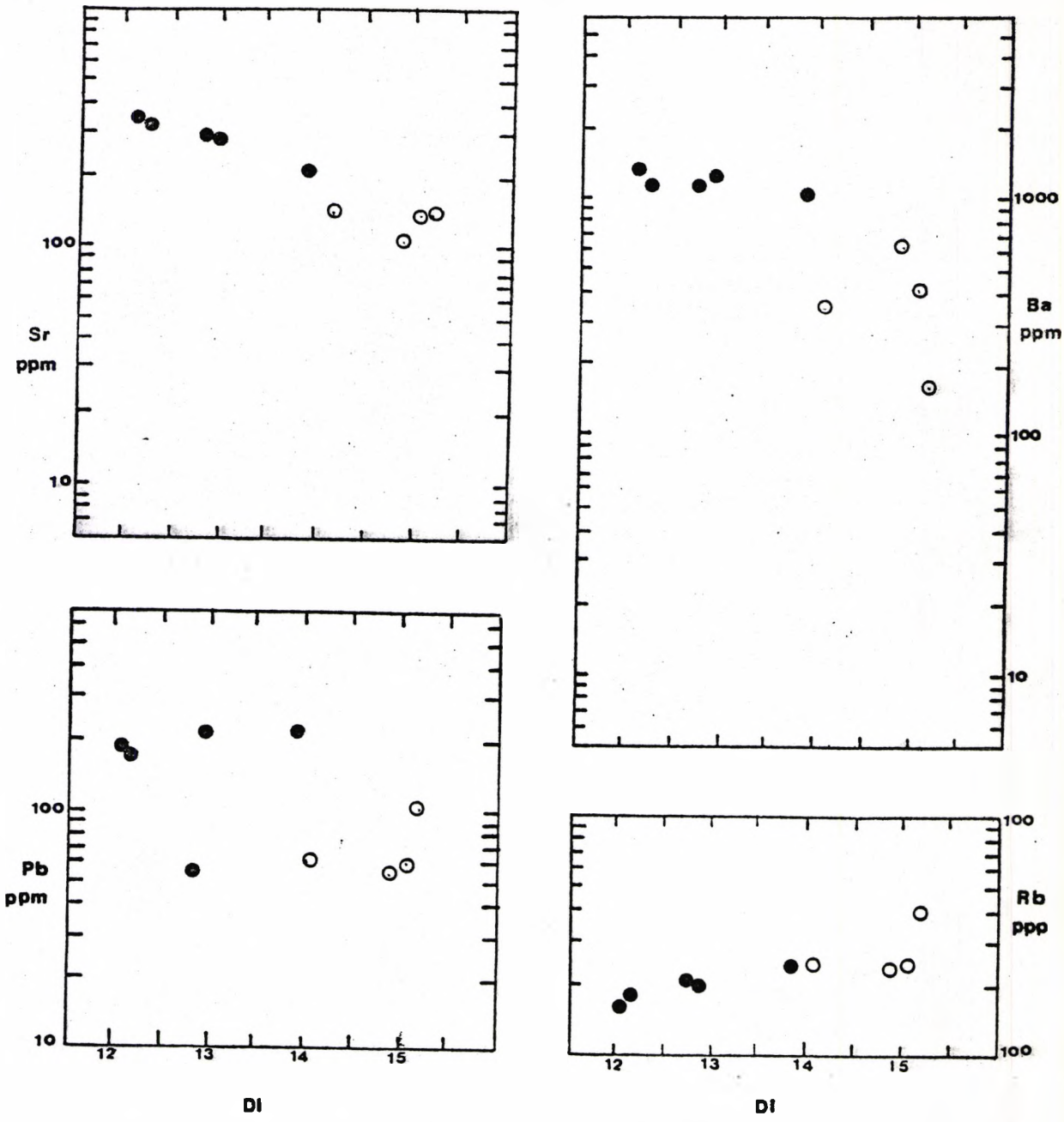

Figure 3.5.2b Plots of trace element content vs. Differentian Index for the plutonic rocks of the Mae-Salit Pluton.
solid circles - inner facies - monzogranite
open circles - outer facies - monzogranite

(petrography section, 3.4). Thus Zn shows compatible behaviour in this pluton, particularly in the outer facies.

Scandium and Vanadium

Sc varies from 4 ppm to 1 ppm, and V varies from 32 ppm to 5 ppm in the rocks of the pluton and they show negative correlations with DI (Fig. 3.5.2a). During fractionation Sc^{+3} (radius = 0.81Å) and V^{+3} (radius = 0.74Å) preferentially enter ferromagnesian minerals, occupying the Mg^{+2} (radius = 0.66Å), and Fe^{+2} (radius = 0.74Å) or Fe^{+3} (radius = 0.64Å) sites, thereby becoming depleted in the liquid. Both Sc and V are strongly concentrated in hornblende (Ewart and Taylor, 1969). Magnetite and ilmenite ore also contain abundant V (Wager and Mitchell, 1951). The concentration of V in the Mae-Salit pluton much resembles the average (44 ppm) for the low calcium granite of Turekian and Wedepohl (1961). The decrease of Sc and V in the Mae-Salit pluton as the differentiation increases from the rocks in the inner facies to the outer facies may be related to the decrease of hornblende (see modal data table 3.4) as well as magnetite which is commonly associated with the ferromagnesian minerals. Therefore, the variation of Sc and V emphasises the compatible behaviour of these elements in this pluton.

Thorium

The Th contents in the rocks of the Mae-Salit Pluton vary between 263 ppm to 49 ppm in the rocks of the inner facies and 102 ppm to 54 ppm in the rocks of the outer facies. The high values of Th in the rocks of the inner facies correlate with the high values of Pb. The Th contents in the outer facies are much the same as in the biotite granite of the White Mountain Series; North America (65 - 98 ppm Th, with K 4.00%, Rogers and Ragland, 1961). The Th value of average granite with a K content 3.47% is 17.36 ppm (Heier and Rogers, 1963). The anomalous high

Th values in this granite can be related to the presence of sphene and allanite (Ragland et al., 1967, and see section 3.4).

Titanium and Zirconium

Ti varies from 2302 ppm to 664 ppm and Zr varies from 237 ppm to 57 ppm in the rocks of the inner facies to the rocks of the outer facies and both of these variations show a crude negative correlation with DI (Fig. 3.5.2a), although the values of both elements in the inner facies are constant.

The plot of Ti versus Zr (Fig. 3.5.2c), shows a decrease of both Ti and Zr from the inner facies to the outer facies. The mineral vector and data indicate that fractionation of some combination of biotite, hornblende $\pm$ magnetite $\pm$ zircon could cause the depletion of Ti and Zr shown.

Both hornblende and biotite show a decrease from the inner facies to the outer facies (see modal data table 3.4.1), and zircon is commonly present as inclusions in biotite (see section 3.4). It would appear therefore that these minerals are responsible for the trend and that Ti and Zr behave compatibly in this pluton.

Yttrium

Y varies from 27 ppm to 8 ppm in the rocks of the inner facies to the rocks in the outer facies and shows a negative correlation with DI (Fig. 3.5.2a). Again the inner facies shows little variation when Y is plotted against CaO (Fig. 3.5.2d), a stunted J-type trend, similar to that of Lambert and Holland (1974) is seen.

They show that, at low CaO levels, the decrease of Y as CaO decreases may be due to the fractionation of hornblende $\pm$ apatite $\pm$ sphene. The rocks of the Mae-Salit Pluton decrease in hornblende abundance from the inner facies to the outer facies (see modal data table 3.4.1), and these

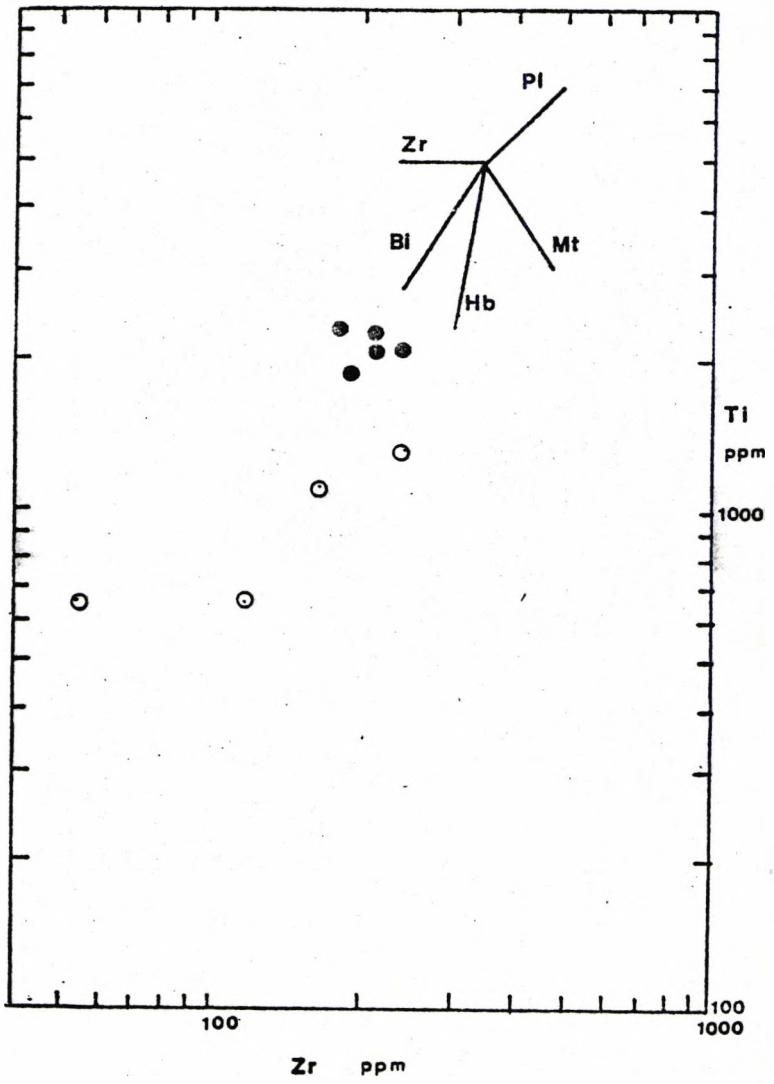

Figure 3.5.2c Plot of Ti vs. Zr for the plutonic rocks of the Mae-Salit Pluton.
solid circles - inner facies - monzogranite
open circles - outer facies - monzogranite
Mineral vectors shown are taken from Pearce and Narry (1979), and indicate the relative change in these elements upon extraction of each mineral.
Bi = biotite; Hb = hornblende; Mt = magnetite;
Pl = plagioclase; Zr = zircon.

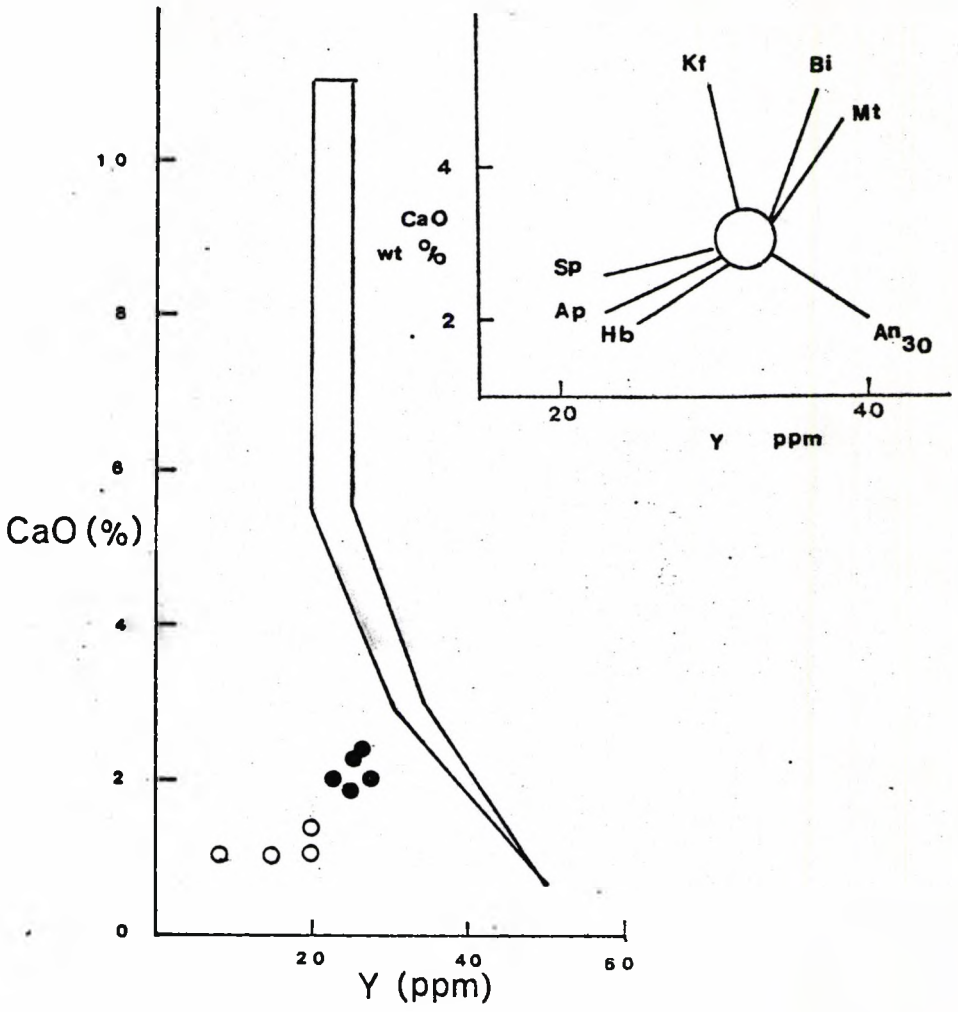

Figure 3.5.2d Plot of CaO vs. Y for the plutonic rocks of the Mae-Salit Pluton.
solid circles - inner facies - monzogranite
open circles - outer facies - monzogranite
Enclosed area represents "standard Calc-alkali trend"
inset shows "liquid fractionation trends" for minerals (after Lambert and Holland, 1974).
Sp = sphene; Ap = apatite; Hb = hornblende;
An_{30} = plagioclase of anorthite 30%; Mt = magnetite;
Bi = biotite; Kf = K-feldspar.

rocks also contain distinctive sphene and apatite (see section 3.4). Therefore, Y behaves compatibly in this pluton, being extracted from the liquid by a combination of these three minerals.

Rubidium, Strontium and Barrium

Rb contents in the rocks of the Mae-Salit Pluton vary from 178 ppm to 412 ppm in the rocks of the inner facies to the rocks of the outer facies and shows a positive correlation with DI (Fig. 3.5.2b).

Sr contents vary from 320 ppm to 100 ppm and Ba contents vary from 1392 ppm to 145 ppm, in the rocks of the inner facies to the rocks of the outer facies. These variations show negative correlations with DI (Fig. 3.5.2b). This incompatible and compatible behaviour respectively is characteristic of these elements in acid rocks. It is related to the crystallization of K-feldspar and biotite versus plagioclase, as discussed earlier.

Ba - Sr diagram

The plot of Ba versus Sr (Fig. 3.5.2e), shows that both Ba and Sr contents decrease from the rocks in the inner facies to the rocks of the outer facies of the Mae-Salit Pluton. The mineral fractionation vectors indicate that plagioclase ($\pm$ K feldspar) and biotite can cause the depletion as seen here. Ba^{+2} (radius = 1.34Å) is preferentially incorporated into biotite by substitution for K^{+} (radius = 1.33Å), the closely similar size of Sr^{+2} (radius = 1.18Å) and Ca^{+2} (radius = 1.02Å) enables Sr to be incorporated in plagioclase and hornblende by substitution for Ca. The extraction of Ba and Sr by K feldspar during fractionation seems very unlikely as it is the last mineral to crystallise and physical separation is difficult to visualise.

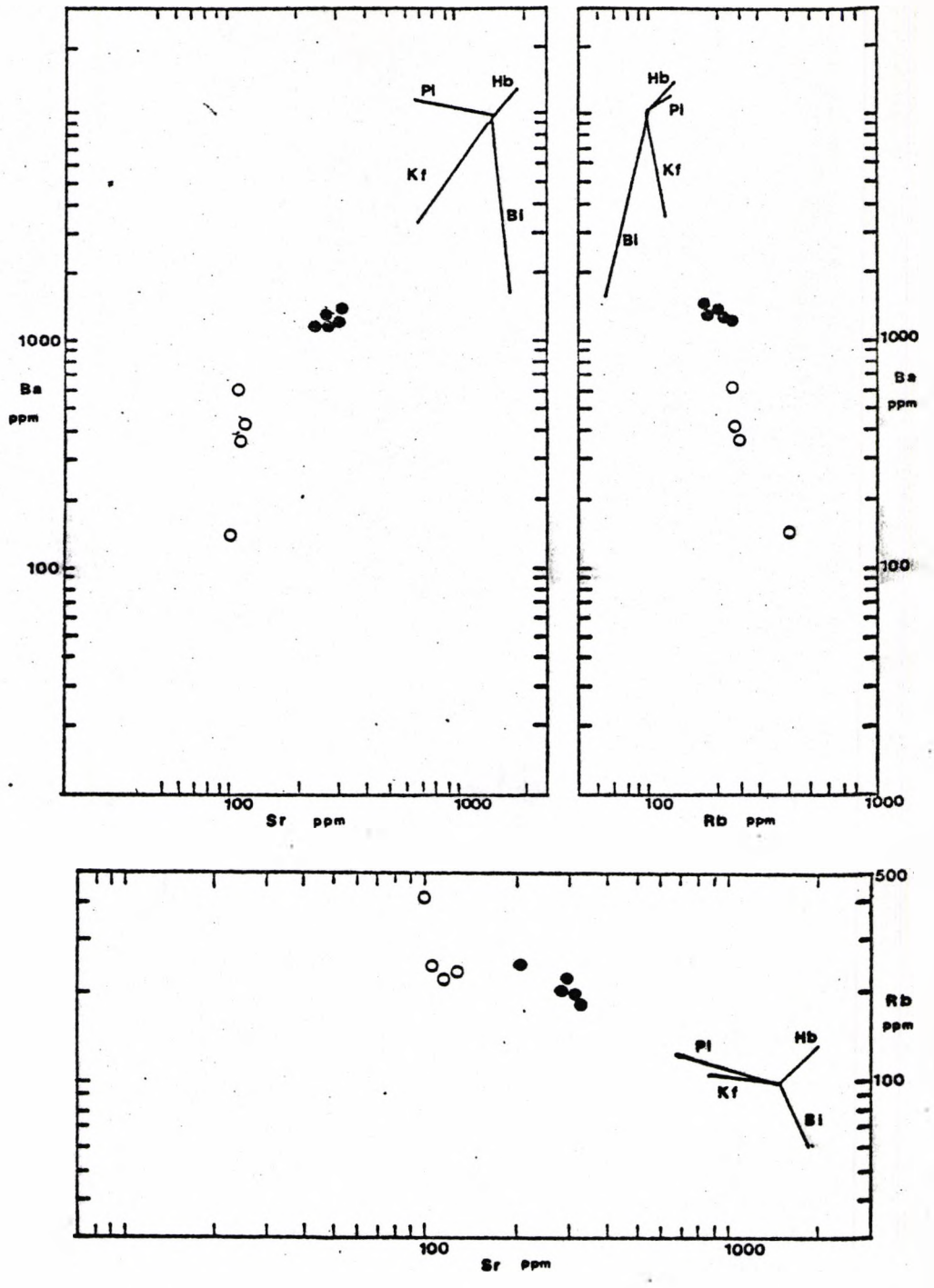

Figure 3.5.2e Plots of Rb, Sr, Ba for the plutonic rocks of the Mae-Salit Pluton.
solid circles - inner facies - monzogranite
open circles - outer facies - monzogranite
Mineral vectors calculated from the distribution co-efficients for acid plutonic rocks (Table 14.1 from Cox et al, 1979). Length of vector indicates 20% fractionation of mineral Kf = K-feldspar; Bi = biotite; Hb = hornblende; Pl = plagioclase.

Ba - Rb diagram

The plots of Ba versus Rb (Fig. 3.5.2e), show a clear trend, with the inner facies here and in the other diagrams, showing a coherent grouping. The mineral vectors indicate that fractionation of plagioclase plus hornblende, and even K-feldspar could deplete Ba and enrich Rb in the liquid. Ba^{+2} (radius = 1.34Å) is preferentially incorporated into biotite and K-feldspar by direct substitution for K^{+1} (radius = 1.33Å), and becomes depleted in the liquid. The larger size of Rb^{+1} (radius = 1.47Å) makes it difficult for Rb to substitute for K in biotite or incorporated into plagioclase and hornblende by substitution for Ca^{+2} (radius = 1.02Å). It therefore becomes enriched in the liquid. The fractionation is compatible with the early precipitation of plagioclase + hornblende as noted in the petrography section.

Rb-Sr diagram

The plot of Rb versus Sr is shown in Fig. 3.5.2e and the mineral vectors indicate that plagioclase ($\pm$ K-feldspar) and hornblende can cause enrichment of Rb and depletion of Sr in the liquid during fractional crystallisation. These relationships are due to the compatible nature of Sr^{+2} (radius = 1.18Å) with plagioclase and hornblende by substitution for Ca^{+2} (radius = 1.02Å), whereas Rb^{+1} (radius = 1.47Å) is incompatible with respect to plagioclase and hornblende, and is preferentially incorporated into K-feldspar. Again these trends emphasise the importance of plagioclase, hornblende and K-feldspar precipitation in the evolution of these rocks.

Summary

The important chemical characteristics of the rocks in the Mae-Salit Pluton are as follows:

1. The decrease of Sr and Ba with the increase of Rb contents from the

rocks in the inner facies to the outer facies reflect the fractionation of plagioclase, hornblende and biotite.

2. The decrease of Y, Ti and Zr contents from the rocks in the inner facies towards the outer facies reflect the fractionation of sphene, apatite, zircon, hornblende, biotite and magnetite.

3. The decrease of La, Ce and Nd from the rocks in the inner facies towards the rock in the outer facies as differentiation increases may indicate the fractionation of LREE-bearing accessory minerals, especially sphene and allanite but hornblende extraction also may be important.

4. The anomalous high Pb values in the rocks of the Mae-Salit Pluton may be related to the high values ofTh and both are apparently related to the distinctive abundance of thorium-bearing accessory minerals, viz. sphene, allanite.

5. Co, Cr and Ni in the rocks of the Mae-Salit Pluton show incompatible characteristics which may be due to the nature of crystallisation of an acid magma rich in volatiles.

6. Sc and V show compatible characteristics in this pluton, presumable being extracted by the ferromagnesian silicates, particularly hornblende.

7. Finally, the overall chemical characteristic of the Mae-Salit Pluton suggest fractional crystallisation of plagioclase + hornblende + biotite and accessory minerals sphene, allanite, apatite, zircon and magnetite may be responsible for the variation in the rocks in the inner facies towards the rocks in the outer facies.

CHAPTER 4

THE WESTERN MAIN RANGE PLUTON

4.1 Introduction

The Western Main Range Pluton is situated on the western flank of the Tak Batholith and covers an area of approximately 950 sq. km. It is a roughly elongated body, forming the main high topographic range, and it has a N-S trend (Fig. 1.2.1).

The pluton cuts the western part of the Eastern Pluton and is itself cut by the later Mae-Salit and Tak Plutons on its western and southern peripheries respectively.

Detailed studies of the granitic rocks in this pluton have not previously been made, except for a short report on their chemistry (Pongsapitch and Mahawat, 1977) and reconnaissance mapping on a scale of 1:250,000 (Piyasin, 1974; Bunopas, 1974).

4.2 The components of the pluton

The Western Main Range Pluton is a crudely zoned pluton which is composed mainly of monzonite and monzogranite (Fig. 4.2.1). Leucogranite and porphyritic rock occur locally around the periphery of the pluton together with pegmatite dykes and felsite. Several small exposures of appinitic rocks crop out throughout the mapped pluton.

Among the major rock units, monzonite outcrops extensively in the central part of the mapped area and forms over 60% of the pluton. Monzogranite crops out marginally, especially near the northern and southern edges of the pluton, and it forms approximately 30% of the pluton's outcrop area. The boundary between the monzonite and the monzogranite has not been established accurately, due to the poor nature of the exposure, but it is considered that the contact may well be gradational.

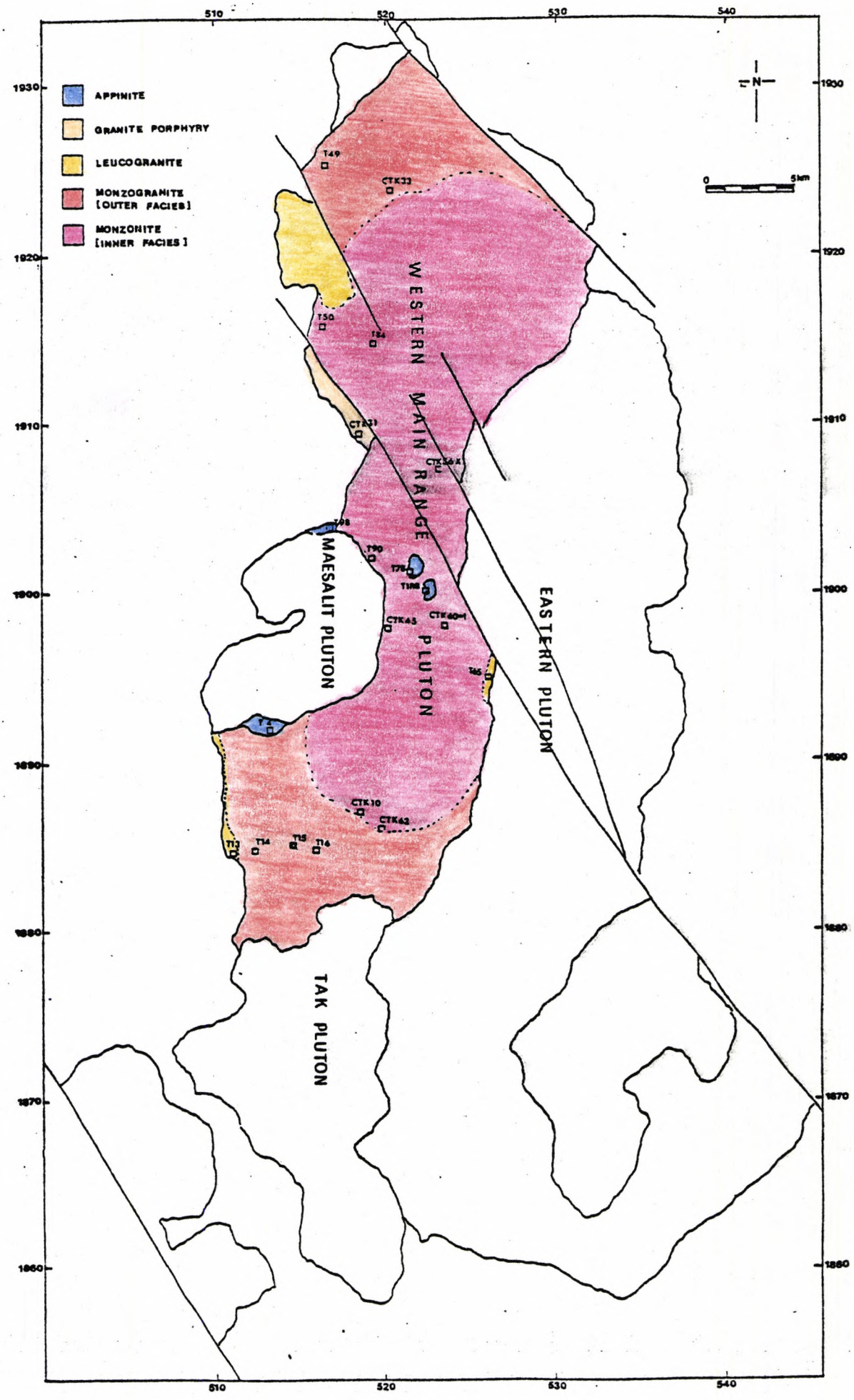

Figure 4.2.1 Outcrop map of the Tak Batholith, showing the different facies and sample localities of the Western Main Range Pluton.

The terms inner facies and outer facies are used to represent the monzonite in the inner part and the monzogranite in the outer part of the pluton respectively.

Among the minor acid intrusive rocks, leucogranite is the predominant rock type. A small outcrop of granite porphyry is exposed in one location (grid ref: 5190 19110). Feldspathic pegmatite is less common than quartz dykes and felsites. All of these occur as late intrusions which cut the monzogranite along the periphery of the pluton.

Several small exposures of appinitic rocks related to the Western Main Range Pluton are also present (Fig. 4.2.1). The relationship between the appinites and the granitic rocks will be discussed in the following section.

4.3 Field relationships

The Western Main Range Pluton is not often in contact with stratified country rocks, since most of the pluton's contacts are either with the granitic rocks of the adjacent composite pluton or are concealed under alluvium. Part of the contact with the Permo-Triassic volcanics at the northern margin of the pluton is faulted and is obscured by minor intrusive leucogranite, quartz dykes and pegmatitic dykes.

The Western Main Range Pluton intrudes into the eastern part of the Eastern Pluton and displaces the northern tip of the latter (see map Fig. 4.2..1). The Western Main Range Pluton is also cut by the Mae-Salit Pluton on its eastern side and by the Tak Pluton on its southern margin.

The relationship of the appinites with the granitic rocks of the Western Main Range Pluton can be broadly recognised as appinitic rafts and appinitic dykes.

Plate 4.3.1. Rounded appinitic xenoliths (one arrowed) in the granitic rocks of the Western Main Range Pluton.

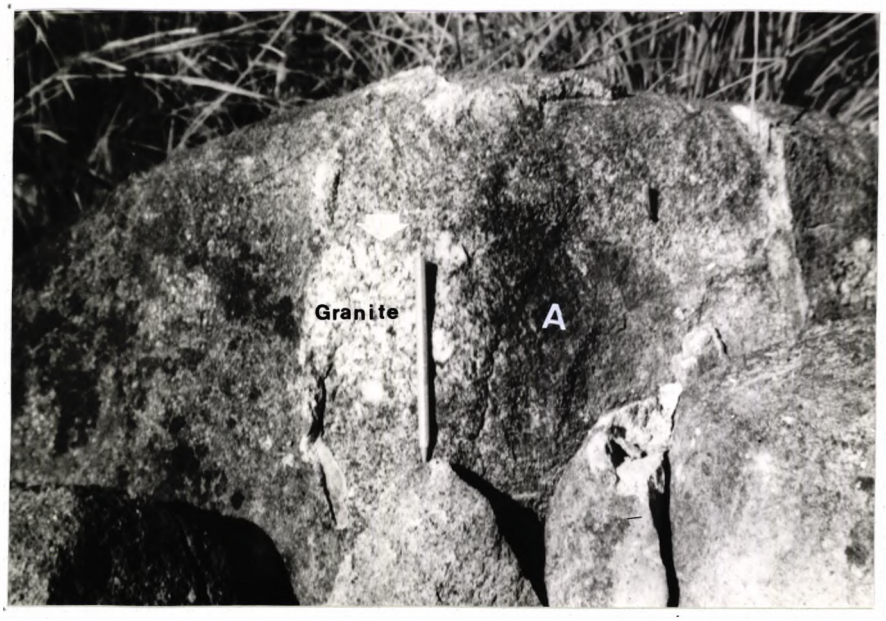

Plate 4.3.2. Enclaves of the granitic rock of the Western Main Range Pluton in the appinitic dyke[A].

The appinitic rafts occur as small bodies (50-100 m. in diameter) within the monzonite (inner facies). Numerous small angular appinitic xenoliths occur within the monzogranite adjacent to the appinite rafts. This feature indicates that the appinitic bodies may have formed from basic rafts which were incorporated within the granitic magma during the emplacement of the pluton. The clusters of rounded appinitic xenoliths in the granite (Plate 4.3.1) may have been formed by eruption of mafic magma as pillows into a acid magma reservoir, as suggested by Blake et al (1966) and Spark et al (1977). The appinitic rafts and xenoliths enclosed within the granite will be referred to in this thesis as the "older appinites".

Some of the appinitic rocks occur as dykes and bosses, and show sharp intrusive contacts with the monzonite or monzogranite. Enclaves of coarse-grained monzonite within the appinitic dykes occur where these rocks are in contact (Fig. 4.3.2). The appinitic dykes will be referred to in this thesis as "younger appinites".

4.4 Petrography

The monzonite (inner facies) occurs as a pinkish, coarse-grained equigranular rock containing large plagioclase and K-feldspar megacrysts and appreciable amounts of large stubby hornblende and biotite. Small resinous brown sphene crystals are commonly present. A plot showing the relative proportions of modal quartz-alkali feldspar-plagioclase is shown in Fig. 4.4.1.

Plagioclase (An_{10-25}) occurs both as clusters of large euhedral to subhedral crystals, and as small discrete crystals. Large plagioclase crystals generally show weakly developed oscillatory zoning and myrmekitic margins when in contact with K-feldspar. Small plagioclase phenocrysts are often poikilitically enclosed by K-feldspar. K-feldspar is microcline perthite and occurs as large twinned subhedral to anhedral

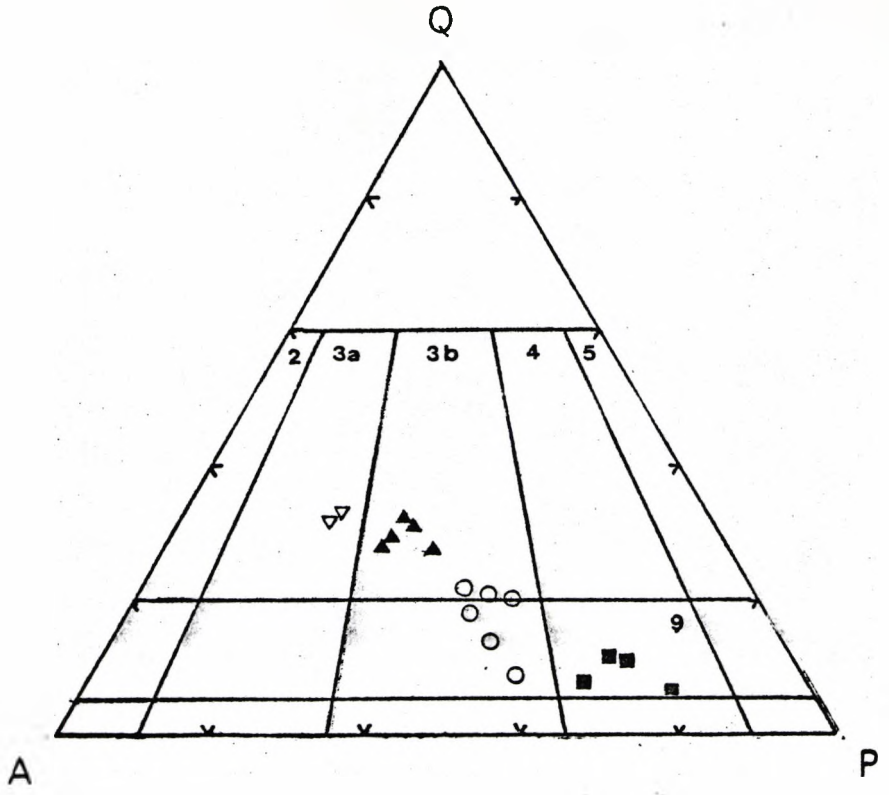

Figure 4.4.1 Classification of the Plutonic rocks of the Western Main Range Pluton (following Streckeisen, 1976) symbols as follows:-
open circles - inner facies - monzonite
solid triangles - outer facies - monzogranite
open triangles - leucogranite
solid square - appinite
(calculated from modes in Table 4.4.1).

TABLE 4.4.1

Modes of the rocks from the Western Main Range Pluton

	inner facies					
	CTK45	CTK60-1	T84	T50	T90	CTK56x
plagioclase	48.58	41.00	41.16	40.70	38.80	40.50
k-feldspar	32.90	33.75	31.54	32.30	34.10	33.60
quartz	8.43	17.43	19.31	20.65	20.60	18.85
hornblende	4.20	3.08	3.61	2.20	2.70	2.60
biotite	4.88	4.05	3.46	3.40	2.25	3.40
others	1.01	0.69	0.92	0.75	1.55	1.05

	outer facies						
	CTK10	T14	T15	T16	CTK33	T49	CTK62
plagioclase	25.69	26.00	26.60	25.47	24.41	23.66	26.44
k-feldspar	42.87	37.90	40.60	38.67	45.29	48.94	40.63
quartz	28.00	31.00	29.50	30.79	25.80	23.62	27.71
hornblende	0.50	0.30	0.25	0.67	L.71	0.33	1.26
biotite	2.25	2.90	2.50	2.90	3.73	2.88	3.17
others	0.69	1.90	0.55	1.50	0.86	0.57	0.79

	leucogranite		appinite			
	T65	T13	T18b	T4	T98	T78
plagioclase	19.10	20.05	44.50	40.43	41.50	37.10
k-feldspar	47.83	46.48	10.20	12.46	16.90	13.50
quartz	31.93	32.94	4.10	7.53	6.50	9.80
hornblende	0.05	-	34.70	34.10	29.40	33.40
biotite	0.68	0.33	4.10	3.11	2.70	4.60
others	0.41	0.20	2.40	2.37	3.00	1.60

*porphyry (CTK31) contains mineral proportions of 19.85% plagioclase, 20.00% k-feldspar, 8.00% quartz, 0.80% hornblende, 3.10% biotite, 0.60% accessory minerals and 47.65% groundmass.

crystals which poikilitically enclosed other minerals. Quartz occurs both as large anhedral patches and as aggregates of small grains which are interstitial to other minerals.

Hornblende (x = pale green, y = z = dark green), forms euhedral to subhedral crystals, mostly twinned and is partially altered to chlorite or replaced by biotite. Hornblende shows well developed cleavages and lacks any pyroxene cores. Biotite (x = brown, y = z = greenish brown) occurs as clusters of flakes in association with hornblende and it is commonly partially altered to chlorite.

Among the accessory minerals, sphene commonly forms aggregates of well-formed wedge-shaped crystals associated with biotite and hornblende (Plate 4.4.1). Zircon and apatite mostly occur as inclusions in biotite. Magnetite usually occurs both as inclusions in mafic minerals and as clusters with other accessory minerals. Allanite occurs mostly as large dark brown, discrete, euhedral prismatic crystals. Some allanite crystals are zoned.

The monzogranite (outer facies) is a pinkish, equigranular, coarse to medium-grained rock containing more pink K-feldspar than plagioclase and small amounts of hornblende and biotite. A plot showing the relative proportions of modal quartz-plagioclase-alkali feldspar is shown in Fig. 4.4.1.

Plagioclase (An_{8-15}) occurs as subhedral crystals, some of which are weakly zoned and have intensely altered cores. Small plagioclase crystals are commonly enclosed by K-feldspar. K-feldspar is microcline-perthite and occurs as large subhedral twinned crystals. The K-feldspar is often highly turbid and has suffered sericitization. Small aggregates of quartz grains are commonly developed along the K-feldspar twinning planes. Granophyric intergrowths are locally well developed (Plate 4.4.2).

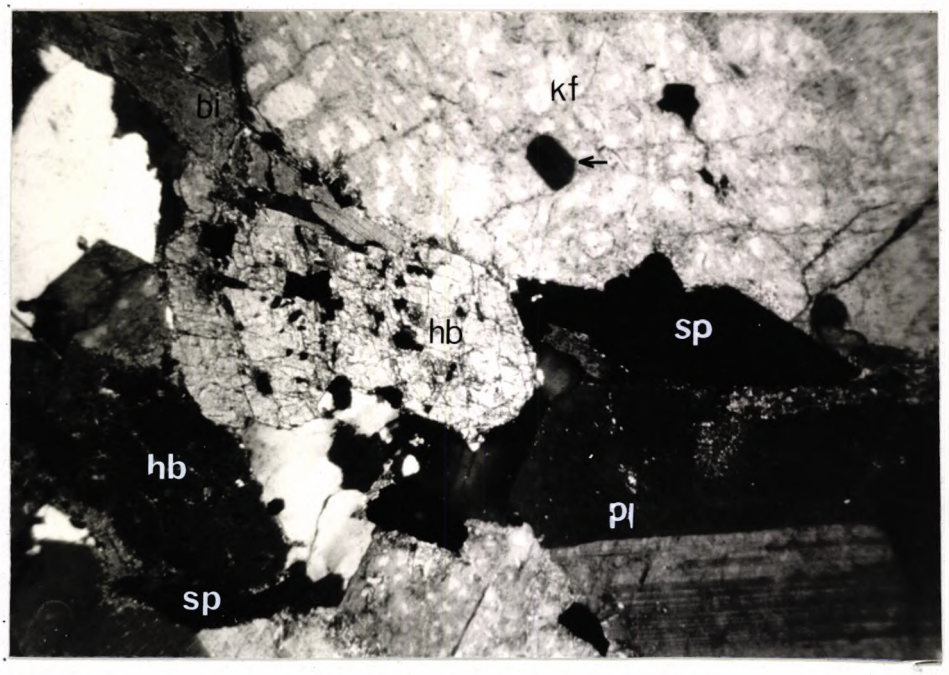

Plate 4.4.1. Photomicrograph of the monzonite (inner facies) of the Western Main Range Pluton, showing wedge-shaped sphene (sp in association with hornblende (hb) and biotite (bi). Subhedral plagioclase (pl) commonly shows twinning; large anhedral K-feldspar enclosing small plagioclase grain (pointed arrow). (Sample T90, X nicol, 2.5 x 8 x)

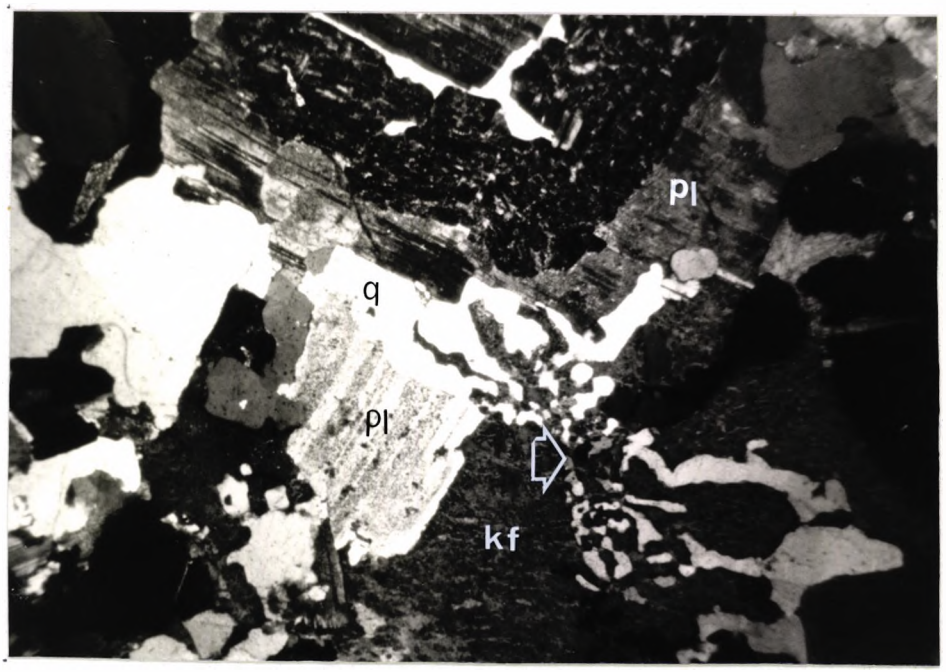

Plate 4.4.2. Photomicrograph of the monzogranite (outer facies) of the Western Main Range Pluton, showing local development of granophyric intergrowth (pointed arrow) between the contact of quartz (q) and K-feldspar (Kf). Some plagioclase (pl) has an intensive altered core. (Sample T49, X nicol, 2.5 x 8 x).

Quartz occurs both as large patches and aggregates of small grains interstitial to other minerals. Biotite (x = brown, y = z = greenish brown) occurs mostly as clusters of flakes and is intensively altered to chlorite. Hornblende (x = green, y = z = yellow green) forms subhedral prismatic twinned crystals. Hornblende is less common than in the monzonite and is commonly replaced by biotite and altered to chlorite. Common accessories are sphene, magnetite, zircon, apatite and allanite.

The leucogranite is a medium to fine-grained leucratic rock, consisting mostly of feldspar and quartz. A plot showing the relative proportions of modal quartz-alkali feldspar-plagioclase is shown in Fig. 4.4.1.

Plagioclase (An_{5-8}) occurs as subhedral crystals and generally lacks zoning. K-feldspar is microcline perthite and shows well developed cross-hatched twinning. Large K-feldspar crystals show carlsbad twinning and enclose plagioclase crystals. Quartz occurs as large anhedral patches and show interlocking boundaries with K-feldspar. In some places, granophyric intergrowths are locally well developed. Small biotite flakes are completely altered to chlorite. Muscovite is not present in these rocks. Small granules of sphene and magnetite are occasionally present in minor amount as accessory minerals.

The granite porphyry is a pinkish porphyritic rock, consisting of large plagioclase and K-feldspar megacrysts with some crystals of hornblende and biotite set in a fine-grained matrix of quartz and feldspar.

Plagioclase (An_{8-15}) phenocrysts generally show weak oscillatory zoning and occasionally have partially resorbed margins (Plate 4.4.3). K-feldspar occurs as twinned microcline-perthite phenocrysts which occasionally enclose plagioclase. Quartz phenocrysts usually shows corroded rims. Hornblende phenocrysts (x = green, y = z = pale green)

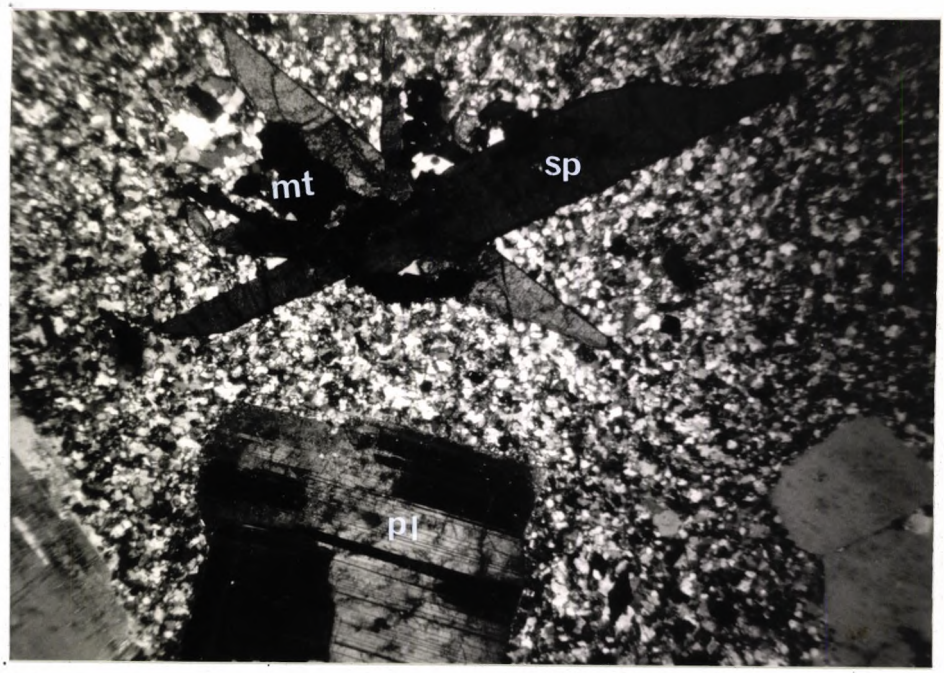

Plate 4.4.3. Photomicrograph of the granite porphyry of the Western Main Range Pluton, showing a phenocryst of plagioclase (pl) and clusters of sphene (sp), magnetite (mt) in a fine grained quartz and feldspar groundmass. (Sample CTK31, X nicol, 2.5 x 8 x).

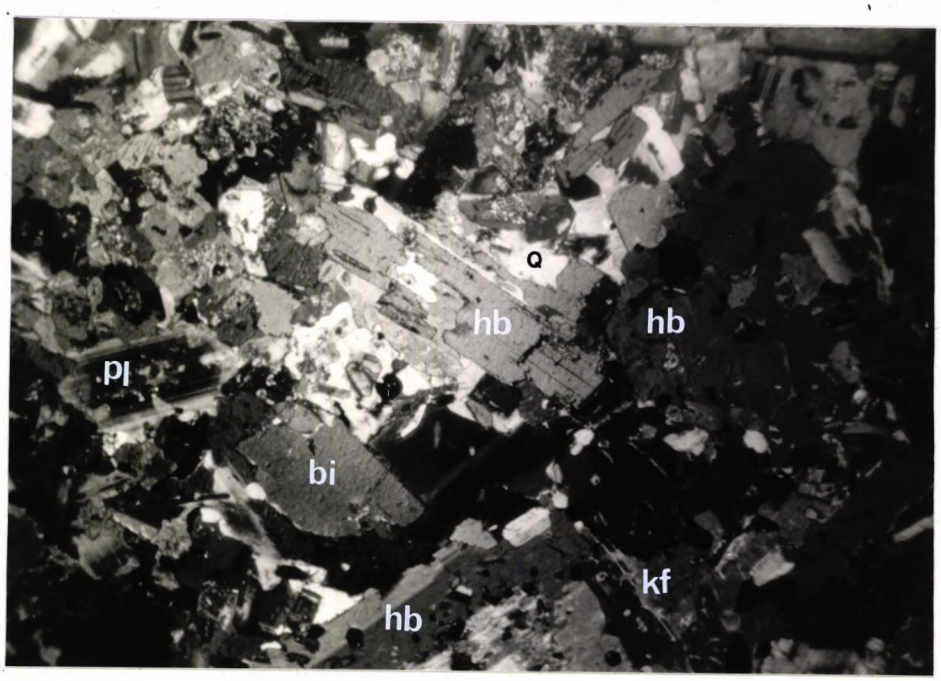

Plate 4.4.4. Photomicrograph of the appinite associated with the Western Main Range Pluton showing clusters of subhedral hornblende (hb), biotite (bi), plagioclase (pl) with interstitial quartz (q) and K-feldspar (Kf). (Sample CTK24, X nicol, 2.5 x 8 x).

occur as subhedral twinned prismatic crystals. Small flakes of biotite and accessory minerals such as sphene, zircon, magnetite are also present. The groundmass consists of fine-grained quartz and K-feldspar with granophyric intergrowth.

The appinites are a medium to fine grained melanocratic rock which consist predominantly of hornblende. A plot of the relative proportions of modal quartz-alkali feldspar-plagioclase (Fig. 4.4.1) shows points within the field of monzodiorite.

The rock consist essentially of hornblende, biotite, plagioclase, K-feldspar, and quartz with accessory sphene, apatite, magnetite (Plate 4.4.4).

Plagioclase (An_{20-37}) occurs both as euhedral to subhedral twinned and zoned crystals. Large plagioclase crystals commonly show patchy zoning and contain mafic inclusions, whereas small plagioclase crystals mostly show twinning on albite, pericline and carlsbad laws. The K-feldspar is microcline, showing poorly developed perthitic textures and lacking carlsbad twinning. K-feldspar occurs as small anhedral crystals interstitial to plagioclase and the mafic minerals. Quartz occurs as small patches interstitial to plagioclase. Hornblende (x = deep green, y = z = yellow green) occurs as clusters of twinned euhedral crystals. Biotite (x = brown, y = z = yellow brown) occurs as small flakes in association with hornblende. Among accessory minerals, sphene occurs mostly as granules rather than as well formed wedge-shaped crystals. Apatite occurs as stout crystals rather than acicular crystals and commonly it forms inclusions within plagioclase and mafic minerals.

Summary

The important points gained from the petrographic features of these rocks are as follows:-

1. K-feldspar is a particularly distinctive mineral constituent of both the monzonite and monzogranite, and occurs as large subhedral to anhedral twinned grains. The turbid K-feldspar and granophyric intergrowth of quartz and K-feldspar are not common in the monzonite, whereas these features are very common in the monzogranite.
2. The clusters of large zoned plagioclase crystals are common in the monzonite, whereas small weakly zoned plagioclase crystals, which are poikilitically enclosed by K-feldspar, are common in the monzogranite.
3. Hornblende and biotite are equally abundant in the monzonite, whereas biotite is the predominant mafic mineral in the monzogranite.
4. Chlorite and sericite are intensely developed both in the monzonite and the monzogranite.
5. Sphene and allanite are common accessory minerals both in the monzonite and the monzogranite.

4.5 Chemical characteristics

4.5.1 Major elements

The analysed samples from the Western Main Range Pluton show a range of SiO_2 values varying from 59-76 wt% (Table 4.5.1). Consideration of the analysed samples plotted on the Fe-(Na+K)-Mg and Ca-Na-K ternary diagrams (Fig. 4.5.1a) shows that Fe, Mg and Ca decrease while Na and K increase from the monzogranite of the inner facies outwards.

The plots for the leucogranite indicate it is higher in Na and K contents than the monzogranite, whereas the plot for the granite porphyry is closely related to the monzogranite.

Consideraration of the ternary plots of Q-Ab-Or and An-Ab-Or (Fig. 4.5.1b), for the analysed samples of the Western Main Range

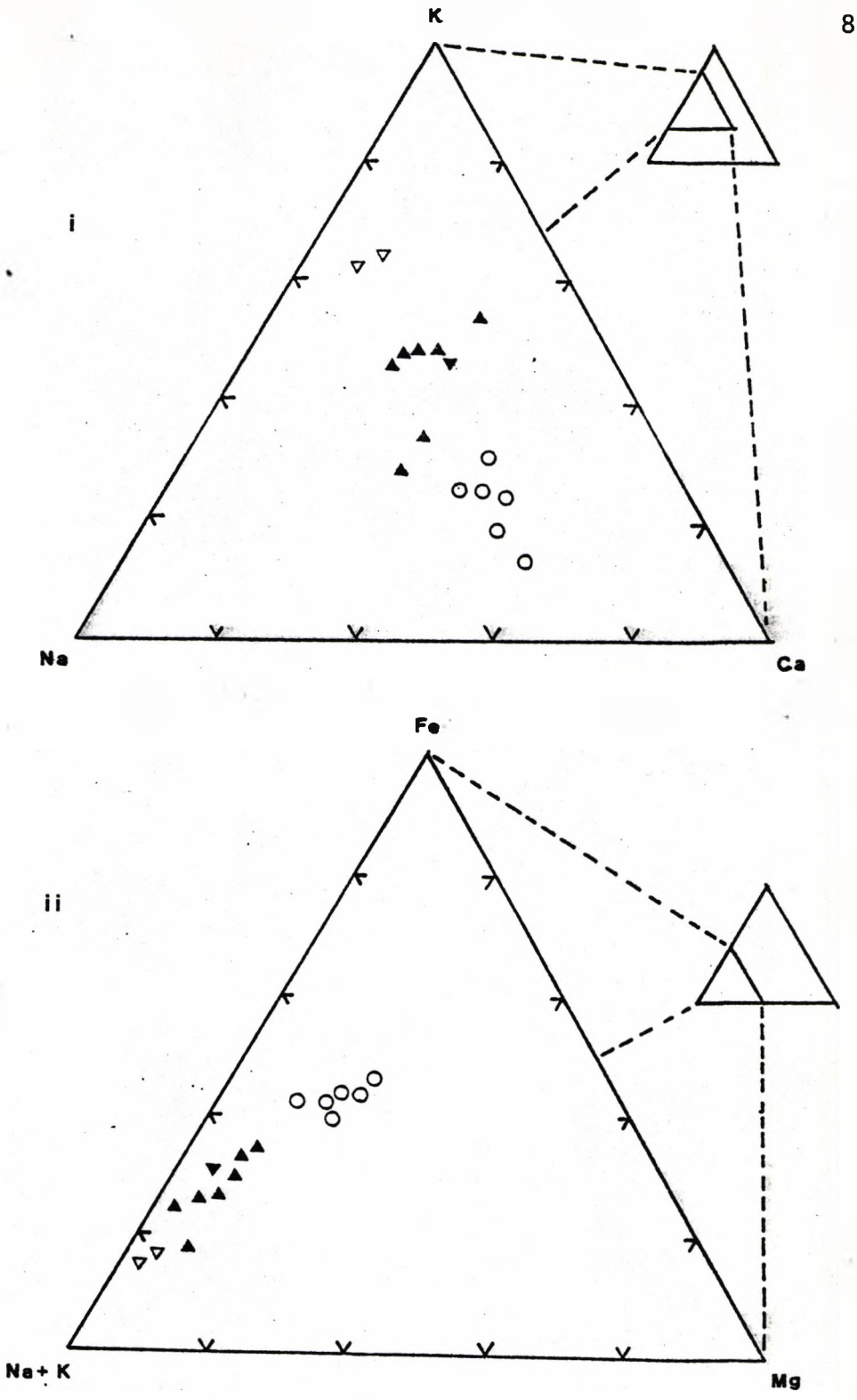

Figure 4.5.1a Triangular plots of the plutonic rocks of the Western Main Range Pluton symbols as follows:-
open circles - inner facies - monzonite
solid triangles, point up - outer facies - monzogranite
solid triangles, point down - porphyry
open triangle - leucogranite
solid square - appinite

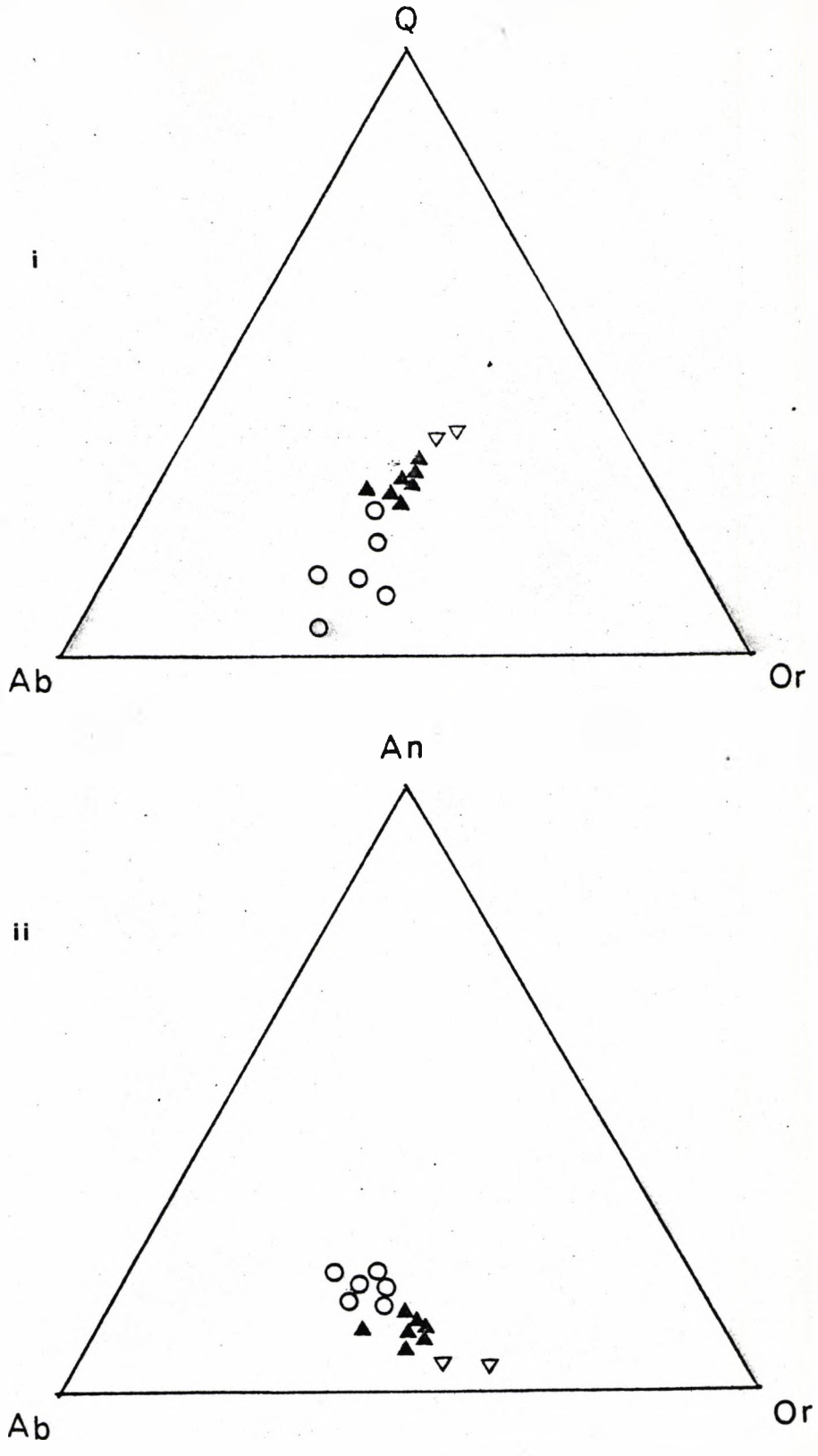

Figure 4.5.1b Triangular plots of the plutonic rocks of the Western Main Range Pluton, symbols as follows:-
open circles - inner facies - monzonite
solid triangles - outer facies - monzogranite
open triangles - leucogranite
(calculated from C.I.P.W. norms in Table 4.5.2).

TABLE 4.5.1

Analyses of the rocks from the Western Main Range Pluton

	inner facies					
Sample	CTK45	CTK60-1	T84	T50	T90	CTK56x
SiO_2	59.72	61.79	62.94	65.75	65.41	67.22
TiO_2	0.57	0.45	0.46	0.41	0.38	0.38
Al_2O_3	18.72	18.49	17.51	16.62	16.91	15.91
Fe_2O_3	1.49	1.78	1.53	1.34	0.59	1.36
FeO	2.52	1.34	1.75	1.41	2.30	1.28
MnO	0.10	0.08	0.09	0.08	0.09	0.08
MgO	1.58	1.24	1.47	1.27	1.52	1.24
CaO	4.01	3.30	3.06	2.75	3.10	2.56
Na_2O	4.86	4.35	4.52	4.07	3.90	4.28
K_2O	4.21	5.35	4.76	4.63	4.52	4.16
P_2O_5	0.24	0.17	0.20	0.19	0.19	0.14
Ba	2563	3102	2499	1843	2135	1582
Ce	124	140	95	88	117	85
Co	58	82	40	90	59	59
Cr	12	8	12	11	7	13
La	93	99	69	49	80	65
Nd	50	49	42	41	39	36
Ni	7	9	6	8	4	6
Pb	67	257	64	59	59	65
Rb	139	177	164	204	179	179
Sc	5	3	4	5	5	4
Sr	642	577	544	1137	462	411
Th	81	348	77	96	74	70
Ti	3703	3121	3162	2746	2997	2399
U	-	-	12	15	13	-
V	60	42	47	41	42	35
Y	26	26	26	24	25	30
Zn	53	38	45	41	46	40
Zr	449	345	342	1831	279	256

TABLE 4.5.1

(continued)

	outer facies						
Sample	CTK10	T14	T15	T16	CTK33	T49	CTK62
SiO_2	71.27	72.34	71.13	72.21	70.62	70.58	71.07
TiO_2	0.28	0.16	0.19	0.17	0.24	0.19	0.24
Al_2O_3	14.02	03.82	14.89	14.41	14.67	14.97	14.69
Fe_2O_3	1.01	0.81	0.90	1.07	1.13	1.09	0.92
FeO	1.17	0.53	0.73	0.77	0.85	0.54	0.83
MnO	0.07	0.10	0.07	0.08	0.12	0.12	0.06
MgO	0.81	0.68	0.49	0.41	0.62	0.58	0.61
CaO	1.89	1.29	1.43	1.34	1.74	1.29	1.74
Na_2O	3.60	3.72	3.78	3.56	4.48	4.11	3.57
K_2O	4.74	5.26	5.42	5.36	4.42	5.43	5.27
P_2O_5	0.11	0.05	0.06	0.05	0.09	0.05	0.08
Ba	933	405	499	644	266	262	699
Ce	88	74	72	81	104	86	80
Co	83	99	89	116	46	47	111
Cr	8	3	5	8	9	7	8
La	53	39	37	40	70	54	60
Nd	39	31	33	33	44	35	37
Ni	3	3	5	5	4	4	4
Pb	66	83	81	79	60	57	74
Rb	204	452	371	344	333	479	214
Sc	2	1	2	2	3	0	0
Sr	283	147	157	187	243	99	280
Th	95	77	55	83	84	61	80
Ti	1699	1036	1040	1197	1448	1089	1531
U	12	30	-	20	-	20	-
V	27	14	17	18	23	16	20
Y	24	24	16	17	30	23	13
Zn	30	25	25	25	35	28	26
Zr	246	168	154	165	1777	94	191

TABLE 4.5.1

(continued)

	leucogranite		porphyry
Sample	T65	T13	CTK31
SiO_2	76.33	75.83	68.85
TiO_2	0.10	0.08	0.28
Al_2O_3	12.42	13.01	15.36
Fe_2O_3	0.67	0.65	1.33
FeO	0.30	0.20	0.90
MnO	0.03	0.02	0.08
MgO	0.16	0.12	0.70
CaO	0.57	0.64	2.01
Na_2O	2.73	3.37	3.83
K_2O	6.29	5.69	5.43
P_2O_5	0.00	0.00	0.08
Ba	260	35	554
Ce	45	24	95
Co	130	95	40
Cr	8	10	7
La	39	22	55
Nd	24	15	30
Ni	6	4	0
Pb	67	70	211
Rb	218	279	302
Sc	0	0	2
Sr	94	39	247
Th	53	23	329
Ti	614	415	1619
U	8	-	-
V	7	6	26
Y	10	5	22
Zn	2	0	41
Zr	81	64	263

TABLE 4.5.1
(continued)

	Appinite			
Sample	T18b	T4	T98	T78
SiO_2	48.31	49.95	50.09	55.22
TiO_2	1.12	1.18	1.15	0.79
Al_2O_3	19.90	16.86	17.10	16.55
Fe_2O_3	3.01	1.41	2.32	2.15
FeO	3.95	6.02	4.96	3.90
MnO	0.12	0.13	0.09	0.13
MgO	6.14	6.32	5.96	6.07
CaO	8.10	7.56	6.92	6.05
Na_2O	2.30	2.57	2.55	2.74
K_2O	3.54	3.88	4.23	2.76
P_2O_5	0.28	0.48	0.50	0.26
Ba	2001	1981	1999	1162
Ce	62	78	117	60
Co	46	17	40	59
Cr	44	181	165	155
La	30	45	62	34
Nd	35	46	61	35
Ni	25	63	60	82
Pb	32	42	49	29
Rb	208	214	218	145
Sc	34	4	29	21
Sr	505	430	419	539
Th	19	49	51	19
Ti	7342	6910	7374	4924
V	231	185	195	128
Y	17	22	21	17
Zn	54	63	63	74
Zr	153	233	279	121

TABLE 4.5.2

C.I.P.W. norms of the rocks from the Western Main Range Pluton

	inner facies					
Sample	CTK45	CTK60-1	T84	T50	T90	CTK56x
Q	4.19	7.41	9.63	20.54	15.56	19.31
Or	24.88	31.56	28.13	27.78	27.30	24.59
Ab	41.12	36.80	38.24	31.30	33.00	36.21
An	16.84	15.16	13.44	9.27	14.14	11.79
Le	-	-	-	-	-	-
Ne	-	-	-	-	-	-
C	-	-	-	0.54	0.31	0.05
Ac	-	-	-	-	-	-
DiCa	0.62	0.04	0.18	-	-	-
DiMg	0.36	0.03	0.12	-	-	-
DiFe	0.24	-	0.05	-	-	-
Wo	-	-	-	-	-	-
HyMg	3.58	3.05	3.54	2.42	3.79	3.09
HyFe	2.40	0.39	1.31	0.56	2.45	0.75
OlMg	-	-	-	-	-	-
OlFe	-	-	-	-	-	-
Mt	2.16	2.58	2.22	1.74	0.86	1.97
He	-	-	-	-	-	-
Il	1.08	0.85	0.87	0.78	1.67	0.72
Ap	0.56	0.39	0.46	0.30	0.44	0.32

TABLE 4.5.2

(continued)

	outer facies						
Sample	CTK10	T14	T15	T16	CTK33	T49	CTK62
Q	26.92	26.96	24.59	27.35	23.30	22.41	25.51
Or	28.01	31.09	32.03	31.85	26.12	32.09	31.15
Ab	30.46	31.47	31.98	30.12	37.90	34.77	30.20
An	8.10	5.48	6.70	6.32	6.87	6.07	8.11
Le	-	-	-	-	-	-	-
Ne	-	-	-	-	-	-	-
C	-	-	0.35	0.40	-	0.11	0.14
Ac	-	-	-	-	-	-	-
DiCa	0.23	0.25	-	-	0.49	-	-
DiMg	0.15	0.21	-	-	0.35	-	-
DiFe	0.07	0.02	-	-	0.10	-	-
Wo	-	-	-	-	-	-	-
HyMg	1.87	1.49	1.22	1.02	1.20	1.44	1.52
HyFe	0.97	0.20	0.41	0.40	0.35	-	0.48
OlMg	-	-	-	-	-	-	-
OlFe	-	-	-	-	-	-	-
Mt	1.46	1.17	1.30	1.55	1.64	1.58	1.33
He	-	-	-	-	-	-	-
Il	0.53	0.03	0.36	0.32	0.46	0.36	0.46
Ap	0.23	0.12	0.14	0.12	0.21	0.12	0.23

TABLE 4.5.2

(continued)

	leucogranite		porphyry
Sample	T65	T13	CTK31
Q	34.92	32.92	20.74
Or	37.17	33.63	32.09
Ab	23.10	28.51	32.40
An	2.83	3.18	8.69
Le	-	-	-
Ne	-	-	-
C	0.09	0.15	-
Ac	-	-	-
DiCa	-	-	0.26
DiMg	-	-	0.21
DiFe	-	-	0.03
Wo	-	-	-
HyMg	0.40	0.30	1.54
HyFe	-	-	0.21
OlMg	-	-	-
OlFe	-	-	-
Mt	0.77	0.48	1.93
He	0.14	0.32	-
Il	0.19	0.15	0.53
Ap	-	-	0.19

TABLE 4.5.2

(continued)

	Appinite			
Sample	T18b	T4	T98	T78
Q	-	-	-	3.52
Or	20.92	22.93	25.00	16.31
Ab	19.46	21.66	21.57	23.18
An	33.52	23.01	22.72	24.71
Le	-	-	-	-
Ne	-	0.05	-	-
C	-	-	-	-
Ac	-	-	-	-
DiCa	2.02	4.74	3.48	1.51
DiMg	1.53	2.94	2.41	1.09
DiFe	0.28	1.53	0.81	0.27
Wo	-	-	-	-
HyMg	0.38	-	2.58	14.02
HyFe	0.07	-	0.87	3.47
OlMg	9.37	8.97	6.91	-
OlFe	1.88	5.14	2.57	-
Mt	5.00	2.04	4.16	4.13
He	-	-	-	-
Il	2.13	2.24	2.18	1.50
Ap	0.65	1.11	1.16	-

Pluton show that normative quartz and orthoclase increase at the expense of albite (Fig. 4.5.1b - i), and anorthite decreases as orthoclase increased (Fig. 4.5.1b - ii) from the monzonite to the monzogranite. These are in agreement with the petrographic observation (Section 4.4). The same diagrams (Fig. 4.5.1b) show that the plots for the leucogranites are located in the field of higher normative quartz and orthoclase than the monzogranite.

In brief, all the diagrams show good trends in major elements which indicate progressive change in chemical characteristics from the inner part of the pluton towards the outer part of the pluton.

4.5.2 Trace elements

Cobalt, Chromium and Nickel

Co varies from 40 ppm to 116 ppm in the monzonite to the monzogranite and shows a slight positive correlation with DI (Fig. 4.5.2a). The leucogranite has a concentration of Co slightly higher than the monzogranite, and the granite porphyry has as low a concentration as some of the monzogranites.

The overall distribution of Co in the rocks of the Western Main Range Pluton is much higher than the average for intermediate rocks (20 ppm) given by Wager and Mitchell (1951).

The behaviour of Co in the rocks of the Western Main Range Pluton is contradictory to the generally observed trend that Co^{+2} (radius = 0.72Å) has a tendency to enter the early crystallized ferromagnesian minerals by substitution for Mg^{+2} (radius = 0.65Å or Fe^{+2} (radius 0.74Å and become depleted in the liquid, i.e. the concentration of Co decreases as the differentiation increases. Ringwood (1955b) considered Co^{+2} with Ni^{+2}, Zn^{+3}, Cr^{+3}, Sc^{+3}, Mg^{+2} and Cu^{+2} which have ionic potentials intermediate between those of "network formers" and "network modifiers". He suggests that sometimes these

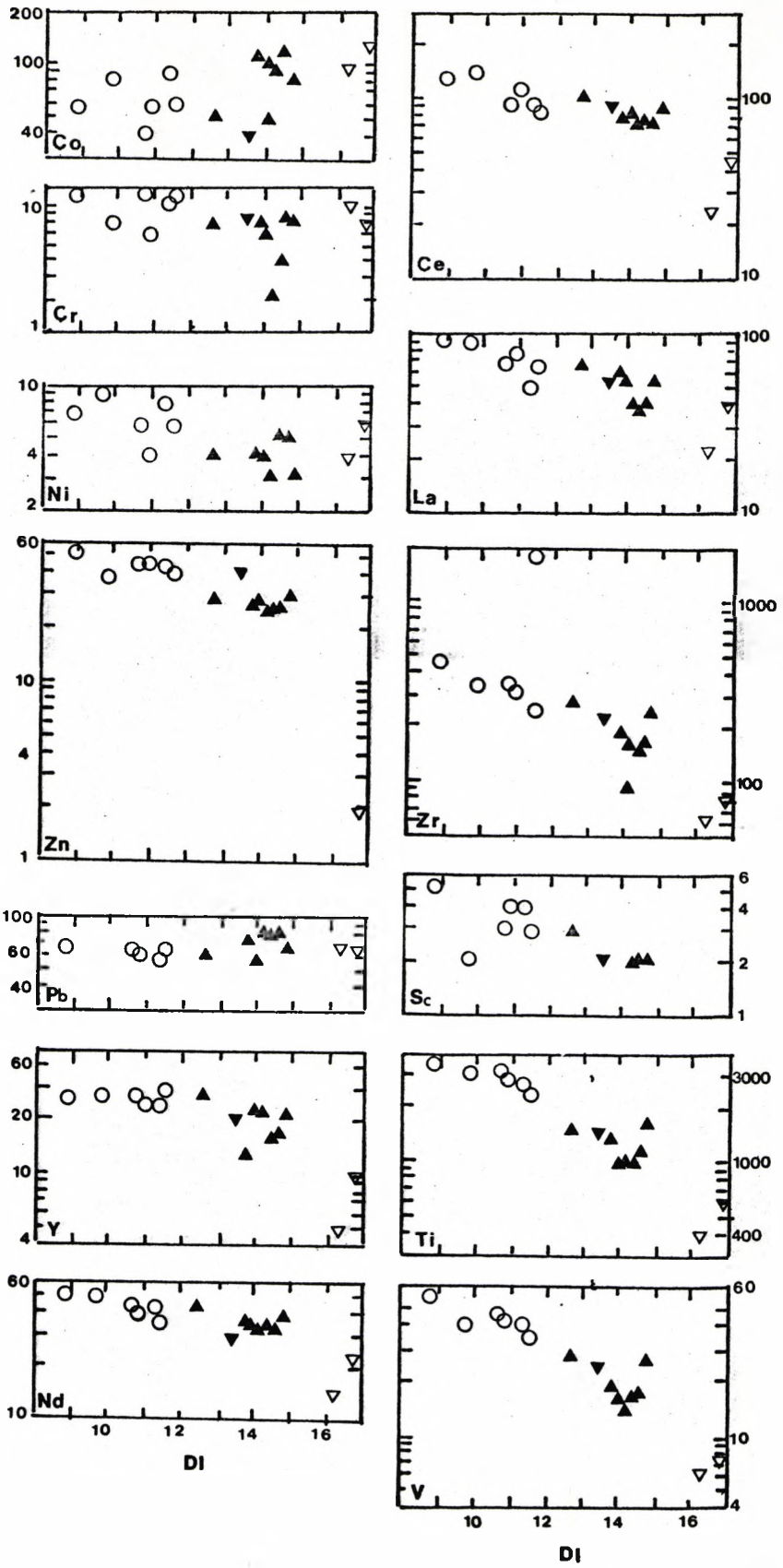

Figure 4.5.2a Plots of trace elements contents vs. Differentiation Index for the plutonic rocks of the Western Main Range Pluton. Symbols as follows:-
open circles - inner facies - monzonite
solid triangles, point up - outer facies - monzogranite
solid triangles, point down - porphyry
open triangles - leucogranite

ions tend to become concentrated in residual magmas during the later stages of magmatic crystallization, because the position which these intermediate ions occupy in the magma depends upon the ratio of anions - mainly (O^{-2}+ OH^{-1} + F^{-1}) to (Si^{+4} + Al^{+3}). They have to compete with the ions of high ionic potential for the available anions, in order to form MO_4 complexes. Under conditions where anion supply is low, the intermediate ions are unable to form their own tetrahedral complexes. Hence they behave as free ions. Under conditions where the magma is rich in volatiles, the supply of anions is much greater, and the intermediate ions are able to form tetrahedral complexes. The large size of these tetrahedral complexes means that they are not accepted in silicate minerals and are therefore concentrated in the residual magma.

The increase of Co content in the late differentiated rocks of the Western Main Pluton may be due to the volatile rich granitic magma as indicated by the granophyric texture in the monzonite (outer facies) and noted in the petrographic observations. Thus Co in the Western Main Range Pluton shows incompatible character.

Ni varies from 9 ppm to 3 ppm, and Cr varies from 12 ppm to 3 ppm, both showing negative correlation with DI (Fig. 4.5.2a). The leucogranites and granite porphyry have much the same concentration of Ni and Cr as the monzogranite. The size of Ni^{+2} (radius = 0.69Å) and Cr^{+3} (radius = 0.63Å) are similar to Mg^{+2} (radius = 0.65Å) and Fe^{+3} (radius = 0.64Å), which enables Ni and Cr to substitute in ferromagnesian minerals, viz, hornblende and biotite. Thus the fractionation of hornblende, biotite and magnetite caused Ni and Cr to be depleted in the liquid. The decrease in Ni and Cr contents from the monzonite to the monzogranite in the Western Main Range Pluton coincides with the decrease of hornblende and biotite as indicated by the modal proportions (see Table 4.4.1). Therefore, the decrease

of Ni and Cr is compatible with the extraction of these elements by hornblende and biotite and emphasises their compatible character, in contradiction to Co.

Lanthanum, Cerium and Neodynium

La varies from 99 ppm to 37 ppm, Ce varies from 140 ppm to 74 ppm and Nd varies from 50 ppm to 31 ppm, in the monzonite to the monzogranite. These variations show negative correlation with DI (Fig. 4.5 2a). La, Ce and Nd in the leucogranite have low concentrations than in the monzogranite, whereas the granite porphyry has much the same concentration of these elements as the monzogranite.

Accessory minerals, viz. sphene, allanite, xenotime, monazite, zircon and apatite are the main sources of La, Ce and Nd in granitic rocks (Condie, 1978). The fractionation of these accessory minerals will be reflected in the decrease of these LREE in the liquid. Sphene, allanite, apatite and zircon are distinctively abundant in the rocks with mafic minerals, as noted in the petrography (see Section 4.4). The decrease in LREE concentration with increasing DI from the monzonite to the monzogranite may be related to the crystallization of LREE-bearing minerals as mentioned above. It may also relate to the crystallization of hornblende which has K_D values greater than 1.0 in acid rocks (Hanson 1980). Therefore, the LREE's behave compatibly in this pluton.

Scandium and Vanadium

Sc varies from 5 ppm to zero, and V varies from 60 ppm to 14 ppm from the monzonite to the monzogranite. The variation of these elements shows a negative correlation with DI (Fig. 4.5.2a). Sc and V are strongly concentrated in the ferromagnesian phenocrysts, the highest concentrations occurring in hornblende and to a less extent in the augites (Ewart and Taylor, 1969). Ringwood (1955a) mentioned that V^{+3} (radius 0.74Å, electronegativity = 1.35) displays a high degree of preferential concentration relative to Fe^{+3} (radius = 0.64Å, electronegativity = 1.8) and is rapidly moved from the magma as soon

as Fe^{+3} is precipitated in any abundance, for instance in magnetite.

In the case of the Western Main Range Pluton, the decrease in hornblende (see modal data Table 4.4.1) from the monzonite to the monzogranite is reflected in the decrease of Sc and V. Magnetite, which commonly occurs in association with hornblende (as noted in the Section 4.4) in these rocks, may also be responsible for the decrease of V. These variations emphasise the compatible character of these two elements. The leucogranites contain lower Sc and V contents than the monzogranite, whereas the granite porphyry has Sc and V concentration much the same as the monzogranite.

Lead and Zinc

The Pb content in the rocks of the Western Main Range varies from 59 ppm to 83 ppm in the monzonite to the monzogranite and shows positive correlation with Di (Fig. 4.5.2a). The leucogranites have Pb contents much the same as the monzogranite. (Two analysed samples from the granite porphyry, CTK31, and from the monzonite of the inner facies show abnormally high values, 211 ppm and 257 ppm respectively).

Pb^{+2} (radius = 1.20Å occurs in silicates by direct substitution of K^{+1} (radius = 1.33Å), but does not enter into K-feldspar lattice and tends to accumulate in the residual magma (Ringwood, 1955a).

Zn varies from 53 ppm to 25 ppm from the monzonite to the monzogranite and shows a negative correlation with DI (Fig. 4.5.2a). The leucogranites have very low Zn concentrations (0-2 ppm), while the granite porphyry has a concentration much the same as the monzogranite.

Zn is camouflaged in minerals containing ferous-iron because the ionic radii of Zn^{+2} and Fe^{+2} are similar (0.74Å).

The increase of Pb and the decrease of Zn from the monzonite to the monzogranite may be related to the decrease in ferromagnesian minerals and the increase of K-feldspar as shown in the modal data (Table 4.4.1). Thus Zn behaves compatibly and Pb does not.

Thorium

The Th contents in the rocks of the Western Main Range Pluton mostly varies between 55 ppm to 96 ppm and shows a slight increase with DI (Fig. 4.5.2a). The leucogranites have lower concentrations of Th (53-23 ppm) than the monzogranite. Two analysed samples from the granite porphyry (CTK31) and from the monzonite of the inner facies (CTK60-1) contain abnormally high Th concentration, 329 ppm and 348 ppm respectively - cf. with the Pb values.

The high values of Th content in the rocks of the Western Main Range Pluton which also contains high K are similar to the values of the biotite granite White Mountain Series (65-98 ppm Th with K 4.00%; Rogers and Ragland, 1961). The Th values of average granite with K content 3.45%, is 17.36 ppm (Heier and Rogers, 1963). The anomalous high Th values in these granite rocks can be related to the presence of sphene or allanite (Ragland et al, 1967). This notion is in agreement with the rocks of the Western Main Range Pluton, which contain abundant sphene and allanite as noted in the petrographic observations (see Section 4.4).

Titanium and Zirconium

Ti varies from 3703 ppm to 1036 ppm, and Zr varies from 449 ppm to 94 ppm from the monzonite to the monzogranite and both show negative correlation with DI (Fig. 4.5.2a). The leucogranites contain lower Ti and Zr contents than the monzogranite, whereas the granite porphyry has much the same concentration as the monzogranite.

The plot of Ti versus Zr (Fig. 4.5.2c) shows a decrease of both Ti and Zr from the monzonite to the monzogranite. The mineral vectors for Ti-Zr are similar to those proposed by Pearce and Norry (1979), and are superimposed on this diagram, and indicate that fractionation of some combination of biotite, hornblende, $\pm$ magnetite, $\pm$ zircon can cause depletion of Ti and Zr in the liquid.

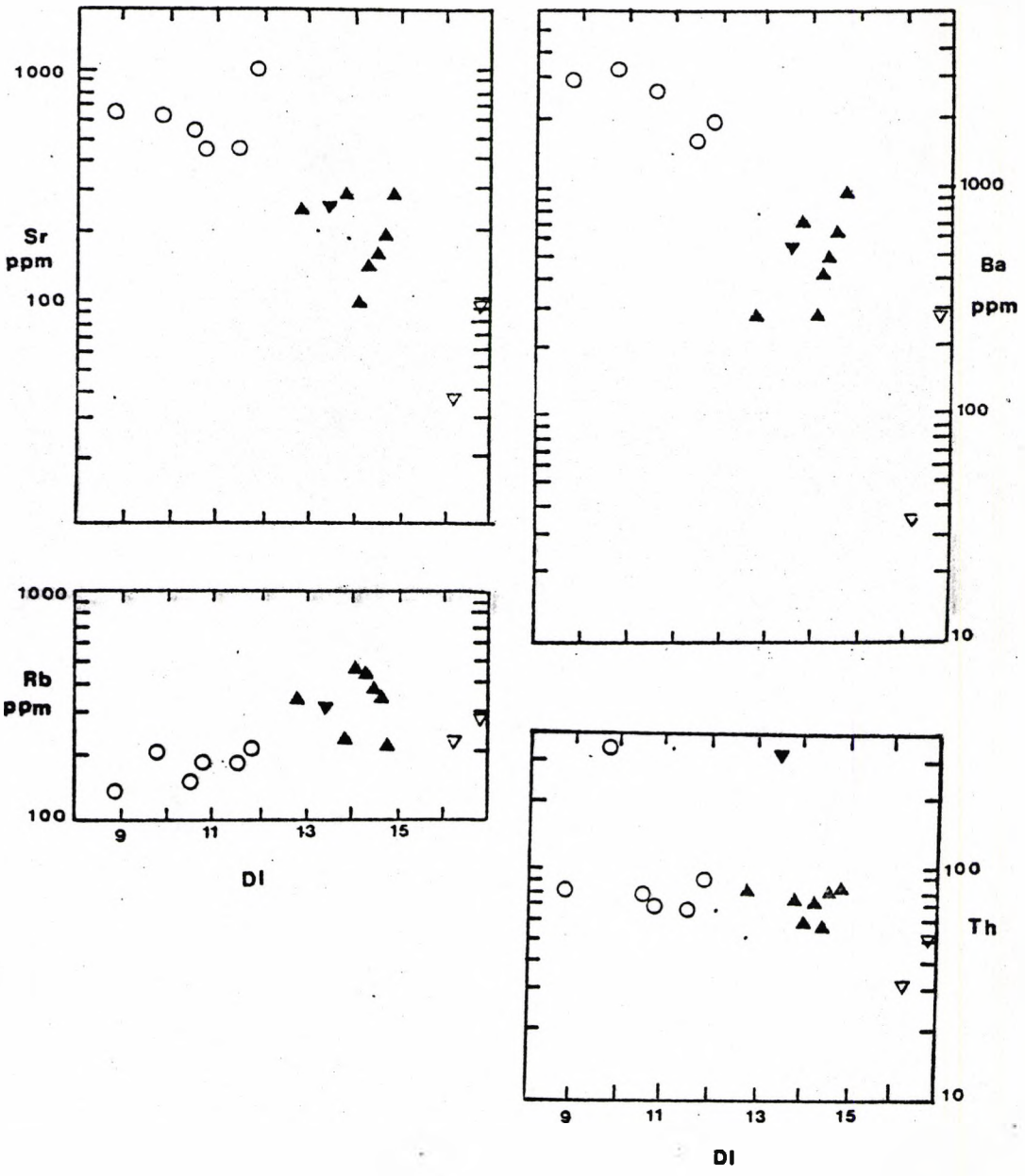

Figure 4.5.2b Plots of trace elements contents vs. Differentiation Index for the plutonic rocks of the Western Main Range Pluton. Symbols as follows:-
open circles - inner facies - monzonite
solid triangles, point up - outer facies - monzogranite
solid triangles, point down - porphyry
open triangles - leucogranite

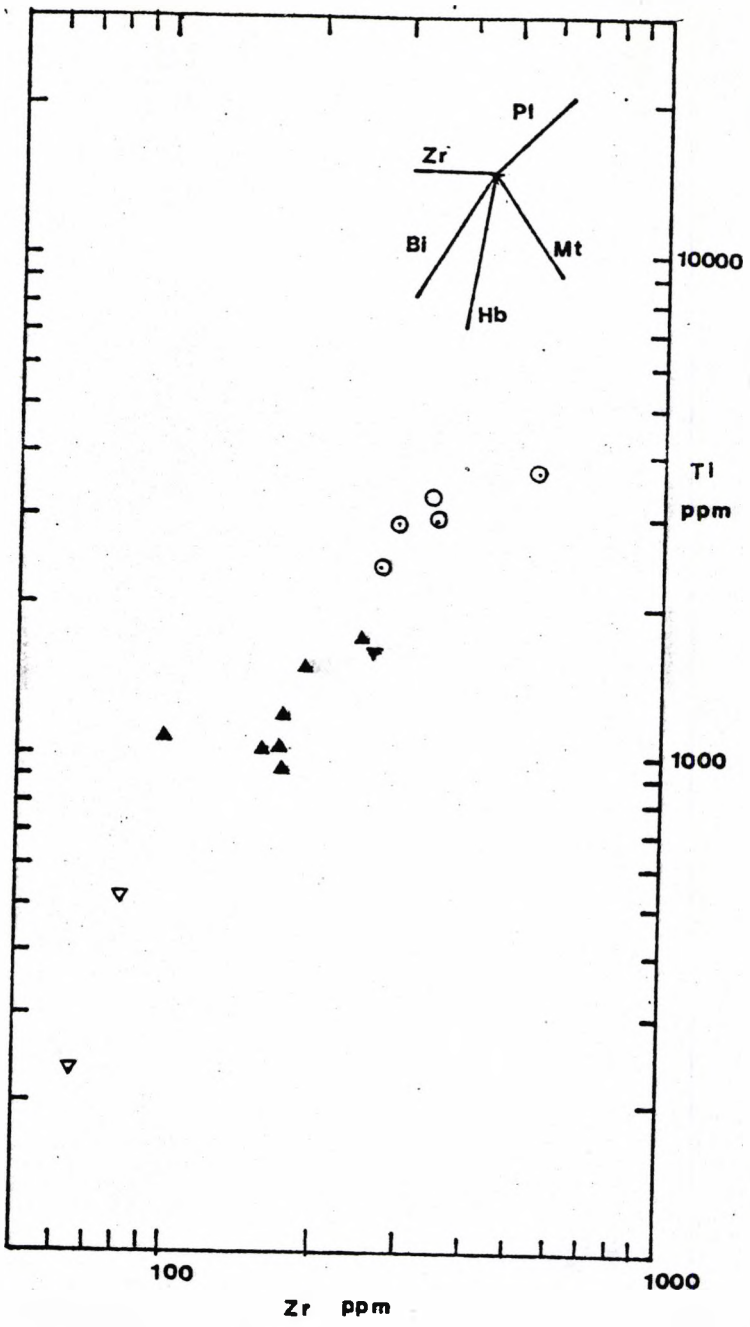

Figure 4.5.2c Plot of Ti Vs Zr for the plutonic rocks of the Western Main Range Pluton, symbols as follows:-
open circles - inner facies - monzonite
solid triangle, point up - outer facies - monzogranite
solid triangle, point down - porphyry
open triangle - leucogranite
The mineral vectors shown are taken from Pearce and Narry (1979), and indicate the relative change in these elements upon extraction of each mineral.
Bi = biotite; Hb = hornblende; Mt = magnetite;
Pl = plagioclase; Zr = zircon;

Hornblende and biotite show decreases from the monzogranite of the inner facies to the monzogranite of the outer facies (see modal data Table 4.4.1) and zircon is commonly present as inclusions in biotite or occurs in clusters with other accessory minerals associated with mafic minerals, as noted in the petrographic observations (see Section 4.4). Therefore, Ti and Zr show marked depletion and behave compatibly in this pluton.

Yttrium

Y varies from 30 ppm to 14 ppm from the monzonite to the monzogranite, showing a negative correlation with DI (Fig. 4.5.2a). The Leucogranites contain lower concentrations of Y than the monzogranite whereas the granite porphyry has much the same concentration as the monzogranite. When Y is plotted against CaO (Fig. 4.5.2d), the trend shows decreasing Y with decreasing CaO; a J-type trend, similar to that of Lambert and Holland (1974). Their work shows that at low CaO level, the decrease of Y as CaO decreases may be due to fractionation of hornblende, apatite or sphene. The rocks of the Western Main Range show decrease in hornblende abundance from the monzonite to the monzogranite (see modal data Table 4.4.1), and these rocks also contain distinctive sphene and apatite as noted in the petrographic section (see Section 4.4). Therefore, Y behaves compatibly in this pluton.

Rubidium, Strontrium and Barium

Rb varies from 139 ppm to 479 ppm, from the monzonite to the monzogranite and shows a positive correlation with DI (Fig. 4.5.2b), whereas Sr varies from 642 ppm to 99 ppm, and Ba varies from 3102 ppm to 262 ppm; both showing negative correlations with DI (Fig. 4.5.2b). The granite porphyry has Rb, Sr and Ba concentrations much the same as the monzogranite, while the leucogranite has a Rb concentration much the same as monzogranite but with lower Ba and Sr contents.

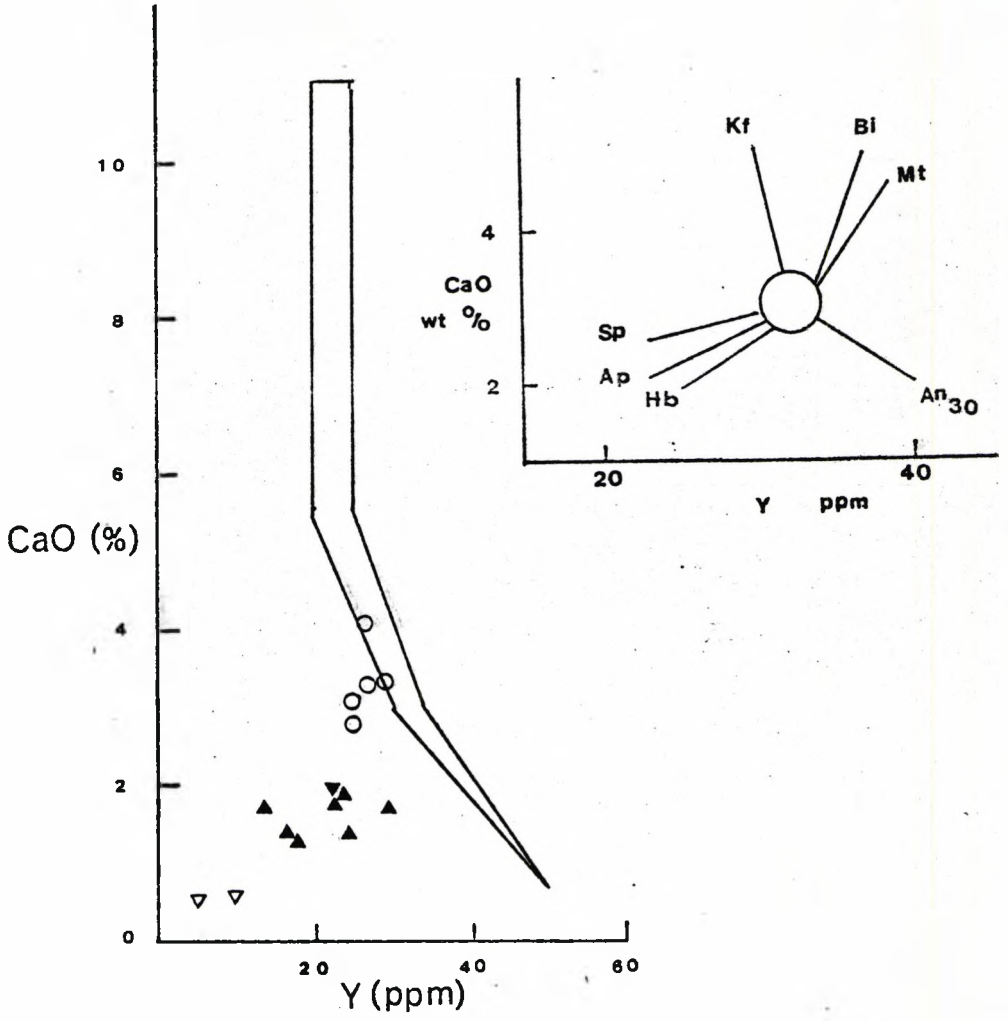

Figure 4.5.2d Plot of Cao vs Y for the plutonic rocks of the Western Main Range Pluton. Symbols as follows:
open circles - inner facies - monzonite
solid triangles, point up - outer facies - monzogranite
solid triangles, point down - porphyry
open triangles - leucogranite
Enclosed area represents "standard calc-alkali trend"
inset shows "liquid fractionation trends" for minerals (after Lambert and Holland, 1974). Sp = sphene; Ap = apatite; Hb = hornblende; An_{30} = plagioclase of anorthite 30%; Mt = magnetite; Bi = biotite; Kf = K-feldspar.

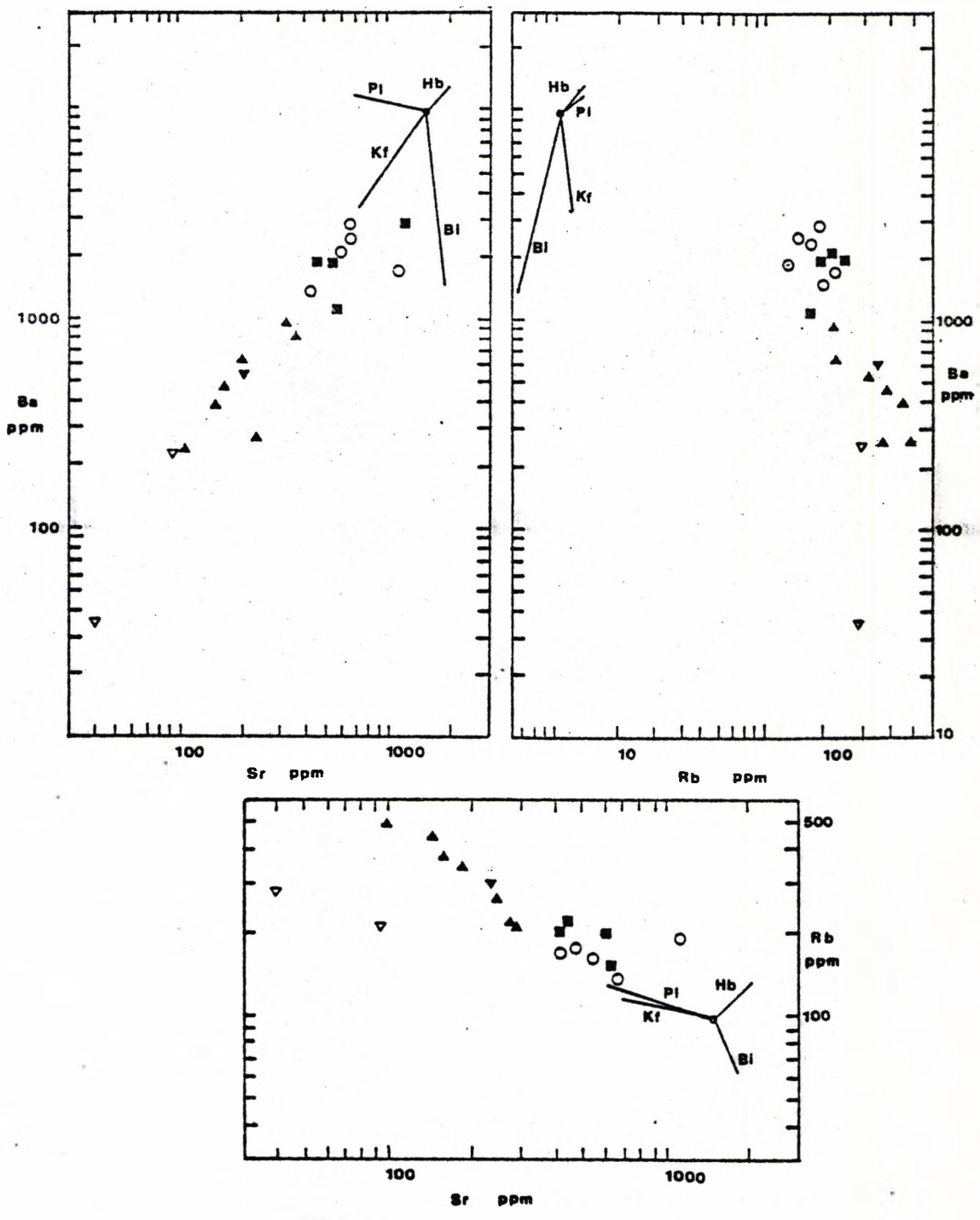

Figure 4.5.2e Plot of Rb, Sr, Ba for the plutonic rocks of the Western Main Range Pluton. Symbols as follows:-
open circles - inner facies - monzonite
solid triangle, point up - outer facies - monzogranite
solid triangle, point down - porphyry
open triangle - leucogranite
solid square - appinite.
Mineral vectors calculated from the distribution coefficients for acid plutonic-rocks (Table 14.1 from Cox et al. 1979). Length of vector indicates 20% fractionation of mineral. Kf = K-feldspar; Bi = biotite; Hb = hornblende; Pl = plagioclase.

Ba-Sr diagram

The plot of Ba versus Sr (Fig. 4.5.2e) shows that both Ba and Sr contents decrease from the monzonite to the monzogranite. The Ba-Sr fractionation vectors indicate that plagioclase (plus hornblende) and biotite can cause depletion both of Ba and Sr during fractionation as seen here because Ba^{+2} (radius = 1.34Å) is preferentially incorporated into biotite by substitution for K^{+} (radius = 1.33Å), and Sr^{+2} (radius = 1.18Å) is preferentially incorporated in plagioclase and hornblende by substitution for Ca^{+2} (radius = 1.02Å). The plots of Ba versus Sr for the appinites shows the points lie close to those of the monzonite whereas the plot for the granite and the plots for the leucogranite indicate lower concentrations of Ba and Sr than in the monzogranite.

Ba-Rb diagram

The plots of Ba versus Rb (Fig. 4.5.2e) show that Ba decreases whereas Rb increases from the monzonite to the monzogranite. The fractionation vectors for Ba-Rb indicate that fractionation of plagioclase (plus hornblende) and biotite and even K-feldspar can deplete Ba and enrich Rb in the liquid. Ba^{+2} (radius = 1.34Å) is more similar in size to K^{+1} (radius = 1.33Å) than Rb^{+1} (radius = 1.47Å); therefore Ba can be incorporated in biotite by direct substitution for K greater than Rb. Also Rb is not preferentially incorporated into plagioclase and hornblende because of the size of Ca^{+2} (radius = 1.08Å) is much smaller than Rb.

The plots of Ba versus Rb for the appinites also fall close to those of the monzonites, whereas the plot for the granite porphyry fall close to the monzogranite and the plots for the leucogranite lie away from the other rocks.

Rb-Sr diagram

The plot of Rb versus Sr (Fig. 4.5.2e), shows that the Rb contents increase, whereas the Sr decrease from the monzonite to the monzogranite.

The mineral vectors for Rb-Sr indicate that plagioclase ($\pm$ K-feldspar) and hornblende can cause enrichment of Rb and depletion of Sr in the liquid during fractional crystallization. These relationships are due to the compatible of the nature of Sr^{+2} (radius = 1.18Å) with plagioclase and hornblende by substitution for Ca^{+2} (radius = 1.02Å), whereas Rb^{+1} (radius = 1.47Å) is compatible with respect to plagioclase and hornblende, and preferentially incorporated in K-feldspar by substitution for K^{+} (radius = 1.33Å).

The plots of Rb and Sr contents for the appinites fall close to the monzonite whereas the plot for the granite porphyry fall close to the monzogranite, but the plots for the leucogranites are away from the trend of the other rocks.

Summary

The important points gained from the chemical characteristics of the rocks in the Western Pluton are as follows:

1. The decreasing contents of the trace elements compatible with calcium-bearing mineral (Sr, Y), as well as the trace element compatible with potassium-bearing minerals (Ba), together with the increase of Rb which is the compatible element with respect to calcium-bearing minerals, from the monzonite of the inner facies to the monzogranite of the outer facies, indicates the importance of the fractionation of plagioclase, hornblende and biotite in these rocks. (Fig. 4.5.2d and Fig. 4.5.2e). Fractionation of plagioclase, hornblende and biotite in these rocks coincides with the decrease of these minerals from the monzonite towards the monzogranite (see modal data Table 4.4.1). The plot of normative An-Ab-Or also indicates the trend of decreasing anorthite content simultaneous with increasing orthoclase from the monzonite towards the monzogranite (Fig. 4.5.1b).

2. The decreasing contents of the trace elements compatible with ferromagnesian minerals, (Cr, Ni, V, Sc) from the monzonite of the inner facies towards the monzogranites of the outer facies is in agreement with the trend of decreasing Fe and Mg in the Fe-(Na+K)-Mg diagram (Fig. 4.5.1a), and compatible with the extraction of these elements from the liquid by hornblende and biotite as indicated in the decrease of these mineral proportions in the rocks (see modal data Table 4.4.1).

3. The decrease in Ti and Zr contents from the monzonite of the outer facies towards the monzogranite of the inner facies reflects the fractionation of hornblende, biotite (with possibly titanomagnetite) and zircon, which is in agreement with the petrographic observation as noted in Section 4.4.

4. The decrease of LREE contents (La, Ce, Nd) from the monzonite of the inner facies towards the monzogranite of the outer facies may be due to the fractionation of the LREE-bearing minerals, viz. sphene, allanite and possibly hornblende. The presence of these accessory minerals is observed in the thin sections of the monzonite and the monzogranite.

5. The high concentration of Th in the rocks of the Western Main Range Pluton may be related to the presence of the Th-bearing accessory minerals similar to the high thorium granite observed by Ragland, et al (1967), plus the characteristic of high K content (4-5 wt%) which commonly relates to high Th content as documented in Rogers and Ragland (1961). Note also the associated high Pb content.

6. The abnormal increasing trend of Co as differentiation increases from the monzonite of the inner facies to the monzogranite of outer facies may be related to the volatile-rich acid magma prior to crystallization as indicated by the granophyric textures commonly

observed in the outer facies, which cause the elements of intermediate ionization potential such as Co to be concentrated in the liquid as the differentiation increases (Ringwood, 1955b)

7. Among the late minor intrusives, the leucogranites have chemical compositions close to or indistinguishable from those of the monzogranite, and the granite porphyry shows chemical characteristics similar to the monzogranite rather than to the monzonite.
8. In brief, the Western Main Range Pluton shows chemical characteristics of differentiation from the monzonite of the inner facies towards the monzogranite of the outer facies.
9. Note that the appinitic rocks have Rb, Sr and Ba contents much the same as the monzonite of the inner facies of the Western Main Range Pluton (Fig. 4.5.2e). This may imply that the appinites, which commonly occur as enclaves and dykes in the monzonite and monzogranite, are not generally related in the fractionation and differentiation.

CHAPTER 5

THE EASTERN PLUTON

5.1 Introduction

The Eastern Pluton is situated on the eastern flank of the Tak Batholith, and covers an area of approximately 1600 sq. km. It is roughly elongated along a NS-axis.

The pluton intrudes limestones, phyllites, tuffs and agglomerates of Permo-Triassic age. The roof of the pluton is locally made up of volcanics (metatuffs, agglomerate with several dykes and sills of andesite porphyry and dacite porphyry), and micaschists of presumably Silurian-Devonian age (Piyasin, 1974; Bunopas, 1974).

Detailed studies of the granitic rocks in this pluton have not previously been made except for a short report on the chemistry (Pongsapitch and Mahawat, 1977), and reconnaissance mapping (Piyasin, 1974; Bunopas, 1974) on a scale of 1:250,000.

5.2 Components of the pluton

The Eastern Pluton is a zoned pluton consisting principally of quartz diorite, granodiorite and monzogranite (Fig. 5.2.1). Aplites and microgranites occur as late minor intrusive phases. Porphyry occurs locally along the contact of the granodiorite and the overlying country rocks which form the roof of the pluton.

The pluton was intruded by the Western Main Range pluton and the Tak pluton on the west. The details of the relationship of these plutons are discussed in the following section. The northern part of the eastern pluton was off-set and uplifted by late faulting. Tectonites and cataclasites are well developed along these fault zones. The uplifting of the northern part of the pluton facilitated the exposure of the inner part of the pluton whereas the exposures on the southern area of the pluton

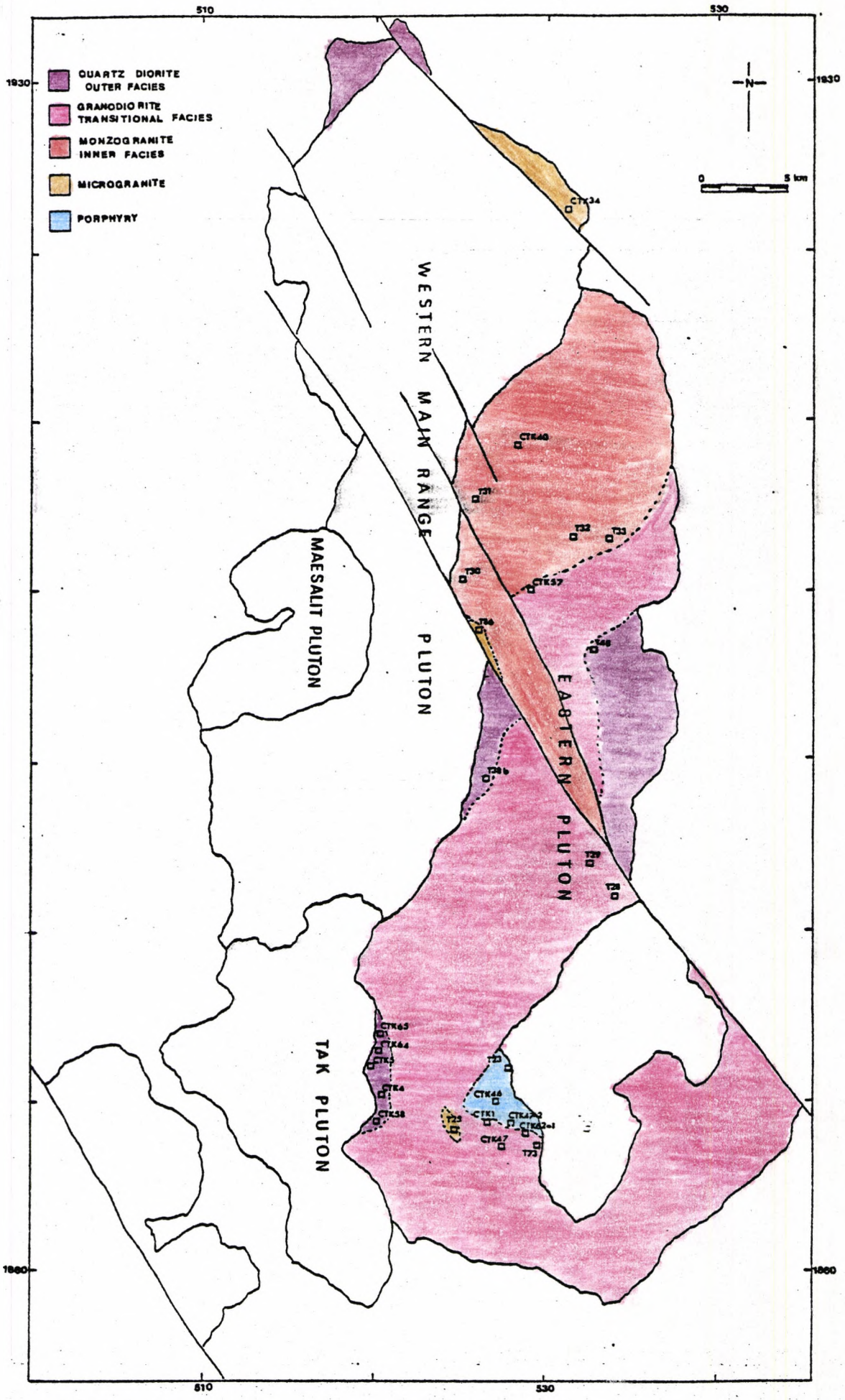

Figure 5.2.1 Outcrop map of the Tak Batholith, showing the different facies and sample localities of the Eastern Pluton.

are close to the roof of the pluton (based on the overall level of exposure close to the contact of the overlying country rocks).

Among the major rock units of the pluton, quartz diorite occurs mostly along the outer part of the pluton and locally crops out as a thin carapace on the granodiorite.

Granodiorite is extensively exposed all over the southern area.

In the northern area, monzogranite occurs in the inner part of the pluton and quartz diorite occurs along the outer part of the pluton. The rock occurring intermediate between these two units is granodioritic in composition (based on modes). The precise contact boundary between monzogranite and granodiorite or between granodiorite and quartz diorite has not been established. The terms of inner facies, transitional facies and outer facies are used to represent monzogranite in the inner part, granodiorite in the intermediate part and quartz diorite in the outer part of the pluton respectively, in order to understand the structure of the pluton in accordance with the petrological and chemical characteristics resulting from these studies.

5.3 Field relationships

The relation with the Tak Pluton

Along the southwestern periphery of the Eastern Pluton, quartz-diorite and granodiorite of the outer facies and transitional facies are mostly in sharp contact with steep or sub-vertical intrusive aplite, microgranite, leucogranite, felsite and pegmatite of the late intrusive border zone of the Tak Pluton, and enclaves of the former in the latter are present in several places.

The relation with the Western Main Range Pluton

The contacts along the western margin are entirely with the outer facies or the late intrusives border zone of the Western Main Range Pluton. Distinctive apophyses of late phases of aplite, microgranite

and felsite of the Western Main Range Pluton penetrate the rocks of the Eastern Pluton and are well exposed in the creek of "Huai Mae-Salit Laeng".

The intrusion of the Western Main Range pluton into the Eastern Pluton results in the disruption of exposures in the northern part of the Eastern Pluton as shown in the map (Fig.5.2.1). The contacts of the intrusion are steep or sub-vertical and show chilled contacts in the rock of the Western Main Range Pluton against the rocks of the Eastern Pluton.

The relation with metasedimentary and metavolcanic wall rocks and envelope.

The eastern flank of the Eastern Pluton is mostly in contact with limestones, phyllites and volcanic tuffs of Permo-Triassic age. This contact is sharp and sub-vertical. The contact zone shows no diffuse features with the wall rocks and the granite does not contain xenoliths. The country rocks along the contact zone are not strongly folded or strongly metamorphosed. Cataclastic granite or tectonite occurs in some places in the granite where it is in fault contact with the wall rocks. In some places on the northern margin of the pluton where it is in contact with andesitic rocks, the contact zone is sharp and intrusive and there are numerous andesitic enclaves in the granite (location 5245, 1929).

Small remnants of roof contacts of the granite with micaschist are found near to the south-western flank of the pluton (location 5025, 1859). The granite contains small xenoliths of micaschist and does not show a gradational contact with the envelope (plate 5.3.1).

On the roof of the Eastern Pluton, where the granodiorite is in contact with the overlying volcanics, there is a thin zone of porphyritic rock, which is recognised by the author as chilled marginal rock.

Plate 5.3.1. Bird's eye view of the roof contact (pointed arrow) of the granite (gr) of the Eastern Pluton with the overlying mica schist (mi).

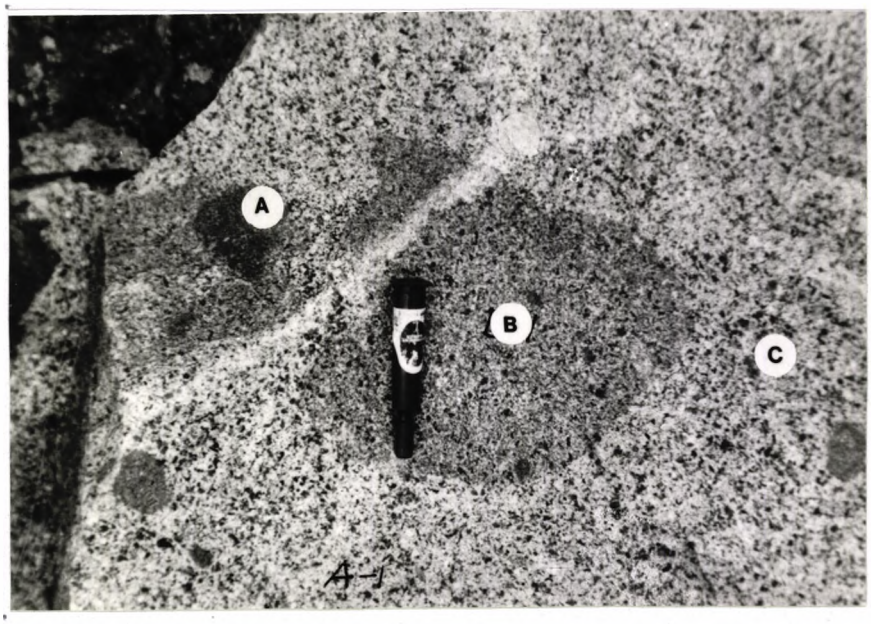

Plate 5.3.2. Enclaves of andesite (A) in the chilled marginal rocks (B), subsequently enclosed by the granodiorite (C), of the Eastern Pluton.

The chilled marginal rocks consist mainly of hornblende and plagioclase phenocrysts set in a fine-grained groundmass of quartz and feldspar. The rocks contain numerous enclaves of volcanics. In some places, composite enclaves occur (plate 5.3.2).

The contact between the chilled marginal rock and the underlying granodiorite is partly gradational and partly intrusive.

The formation of the chilled marginal rock with multiple enclaves along the roof contact of the granitic pluton is well explained by Dier (1973). Thus the part of it that first comes into contact with the country rocks is chilled as a result of quick cooling and encloses some of the fragments of the country rocks as enclaves. However, under the pulsatory pressure of the underlying magma, the first chilled shell is disrupted and allows the granite to advance higher. By this process, the first chilled shell with inclusions can be broken and is incorporated in the normal crystallizing granitic body.

5.4 Petrography

The quartz diorite (outer facies) is a leucocratic medium-grained rock with predominant prismatic hornblende and subordinate biotite. Within the mapped quartz diorite there is a variation in the amount of hornblende, biotite and K-feldspar (table 5.4.1). A plot of the relative proportions of modal quartz, alkali feldspar, plagioclase (Fig. 5.4.1) shows a scatter of points across the fields of quartz diorite and the upper field of diorite and monzodiorite.

The essential minerals are plagioclase, K-feldspar, quartz, hornblende and biotite. Accessory minerals present are magnetite, apatite and zircon. Chlorite and sericite occur as alteration products of the essential minerals. Plagioclase (An_{25-37}) forms euhedral well twinned crystals, and commonly occurs as clusters associated with the mafic minerals. Oscillatory zoning is weakly developed and patchy zoning is very much less developed. Some small twinned plagioclase occur as inclusions in the mafic minerals.

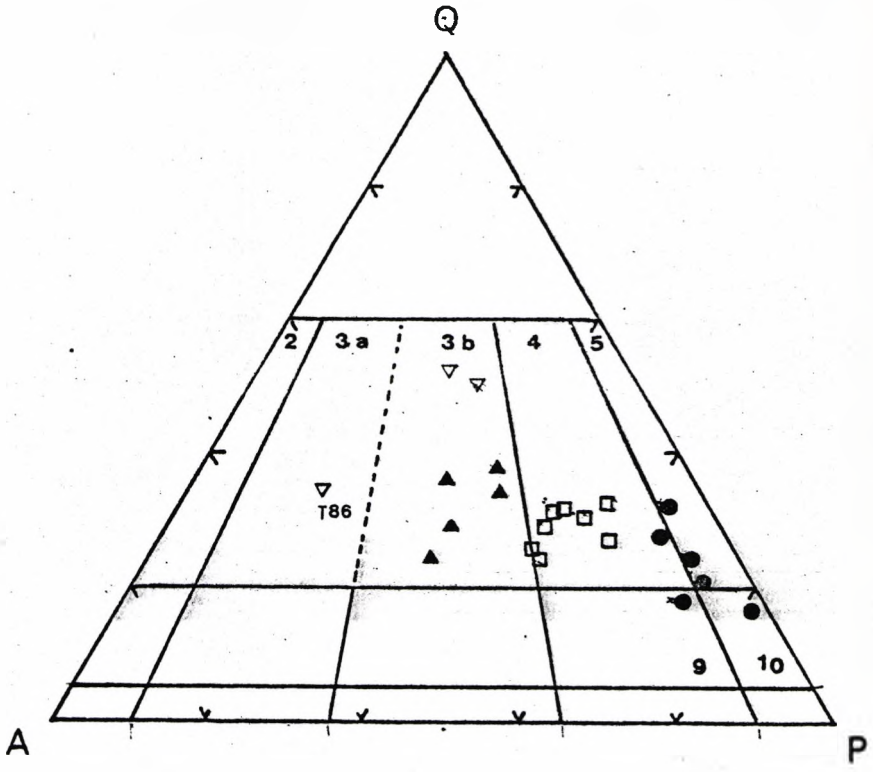

Figure 5.4.1 Classification of the plutonic rocks of the Eastern Pluton (following Streckeisen, 1976).
solid circles - outer facies - quartz-diorite
open squares - transitional facies - granodiorite
solid triangles - inner facies, monzogranite
open triangles - microgranite and aplite(T86).
(calculated from modes in Table 5.4.1)

TABLE 5.4.1

Modes of the rocks from the Eastern Pluton

	outer facies				
	T38b	CTK58	T48	CTK65-1	CTK5
plagioclase	47.84	47.56	54.44	52.21	49.06
k-feldspar	8.66	5.34	5.16	2.56	8.06
quartz	12.43	10.65	19.94	28.83	26.44
hornblende	19.17	23.00	9.75	3.32	7.00
biotite	10.57	12.60	10.69	13.02	8.56
others	1.33	0.85	0.02	0.06	0.88

	transitional facies							
	CTK64	CTK57	T28	T29	CTK1	CTK62-1	CTK47	T73
plagioclase	44.40	43.90	46.79	44.09	40.40	41.38	42.23	43.40
k-feldspar	5.90	16.65	12.11	10.16	15.91	19.50	16.90	19.13
quartz	27.70	20.21	22.26	20.90	25.10	22.06	27.12	27.14
hornblende	7.05	9.33	15.17	18.90	8.00	9.25	5.06	4.00
biotite	14.90	9.70	3.61	5.88	10.55	7.50	8.67	6.00
others	0.05	0.17	0.06	0.07	0.04	0.31	0.06	0.33

	inner facies					micro-granite		aplite
	CTK40	T30	T31	T33	T32	CTK34	T25	T86
plagioclase	34.00	34.50	36.48	33.78	26.25	26.00	24.60	18.00
k-feldspar	32.30	23.13	22.10	36.82	35.12	23.80	26.00	37.00
quartz	26.40	35.40	31.78	20.94	32.69	48.60	47.40	44.00
hornblende	-	0.29	-	-	-	-	-	-
biotite	7.30	6.63	9.45	8.30	5.83	1.10	1.90	1.00
others	0.00	0.05	0.19	0.16	0.11	0.50	0.10	-

	porphyry			
	T76	T23	CTK46	CTK47-2
plagioclase	28.05	27.10	26.00	24.00
quartz	0.20	3.70	2.40	4.60
hornblende	8.50	9.83	8.70	8.00
biotite	0.85	0.90	0.05	0.60
others	0.65	0.27	0.50	0.30
groundmass	61.75	58.20	62.35	62.50

K-feldspar is weakly perthitic and occurs as small anhedral patches interstitial to other minerals. Quartz is very common, typically as late granular aggregates, interstitial to plagioclase and mafic minerals which it characteristically embays. Hornblende (x = pale green, y = z = greenish brown) forms euhedral to subhedral twinned crystals with a well-developed cleavage (plate 5.4.1).

Significantly the hornblende shows no evidence of pyroxene cores which might indicate replacement of earlier pyroxene. This indicates that hornblende occurs as primary magmatic hornblende. Biotite (z = deep brown, y = x = yellow brown) occurs as clusters of large flakes associated with hornblende. Apatite, zircon and magnetite commonly occur as inclusions in biotite.

The granodiorite (transitional facies) is also a leucocratic medium-grained rock but has less abundant hornblende and much more potash K-feldspar than the quartz diorite. A plot showing the relative proportion of modal quartz, alkali feldspar, plagioclase is shown in Fig. 5.4.1).

The essential minerals are plagioclase, K-feldspar, quartz, hornblende and biotite. Accessory minerals are magnetite, apatite and zircon as commonly found in the quartz diorite. Plagioclase (An_{17-25}) occurs as euhedral to subhedral crystals, some of which are zoned, with the development of saussuritized cores. It commonly occurs as individual grains, and zoned crystals usually have albitic rims. K-feldspar occurs as large subhedral to anhedral plates and usually encloses plagioclase and other minerals. Perthite is weakly developed and twinning is very uncommon. Quartz forms large anhedral patches and partly encloses plagioclase, hornblende and biotite. Some small quartz grains are enclosed by K-feldspar. The intergrowth of quartz and K-feldspar is not present in these rocks. Hornblende (x = yellow green, y = z = green) forms euhedral to subhedral crystals, often twinned and usually occurring as clusters with biotite.

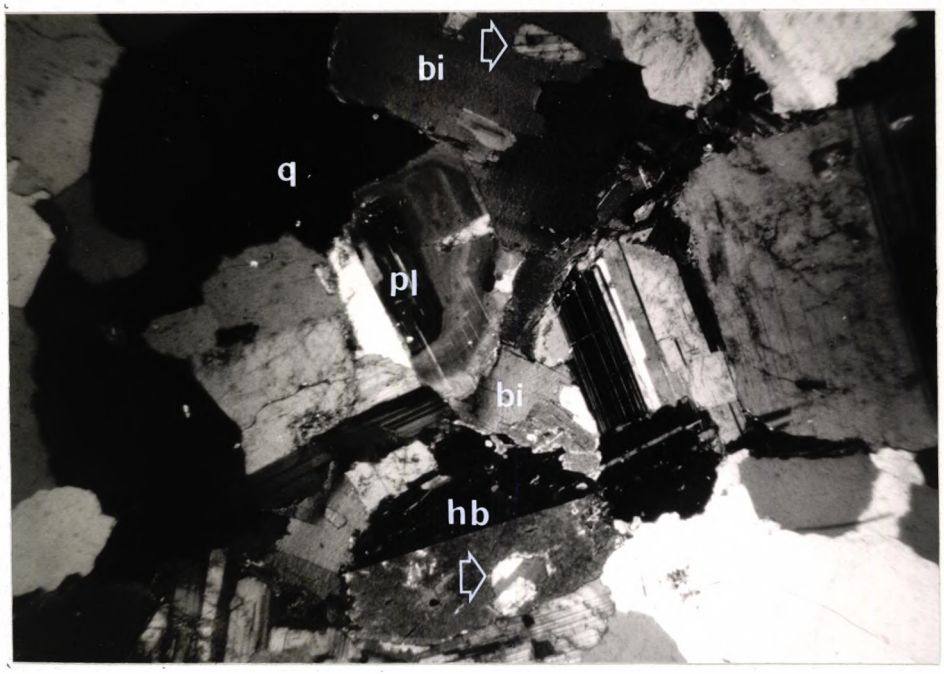

Plate 5.4.1. Photomicrograph of the quartz diorite (outer facies) of the Eastern Pluton, showing clusters of twinned and oscillatory zoned plagioclase (pl) with biotite (bi) and hornblende (hb). Arrows indicate inclusions of plagioclase in hornblende and biotite; quartz (q) occurs as large patches (Sample CTK65, X nicol, 2.5 x 8 x).

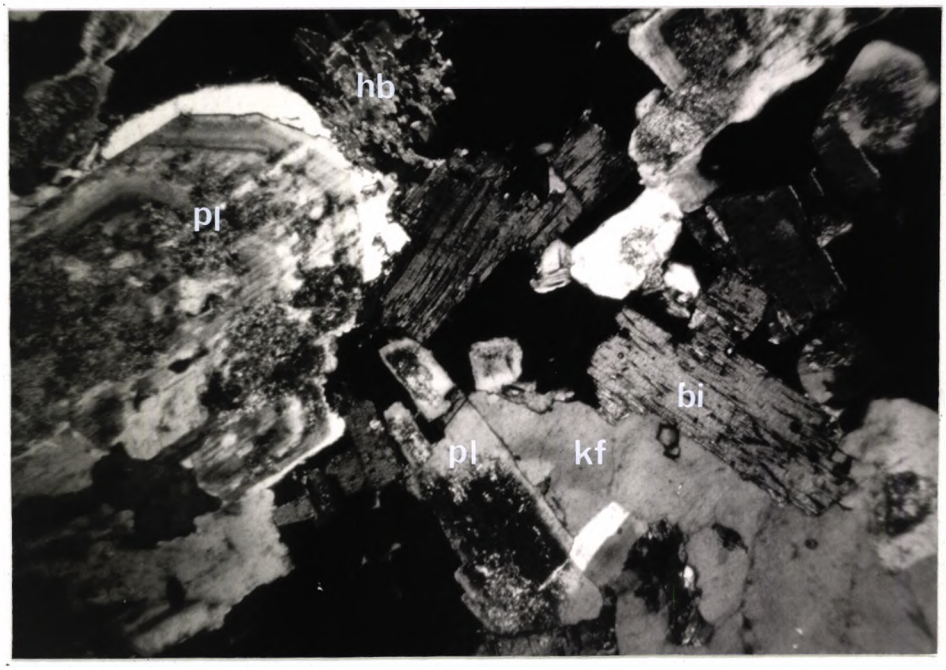

Plate 5.4.2. Photomicrograph of the granodiorite (transitional facies) of the Eastern Pluton, showing large subhedral K-feldspar (Kf) enclosing weakly zoned plagioclase (pl), biotite (bi) and hornblende (hb). (Sample CTK1, X nicol, 2.5 x 8 x).

Hornblende rims commonly show replacement by biotite. Biotite (x = yellow brown, y = z = dark brown), occurs as clustered flakes, some of which are partly enclosed by plagioclase rims. It is commonly altered to chlorite. Accessory minerals of zircon, apatite, magnetite commonly occur as inclusions in biotite or associated with clusters of mafic minerals (plate 5.4.2).

The monzogranite (inner facies) is a leucocratic medium-grained rock which has less abundant mafic minerals compared to the quartz diorite and granodiorite. Modal analyses are given in Table 5.4.1 where it is seen that biotite is predominant over hornblende. A plot showing the relative proportion of quartz-alkali feldspar - plagioclase is shown in Fig. 5.4.1.

The rock consists essentially of plagioclase, K-feldspar, quartz, biotite and some hornblende. Accessories are magnetite, apatite and zircon (plate 5.4.3).

Plagioclase (An_{12-15}) occurs mostly as discrete small euhedral to subhedral crystals. Plagioclase crystals are partly surrounded or poikilitically enclosed in K-feldspar. K-feldspar is microcline perthite and occurs as large subhedral to anhedral twinned grains. Myrmekitic intergrowths commonly develop along the contact of K-feldspar and plagioclase grains. Large K-feldspar grains commonly enclose other minerals. Quartz occurs both as large patches and as aggregates of small grains interstitial to plagioclase and K-feldspar. Biotite (x = yellow brown, y = z = brown) occurs as small flakes, and is intensely chloritized. Hornblende (x = pale green, y = z = deep green) occurs as subhedral twinned crystals. It is strongly altered and less common in these rocks. Accessory magnetite, apatite and zircon commonly occur in aggregates or as inclusions in mafic minerals.

Aplite and microgranite occur as leucocratic fine-grained rocks and

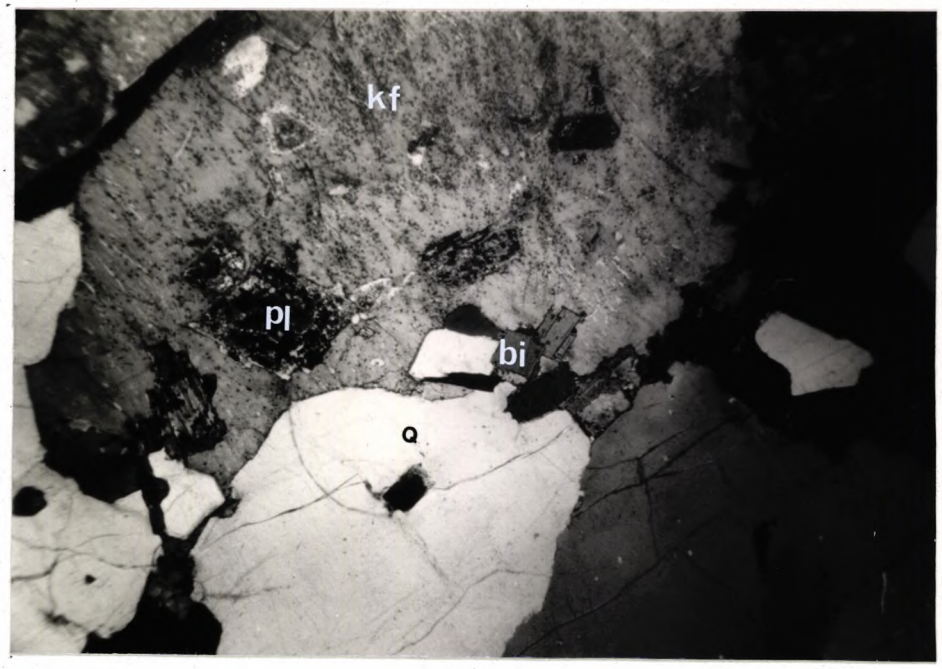

Plate 5.4.3. Photomicrograph of the monzogranite (inner facies) of the Eastern Pluton, showing large anhedral K-feldspar (Kf) enclosing biotite (bi), plagioclase (pl), quartz (q) forms large anhedral patches. (Sample T33, X nicol, 2.5 x 8 x).

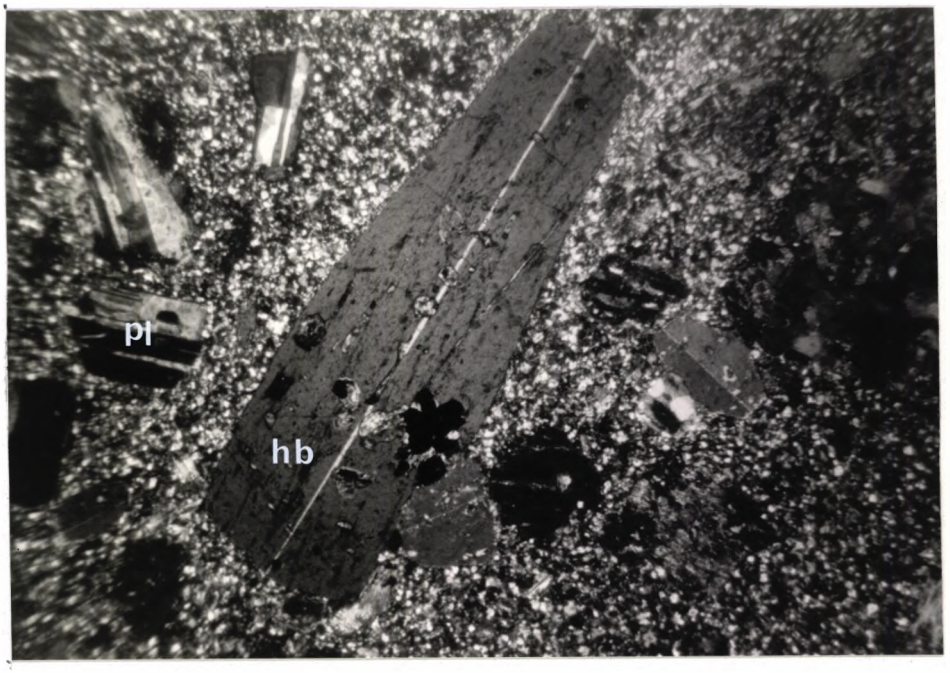

Plate 5.4.4. Photomicrograph of the porphyry (chilled marginal rock) of the Eastern Pluton, showing phenocrysts of hornblende (hb) and plagioclase (pl) set in a fine grained quartz and feldspar groundmass. (Sample T23, X nicol, 2.5 x 8 x).

are composed mainly of quartz and feldspar with minor amounts of biotite. A plot showing the relative proportion of modal quartz, alkali feldspar - plagioclase is shown in Fig. 5.4.1.

In thin section, plagioclase (An_{5-7}) occurs as twinned subhedral crystals, and they are usually altered to sericite. Some small plagioclase crystals are poikilitically enclosed in K-feldspar. Large plagioclase crystals have irregular rims and are partly embayed by quartz and K-feldspar. K-feldspar is microcline perthite and occurs as large irregular grains. Graphic intergrowths of quartz and K-feldspar are common. Quartz occurs as large clear patches. Some small quartz grains occur as inclusions in K-feldspar. Biotite (x = y = z = pale brown) occurs as discrete small flakes and is usually chloritized.

The porphyry is a prophyritic rock with phenocrysts of dark green stubby hornblende 2-5 mm in length and feldspar set in a fine-grained matrix of quartz and feldspar.

In thin section, it is composed of phenocrysts of hornblende, biotite, plagioclase and quartz, set in a fine-grained matrix of quartz and alkali feldspar (plate 5.4.4).

Plagioclase (An_{20-28}) occurs mostly as discrete crystals with corroded rims. Zoned plagioclase crystals are strongly saussuritized. Hornblende (x = yellow brown, y = z = greenish brown) occurs as large, discrete, twinned prismatic crystals. Some hornblende is replaced by biotite and is usually altered to chlorite. Inclusions in hornblende are mostly magnetite.

Biotite (x = y = z = yellow brown), occurs as small flakes and is intensely altered to chlorite.

Quartz occurs as large corroded grains. Granophyric intergrowths are commonly developed along the contact of quartz grain and the groundmass.

The groundmass consists chiefly of fine-grained quartz and alkali feldspar.

Summary:-

The important points gained from petrographic studies of the components of the Eastern Pluton are as follows:-

1. Hornblende is the predominant mafic mineral in the quartz diorite, and granodiorite, and becomes a subordinate mineral to biotite in the monzogranite. Pyroxene does not occur in any component of the Eastern Pluton.
2. Plagioclase in the quartz diorite occurs as clusters of zoned and twinned crystals whereas it occurs as discrete weakly zoned crystals in the granodioritic and monzogranite. Patchy zoned plagioclase does not occur in the Eastern Pluton.
3. K-feldspar changes from small interstitial grains in quartz diorite to large untwinned poikilitic microcline perthite in the granodiorite and to large twinned well developed microcline perthite in the monzogranite.
4. Magnetite, apatite and zircon are the only common accessories in all rocks of the Eastern Pluton. Sphene and allanite are not present in these rocks.

5.5 Chemical characteristics

5.5.1 Major elements

The analysed samples from the Eastern Pluton show a range of SiO_2 values varying from 57-76 wt% (Table 5.5.1).

Consideration of the analysed samples plotted on the Fe-(Na^+K)-Mg and Ca-Na-K ternary diagrams (Fig. 5.5.1a) shows that Mg, Fe and Ca decreases while Na and K increase from the quartzdiorite of the outer facies, through the granodiorite of the transitional facies to the monzogranite of the inner facies.

The plots for the microgranites and aplite in these diagrams show that the microgranites are closely related to the monzogranites, whereas the aplite is very different and close to the Na apex.

The plots for the porphyrites show that they closely relate to the granodiorites of the transitional facies.

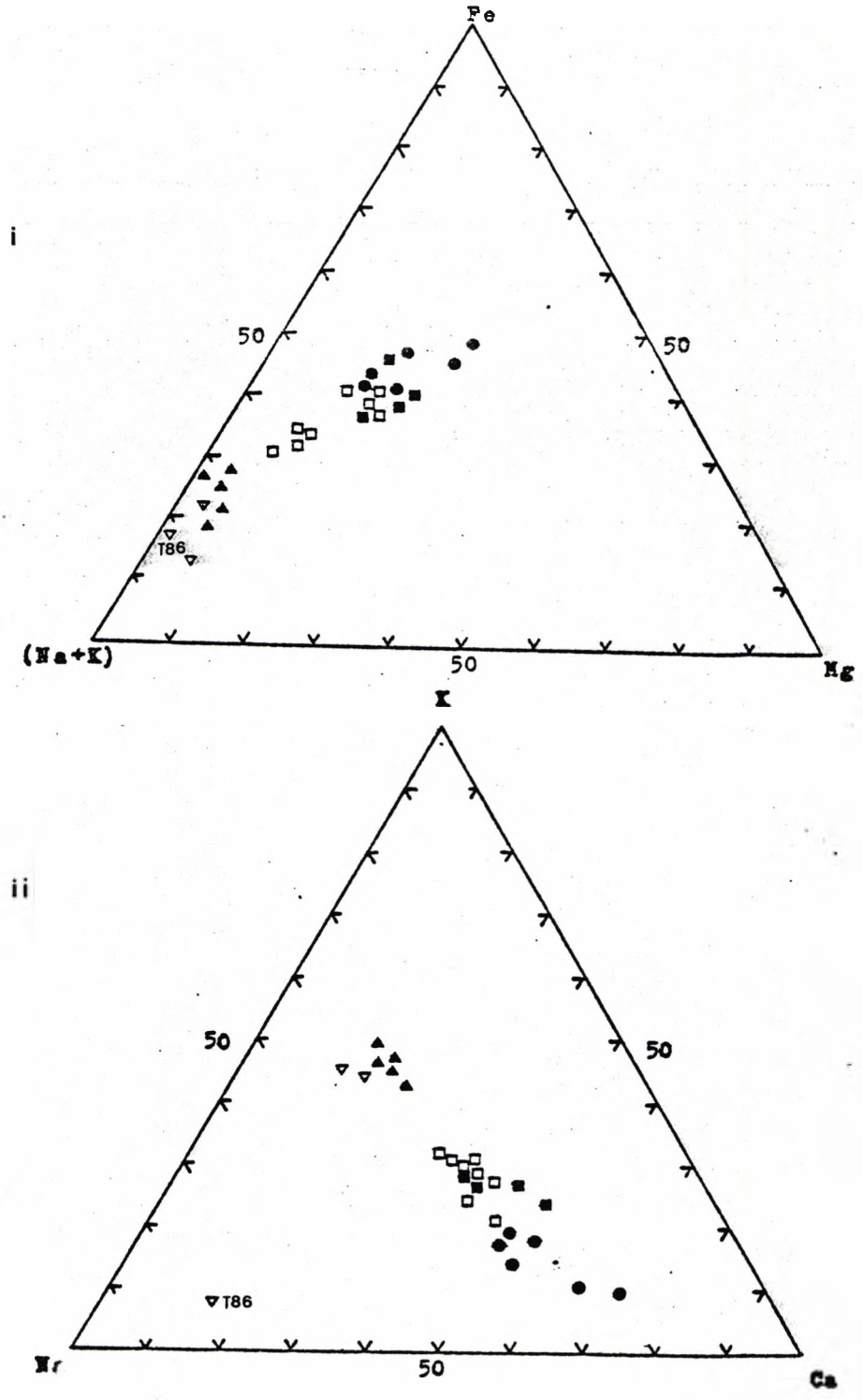

Figure 5.5.1a Triangular plots of the plutonic rocks of the Eastern Pluton. Symbols as follows:
solid circles - outer facies - quartz-diorite
open squares - transitional facies - granodiorite
solid triangles - inner facies - monzogranite
open triangles - microgranite and aplite (T86)
solid squares - porphyry

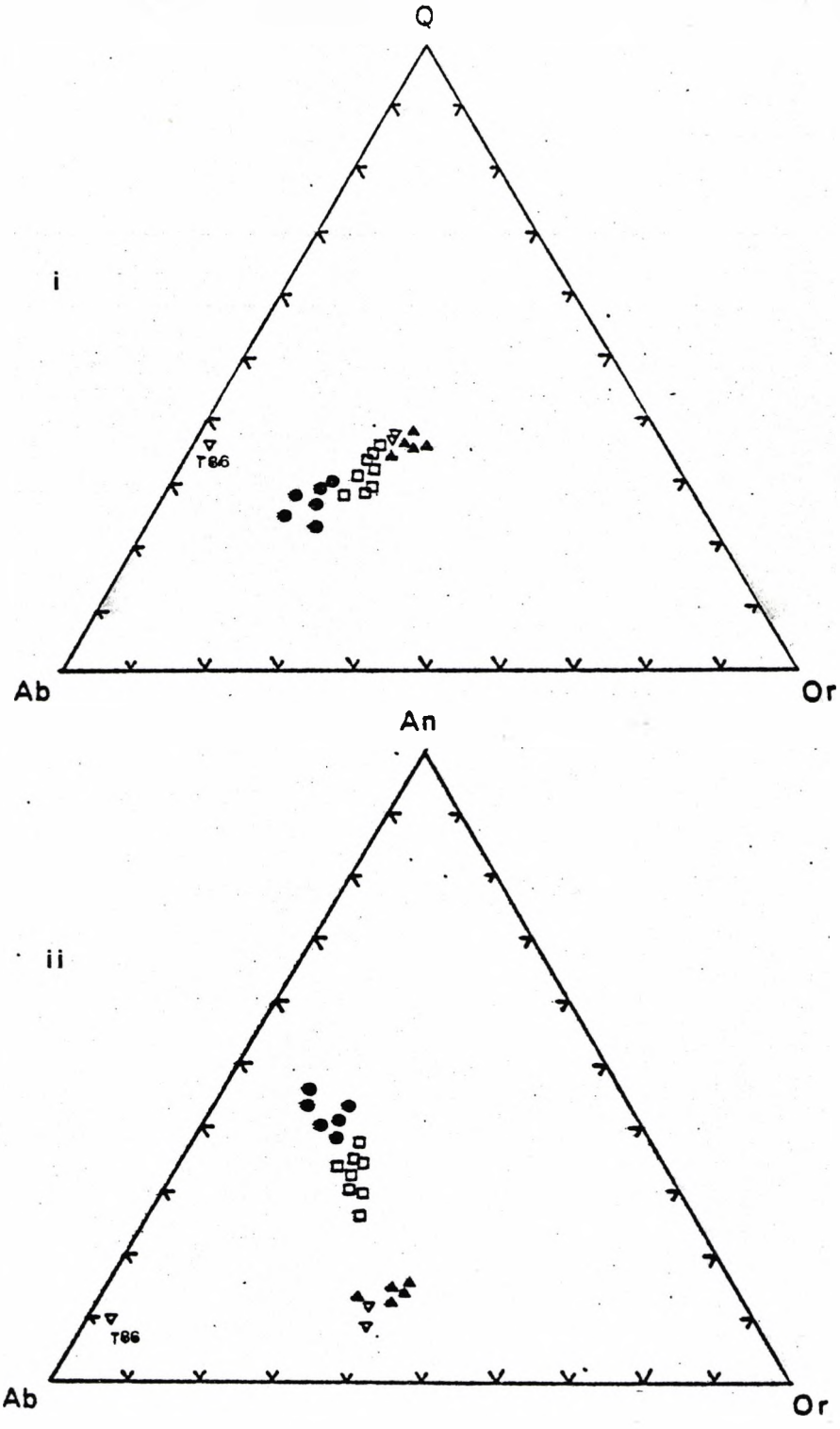

Figure 5.5.1b Triangular plots of the plutonic rocks of the Eastern Pluton. Symbols as follows:
solid circles - outer facies - quartz-diorite
open squares - transitional facies - granodiorite
solid triangles - inner facies - monzogranite
open triangles - microgranite and aplite (T86)
(calculated from C.I.P.W. norms in Table 5.5.2).

TABLE 5.5.1

Analyses of the rocks from the Eastern Pluton

	outer facies				
Sample	T38b	CTK58	T48	CTK65-1	CTK5
SiO_2	57.16	57.16	60.12	60.73	62.03
TiO_2	0.85	0.95	0.58	0.73	0.66
Al_2O_3	18.25	16.90	18.59	17.04	16.47
Fe_2O_3	2.34	0.13	0.27	0.34	1.57
FeO	4.69	6.59	4.56	4.99	3.54
MnO	0.14	0.12	0.10	0.11	0.09
MgO	2.66	3.29	1.94	2.60	2.61
CaO	6.35	6.69	6.41	5.56	5.28
Na_2O	3.38	2.95	3.66	3.26	2.91
K_2O	1.47	1.96	1.50	1.97	2.43
P_2O_5	0.23	0.23	0.15	0.15	0.14
Ba	381	556	372	527	511
Ce	27	63	26	34	36
Co	55	91	46	105	152
Cr	39	37	27	31	42
La	12	38	13	21	14
Nd	20	31	16	18	44
Ni	0	6	6	8	0
Pb	55	21	23	20	62
Rb	58	81	52	92	99
Sc	18	24	14	12	15
Sr	332	381	375	517	331
Th	9	22	10	10	36
Ti	4816	5107	3262	3761	3602
U	-	4	-	-	-
V	112	150	73	101	100
Y	21	31	21	18	23
Zn	82	75	78	66	57
Zr	191	132	177	118	127

TABLE 5.5.1

(continued)

	transitional facies							
Sample	CTK64	CTK57	T28	T29	CTK1	CTK62-1	CTK47	T73
SiO_2	62.66	62.68	62.27	60.41	64.35	67.19	67.07	66.25
TiO_2	0.64	0.47	0.17	0.19	0.51	0.42	0.49	0.45
Al_2O_3	16.63	15.97	16.74	15.97	16.31	15.33	15.13	16.08
Fe_2O_3	0.33	0.87	1.32	2.70	0.06	0.28	0.53	0.89
FeO	4.37	3.99	3.73	3.79	3.90	3.09	3.28	2.70
MnO	0.10	0.09	0.09	0.09	0.07	0.06	0.07	0.06
MgO	2.41	3.05	3.54	3.87	1.95	1.43	1.64	1.56
CaO	5.42	4.50	3.81	5.31	4.50	3.81	3.84	4.07
Na_2O	3.25	3.47	3.05	2.96	3.41	3.51	3.23	3.20
K_2O	1.73	2.43	2.74	2.63	2.96	3.12	2.92	2.89
P_2O_5	0.14	0.13	0.15	0.13	0.10	0.09	0.11	0.12
Ba	499	607	515	482	495	559	566	570
Ce	56	38	40	49	37	45	57	54
Co	77	22	69	69	75	75	103	63
Cr	30	69	134	120	40	32	37	30
La	11	24	20	19	22	26	34	23
Nd	16	22	23	26	22	24	30	27
Ni	8	15	24	27	8	8	8	7
Pb	18	26	14	16	27	24	25	21
Rb	84	98	116	109	124	132	120	118
Sc	12	14	21	20	13	10	14	12
Sr	399	305	249	219	205	231	224	252
Th	8	15	11	15	16	18	22	12
Ti	3425	2912	3914	4143	2716	2345	2715	2641
U	-	-	-	4	-	-	-	2
V	89	92	118	119	70	55	61	60
Y	18	23	19	23	28	27	29	28
Zn	57	64	55	57	45	37	44	48
Zr	124	134	103	134	136	126	138	135

TABLE 5.5.1

(continued)

	inner facies					micro-granite		aplite
Sample	CTK40	T30	T31	T33	T32	CTK34	T25	T86
SiO_2	71.82	69.44	71.34	70.73	74.45	73.41	73.73	75.59
TiO_2	0.28	0.34	0.28	0.30	0.21	0.22	0.16	0.18
Al_2O_3	14.09	14.99	14.28	14.55	11.35	13.49	13.65	13.30
Fe_2O_3	0.26	1.32	0.89	0.95	1.09	0.32	0.47	0.92
FeO	2.35	2.11	1.79	2.17	1.31	1.99	1.33	0.28
MnO	0.06	0.15	0.06	0.06	0.06	0.05	0.04	0.03
MgO	0.70	0.77	0.71	0.67	0.49	0.53	0.24	0.69
CaO	1.97	1.87	1.99	2.15	2.03	1.83	1.36	1.43
Na_2O	3.16	3.87	3.26	3.35	3.42	3.59	4.06	6.47
K_2O	4.11	3.74	4.24	4.02	4.80	3.84	4.13	0.35
P_2O_5	0.08	0.09	0.08	0.10	0.08	0.06	0.04	0.04
Ba	674	1138	752	802	933	652	489	39
Ce	39	67	41	59	40	36	41	64
Co	94	79	107	109	116	128	102	140
Cr	20	14	16	16	7	12	9	7
La	19	38	22	24	21	20	19	45
Nd	21	32	37	32	21	22	24	24
Ni	8	0	4	5	5	3	2	4
Pb	32	127	98	26	40	29	29	21
Rb	163	137	176	179	146	163	167	20
Sc	6	8	5	9	5	4	4	1
Sr	192	205	127	197	226	145	100	233
Th	15	68	54	13	10	20	31	64
Ti	1614	2004	1574	1778	221	1297	935	1034
U	-	-	-	2	-	-	8	-
V	31	34	27	32	20	22	13	12
Y	26	34	30	34	26	29	41	18
Zn	33	103	37	67	37	23	26	2
Zr	133	183	150	148	102	114	109	134

TABLE 5.5.1

(continued)

	porphyry			
Sample	T76	T23	CTK46	CTK47-2
SiO_2	57.86	63.34	61.61	64.13
TiO_2	0.70	0.69	0.56	0.56
Al_2O_3	17.01	16.21	16.30	16.17
Fe_2O_3	2.82	1.67	0.48	0.63
FeO	4.54	3.81	5.46	4.21
MnO	0.13	0.02	0.09	0.09
MgO	3.94	2.55	2.98	1.69
CaO	5.53	4.09	4.76	4.25
Na_2O	2.70	3.18	3.19	3.61
K_2O	2.52	2.71	2.42	2.90
P_2O_5	0.17	0.16	0.15	0.18
Ba	533	575	529	530
Ce	48	48	34	39
Co	37	37	48	79
Cr	56	42	53	31
La	18	23	19	20
Nd	28	25	20	26
Ni	15	12	16	6
Pb	17	16	24	23
Rb	91	102	94	139
Sc	21	14	16	10
Sr	298	373	318	265
Th	5	9	14	15
Ti	4478	3294	3281	3102
U	-	-	-	-
V	138	94	98	63
Y	24	26	21	33
Zn	76	54	53	54
Zr	142	118	124	160

TABLE 5.5.2

C.I.P.W. norms of the rocks from the Eastern Pluton

	outer facies				
Sample	T38b	CTK58	T48	CTK65-1	CTK5
Q	14.82	10.79	14.67	15.39	19.17
Or	8.75	11.88	9.04	11.64	14.36
Ab	28.60	25.55	31.56	27.58	24.62
An	30.00	27.74	30.08	26.05	24.71
Le	-	-	-	-	-
Ne	-	-	-	-	-
C	0.09	-	0.14	-	-
Ac	-	-	-	-	-
DiCa	-	1.95	-	0.23	0.24
DiMg	-	0.89	-	0.10	0.14
DiFe	-	1.04	-	0.13	0.09
Wo	-	-	-	-	-
HyMg	6.62	7.50	4.91	6.37	6.36
HyFe	0.21	8.77	6.86	7.75	4.19
ClMg	-	-	-	-	-
OlFe	-	-	-	-	-
Mt	6.29	1.51	1.28	0.49	2.28
He	-	-	-	-	-
Il	1.61	1.84	1.12	1.39	1.25
Ap	0.53	0.56	0.35	0.35	0.32

TABLE 5.5.2

(continued)

	transitional facies							
Sample	CTK64	CTK57	T28	T29	CTK1	CTK62-1	CTK47	T73
Q	19.25	16.78	16.85	15.93	19.00	22.95	24.55	24.30
Or	10.22	14.36	16.19	15.54	17.73	18.44	17.26	17.08
Ab	27.50	29.36	25.80	21.04	29.27	29.70	27.33	27.07
An	25.68	20.83	21.17	21.43	20.83	16.59	18.17	19.41
Le	-	-	-	-	-	-	-	-
Ne	-	-	-	-	-	-	-	-
C	-	-	-	-	-	-	-	0.58
Ac	-	-	-	-	-	-	-	-
DiCa	0.12	0.27	0.69	1.20	0.50	0.72	0.07	-
DiMg	0.06	0.15	0.41	0.82	0.22	0.30	0.03	-
DiFe	0.06	0.12	0.25	0.29	0.28	0.42	0.04	-
Wo	-	-	-	-	-	-	-	-
HyMg	5.95	7.45	8.40	8.82	4.46	3.26	4.05	3.96
HyFe	6.82	5.88	5.06	3.12	5.72	4.44	4.87	3.34
OlMg	-	-	-	-	-	-	-	-
OlFe	-	-	-	-	-	-	-	-
Mt	0.48	1.26	2.51	4.52	0.77	0.41	0.77	1.73
He	-	-	-	-	-	-	-	-
Il	1.22	0.89	0.32	1.31	0.99	0.80	0.93	0.85
Ap	0.32	0.30	0.35	0.72	0.23	0.21	0.25	0.28

TABLE 5.5.2

(continued)

	inner facies					micro-granite		aplite
Sample	CTK40	T30	T31	T33	T32	CTK34	T25	T86
Q	30.97	26.58	30.05	29.26	32.51	31.87	30.36	32.78
Or	24.29	22.10	25.06	23.76	28.37	22.69	24.41	2.07
Ab	26.73	32.74	27.58	28.34	28.93	30.37	34.35	54.74
An	9.25	8.69	9.35	10.01	1.45	8.69	6.49	6.22
Le	-	-	-	-	-	-	-	-
Ne	-	-	-	-	-	-	-	-
C	1.05	1.34	0.90	1.02	-	0.25	0.13	-
Ac	-	-	-	-	-	-	-	-
DiCa	-	-	-	-	-	-	-	0.26
DiMg	-	-	-	-	-	-	-	0.22
DiFe	-	-	-	-	-	-	-	-
Wo	-	-	-	-	-	-	-	-
HyMg	1.74	1.92	1.77	1.67	-	1.32	0.60	1.50
HyFe	3.75	2.50	2.20	2.82	-	3.12	1.74	-
OlMg	-	-	-	-	-	-	-	-
OlFe	-	-	-	-	-	-	-	-
Mt	0.38	1.91	1.29	1.38	1.58	0.46	0.90	0.48
He	-	-	-	-	-	-	-	0.59
Il	0.53	0.65	0.53	0.57	0.40	0.42	0.30	0.34
Ap	0.09	0.21	0.19	0.23	0.19	0.14	0.09	0.09

TABLE 5.5.2

(continued)

	porphyry			
Sample	T76	T23	CTK46	CTK47-2
Q	13.12	20.28	15.50	18.10
Or	14.89	16.02	14.36	17.14
Ab	22.84	29.90	26.99	30.54
An	26.32	19.31	22.64	19.36
Le	-	-	-	-
Ne	-	-	-	-
C	0.19	0.97	0.13	-
Ac	-	-	-	-
DiCa	-	-	-	0.23
DiMg	-	-	-	0.09
DiFe	-	-	-	0.14
Wo	-	-	-	-
HyMg	9.81	6.35	7.42	4.12
HyFe	4.73	4.51	8.87	6.31
OlMg	-	-	-	-
OlFe	-	-	-	-
Mt	4.09	2.42	0.70	0.91
He	-	-	-	-
Il	1.33	1.31	1.06	1.06
Ap	0.39	0.35	0.35	0.42

Consideration of the ternary plots of Q-An-Or and An-Ab-Or (Fig. 5.5.1b), calculated from the CIPW norms given in Table 5.5.2 for the analysed samples of the Eastern Pluton, shows that normative quartz and orthoclase increase at the espense of albite (Fig. 5.5.1b - i), and anorthite increases (Fig. 5.5.1b - ii) from quartzdiorite through granodiorite to the monzogranite (compare with Petrography Section 5.4). The same diagrams (Fig. 5.5.1b), show that the plotted points for the microgranites are close to those of monzogranite, whereas the plotted point for the aplite indicates very high normative albite and quartz and little else.

In brief, all the diagrams for this pluton, show good trends in major elements, similar to many other zones plutons (Atherton 1981), with an apparent calc-alkali trend on the Fe-(Na+K)-Mg diagram.

5.3.2 Trace elements

Cobalt

Co varies from 55 ppm to 103 ppm from quartzdiorite to monzogranite and shows a slight positive correlation with DI (Fig. 5.5.2a). Co^{2+} (radius = 0.72Å) in the iron-magnesium bearing-minerals rather than Mg (Mg^{+2} radius = 0.65Å.

The decrease in modal content of hornblende from quartz diorite to monzogranite (Table 5.4.1) may be reflected in the increase in Co. The minor intrusions, aplite and microgranite contain similar levels of Co. (102-140 ppm) to the monzogranite. The porphyries have much the same concentration as the granodiorite.

The co content in the rocks of the Eastern Pluton is relatively high compared with Wager and Mitchell's (1951) 40 and 10 ppm for the Caledonian intermediate and acid plutonics.

Chromium and Nickel

Ni varies from 27 ppm to 4 ppm and Cr varies from 134 ppm to 14 ppm in quartzdiorite to monzogranite, showing negative correlation with DI

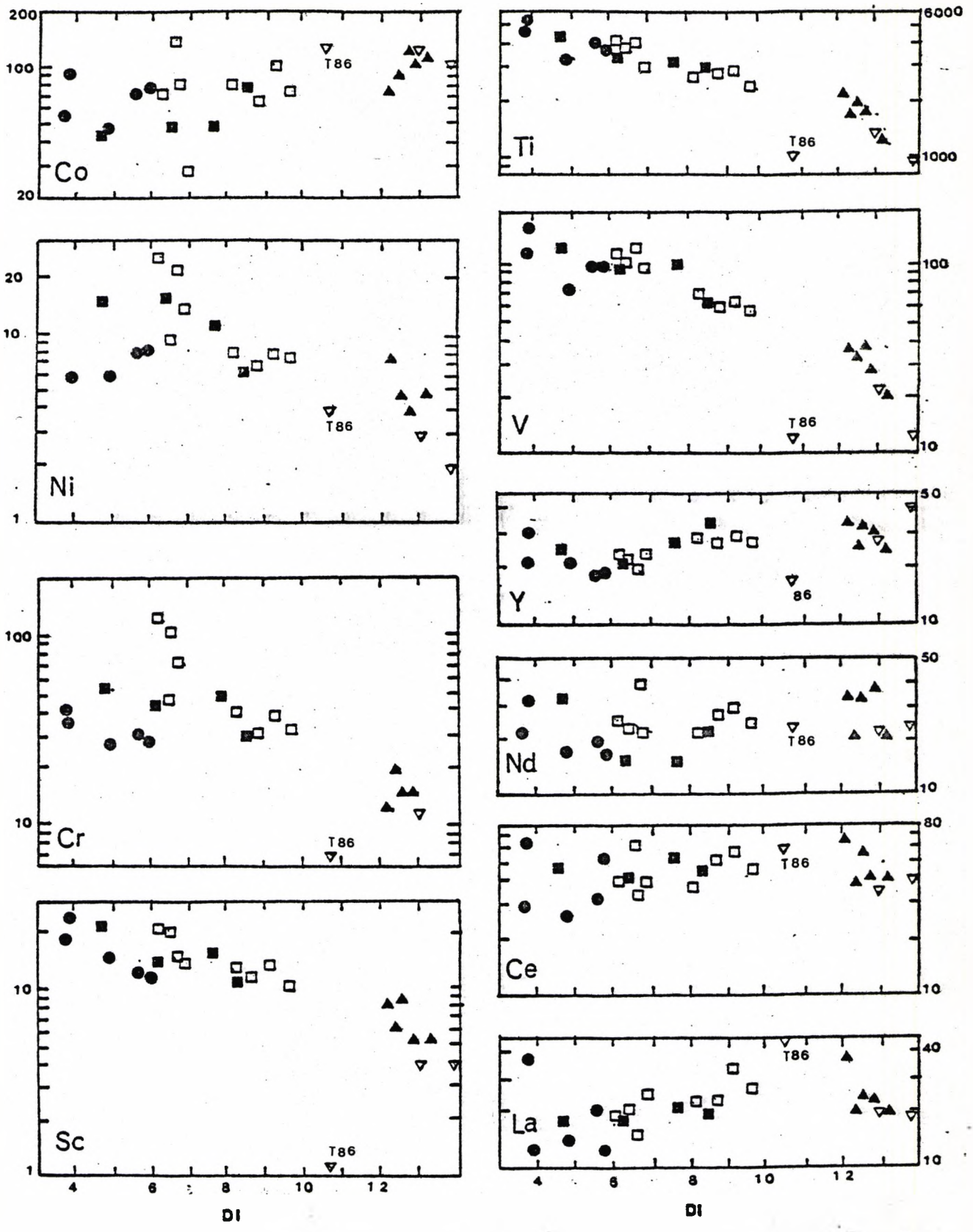

Figure 5.5.2a Plots of trace element content vs. Differentiation Index for the plutonic rocks of the Eastern Pluton.
Symbols as follows:
solid circles - outer facies - quartz diorite
open squares - transitional facies - granodiorite
solid triangles - inner facies - monzogranite
open triangles - microgranite and aplite (T86)
solid squares - porphyry

(Fig. 5.5.2a). Ni^{+2} (radius = 0.69Å) and Cr^{+3} (radius = 0.63Å) preferentially replace Fe^{+2} (radius = 0.74Å) rather than Mg^{+2} (radius = 0.65Å). Therefore, Ni^{+2} and Cr^{+3} are preferentially incorporated in iron bearing-minerals, viz hornblende, compared to magnesium bearing minerals. Thus the fractionation of hornblende causes Ni and Cr to be depleted in the liquid. Aplite and microgranites contain contents of Ni (2-4 ppm) and Cr (7-12 ppm) similar to the monzogranite. The porphyries have much the same concentration of Cr and Ni as the granodiorite.

Ni contents in the Eastern Pluton are similar to Wager and Mitchell's (1951) 20 ppm for the Caledonian acid plutonics and Teggin's (1975) 10-35 ppm for some Triassic granites in North Thailand.

Cr contents in the Eastern Pluton are also closely similar to Teggin's (1975) 10-60 ppm for the Triassic granites in North Thailand.

Scandium and Vanadium

Sc varies from 24 ppm to 4 ppm and V varies from 150 ppm to 20 ppm in quartzdiorite through granodiorite to monzogranite. The variation of these elements shows a negative correlation with DI (Fig. 5.5.2a).

Both Sc and V are strongly concentrated in the ferromagnesian minerals presumably substituting for Fe^{+3} (Curtis, 1964), and the highest concentrations occur in hornblende, and to a lesser extent in augite (Ewart and Taylor, 1969).

In the case of the Eastern Pluton, the decrease in hornblende (see modal data, Table 5.4.1) from quartzdiorite through granodiorite to monzogranite is reflected in the decrease of Sc and V. This is compatible with the extraction of these elements by hornblende during fractionation and emphasises their compatible character. The aplite and microgranite contain lower concentrations of Sc and V than the monzogranite. The porphyries have much the same concentration of these elements as the granodiorite.

Lanthanum, Cerium and Neodymium

La varies from 12 ppm to 38 ppm; Ce varies from 29 ppm to 67 ppm; and Nd varies from 20 ppm to 37 ppm in the sequence quartzdiorite through granodiorite to monzogranite. All of these trace elements increase slightly with increasing DI (Fig. 5.5.2a). The aplite and microgranites have much the same concentration as the monzogranite, whereas the porphyries have much the same concentration as the granodiorite.

Accessory minerals, viz. sphene, allanite, xenotime and monazite are the main sources of La, Ce and Nd in granitic rocks (Condie, 1978). These elements are also contained in small amounts of zircon and other minerals. The slight increase in LREE concentration with increasing DI in the rocks of the Eastern Pluton may be related to a lack of crystallisation of LREE-bearing minerals as noted in the petrographic observations on these rocks (see Section 5.4). Clearly the LREE's behave uncompatibly in this pluton.

The positive correlation of the content with DI and K in the Eastern Pluton can be related to the increase of K-feldspar from quartzdiorite through granodiorite to monzogranite as indicated in the modal data (Table 5.4.1). Sphene and allanite are not present in these rocks (as stated in the Section 5.4); so the increase cannot be due to the enrichment often due to the presence of these minerals (Smith et al. 1957).

Titanium and Zirconium

Ti varies from 4816 ppm to 1574 ppm in quartzdiorite through granodiorite to monzogranite showing negative correlation with DI (Fig. 5.5.2a). The aplite and microgranite contain lower Ti contents (935-1295 ppm) than the monzogranite.

Zr varies from 191 ppm to 102 ppm in quartzdiorite through granodiorite to monzogranite and varies very little with the increase of DI (Fig. 5.5.2b). The aplite and microgranite have much the same concentration of Zr as the monzogranite. The porphyries contain contents of Ti (3102-4478 ppm) and

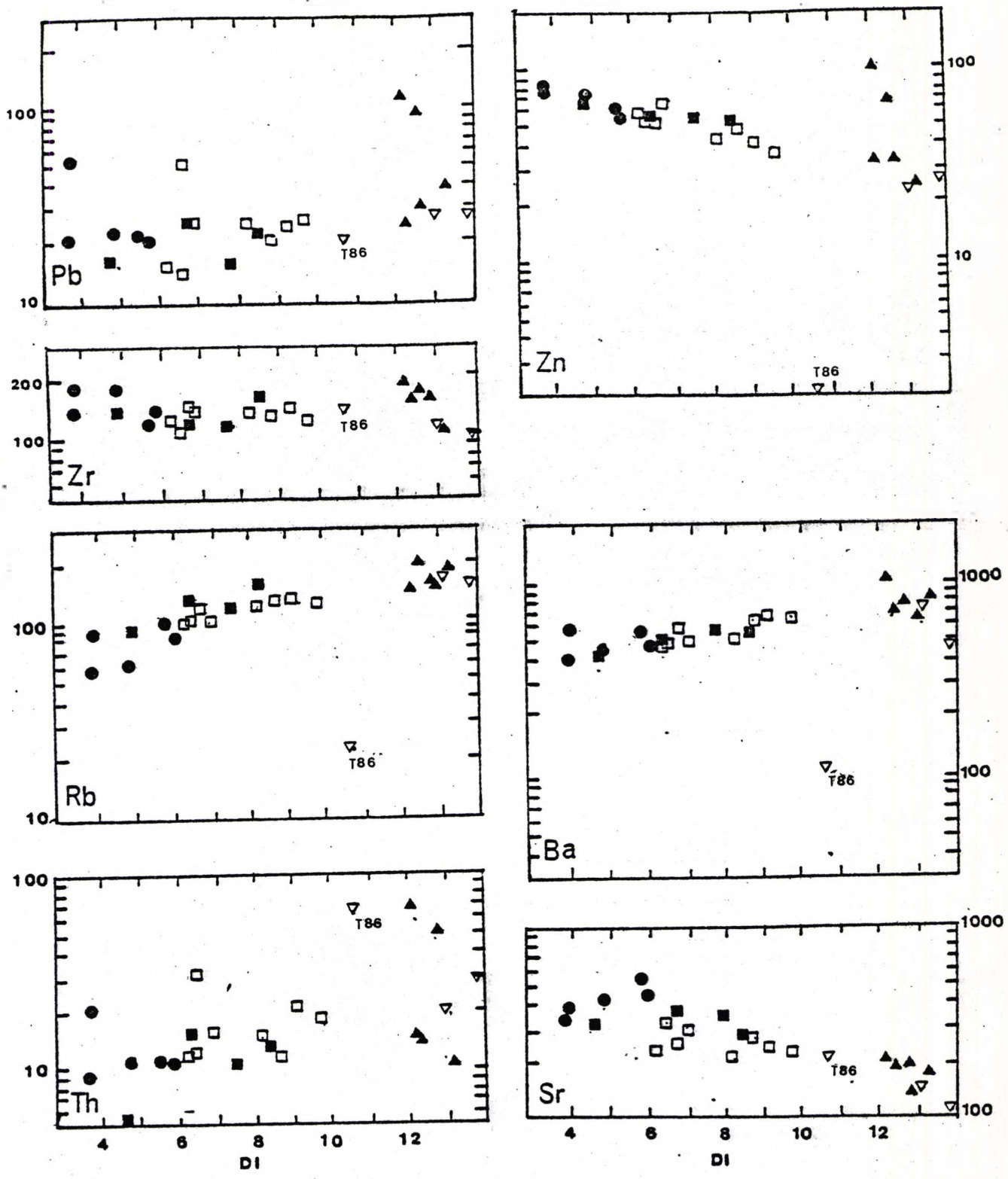

Figure 5.5.2b Plots of trace element content vs. Differentiation Index for the plutonic rocks of the Eastern Pluton.
Symbols as follows:
solid circles - outer facies - quartz diorite
open squares - transitional facies - granodiorite
solid triangles - inner facies - monzogranite
open triangles - microgranite and aplite(T86)
solid squares - porphyry

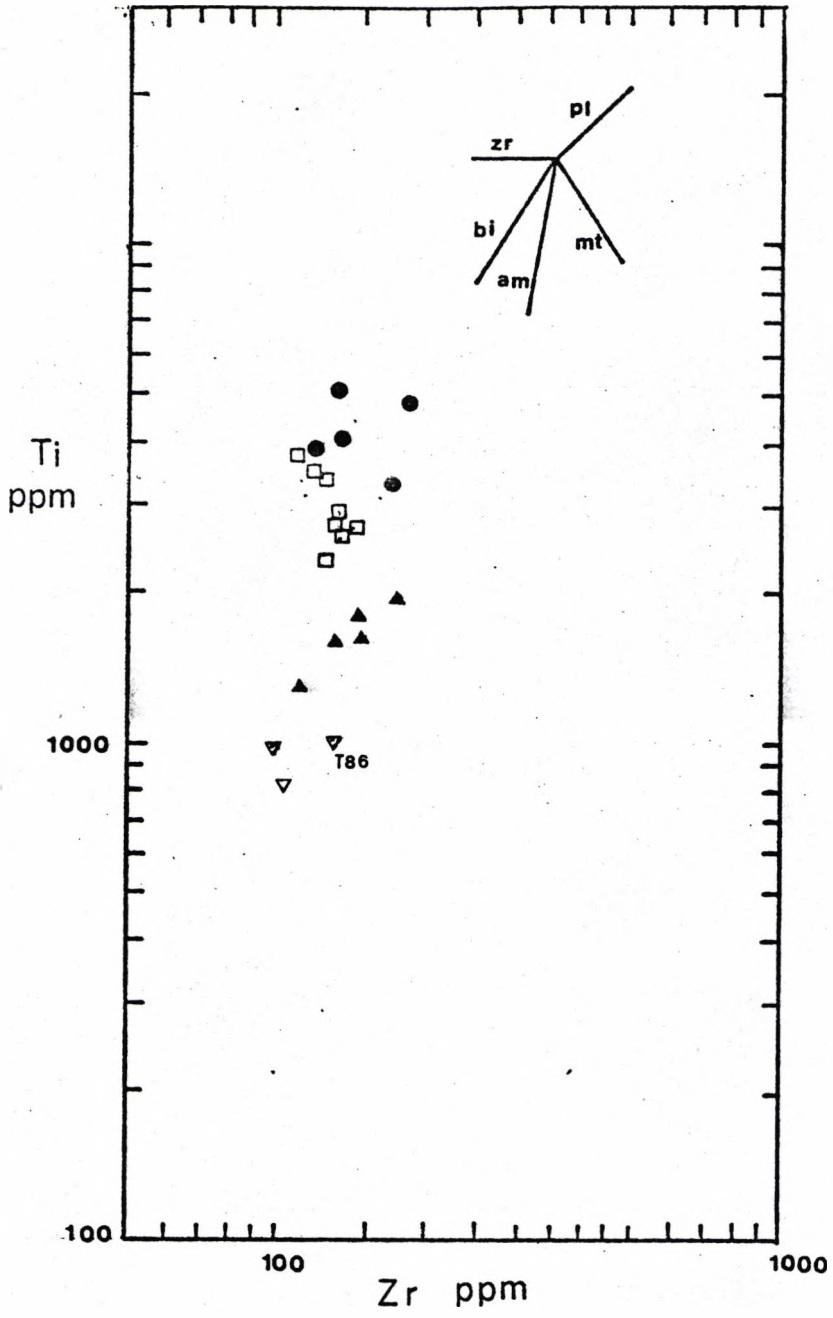

Figure 5.5.2c Plot of Ti vs. Zr for the plutonic rocks of the Eastern Pluton. Symbols as follows:-
solid circles - outer facies - quartz diorite
open squares - transitional facies - granodiorite
solid triangles - inner facies - monzogranite
open triangles - microgranite and aplite (T86)
The mineral vectors shown are taken from Pearce and Narry (1979) and indicate the relative change in these elements upon extraction of each mineral.
bi = biotite; am = hornblende; mt = magnetite;
pl = plagioclase; zr = zircon.

Zr (118-160 ppm) similar to the granodiorite. The high field strength elements Zr^{+4} and Ti^{+4} can form complex ions in magmas (Ringwood, 1955b). Zircon is the main source of Zr^{+4}, while hornblende, biotite, magnetite and ilmenite are common Ti-bearing minerals.

Plots of Ti versus Zr (Fig. 5.5.2c) show a strong decrease of Ti with a slight decrease of Zr from quartzdiorite through granodiorite to monzogranite. The mineral vectors for Ti-Zr are similar to those proposed by Pearce & Norry (1979) and are superimposed on this diagram, and indicate that strong fractionation of biotite, hornblende, $\pm$ magnetite, $\pm$ zircon can cause a sharp decrease in Ti in the liquid, and the slight decrease in Zr. Notably the data allow a variety of crystallising options, and the likely ores will be discussed later.

Thorium

Th varies from 9 ppm to 68 ppm in the rocks of the Eastern Pluton, showing positive correlation with DI (Fig. 5.5.2b). The microgranites and aplite have concentrations (31-64 ppm), which are higher than those of the monzogranite. The porphyries have much the same concentration as the granodiorite.

The sympathetic relation between Th and K contents in plutonic rocks has been recognised by Heier and Rogers (1963), Clark et al. (1966), Adam et al. (1959) and Lambert and Heier (1967). K also increases in this pluton as there is a sympathetic relation between K and Th.

Lead and Zinc

Pb varies from 14 ppm to 127 ppm in quartzdiorite to granodiorite and monzogranite, and shows positive correlation with DI (Fig. 5.5.2b). Zn in these rocks varies from 82 ppm to 26 ppm, and show negative correlation with DI (Fig. 5.5.2a). Aplite and microgranites have lower Pb than and similar Zn concentrations to the monzogranite. The porphyries have much the same concentration of Pb and Zn as the granodiorite.

Pb^{+2} (radius = 1.20Å) can substitute for K^{+} (radius = 1.33Å) and Zn^{+2} (radius = 0.74Å) can substitute for Fe^{+2} (radius = 0.74Å), but

both Pb and Zn have a tendency to accumulate in the residual liquid due to high electronegativity of Pb^{+2} (1.8) compared to K^{+1} (0.8) and high electronegativity of Zn^{+2} (1.7) compared to Fe^{+2} (1.65), as suggested by Ringwood (1955a).

The increase of Pb and decrease of Zn from quartzdiorite through granodiorite to monzogranite in the Eastern Pluton may be related to the decrease in ferromagnesian minerals and the increase in residual liquid as intimated in the modal data (Table 5.4.1). It is notable that the increase of Pb contents in these rocks coincides with the increase of Th concentration (see variation of Th). Thus Zn behaves compatibly and Pb does not.

Zr contents in the Eastern Pluton are similar to Wager and Mitchell's (1951) 150-200 ppm for the Caledonian intermediate and acid plutonic rocks, and lower than Teggin's (1975) 35-380 ppm for the Triassic granites in North Thailand.

Yttrium

Y varies from 19-34 ppm in quartzdiorite through granodiorite to monzogranite and shows a positive correlation with DI (Fig. 5.5.2a). When plotted against CaO (Fig. 5.5.2d), the trend is of slightly increasing Y with decreasing CaO and follows the "standard Calc-alkali trend) of Lambert and Holland (1974).

The plots for the microgranites are close to those of monzogranite, whereas the plots for aplite deviate markedly from the trend. The porphyries have much the same concentration of Y as the granodiorite. The work of Lambert and Holland (1974) shows that the slight increase of Y as CaO decreases can be due to the fractionation of plagioclase, which is a Y-acceptors, will deplete Y in the liquid. This is compatible with the petrographic variation seen in the pluton.

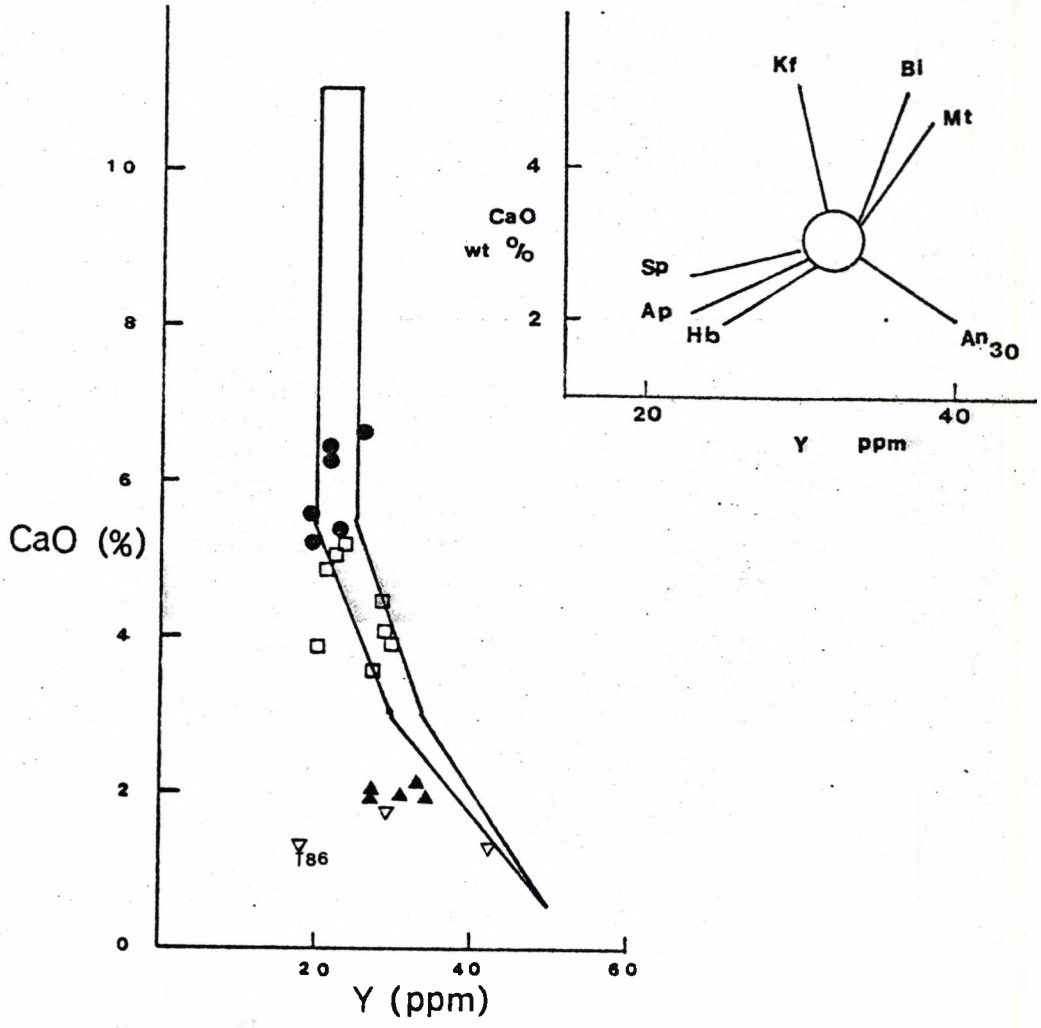

Figure 5.5.2d Plot of CaO vs. Y for the plutonic rocks of the Eastern Pluton. Symbols as follows:-
solid circles - outer facies - quartz diorite
open squares - transitional facies - granodiorite
solid triangles - inner facies - monzogranite
open triangles - microgranite and aplite (T86)
Enclosed area represents "standard calc-alkali trend" inset shows "liquid fractionation trends" for minerals (after Lambert and Holland, 1974).
Sp = sphene; Ap = apatite; Hb = hornblende; An_{30} = plagioclase of anorthite 30%; Mt = magnetite; Bi = biotite; Kf = K-feldspar.

Y contents in the Eastern Pluton are similar to Teggin's (1975) 15-35 ppm for the Triassic granites in North Thailand.

Rubidium, Strontium and Barium

The variation of Rb, Sr and Ba in the rocks from quartzdiorite through granodiorite to monzogranite are 43 ppm to 179 ppm, 240 ppm to 1138 ppm and 517 ppm to 124 ppm, respectively. The variations of Rb and Ba contents in these rocks show positive correlation with DI, whereas the variation of Sr content shows negative correlation with DI (Fig. 5.5.2b). This incompatible and compatible behaviour, respectively, is characteristic of these elements in acid rocks. It is related to the crystallisation of K-feldspar and biotite versus plagioclase crystallisation.

Ba-Sr diagram

The plot of Ba v Sr (Fig. 5.5.2e) shows that the Ba content increases whereas Sr decreases from quartzdiorite through granodiorite to monzogranite. The mineral vectors for Ba-Sr are superimposed on this diagram and indicate that plagioclase and hornblende can cause Sr to decrease and Ba to increase in the liquid during fractional crystallization. Sr^{+2} (radius = 1.18Å) is preferentially incorporated in the calcium-bearing minerals viz. plagioclase and hornblende by direct substitution for Ca^{+2} (radius = 1.02Å) to a greater extent than in K^{+1} (radius = 1.33Å) sites in the potassium-bearing minerals. In contrast, Ba^{+2} (radius = 1.34Å) is preferentially incorporated in potassium-bearing minerals.

The plots of Ba v Sr for aplite and microgranites, in the same diagram, show that the plotted points for microgranite are close to those of the monzogranites, whereas the plotted point for aplite (T86) is well away from the general trend of the other rocks.

The plots of Ba and Sr for the porphyries are closely similar to those of the monzogranite.

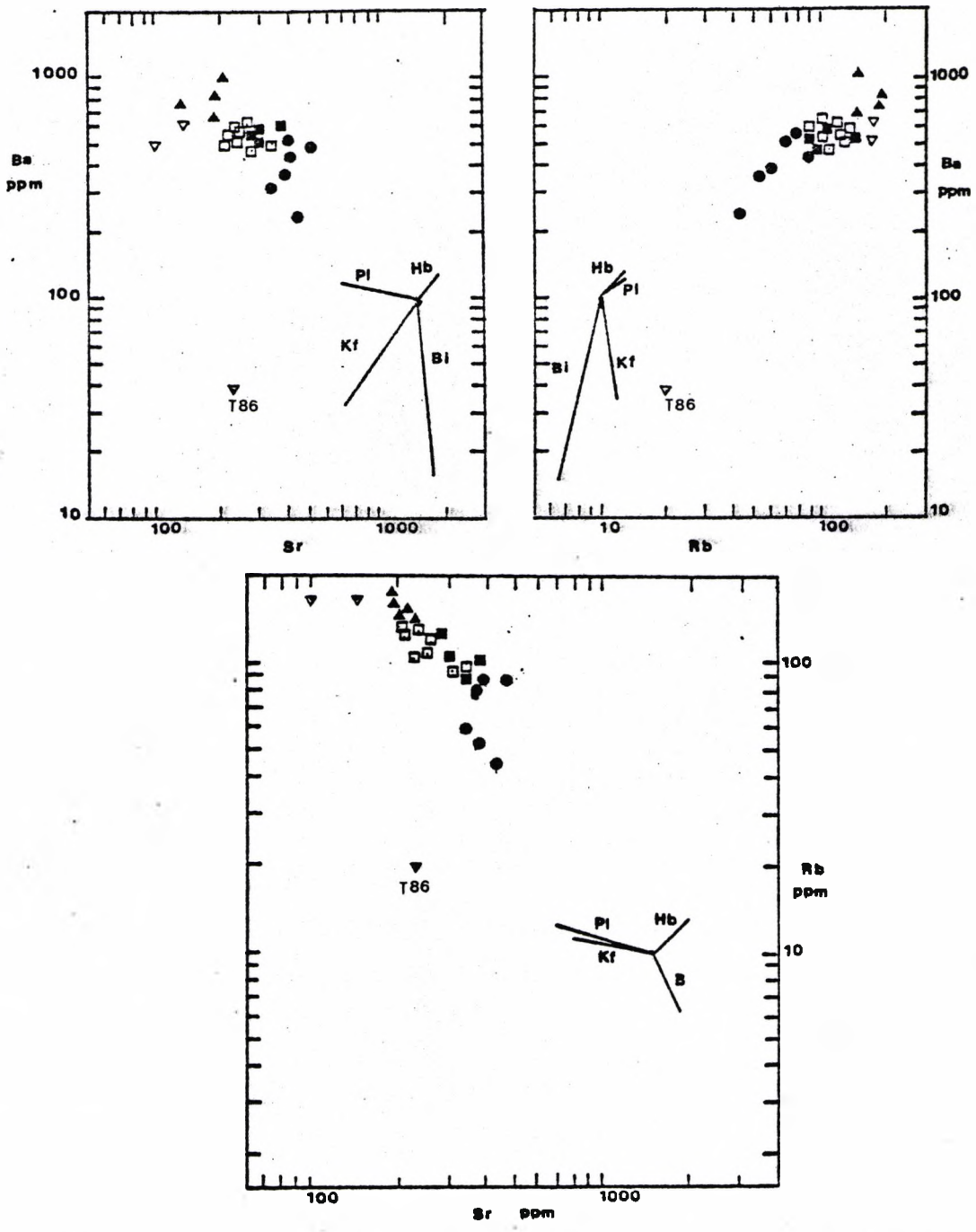

Figure 5.5.2e Plots of Rb, Sr, Ba for the plutonic rocks of the Eastern Pluton. Symbols as follows:
solid circles - outer facies - quartz-diorite
open squares - transitional facies - granodiorite
solid triangles - inner facies - monzogranite
open triangles - microgranite and aplite (T86)
solid squares - porphyry
Mineral vectors calculated from the distribution coefficients for acid rocks (Table 14.1 from Cox et al. 1979). Length of vector indicates 20% fractionation of the mineral.
Kf = K-feldspar; Bi = biotite; Hb = hornblende; Pl = plagioclase.

Ba-Rb diagram

The plot of Ba-Rb (Fig. 5.5.2e) shows that both Ba and Rb contents increase from quartzdiorite through granodiorite to monzogranite. The mineral vectors for Ba-Rb are superimposed on this diagram and they predict that plagioclase and hornblends can cause enrichment of Ba and Rb in the liquid during fractional crystallization.

Both Ba^{+2} (radius = 1.34Å) and Rb^{+1} (radius = 1.47Å) are not readily incorporated in calcium-bearing minerals by substitution for Ca^{+2} (radius = 1.02Å). Therefore these elements will become enriched in the liquid during the fractionation of calcium-bearing minerals.

The plots of Ba and Rb for the porphyries are closely similar to the granodiorites, while the plots for the microgranites are close to the plots of the monzogranite (inner facies), but the plot for aplite (T86) is well away from the general trend of the other rocks, and anomalous.

Rb-Sr diagram

The plot of Rb v Sr (Fig. 5.5.2e) shows that the Rb contents increase, whereas the Sr contents decrease from quartzdiorite through granodiorite to monzogranite.

The mineral vectors for Rb-Sr indicate that plagioclase ($\pm$ K feldspar) and hornblende can cause enrichment of Rb and depletion of Sr in the liquid during fractional crystallization.

The plots of Rb and Sr contents for the porphyries rocks, the microgranites and the aplite, show that the plotted points for porphyry are closely similar to those of granodiorite, whereas the plotted points for the microgranites are close to those of the monzogranite, but the plotted point for aplite (T86) is again anomalous.

Summary

The important points gained from the chemical characteristics of the rocks in the Eastern Pluton are as follows:

1. The increasing content of the trace elements Y, Ba, Rb, incompatible with calcium-bearing minerals, and the decrease of the compatible trace element Sr, from granodiorite to monzogranite, reflect the fractional crystallization of plagioclase and hornblendes (see Section 5.5.2d, and 5.5.2e). Fractionation of plagioclase and hornblende in these rocks is in agreement with the decrease of plagioclase and hornblende in rocks from the outer facies towards the inner facies (see modal data Table 5.4.1). The plot of normative An-Ab-Or also indicates the trend of decreasing anorthite simultaneous with increasing orthoclase from the outer facies towards the inner facies (see Section 5.5.1b).

2. The decreasing content of the trace elements - Cr, Ni, V, Sc - compatible with ferromagnesian minerals, from quartzdiorite through granodiorite to monzogranite, is in agreement with the trend of decreasing Fe and Mg in the Fe-(Na+K)-Mg diagram (Fig. 5.5.1a), and compatable with the extraction of these elements from the liquid by hornblende.

3. The strong decrease in Ti content relative to a very slight decrease in Zr content, from the rocks in the outer facies towards the inner facies, reflects the strong fractionation of hornblende and magnetite and possibly ilmenite (see Section 5.5.2c), and a very slight fractionation of zircon.

4. The very slight increase of LREE contents (La, Ce, Nd) from quartzdiorite through granodiorite to monzogranite may be due to the absence of LREE-bearing minerals, viz. sphene, allanite, in the fractionation. This is confirmed in the thin sections. It is noteworthy that in the lack of sphene and allanite in the rocks of the Eastern Pluton is in contrast to the rocks of the Tak Pluton, the Mae-Salit Pluton and the Western Main Range Pluton.

5. Among the late minor intrusives, the microgranites have chemical compositions close to or indistinguishable from those of the monzogranites, whereas the aplite does not show these characteristics relating to the rest of the pluton. The porphyry shows chemical characteristics similar to the granodiorite rather than the quartz-diorite.

CHAPTER 6

The Rare Earths

6.1 The Tak Pluton

Figure 6.1.1 shows the chondrite normalised REE patterns of the granitic rocks from the Tak Pluton which indicate that the LREE are strongly fractionated and the Eu has a strong negative anomaly, whereas the HREE show a flat pattern. The sample T01 is a rock from the inner facies, whereas the sample T10b and T02 are rocks from the outer facies.

The development of a negative Eu anomaly from the rocks in the inner facies towards the outer facies could be explained by the fractionation of plagioclase. The divalent Eu is geochemically very similar to Sr (Hanson, 1980) and can be preferentially incorporated into divalent sites such as Sr and Ca in plagioclase. Fractionation of plagioclase from the rocks in the inner facies towards the outer facies is also suggested by the variation of Rb, Sr and Ba (see section 2.5.2).

Among the rocks in the outer facies, the sample T10b, collected from the southern periphery, shows less depletion in LREE than the sample T02, collected from the eastern periphery, but conversely shows more depletion in HREE. This may also be due to fractional crystallisation of plagioclase which will result in the enrichment of HREE, relative to the depletion of LREE as suggested by Nagasawa and Schnetzler, (1971).

However, there are two problems to the above explanation, (a) major element modelling (Section 7.3) indicates felspar fractionation plus other likely minerals cannot account for the change in major element composition with increasing acidity; (b) more significantly

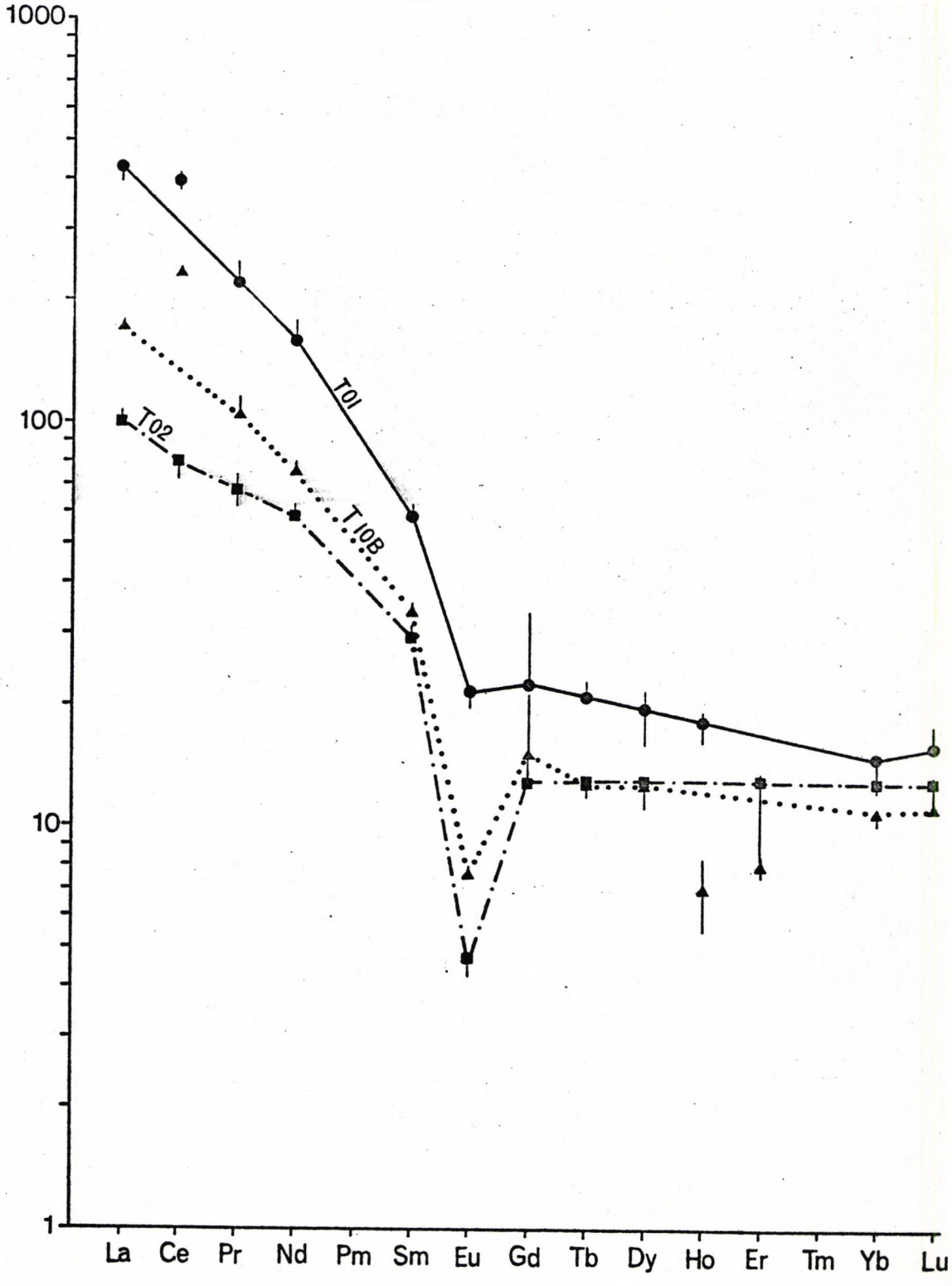

Figure 6.1.1 Chondrite-normalised REE plot for three rocks from the Tak Pluton. Sample T01 is monzogranite (inner facies); T10B and T02 are syenogranite (outer facies).

felspar fractionation of any original Tak magma of a composition appropriate to any combination of the inner and outer facies would increase the REE not decrease them. This characteristic of felsic magmas has been noted by Miller and Mittlefehldt (1982) and explained in a variety of ways (see for example Moll (1981) and Ludington (1981) who thought thermogravitational diffusion (Hildreth 1979) was very likely. The "decoupling" of major and trace elements noted here seems to be better explained in terms of the crystallisation of extremely LREE-rich accessory minerals such as sphene and/or allanite as indicated by the petrology. The depletion is very similar to that noted in the Woman Mountain (Miller and Mittlefehldt 1982) who emphasise, as do Fourcade and Allegre (1981) that modelling of trace elements based on major minerals as has been done is not valid for felsic rocks. This particularly related to the lanthanides (see also McCarthy and Kable (1978) and Shaw (1977)). In the Tak Pluton it seems possible that early and even perhaps continuous crystallisation of allanite and sphene depleted the later magmas, the pegmatite being particularly depleted Hon and Noyes (1977), Pegram et al. (1980); this combined with some plagioclase fractionation and pegmatite separation and mixing gave the observed distributions.

6.2 The Mae-Salit Pluton

Figure 6.2.1 shows the chondrite normalised REE pattern for the rocks in the Mae-Salit Pluton, in which T48b and CTK7 are samples from the central part of the pluton (inner facies). The sample CTK22 is a medium-grained rock intermediate between the inner facies and the outer facies. The sample CTK2 is a medium grained rock from the outer facies and CTK44 is a fine-grained rock from the immediate contact of this pluton with the granite of the Western Main Range Pluton. The diagram

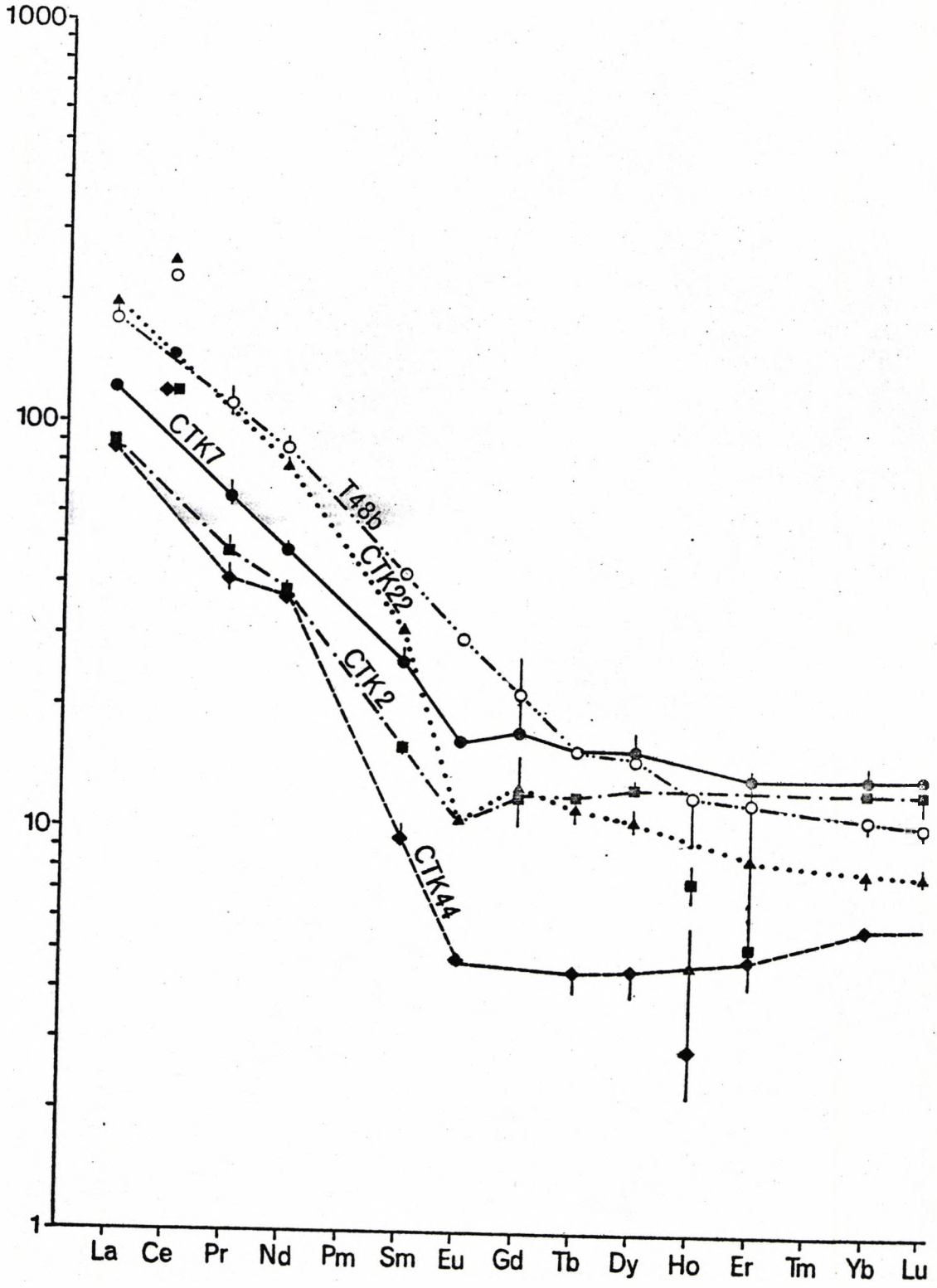

Figure 6.2.1 Chondrite-normalised REE plot for five rocks from the Mae-Salit Pluton. Samples T48b and CTK7 are monzogranite (inner facies); CTK22, CTK2 and CTK44 are monzogranite (outer facies).

shows that while the Eu anomalies are not large, they show a slight development of a negative Eu anomaly from the rocks in the inner facies towards the outer facies (ignoring CTK44). The increase in this negative Eu anomaly indicates the fractionation of plagioclase as suggested by Philpotts and Schnetzler (1968). (See also the variation of Rb, Sr and Ba in section 3.5.2). The LREE depletion from the rocks in the inner facies (T48b) and the outer facies (CTK44) may again be due to the fractionation of LREE-bearing minerals, viz. sphene, allanite, which are common accessory minerals in these rocks (see argument on the Tak Pluton). The erratic variation of the LREE in the rocks intermediate between the inner facies (CTK7) and the outer facies (CTK22) may be due to inhomogeneity in the distribution of the LREE-bearing accessory minerals, Condie (1978), compared to the systematic variation of plagioclase as shown in the Eu anomaly. This also emphasises that the variation in some trace elements is strongly influenced by very minor proportions of certain accessory minerals. The overall fractionation of LREE is from the medium-grained rock (CTK22) intermediate between the inner facies and the outer facies, through the medium-grained rock of the outer facies (CTK2) to the fine grained rock of the outer facies (CTK44). These rocks all show flat HREE patterns. The fine-grained rock from the outer facies (CTK44) is strongly depleted in HREE, and may reflect the removal of accessory apatite and sphene which are the major sources of HREE (Nagasawa, 1970; Condie, 1978) during fractional crystallisation. Sample CTK44 also contains a low Zr content so presumably depletion by zircon is unlikely. The somewhat higher values of the HREE patterns in the samples CTK7 and CTK2 may indicate the inhomogeneous distribution of REE-bearing minerals in these rocks and also the fractional crystallisation of plagioclase, which will enrich HREE relatively in the liquid (Nagasawa and Schnetzler,

1971). The combined effect of plagioclase plus biotite and the accessory minerals fractionation was to produce a subdued Eu anomaly, and the REE distribution shown in Fig. 6.2.1

6.3 The Western Main Range Pluton

6.3.1 The main body

Figure 6.3.1 shows the chondrite-normalised REE distribution in the rocks of the Western Main Range Pluton, in which the sample (T50) is a rock of the inner facies, CTK33 is the rock of the outer facies from the northern periphery, CTK62 and T16 are the rocks of the outer facies from the southern periphery of the pluton.

The chondrite normalised REE patterns indicate that there is a strong LREE fractionation, with a slight Eu anomaly and a flat HREE distribution. The development of a negative Eu anomaly from the rocks in the inner facies towards the rocks in the outer facies could be explained in terms of the removal of plagioclase, which concentrates Eu (Hanson, 1980) during fractional crystallisation. The "fractionation" of plagioclase is also indicated in the variation of Rb, Sr and Ba (see section 4.5.2). The slight decrease of LREE from the rock in the inner facies toward the outer facies may be due to the removal of sphene and allanite, which are the main sources of LREE as indicated earlier (Condie, 1978). The slightly enrichment of HREE in the rocks of the outer facies could be due to the removal of plagioclase (Nagazawa and Schnetzler, 1971). One of the samples of the outer facies (T16) shows depletion of HREE, which could be due to the depletion by apatite and zircon which are the main sources of HREE, especially Yb and Lu (Nagasawa and Schnetzler, 1971; Condie, 1978). As in the previous examples the depletion in REE seems best explained in terms of accessory mineral crystallisation, indeed extraction of the leucogranite from the

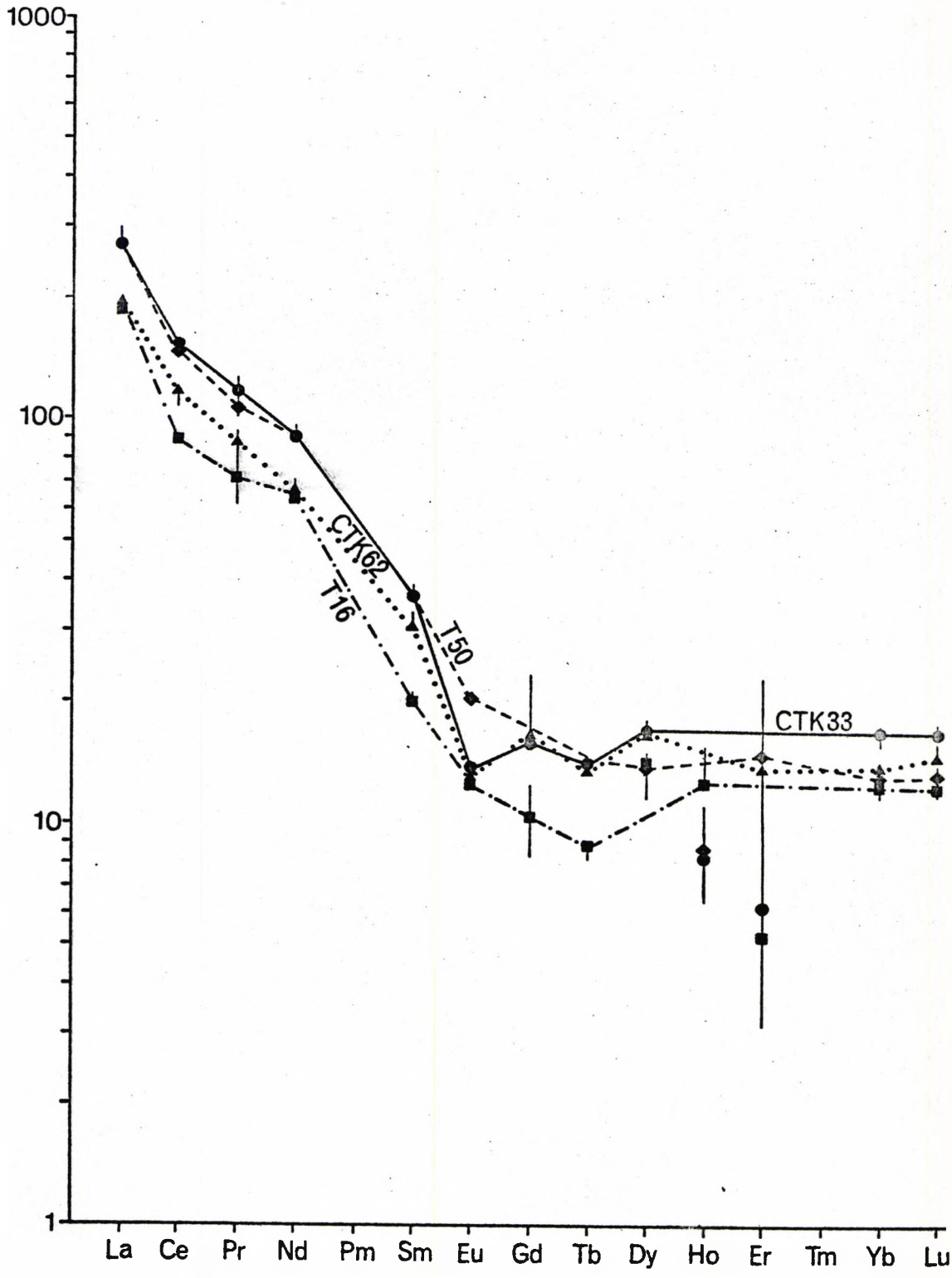

Fig. 6.3.1 Chondrite-normalised REE plot for four rocks from the main body of the Western Main Range Pluton. Sample T50 is monzonite (inner facies); CTK33, CTK62 and T16 are monzogranite (outer facies).

from the average (original composition of the pluton) would produce effects very similar, if not indistinguishable, from crystal fractionation. The late end granite will be impoverished in REE (particularly LREE) presumably leaving these in the accessory minerals and feldspars in the more basic members of the pluton. Thus magma separation, by whatever means, is arithmetically equivalent to fractional crystallisation, but does not pose some of the problems inherent in such a mechanism in acid systems.

6.3.2 The associated appinites

Figure 6.3.2 shows the chondrite normalized REE patterns of the appinitic rocks, which commonly occur as basic xenoliths and dykes in association with the Western Main Range Pluton. The REE patterns (Fig. 6.3.2) of the "older appinites" which occur as large basic rafts (T98 and T18b) within the granites have high LREE, flat HREE and no negative Eu anomaly similar to the REE pattern of the rock in the inner facies (T50) of the Western Main Range Pluton (Fig. 6.3.1). Both "older appinites" and the granitic rocks of the Western Main Range contain sphene which is the main source of LREE. The local variation of the accessory zircon and apatite in these rocks reflects the slight depletion and enrichment of HREE, because these minerals have large K_D values for the HREE (Hanson, 1980). Therefore, the "older appinites" are more likely to be consanguineous with the inner facies of the Western Main Range Pluton. The REE patterns of the "younger appinites" which commonly occur as dykes (T78 and T4) show flatter patterns both in LREE and HREE (Fig. 6.3.2). The REE patterns of the younger appinties are slightly different from the REE patterns of the rocks in the Western Main Range Pluton. Sample T4 in particular shows LREE which are much less similar than almost all the other facies.

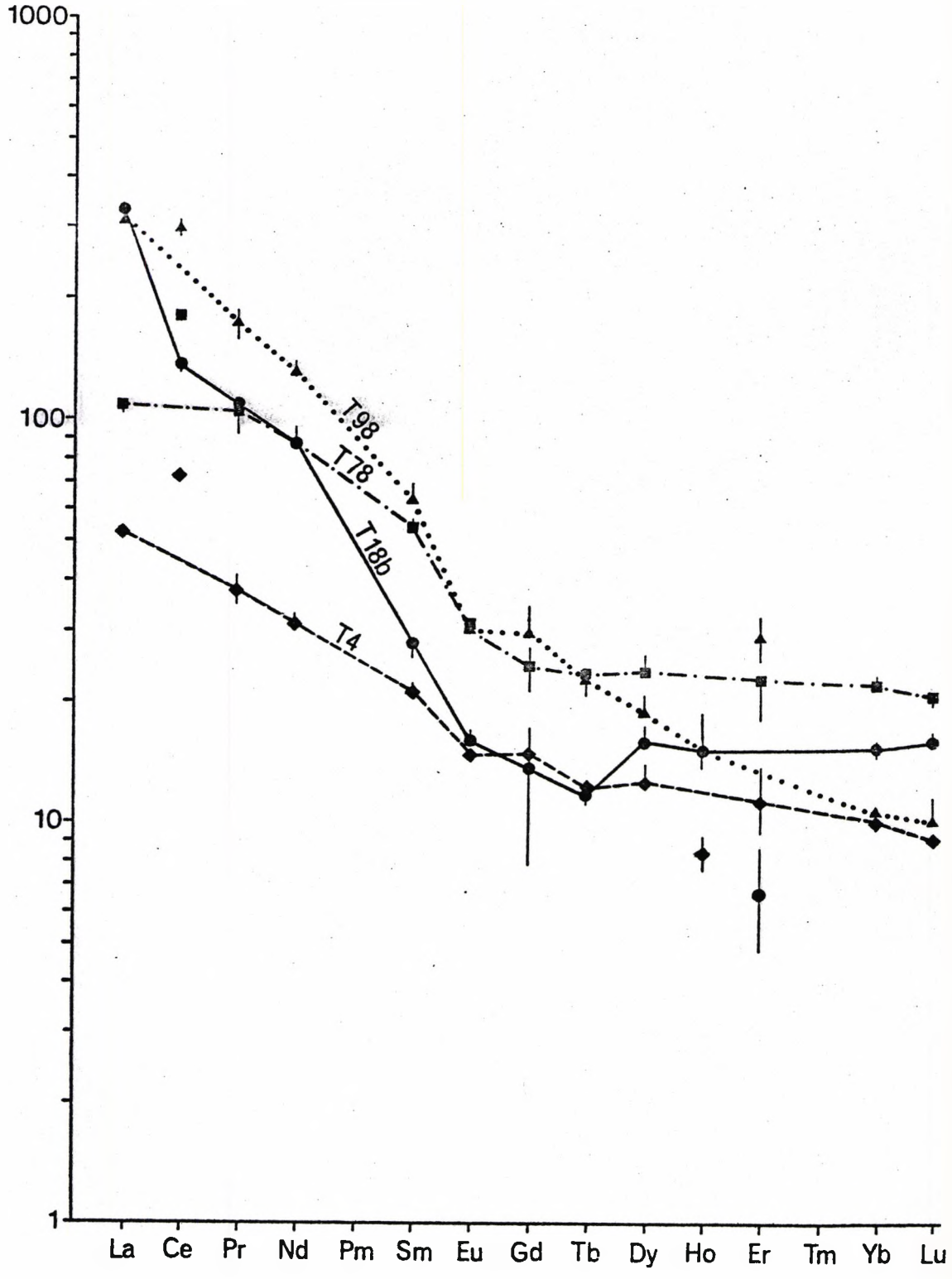

Figure 6.3.2 Chondrite-normalised REE plot for four appinite associated with the Western Main Range Pluton. Samples T98 and T18b are "older" appinites; T78 and T4 are "younger" appinites.

Therefore, the appinitic dykes may not be directly cogenetically related to the rocks of the Western Main Range Pluton.

6.4 The Eastern Pluton

6.4.1 The main body

Figure 6.4.1 shows the chondrite normalised REE patterns for the rocks of the Eastern Pluton, in which sample T48 is from the outer facies, T73 and T29 are from the transitional facies and T33 is from the inner facies.

The diagram shows moderate LREE fractionation and flat HREE. There is only a very slight Eu anomaly, and the Eu decreases from the rocks in the outer facies towards the inner facies. The decrease in Eu may be explained in terms of the fractional crystallisation of plagioclase. Note the combined effect of plagioclase plus hornblende as modelled using major elements (see section 7.2) will not produce a marked Eu anomaly. The rock of the outer facies (T48) shows higher LREE and lower HREE than the other rocks. The LREE decrease from the outer facies towards the inner facies, whereas the HREE increase from the outer facies towards the transitional and inner facies. This could be due to the crystallisation of plagioclase which will result in relative enrichment of HREE over LREE (Nasagawa and Schnetzler, 1971). Crystallisation of hornblende as well as plagioclase, as indicated in the major element modelling would also produce the same effect (see section 7.2). The sample T73, a rock of the transitional facies from the roof of the pluton, which is commonly associated with the porphyry (chilled margin), has higher HREE than the others may be due to the local concentration of HREE bearing accessory minerals, viz. apatite and zircon.

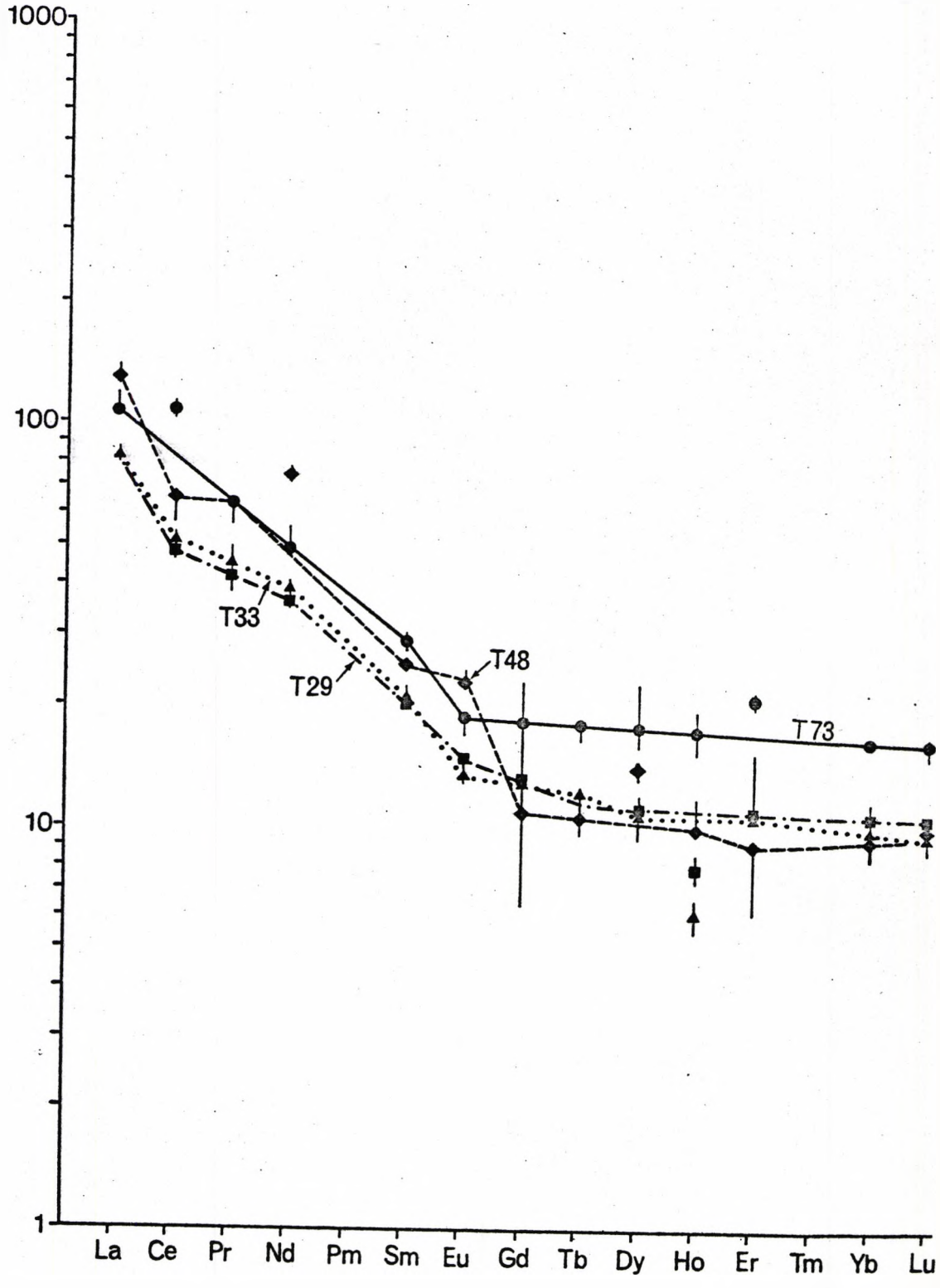

Figure 6.4.1 Chondrite-normalised REE plot for four rocks from the Eastern Pluton. Sample T48 is quartz-diorite (outer facies); T73 and T29 are granodiorite (transitional facies), T33 is monzogranite (inner facies).

The other sample of the rocks in the transitional facies (T29) has a similar REE pattern to the inner facies (T33), even though their major and trace element concentrations are different. It is not clear why this should be so.

6.4.2 The associated porphyry and late intrusive microgranites

Figure 6.4.2 shows the chondrite normalised patterns of the porphyry (T23) and late minor intrusive microgranites (T25 and CTK34), in which the porphyry occurs at the roof contact of the granodiorite of the transitional facies of the Eastern Pluton with the overlying country rocks. It is considered to be a chilled margin along the roof of the pluton (see Chapter 5). The porphyry commonly occurs as enclaves in the granodiorite (T73). The REE pattern of the porphyry (T23), shows less fractionated LREE, lack of Eu anomaly and flat HREE (Fig. 6.4.2) and is very similar to the REE pattern of the granodiorite (T73) of the transitional facies, (Fig. 6.4.1). The similarity of the REE patterns of the porphyry and the associated granodiorite support the notion that the porphyry is a chilled marginal rock, having a composition closely related to the granodiorite of the roof of the pluton. The other trace elements concentrations of the prophyry are much the same as in the rocks of the transitional facies (see section 5.5.2).

The REE pattern (Fig. 6.4.2) for the microgranite (T25) collected from the roof of the Eastern Pluton shows less fractionated LREE's, a well developed negative Eu anomaly and is enriched in HREE, whereas the microgranite (CTK34) collected from the border of the pluton show subdued LREE's, a very small Eu anomaly and an enrichment in HREE (Fig. 6.4.2). The very similar enrichment of HREE in the two microgranites may be due to the local concentration of zircon and apatite

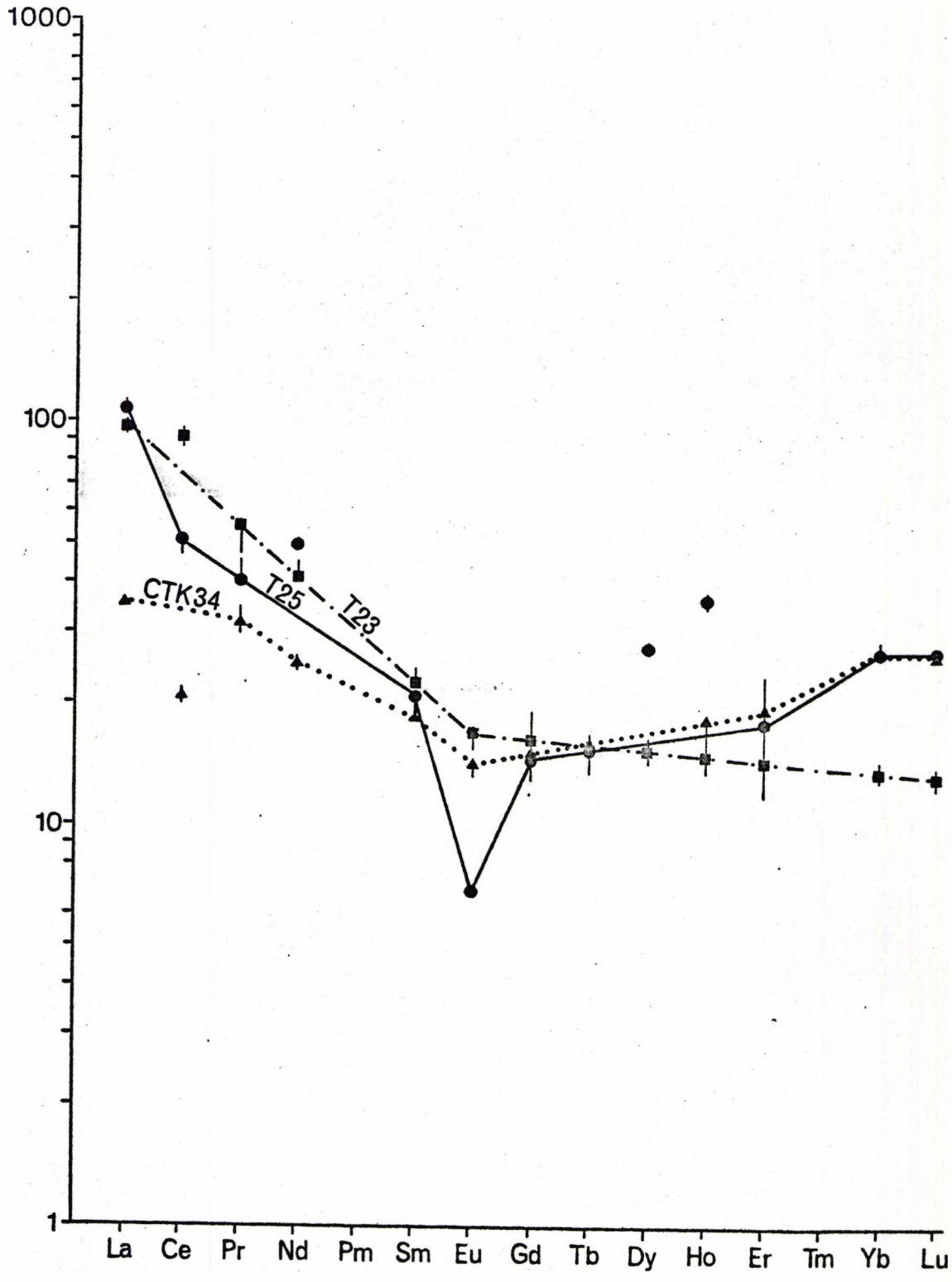

Figure 6.4.2 Chondrite-normalised REE plot for three rocks associated with the Eastern Pluton. Sample T23 is porphyry (chilled margin), T25 and CTK34 are microgranites.

which have larger K_D's for the HREE (Hanson, 1980). The larger negative Eu anomaly in the microgranite from the roof compared to the microgranite from the border of the pluton indicate strong fractionation of plagioclase in the former rather than the latter. The microgranite from the border is depleted in LREE-bearing minerals compared to the microgranite from the roof of the pluton. The REE patterns of the microgranites (Fig. 6.4.2) compared with the REE patterns of the rocks of the Eastern pluton cast uncertainty on the belief that the microgranites are directly differentiated from the Eastern Pluton.

Summary

The important points gained from the study of the characteristics of the REE patterns of the rocks of the composite plutons in the Tak Batholith are as follows:

1. The Tak Pluton, The Mae-Salit Pluton and The Western Main Range Pluton, which all show unusual outward zoning, have strong LREE fractionation with flat HREE's. The characteristic of strongly fractionated LREE patterns in the outward zoned plutons is in agreement with the presence of LREE-rich accessory minerals (sphene and allanite), whereas the Eastern Pluton, which shows less fractionated LREE's, generally lacks sphene and allanite.

2. The strong negative Eu anomaly occurs in the Tak Pluton, whereas the Mae-Salit and The Western Main Range Plutons show less well developed Eu anomalies and it is even less distinctive in the Eastern Pluton. These indicate that plagioclase crystallisation and removal dominated in the Tak Pluton, while conventional fractionation of hornblende plus plagioclase in the Eastern Pluton, resulted in little or no Eu anomaly.

3. The HREE distributions in the rocks of all these plutons are rather variable and complicated probably due to the combination of the crystallisation of plagioclase, which will enrich HREE in the liquid, and the crystallisation of apatite and zircon which will deplete the HREE in the liquid.

4. Perhaps the most interesting aspect of these plutons, apart from their diverse character, is the decrease in total REE with "fractionation" a feature common to felsic rocks (Miller and Mittlefehldt, 1982). Although various explanations have been put forward to explain this; changes in polymerization of the silicate liquid; loss of an exsolved LREE-rich vapour phase; liquid state thermogravitational diffusion; autometasomatism by an HREE-rich vapour phase; pressure of accessory minerals in small quantities with $K_{LREE} >> 1$ (sphene, apatite, and in particular monozite and allanite). The latter explanation in conjunction with pegmatite, leucogranite etc. separation seems in view of the geologic and petrographic evidence, best suited to the genesis of some of the granites described here.

CHAPTER 7

Harker Diagrams and Modelling

7.1 Harker diagrams

The individual analyses for the rocks have been plotted on Harker diagrams (Figures 7.1.1 to 7.1.4) for the Tak, Mae-Salit, Western Main Range and Eastern Plutons respectively. The Tak and the Mae-Salit plutons are acidic and have a restricted range in SiO_2, the rock types ranging from monzogranite to syenogranite. The Western Main Range Pluton includes more basic rocks, extending from monzonite to monzogranite. The Eastern Pluton has even more basic members and ranges from quartz-diorite to monzogranite.

Most of the elements plot as expected, showing a decrease with increasing acidity. The graphs for Fe_2O_3 show some scatter, especially in the case of the Mae-Salit and Eastern Plutons. This is likely to be due to variable amounts of magnetite and/or hematite. The alkalis show interesting differences between the four plutons. The Na_2O shows little change in the Tak Pluton - note the vertical scale is exagerrated - and is almost constant in the Eastern Pluton. In the Mae-Salit and the Western Main Range Plutons there is a clear decrease in Na_2O. The graphs for K_2O show a decrease with increasing SiO_2 in the Tak Pluton, but in the other three plutons an increase can be seen, especially in the Eastern Pluton.

Attempts have been made to explain these changes in chemical composition by modelling, i.e. by removing or crystallising minerals or rocks of chosen composition from a given initial composition, and then observing whether the compositions of the evolved "residues' produce a trend on the Harker diagrams, which fit the observed values. The Eastern Pluton is the only one of these four that shows a classic 'normal' zoning i.e. a basic outer part and an acidic core. This pluton will be discussed

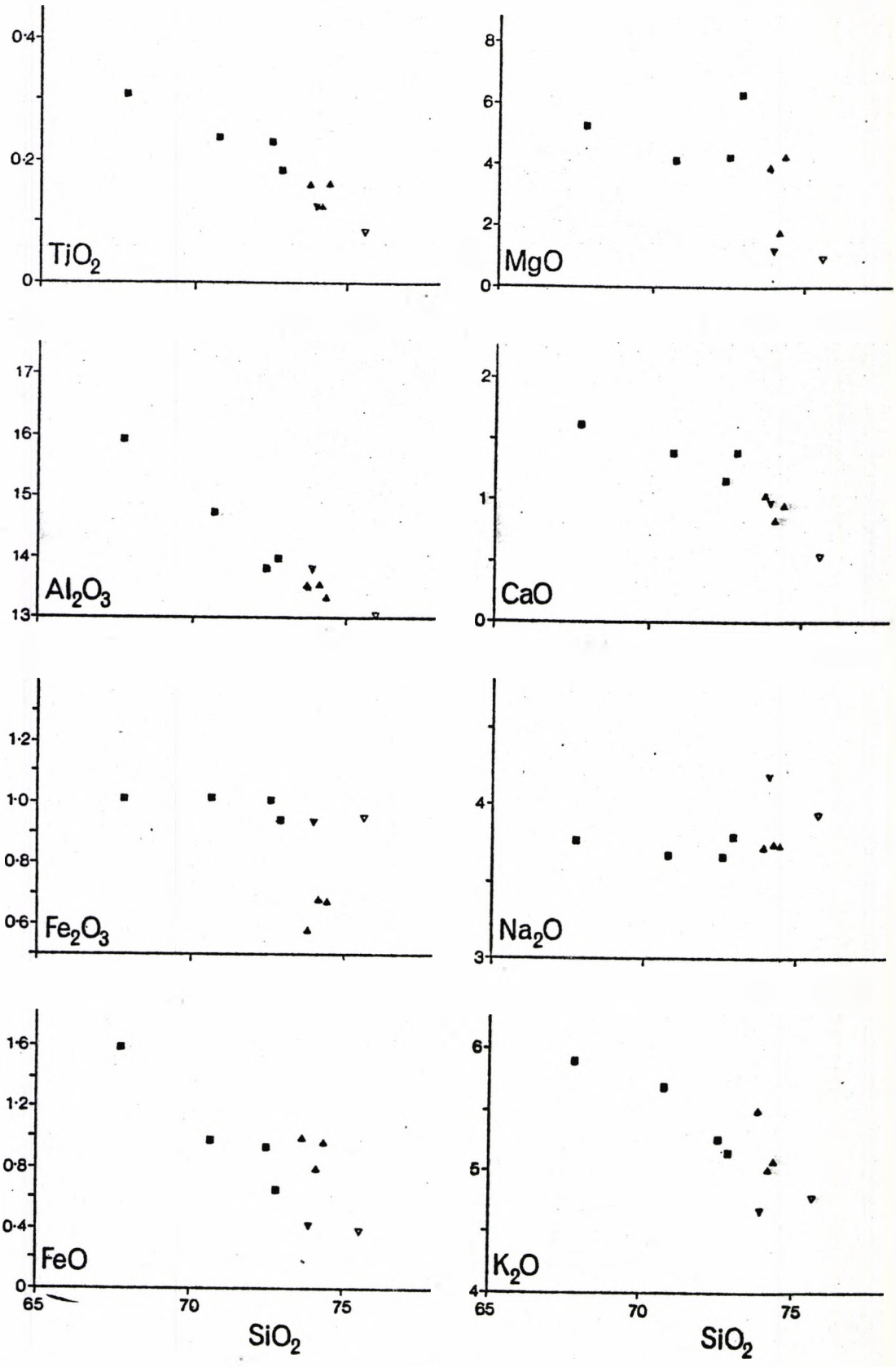

Figure 7.1.1 Harker diagrams for the rocks of the Tak Pluton.
solid squares - inner facies; solid triangles point up - outer facies.
open triangles - microgranites; solid triangles point down - porphyry.

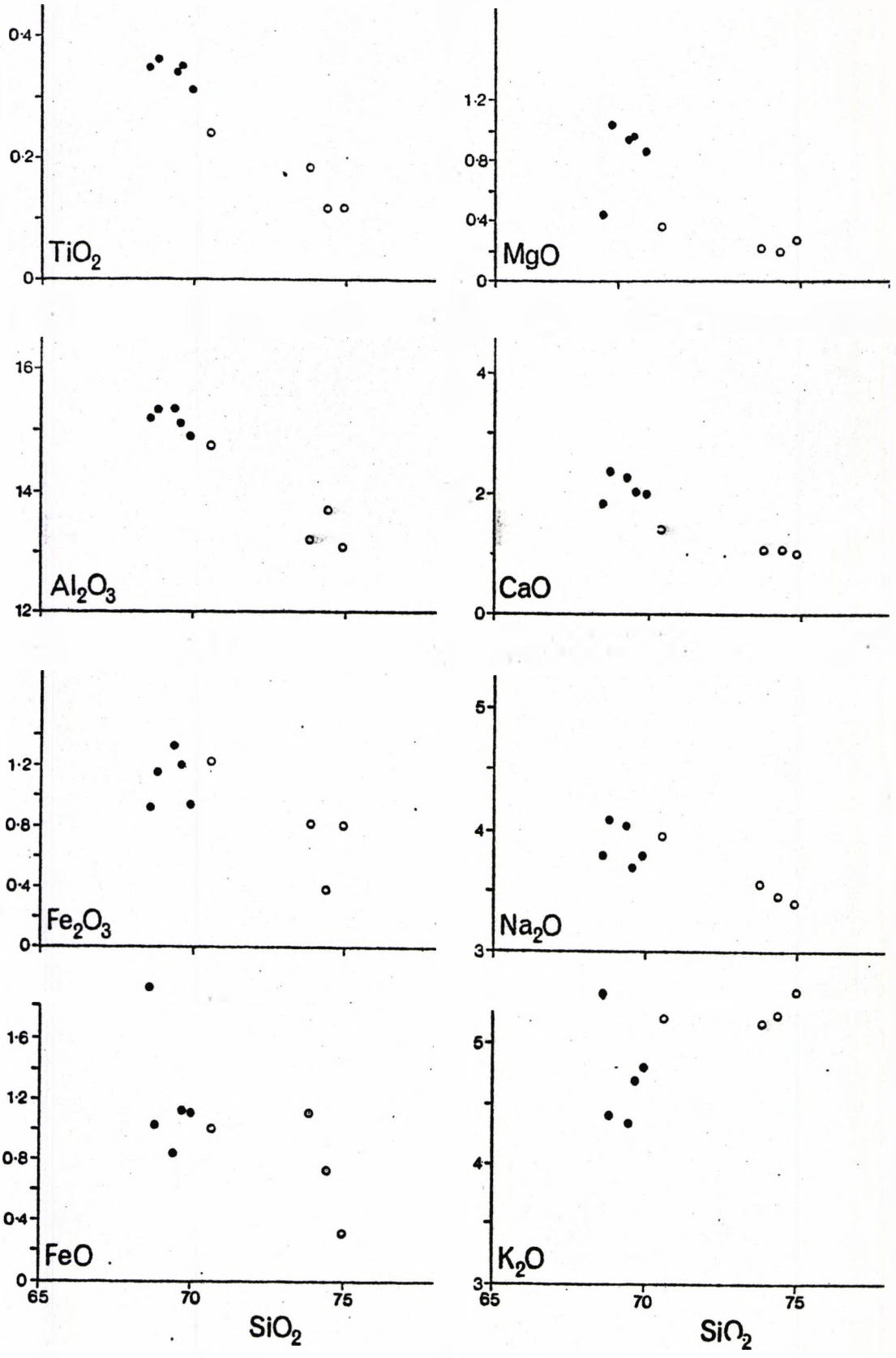

Figure 7.1.2 Harker diagrams for the rocks of the Mae-Salit Pluton
solid circles - inner facies; open circles - outer circles.

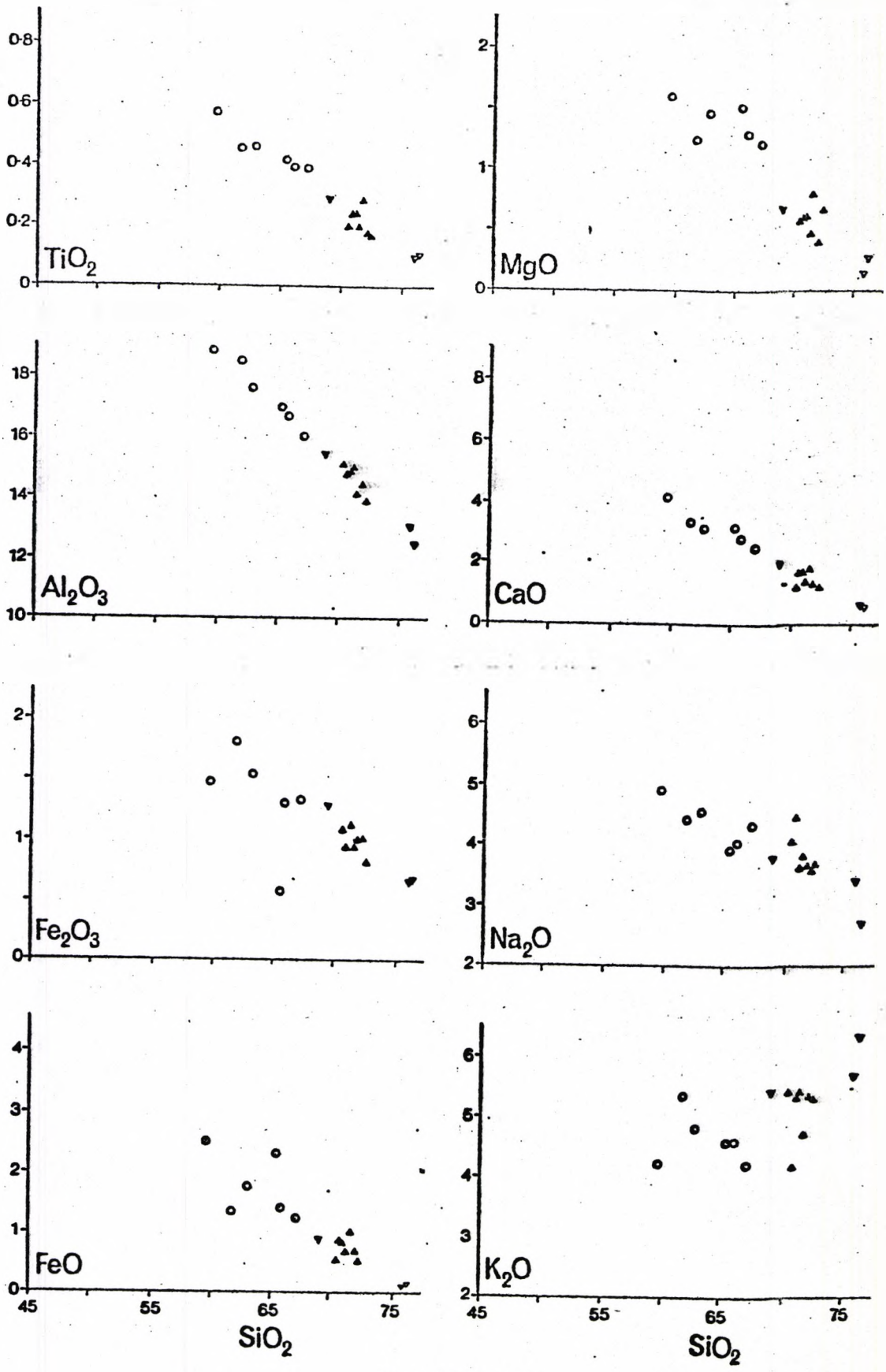

FIGURE 7.1.3

Harker diagrams for the rocks of the Western Main Range Pluton
open circles - inner facies; solid triangles point up - outer facies
open triangles - leucogranites; solid triangles point down - porphyry

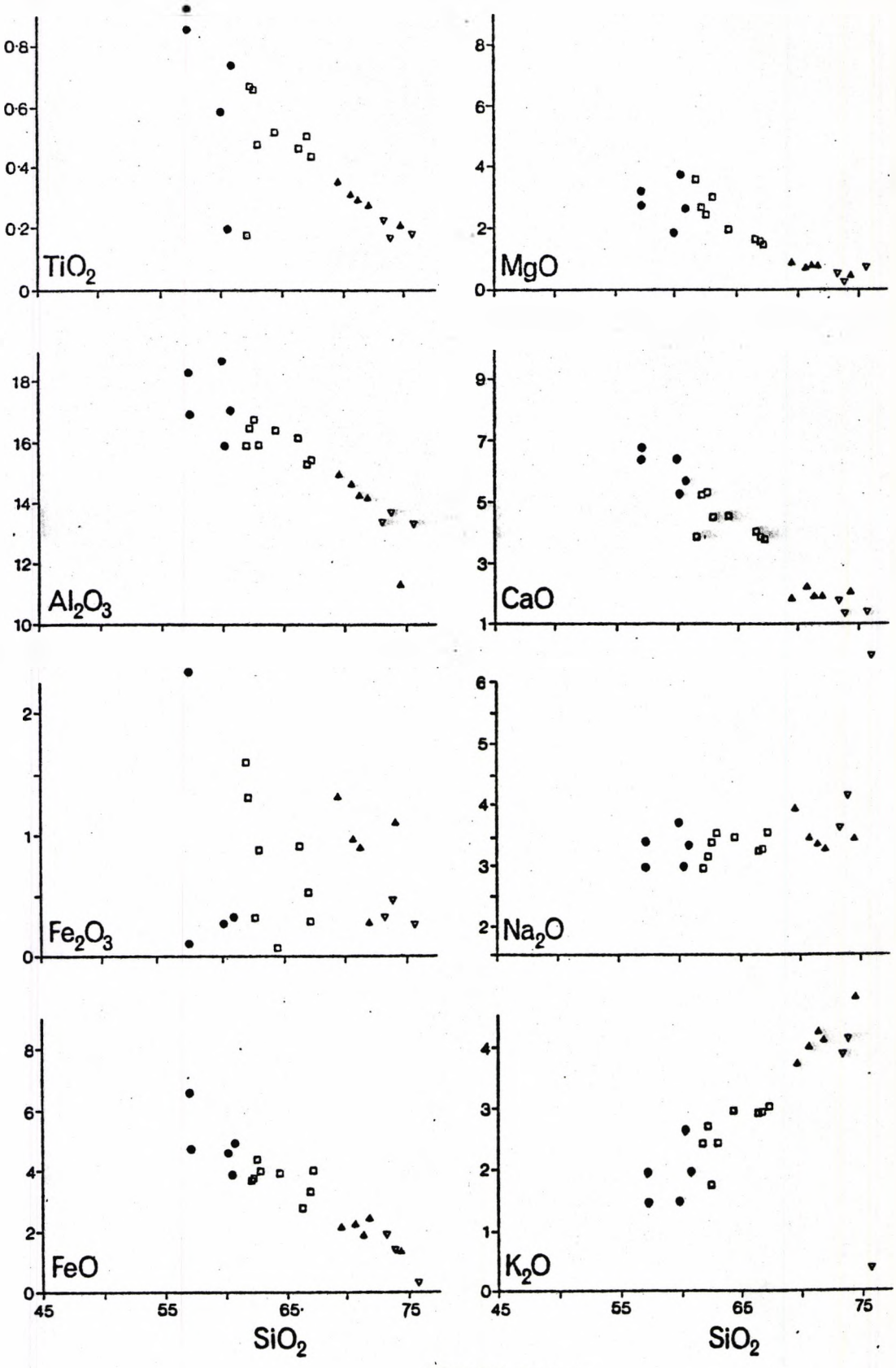

FIGURE 7.1.4

Harker diagrams for the rocks of the Eastern Pluton
solid circles - outer facies; open squares - transitional facies
solid triangles - inner facies; open triangles - microgranites

in detail first.

7.2 Eastern Pluton

The rocks of this pluton fall into three facies; an acidic inner facies, an intermediate transitional facies and a basic outer facies. Thus the pluton can be called 'normally' zoned, and the change in composition observed can be considered to have occurred by crystallisation of early formed basic minerals - plagioclase, hornblende $\pm$ biotite - in the cooling outer part of the pluton. Continued crystallisation of these minerals will fractionate the magma to an acidic facies.

The five samples from the inner facies have been averaged to give an inner average (no. 1, Table 7.2) and similarly four samples representative of the transitional facies and three samples representative of the outer facies have also been averaged (nos. 2 and 3, Table 7.2). Since there are no H_2O^+ analyses for any of these rocks, the difference from 100 has been included. This is an essential precaution, since the arithmetic of the extraction process is not valid, unless all components add to 100. These differences do indicate a sensible water content for the type of rocks expected in these facies.

Field evidence suggests that the proportions of the three facies is 45% inner facies, 45% transitional and 10% outer. These values have been used to calculate an overall weighted average for the pluton (no. 4, Table 7.2). The mineral analyses chosen for extraction are microprobe analyses of minerals in rocks from this pluton. The plagioclase (no. 5, Table 7.2) is from a diorite on the periphery and the hornblende (no. 6, Table 7.2) is from a granite porphyry in the chilled margin. There are only total iron figures available, so all the iron has been assigned to FeO.

TABLE 7.2

Modelling data for the Eastern Pluton

	1	2	3	4	5	6	7	8	9
SiO_2	71.56	66.22	58.15	67.82	55.96	46.62	50.98	72.03	57.77
TiO_2	0.28	0.47	0.79	0.42	-	1.37	1.32	0.19	0.94
Al_2O_3	13.85	15.71	17.91	15.09	28.27	8.24	18.79	14.17	17.32
Fe_2O_3	0.90	0.44	0.91	0.69	-	-	-	0.86	0.28
Feo	1.95	3.24	5.28	2.87	-	15.97	7.27	1.77	5.51
MgO	0.67	1.65	2.63	1.30	-	11.49	5.23	0.32	3.66
CaO	2.00	4.06	6.48	3.38	9.77	10.32	9.89	1.75	7.29
Na_2O	3.41	3.34	3.33	3.37	5.52	1.37	3.56	3.32	3.49
K_2O	4.18	2.97	1.64	3.38	0.48	0.51	0.49	4.10	1.65
Rest	1.20	1.90	2.88	1.68	-	4.11	2.27	1.51	2.04

1 Average of 5 inner facies rocks from the Eastern Pluton

2 Average of 4 transitional facies rocks from the Eastern Pluton (samples T73, CTK1, CTK47, CTK62-1).

3 Average of 3 outer facies rocks from the Eastern Pluton (samples T38b, T48, CTK58).

4 Overall weighted average in the proportions of 45% inner, 45% transitional, 10% outer.

5 Plagioclase from sample CTK4; diorite from the Eastern Pluton.

6 Hornblende from sample CTK47-2; granite porphyry, chilled margin, Eastern Pluton.

7 'Precipitate', mixing 53.2% of (5), 45.5% of (6), 0.7% rutile, 0.5% water.

8 Evolved liquid when 20% of (7) has been removed from (4).

9 'Cumulate', mixing 40.1% of (4) with 59.9% of (7).

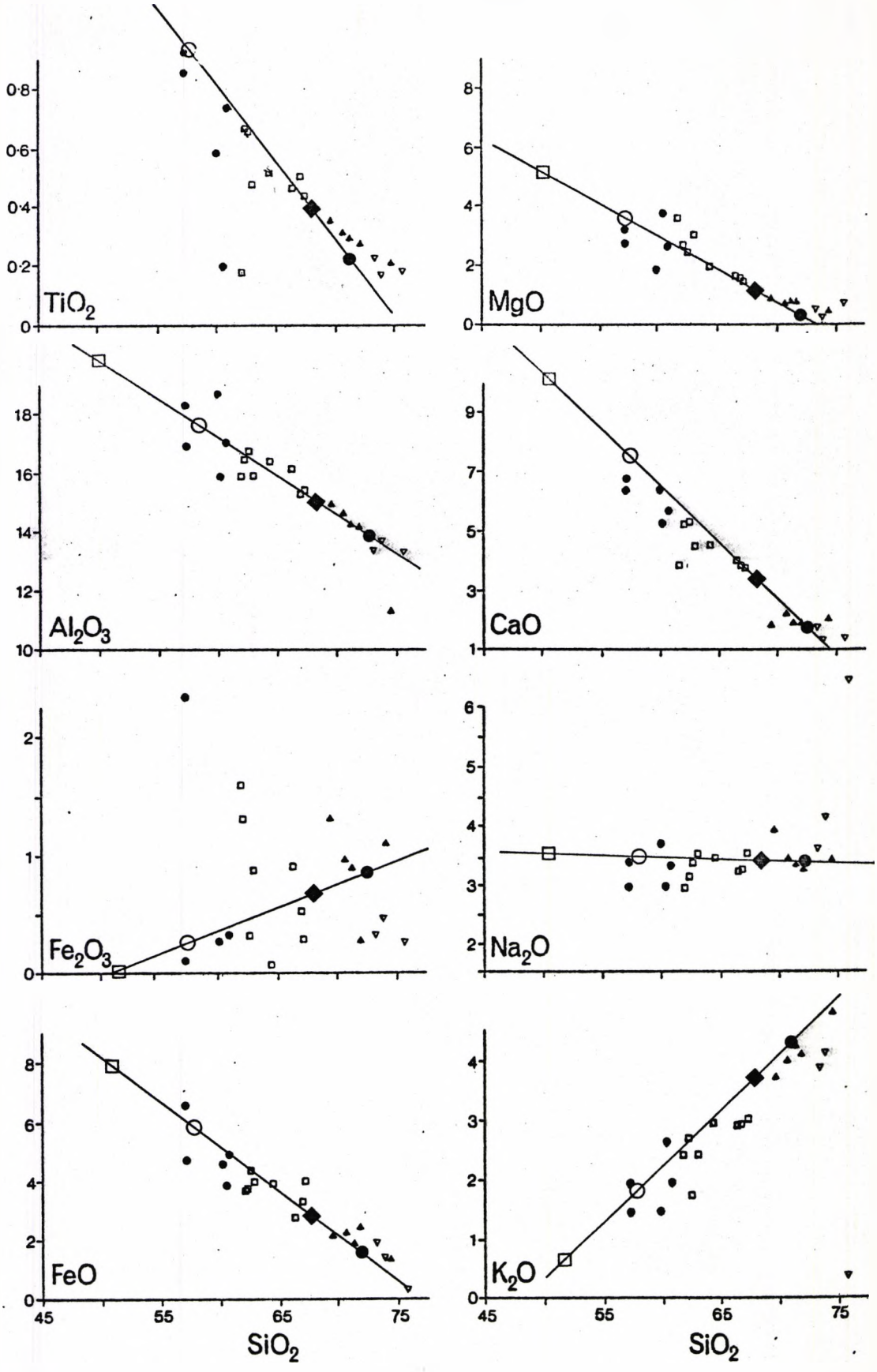

Figure 7.2 Harker diagrams and modelling data for the Eastern Pluton

symbols as in Figure 7.1.4 plus:- solid diamond - overall weighted average ; solid circle - evolved liquid when 20% of solid removed; open circle - 'cumulate'; open square - 'precipitate'.

If an attempt is made to extract a combination of these two minerals only from the overall weighted average, the effect is that, although there is some success in obtaining a composition close to that of the inner facies, better results are obtained by including rutile and water as extra components. The best combination to extract is as follows:- plagioclase 53.2%, hornblende 45.5%, rutile 0.7%, water 0.5% by weight. This would correspond to a modal composition of plagioclase 57.8%, hornblende 40.2%, rutile 0.5%, water 1.5% by volume. When a weight fraction of 20% of the initial magmatic liquid is removed, the evolved liquid composition (no. 8, Table 7.2) can be seen to be close to that of the inner average (no. 1, Table 7.2). The composition of the crystallising solids, the 'precipitate', is also given (no. 7, Table 7.2), but this is unlikely to be seen as a rock, as it will be mixed with some of the remaining liquid. The components considered above have been mixed in the same relative proportions with the overall weighted average as follows:- overall average 40.1%, plagioclase 31.9% hornblende 27.3% rutile 0.4%, water 0.3% by weight, which gives a composition (no. 9, table 7.2) close to that of the average for the outer facies (no. 3, Table 7.2).

The trace elements plots for Rb, Sr, Ba (Figure 5.5.2e) show clearly that the trend in the rocks is explained by a combination of the plagioclase and hornblende vectors and that fractionation of much biotite would cause a change in composition of these elements in the opposite direction. The CaO - Y plot is also consistent with a dominantly plagioclase extraction (Figure 5.5.2d). The Ti - Zr plot suggests that hornblende and biotite could be responsible (Figure 5.5.2c). The omission of biotite in the extract modelling above indicates that hornblende alone was the ferromagnesian mineral involved, possibly with a higher TiO_2 content than the one chosen. In this way, hornblende rather than rutile,

could account for the depletion in TiO_2.

When comparing the modes for these rocks (Table 5.4.1), there is a clear decrease in plagioclase, hornblende (particularly) and biotite, with a corresponding increase in quartz and K-feldspar. This is what would be expected of course, and a calculated mode for the 'cumulate' shows that it is similar to the outer facies, but does indicate rather more hornblende at the expense of quartz and biotite. The use of the term 'cumulate' here is not intended to necessarily imply the same sorts of processes that may occur in closed system basalt to acid fractionation, but rather to imply a mix of liquidus crystals with the original or evolved liquid. It may be that biotite does play some part in the fractionation process, but it is considered that biotite, together with quartz and K-feldspar, crystallise at a later stage, and hence are not involved in the early or middle stages of fractionation. These compositions are shown on the Harker diagrams (Figure 7.2).

7.3 Tak Pluton

This pluton is very different to the Eastern Pluton - namely that the overall composition is fairly acid, with a range in SiO_2 of 67.9 - 74.4%, and in addition it has a basic core and an acidic outer part. If the same process of initial cooling and crystallisation of plagioclase and hornblende, thus causing fractionation of the original magma, is attempted the composition of the 'acidic' member cannot be attained, mainly because the K_2O is lower in the acidic member. The removal of plagioclase and hornblende, both with zero or low K_2O, inevitably causes the K_2O in the evolved liquid to increase. Even if biotite is included in the fractionation process, there is not enough FeO and MgO available to allow sufficient biotite to be used to cause a reduction in the K_2O. Furthermore, so much biotite would be required - 60% plus - that to cause any reduction, that the reduced amount of plagioclase means that Al_2O_3 increases, instead of decreasing as required. The high Al_2O_3 in plagioclase, particularly in an anorthite-rich variety, is the only means

of removing Al_2O_3 in these rocks.

As an example the most basic sample (T01 approximately 68% SiO_2 - no. 12, Table 7.3) has been taken and attempts made to arrive at an acidic end-member (say T10B approximately 74% SiO_2 - Table 2.5.1) by removal of combinations of plagioclase, hornblende and biotite. Even with a mix of plagioclase 20%, hornblende 20%, biotite 60% by weight (no. 16, Table 7.3), it can be seen that after only 8% of the original magma (i.e. sample T01) has been removed, the SiO_2 has only increased to just over 70%, but the Al_2O_3 has increased to 16% (no. 17, Table 7.3). Further fractionation along this path is not possible, as both FeO and MgO are almost depleted; only a small increase in K_2O has been achieved. It became clear that the only mineral capable of reducing the K_2O sufficiently would be K-feldspar, but it is not possible to imagine a fractionation involving both hornblende and K-feldspar, from the textural and physical relations.

A numerical solution can be achieved by extracting a quartz-feldspar mix (= pegmatite) from the overall weighted average and thereby obtain a basic, high K_2O, member. There are extensive late pegmatites, which are mined for K-feldspar, around the Tak Pluton and so a geological model, compatible with the numerical model, can be put forward in which these pegmatites evolved from the original homogeneous magma. This resulted in a more basic 'residue' with the composition of the inner facies. The pegmatites around the Tak Pluton contain mainly quartz and K-feldspar, with some plagioclase. An estimated composition was calculated by mixing quartz 47.5%, K-feldspar 32.5%, plagioclase 20% by weight and the composition is given in Table 7.3 (no. 6). The effects of removing 15, 25 and 35% of this pegmatite from the overall weighted average are given in Table 7.3 (nos. 7, 8 and 9). In order to explain the compositions of the outer facies, i.e. those rocks having SiO_2

TABLE 7.3

Modelling data for the Tak Pluton

	1	2	3	4	5	6	7	8	9
SiO_2	71.02	74.14	72.27	64.80	68.39	82.24	70.51	68.95	66.90
TiO_2	0.24	0.15	0.20	-	-	-	0.24	0.27	0.31
Al_2O_3	14.60	13.45	14.14	19.72	19.85	10.38	14.80	15.39	16.16
Fe_2O_3	1.04	0.65	0.88	-	-	-	1.04	1.17	1.35
FeO	1.04	0.96	1.01	-	-	-	1.19	1.35	1.55
MgO	0.50	0.33	0.43	-	-	-	0.51	0.57	0.66
CaO	1.40	0.94	1.22	0.34	0.21	0.15	1.41	1.58	1.80
Na_2O	3.73	3.75	3.74	3.42	11.27	3.37	3.81	3.86	3.94
K_2O	5.50	5.23	5.39	11.72	0.28	3.86	5.66	5.90	6.21
Rest	0.93	0.40	0.72	-	-	-	0.85	0.96	1.11

1 Average of 4 inner facies rocks from the Tak Pluton.

2 Average of 3 outer facies rocks from the Tak Pluton.

3 Overall weighted average in the proportions 60% inner, 40% outer.

4 K-feldspar from Deer, Howie and Zussman (1963) vol. 4, p. 37, no.10. orthoclase microperthite (moonstone) - slight adjustment to SiO_2.

5 Plagioclase from Deer, Howie and Zussman (1963) vol. 4, p. 110, no. 4, albite - slight adjustment to SiO_2.

6 Empirical pegmatite, mixing quartz 47.5%, no. (4) 32.5%, no. (5) 20%.

7 Evolved liquid when 15% of (6) has been removed from (3).

8 Evolved liquid when 25% of (6) has been removed from (3).

9 Evolved liquid when 35% of (6) has been removed from (3).

cont/....

TABLE 7.3 (continued)

	10	11	12	13	14	15	16	17
SiO_2	74.26	76.26	67.87	55.96	46.62	35.71	41.94	70.12
TiO_2	0.16	0.12	0.31	-	1.37	4.00	2.67	0.10
Al_2O_3	13.39	12.64	15.89	28.27	8.24	13.32	15.29	15.94
Fe_2O_3	0.70	0.53	1.07	-	-	4.02	2.41	0.95
FeO	0.81	0.61	1.59	-	15.97	23.61	17.37	0.22
MgO	0.34	0.26	0.53	-	11.49	6.57	6.24	0.03
CaO	1.01	0.79	1.63	9.77	10.32	0.01	4.02	1.42
Na_2O	3.67	3.59	3.77	5.52	1.37	0.15	1.47	3.97
K_2O	5.08	4.78	5.90	0.48	0.51	9.53	5.81	5.91
Rest	0.58	0.43	1.44	-	4.11	3.26	2.78	1.32

10 'Cumulate', mixing 80% of (3) with 20% of (6).

11 'Cumulate', mixing 60% of (3) with 40% of (6)

12 'Cumulate', mixing 40% of (3) with 60% of (6)

12 Sample T01 from Table 2.5.1

13 Plagioclase no. 5 from Table 7.2

14 Hornblende no. 6 from Table 7.2

15 Biotite from Teggin (1975) Table 7.23 sample TK1

16 'Precipitate', mixing 20% of (13), 20% of (14), 60% of (15).

17 Evolved liquid when 8% of (16) has been removed from (12).

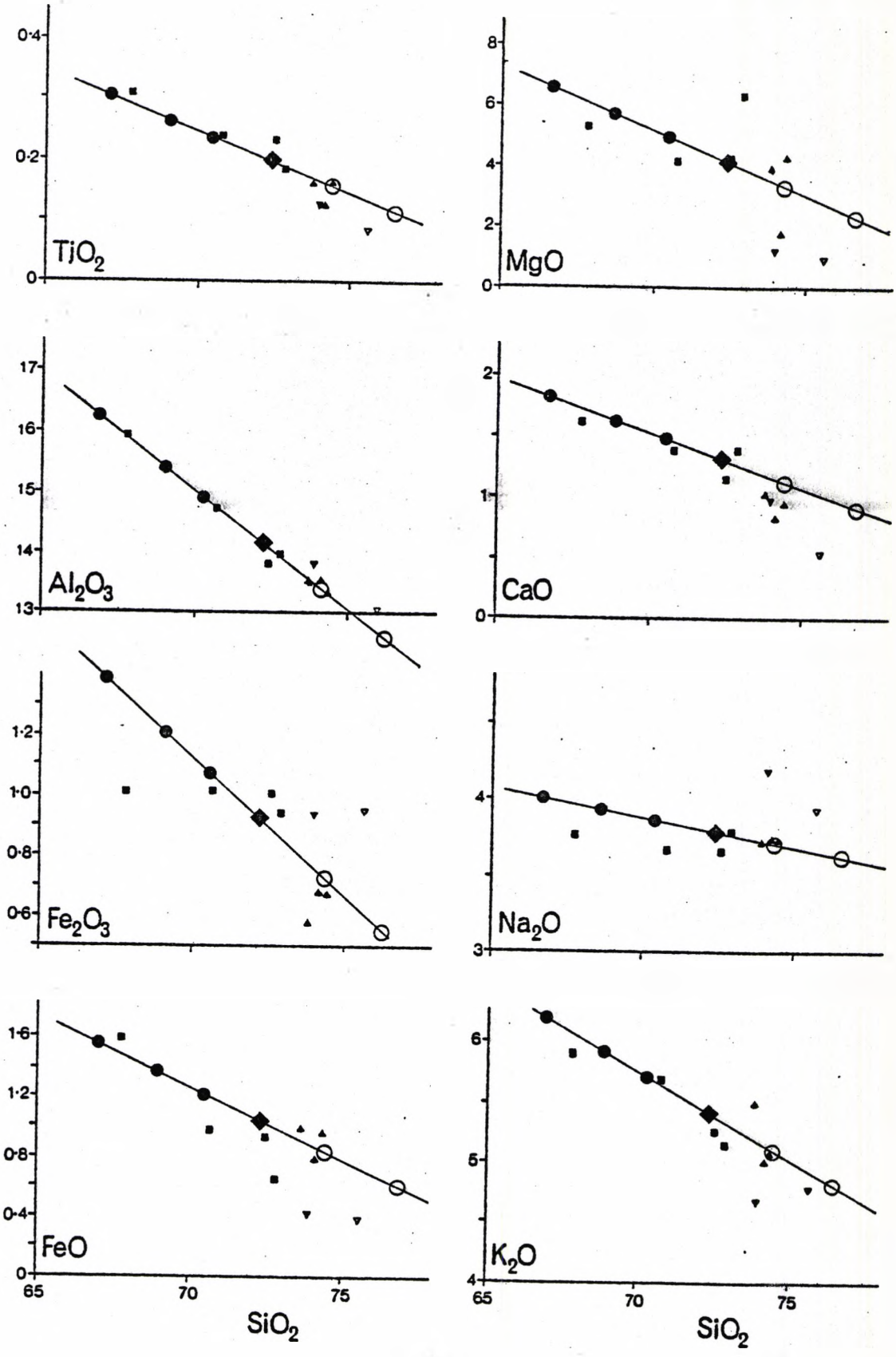

Figure 7.3 Harker diagrams and modelling data for the Tak Pluton symbols as in Figure 7.1.1 plus:- solid diamond - overall weighted average; solid circle - evolved liquids (right to left 15, 25, 35% of solid removed; open circle - 'cumulates' (left to right 80% average plus 20% pegmatite, 60% plus 40%)

contents greater than the overall average, the pegmatite has been mixed with this average in various proportions, and two examples are shown in Table 7.3 (nos. 10 and 11). The above compositions are shown superimposed on the Harker diagrams (Figure 7.3). They are all compatible with the plots of the actual rocks and indicate that unmixing, particularly in the outer facies, was not complete. It can be seen that the most basic rock of the inner facies was derived from the greatest removal of pegmatite (Figure 7.3). The general scatter in Figure 7.3 is related to variable removal and mixing in the inner and outer facies.

7.4 Western Main Range Pluton

This pluton has a range of SiO_2 of 61.8 - 72.3% and shows similar zoning to the Tak Pluton; a basic core and an acidic outer part. The alkalis appear however to behave in a slightly different fashion. The K_2O increases from basic to acidic and Na_2O shows a distinct decrease, whereas in both the Tak and in the Eastern Pluton particularly, there is little significant change in Na_2O content.

An attempt was made to fractionate from the basic to acidic compositions, as in the Eastern Pluton model, Starting with sample T84 (Table 4.5.1), plagioclase and hornblende were removed; the fractionation could not proceed very far in terms of an increasing SiO_2, as CaO soon falls to zero. A change to a more albitic plagioclase (an andesine from Deer, Howie and Zussman (1963) vol. 4, p. 115, no. 8) did not help as expected, since the plagioclase now has a higher SiO_2 and a lower Al_2O_3. Therefore the SiO_2 does not increase rapidly enough, neither does the Al_2O_3 decrease sufficiently. In addition FeO, MgO and CaO all fall too quickly, Na_2O does not decrease sufficiently and K_2O is increasing too much. The inclusion of biotite in the fractionation means that the increase in K_2O is not so rapid, but the overriding problem seems to be

TABLE 7.4

Modelling data for the Western Main Range Pluton

	1	2	3	4	5	6	7	8	9	10
SiO_2	64.62	71.27	66.60	76.08	77.66	64.23	60.28	68.50	70.39	72.29
TiO_2	0.52	0.20	0.42	0.09	-	0.50	0.64	0.35	0.29	0.22
Al_2O_3	17.09	14.58	16.34	12.72	12.84	17.25	18.75	15.62	14.89	14.17
Fe_2O_3	1.32	0.99	1.22	0.66	-	1.36	1.59	1.11	1.00	0.88
FeO	1.62	0.71	1.35	0.25	-	1.63	2.08	1.13	0.91	0.69
MgO	1.35	0.57	1.12	0.14	-	1.37	1.77	0.92	0.73	0.53
CaO	2.95	1.47	2.51	0.61	0.20	2.99	3.78	2.13	1.75	1.37
Na_2O	4.22	3.87	4.12	3.05	3.40	4.39	4.83	3.91	3.69	3.48
K_2O	4.70	5.19	4.85	5.99	5.90	4.57	4.09	5.08	5.31	5.53
Rest	1.61	1.15	1.47	0.41	-	1.74	2.18	1.26	1.05	0.83

1 Average of 5 inner facies rocks from the Western Main Range Pluton (omitting sample CTK45 - rock in contact with Mae-Salit Pluton)

2 Average of 6 outer facies rocks from the Western Main Range Pluton (omitting sample CTK10 - boundary inner/outer facies)

3 Overall weighted average in the proportions 70% inner, 30% outer.

4 Average leucogranite (samples T13 and T65 from Table 4.5.1).

5 Empirical pegmatite, mixing quartz 35%, K-feldspar (no. 4, Table 7.3) 50%, plagioclase (no. 5, Table 7.3) 15%.

6 Evolved liquid when 20% of (4) has been removed from (3).

7 Evolved liquid when 40% of (4) has been removed from (3).

8 'Cumulate', mixing 80% of (3) with 20% of (4).

9 'Cumulate', mixing 60% of (3) with 40% of (4).

10 'Cumulate", mixing 40% of (3) with 60% of (4).

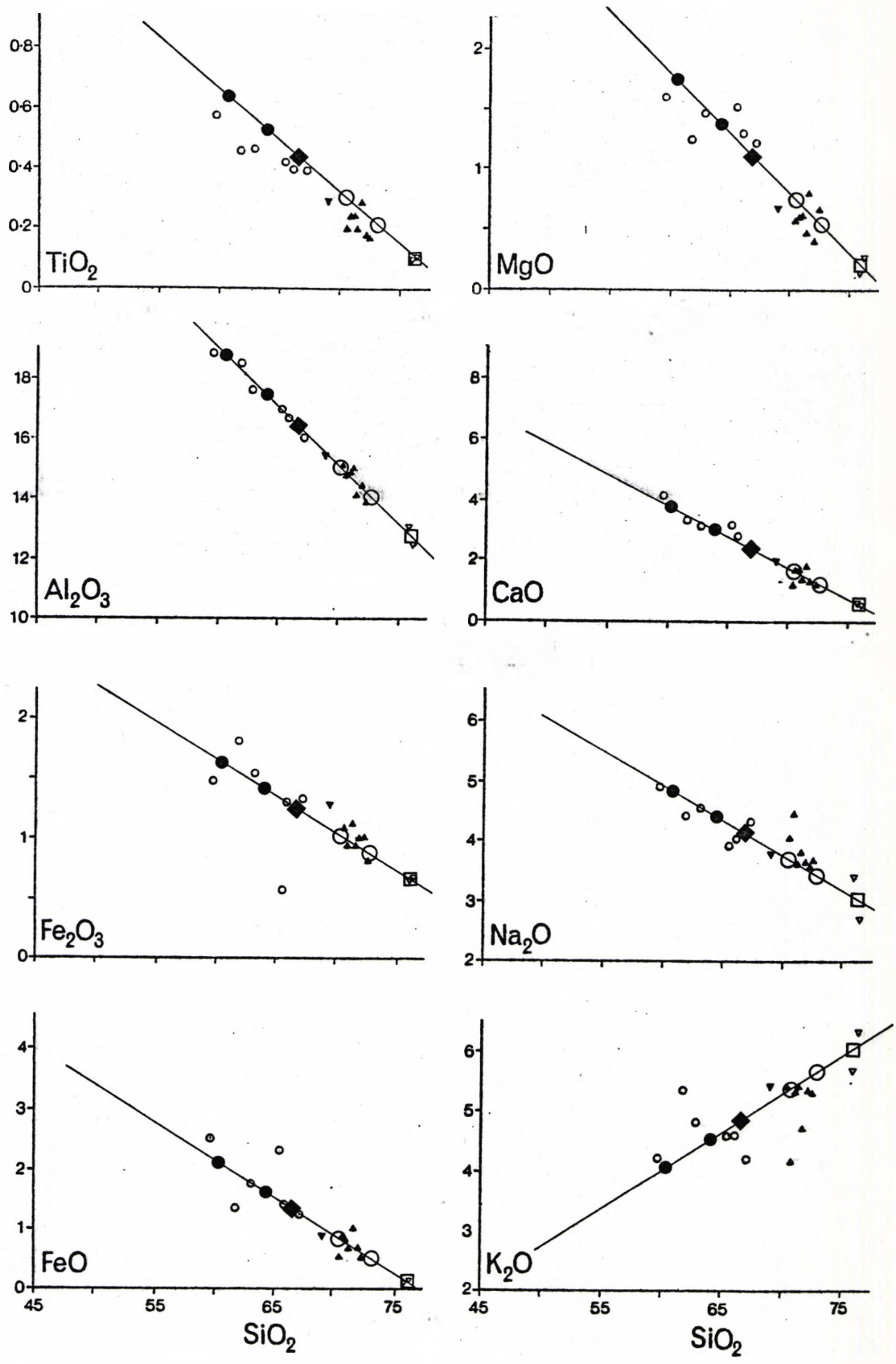

Figure 7.4 Harker diagrams and modelling data for the Western Main Range Pluton

symbols as in Figure 7.1.2 plus:- solid diamond - overall weighted average; solid circle - evolved liquids (right to left 20, 40% of solid removed); open circle - 'cumulates' (left to right 60% average plus 40% leucogranite, 40% plus 60%); open square - average leucogranite.

to get the SiO_2 high enough. There does not appear to be a combination of these three minerals, which are those that are expected to take part in fractionation, which will cause the composition to change in the required manner, i.e. from, say, sample CTK 60-1 to sample T16.

While no pegmatites have been found around the Western Main Range Pluton, there are some late intrusive leucogranites. Two samples have been analysed (T13 and T65) and their average composition (no. 4, Table 7.4) has a K_2O of 5.99%. The results of extracting 20 and 40% of this average from the overall weighted average (no. 3, Table 7.4) are shown in Table 7.4 (nos. 6 and 7). The effect of mixing the average leucogranite with the overall average gives the more acidic compositions (nos. 8, 9 and 10, Table 7.4). All these compositions are shown superimposed on the Harker diagrams (Figure 7.4) and can be seen to fit well with the plots of the actual rocks.

The average modal composition of the intrusive granites (taken from Table 4.4.1) is quartz 32.4%, K-feldspar 47.1%, plagioclase 19.6%, others 0.8% - which converts to weight proportions quartz 32.8%, K-feldspar 46.8%, plagioclase 19.5%, others 0.9%. Converting the average leucogranite (no. 4, Table 7.4) to a CIPW Norm, the proportions are quartz 33.8%, orthoclase 35.6%, albite 25.7%, anorthite 3.1%, others 1.4%, water 0.4%. An empirical mix of quartz 35%, K-feldspar 50%, plagioclase 15%, is shown in Table 7.4 (no. 5) and this gives a composition close to that of the intrusive granites. It is noteworthy that the acidic extract in this pluton has a greater proportion of K-feldspar and hence a higher K_2O, than the acidic extract proposed in the Tak Pluton model.

7.5 Mae-Salit Pluton

This is an acidic pluton, with a range in SiO_2 of 68.8 - 75.0% and like the Tak and Western Main Range Plutons, shows 'reverse' zoning, in

that it has a basic core and an acidic outer part. It is similar to the Western Main Range Pluton, showing an increase in K_2O and some decrease in Na_2O with increasing SiO_2. Field evidence does not show any evidence of pegmatites or intrusive granites associated with this pluton. This suggests that a fractionation model, similar to that for the Eastern Pluton, should be tested. The Harker diagrams show a distinct gap in the SiO_2 content, and sample CTK22, originally assigned to the outer facies on geographical and field evidence, is clearly more closely related to the inner facies on the basis of major element chemistry. This sample has therefore been included in the inner facies average (no. 1, Table 7.5) and excluded from the outer facies average (no. 2).

There are virtually no mineral analyses available from this pluton, but on attempting to extract a combination of plagioclase, hornblende and biotite from the overall weighted average (no. 3, Table 7.5), it became clear that an albitic plagioclase, with some K_2O, was required. Petrographic evidence indicates that the plagioclase phenocrysts in this pluton are less anorthitic than those in the Eastern Pluton (see sections 3.4 and 5.4). A suitable composition was selected from Deer, Howie and Zussman (1963) vol. 4, p. 113, no. 13 and this is given in Table 7.5 (no. 4). It then became apparent that a more Mg-biotite than that used in the Eastern Pluton model was necessary. Teggin (1975) gives several analyses of biotites from what he designated the Tak Batholith. Later work by the author has established the existence of a separate pluton - namely the Mae-Salit - in the north west of the area. The biotite selected on compositional grounds is indeed from the Mae-Salit Pluton (no. 6, Table 7.5). The hornblende used is the same as that used in the Eastern Pluton model (no. 5, Table 7.2). Although theoretically hornblende can vary substantially in composition, in practice the variation seems to

TABLE 7.5

Modelling data for the Mae-Salit Pluton

	1	2	3	4	5	6	7	8	9
SiO_2	69.46	74.40	70.45	60.98	46.62	36.87	55.94	74.08	69.00
TiO_2	0.33	0.14	0.29	0.05	1.37	4.05	0.84	0.15	0.35
Al_2O_3	15.13	13.33	14.77	23.59	8.24	13.82	21.15	13.18	15.41
Fe_2O_3	1.13	0.67	1.04	0.24	-	1.43	0.45	1.19	0.98
FeO	1.19	0.73	1.10	0.32	15.97	16.01	3.86	0.41	1.38
MgO	0.79	0.23	0.68	0.23	11.49	14.25	3.28	0.03	0.94
CaO	2.00	1.10	1.82	4.69	10.32	-	4.06	1.26	2.04
Na_2O	3.91	3.48	3.82	7.39	1.37	0.05	5.79	3.33	4.02
K_2O	4.81	5.25	4.90	1.49	0.51	9.42	2.91	5.40	4.70
Rest	1.25	0.67	1.13	1.01	4.11	4.10	1.71	0.99	1.19

1 Average of 6 inner facies rocks from the Mae-Salit Pluton

2 Average of 3 outer facies rocks from the Mae-Salit Pluton

3 Overall weighted average in the proportions 80% inner, 20% outer.

4 Plagioclase from Deer, Howie and Zussman (1963) vol. 4, p. 113 no. 13 oligoclase - slight adjustment.

5 Hornblende (no. 6 from Table 7.2).

6 Biotite from Teggin (1975) Table 7.23 sample TK14.

7 'Precipitate', mixing 77.4% of (4), 4.2% of (5), 18.4% of (6).

8 Evolved liquid when 20% of (7) has been removed from (3).

9 'Cumulate', mixing 90% of (3) with 10% of (7).

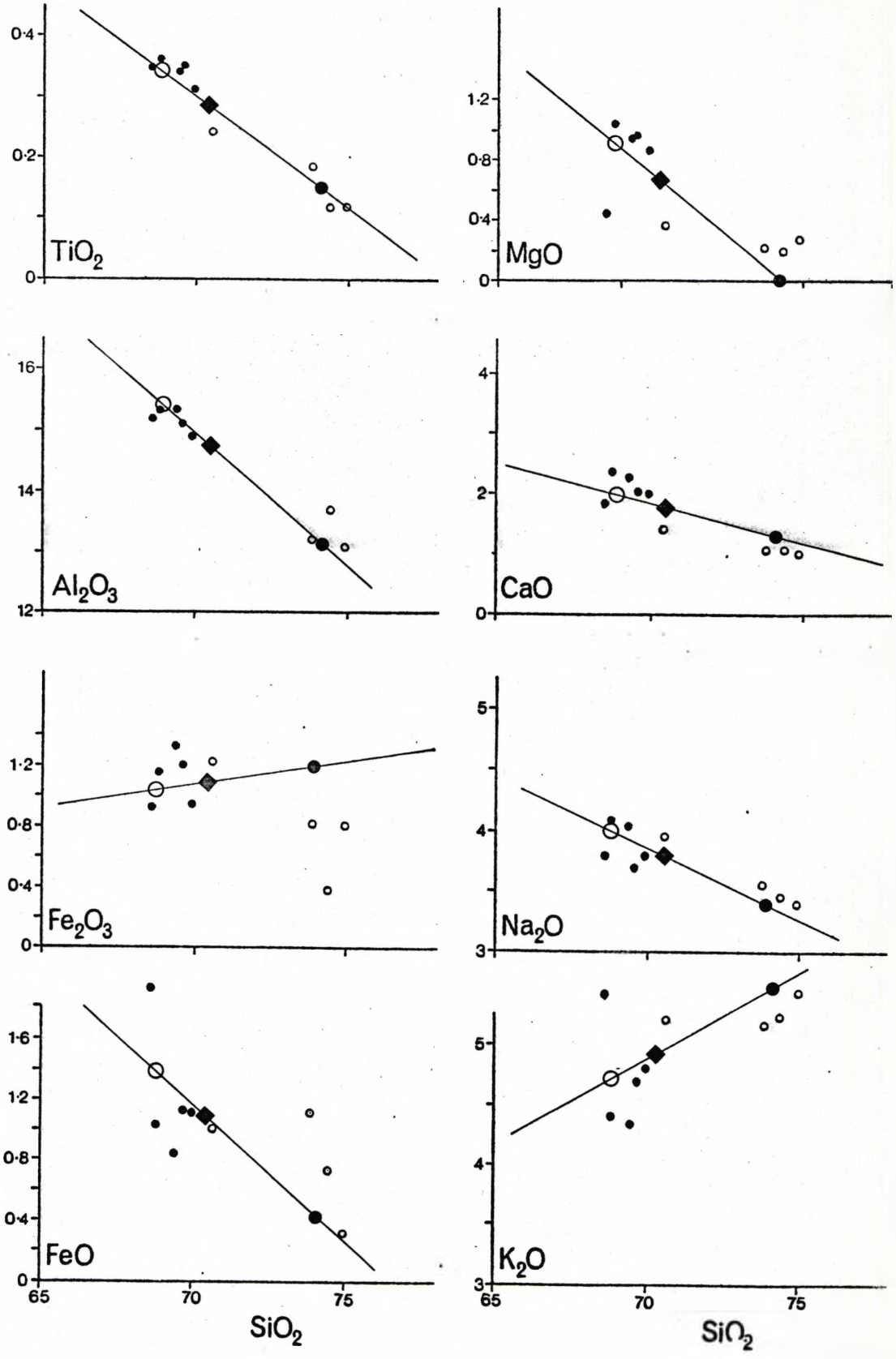

Figure 7.5 Harker diagrams and modelling data for the Mae-Salit Pluton.

. symbols as in Figure 7.1.3 plus:- solid diamond - overall weighted average; solid circle - evolved liquid when 20% of solid removed; open circle - 'cumulate' 90% average plus 10% 'precipitate'.

be small (see Appendix III). The most suitable mix of these minerals needs only a small amount of hornblende, so even a major change in its composition would not materially affect the model.

The results of extracting these three minerals from the overall weighted average (no. 3, Table 7.5) is given in the same table (no. 8); the effect of mixing the 'solid' extract (no. 7, Table 7.5) with the overall average is also given (no. 9). These compositions are shown superimposed on the Harker diagrams (Figure 7.5) and mostly agree well with the plots of the actual rocks observed in the Mae-Salit Pluton. The trend on the plot for Fe_2O_3 does not agree quite so well, but it is a simple matter to remove excess Fe_2O_3 as hematite. One sample (CTK 25) from the inner facies has somewhat aberrant plots on the FeO, MgO and K_2O diagrams (Figure 7.1.2). This rock has a granophyric texture and is different to the other inner facies rocks.

The geological problem of explaining how plagioclase, hornblende and biotite could crystallise in the core during the early stages, whilst presumably at a higher temperature than the outer part of the pluton, will be discussed in the conclusions.

CHAPTER 8

TYPOLOGY OF GRANITES AND MODE OF EMPLACEMENT

8.1 Introduction

An initial classification of granites was put forward by Chappell and White (1974), who divided granite rocks into I- and S- types. The criteria they used were sodium content, level of normative corundum, compositional range, type of mafic minerals and initial $^{87}Sr/^{86}Sr$ ratios (Table 8.1.1). This classification has been extended by White (1979) and by Pitcher (in press) as shown in Table 8.1.2. The latter author appreciated that the I-type of Chappell and White (1974), as defined in the Lachlan Belt in S.E. Australia, is compositionally and environmentally different from the I-type of Andinotype orogenic belts.

Beckinsale (1979) presents a classification of Thai granites using the original scheme of Chappell and White (1974). This will be examined in some detail, before considering the Tak Batholith, in the light of the later classification.

8.2 Previous classification of Thai granites according to Beckinsale (1979)

On the basis of initial $^{87}Sr/^{86}Sr$ ratios, recorded by Snelling et al (1970); Garson et al (1975); von Braun et al (1976); Teggin (1975) and Beckinsdale (1979), indicate that most of the Triassic granites in Thailand appear to be S-types. (Table 8.2.1).

However some of the Cretaceous granites in the Mae Lama and Phuket areas, which have initial $^{87}Sr/^{86}Sr$ ratios of 0.7086 and 0.7073 respectively, are considered to be I-type granites (Beckinsale 1979); although the initial $^{87}Sr/^{86}Sr$ ratios are higher than the range of 0.704-0.706 in the typical I-type granite (Chappell and White, 1974); Beckinsale (op. cit.) points out that the Mae Lama

TABLE 8.1.1 CHARACTERISTIC FEATURES OF I- AND S-TYPE GRANITES

I-TYPES	S-TYPES
Relatively high Sodium, Na_2O normally $>$ 3.2% in felsic varieties, decreasing to $>$ 2.2% in more mafic types.	Relatively low Sodium, Na_2O normally $<$ 3.2% in rocks with approx. 5% K_2O, decreasing to 2.2% in rocks with approx. 2% K_2O.
C.I.P.W. normative diopside or $<$ 1% normative corundum.	$>$ 1% C.I.P.W. normative corundum.
Broad spectrum of compositions from felsic to mafic.	Relatively restricted in composition to high SiO_2 types.
Hornblende and sphene commonly present.	Muscovite, monazite, cordierite, garnet commonly present.
Initial $^{87}Sr/^{86}Sr$ ratios in the range 0.704-0.706.	Initial $^{87}Sr/^{86}Sr$ ratios greater than 0.708.

TABLE 8.1.2 GRANITE-TYPES, THEIR CHARACTER AND GEOLOGICAL ENVIRONMENTS [from Pitcher (in press)]

M-type	I-(Cordilleran) type	I-(Caledonian) type	S-type	A-type
Plagioclase subordinate to gabbro	Tonalite dominant but broad compositional spectrum -	Granodiorite-granite in constrasted association with minor bodies of hornblende diorite and gabbro	Granites with high but narrow range of SiO_2. Leucocratic monzogranites predominate but granitoids with high biotite content locally important	Biotite granite in evolving series with alkalic granite and syenite. Highly contrasted acid-basic relationship
Hornblende and biotite; pyroxene	Hornblende and biotite; magnetite, sphene	Biotite predominates; ilmenite and magnetite	Muscovite and red biotite; ilmenite, monazite, garnet, cordierite	Green biotite. Alkali amphiboles and pyroxenes in alkalic types, astrophyllite
K-feldspar interstitial micrographic	K-feldspar interstitial and xenomorphic	K-feldspar interstitial and invasive	K-feldspar often as megacrysts with protracted history. Autometasomatic variants	
Basic igneous xenoliths	Dioritic xenoliths; may represent restitic material	Mixed xenolith populations	Metasedimentary xenoliths predominant	Cognate xenoliths, also basic magma blebs
Mol. $Al/Na + K + \frac{Ca}{2}$ 1.0	$Al/(Na + K + \frac{Ca}{2})$ 1.1	$Al/(Na + K + \frac{Ca}{2})$ ca. 1	$Al/(Na + K + \frac{Ca}{2})$ 1.05	Often peralkaline, relatively rich in F. Considerable range 0.703 - 0.712
Initial $^{87}Sr/^{86}Sr$ ratios < 0.704	<0.706	>0.705 <0.709	>0.708	
Small quartz diorite-gabbro composite plutons	Great multiple, linear batholiths with arrays of composite cauldrons	Dispersed, isolated complexes of multiple plutons and sheets	Multiple batholiths, plutons and sheets, less voluminous and more commonly diapiric than I-types	Multiple, centred, cauldron-complexes of relatively small volume
Associated island-arc volcanism	Associated with great volumes andesite and dacite	Sometimes associated basalt-andesite lava "plateaux"	Can be associated with cordierite-bearing lavas but characteristically lacking in voluminous volcanic equivalents	Associated with caldera centred alkalic lavas
Short, sustained plutonism	Very long-duration episodic plutonism	Short, sustained plutonism; post-kinematic	Sustained plutonism of moderate duration; syn- and post-kinematic	Short-lived plutonism
Oceanic island arc	Andinotype marginal continental arc (and some island arcs)	Caledonian-type post-closure uplift	Hercynotype continental collision. Also encratonic ductile shear-belts	Post-orogenic or anorogenic situations
Open folding: burial-type metamorphism	Vertical movements, little lateral shortening; burial-type metamorphism	Dip-slip and strike-slip faulting : retrograde metamorphism	Much shortening: low-pressure metamorphism in slate belts; part of a Granite Series	Doming and rifting
Porphyry-Cu, Au mineralization	Porphyry-Cu, Mo mineralization	Rarely strongly mineralized	Sn and W-greisen and vein-type mineralization	Columbite, cassiterite and fluorite

intrusion has a Na_2O content of ca 3.3% at ca 5.2% K_2O and an iron oxidation ratio of ca. 0.15, which confirms that the Mae Lama granite is essentially an I-type. He also discussed the higher initial $^{87}Sr/^{86}Sr$ ratio and thought it could be a result of minor contamination of a mantle derived magma with crystal strontium, a reasoning similar to that of Taylor and Silver (1978) who thought that extensively altered oceanic lithosphere might be involved in the genesis of this kind of granitic magma.

The relationship of the granite in Thailand and Malaysia to a plate tectonic model has been proposed by Mitchell (1977). He recognised three zones of granitic belts, namely the Eastern Belt, the Central Belt and the Western Belt. (Fig. 8.2.1). The Eastern Belt is generally recognised as consisting of hornblende-bearing granites, usually associated with late Palaeozoic to Triassic volcanics, and ranging in age from Carboniferous to Permian or early Triassic. The Central Belt is made up chiefly of porphyritic biotite-granite of Triassic age, usually associated with highly folded Palaeozoic meta-sediments. The Western Belt is composed principally of granitic rocks of Cretaceous to Eocene age. It is argued later that, in my view, Mitchell placed his boundary lines too far to the east. The western belt consists only of Phuket and Mae-Lama I-type granites. The Tak Batholith and several intrusions further north lie in the Eastern belt.

Beckinsale (1979) based on $^{87}Sr/^{86}Sr$ ratios (Table 8.2.1) recognised that there are both I - and S - type granites in Thailand. The Eastern Belt is related to subduction of the oceanic lithosphere during Permo-Triassic times; the Central Belt, an S-type granite, is related to continental collision in Triassic times; the Western Belt, with I - and S-type granites is also related to subduction. Beckinsale (op. cit) mentioned that the change in the tectonic pattern of late Palaeozoic-Triassic subduction and collision is due to the opening

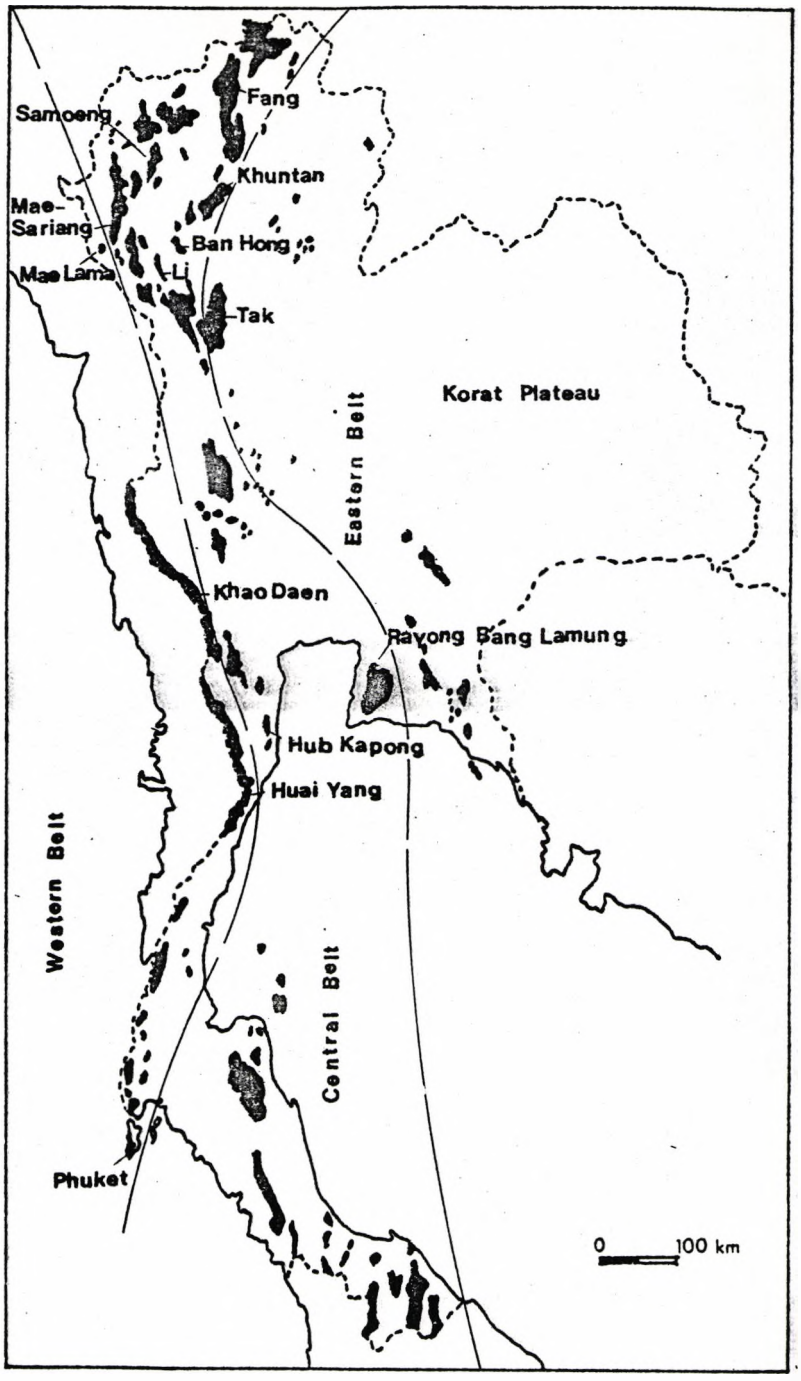

Fig. 8.2.1 Distribution of granites in Thailand.

Those named have Rb-Sr whole rock isochron ages (Table 8.2.1). The long dashed lines show the boundaries of the Western, Central and Eastern granitic belts (modified from Mitchell, 1977).

TABLE 8.2.1

Geochronological data for Thai granites

Location	Rb/Sr age Ma	Classification	Sr^{87}/Sr^{86} ratio	Reference
Mae Sariang	190 ± 7	S-type	0.7280	Braun, V. et al. (1976)
Fang	240 ± 64	S-type	0.7280 ± 66	Braun, V. et al., (1976) Beckinsale et al., (1979)
Li	244 ± 28	S-type	0.7220 ± 44	Braun, V. et al., (1976) Beckinsale et al., (1979)
Ban Hong	342 ± 9	S-type	0.7253 ± 15	Braun, V. et al., (1976) Beckinsale, et al. (1979)
Khuntan	212 ± 12	S-type	0.7244 ± 20	Teggin, (1975) Braun, V. et al., (1976) Beckinsale, et al. (1979)
Mae Lama	130 ± 4	I-type	0.7086 ± 7	Beckinsale et al., (1979)
Samoeng	204 ± 15	S-type	0.7328 ± 21	Teggin, (1975) Beckinsale, et al., (1979)
Tak (pink)	219 ± 12	intermediate I-type	0.710 ± 19	Teggin, (1975)
Tak (white)	213 ± 10	intermediate I-type	0.7158 ± 13	Teggin, (1975)
Khao Daen	93 ± 4	S-type	0.7338 ± 7	Beckinsale et al., (1979)
Hub Kapong	210 ± 4	S-type	0.7237 ± 6	Beckinsale et al., (1979)
Rayong-Bang Lamung	220 ± 13	S-type	0.7265 ± 13	Beckinsale, R.D. (1979)
Phuket Island	108 ± 5	S-type	0.7293 ± 5	Beckinsale, R.D., (1979
Phuket Island	124 ± 4	I-type	0.7072 ± 13	Snelling et al., (1970) Beckinsale, et al., (1979)
Huai Yang	186 ± 11	S-type	0.823 ± 3	Burton and Bignell, (1969)

and closing of a suture which was the site of a 'marginal' basin between the then existing mircoplates in this area. This notion is in agreement with the suggestion of Ridd (1980) that this area was formed by fusion of the Thai-Malay Peninsula Block with the Indo-China Block (see chapter 1). The closure of the Palaeo-Tethys between the Thai-Malay Peninsula Block and the Indo-China Block, with a westward subduction of the latter under the former during early Permian times, as proposed by Ridd (1980) may be related to the granitic intrusions in the Eastern Belt. Therefore, the granitic rocks in the Eastern Belt could be subduction related. This subduction zone may have been present for a short period during early Permian times, but changed to a collision regime during middle or late Triassic times, producing the Central Belt granites of collision related S-type. The Western Belt granites, which are both I- and S-types of Cretaceous and Eocene ages may be related to the eastward subduction of oceanic lithosphere from the marginal basin (Neo-Tethys) lying to the west of Thailand. The relationship of the granitic intrusions with the plate tectonic model is shown in Figure 8.2.2.

The Tak Batholith is geographically located in an intermediate position between the Central Belt and the Eastern Belt (Figure 8.2.1). In contrast to the general features of S-type granites in the Central Belt, the granitic rocks in the Tak Batholith are not associated with highly folded Palaeozoic metasediments, but are usually associated with the Permo-Triassic volcanics. Mineralogically, the granitic rocks in the Tak Batholith are hornblende-biotite bearing which suggests they are similar to the Eastern Belt granites of Malaysia, as described by Mitchell (1977). The similarity of the granitic rocks in the Tak Batholith with those of the Eastern Belt of Malaysia was also recognised by Cobbing (per.comm.)

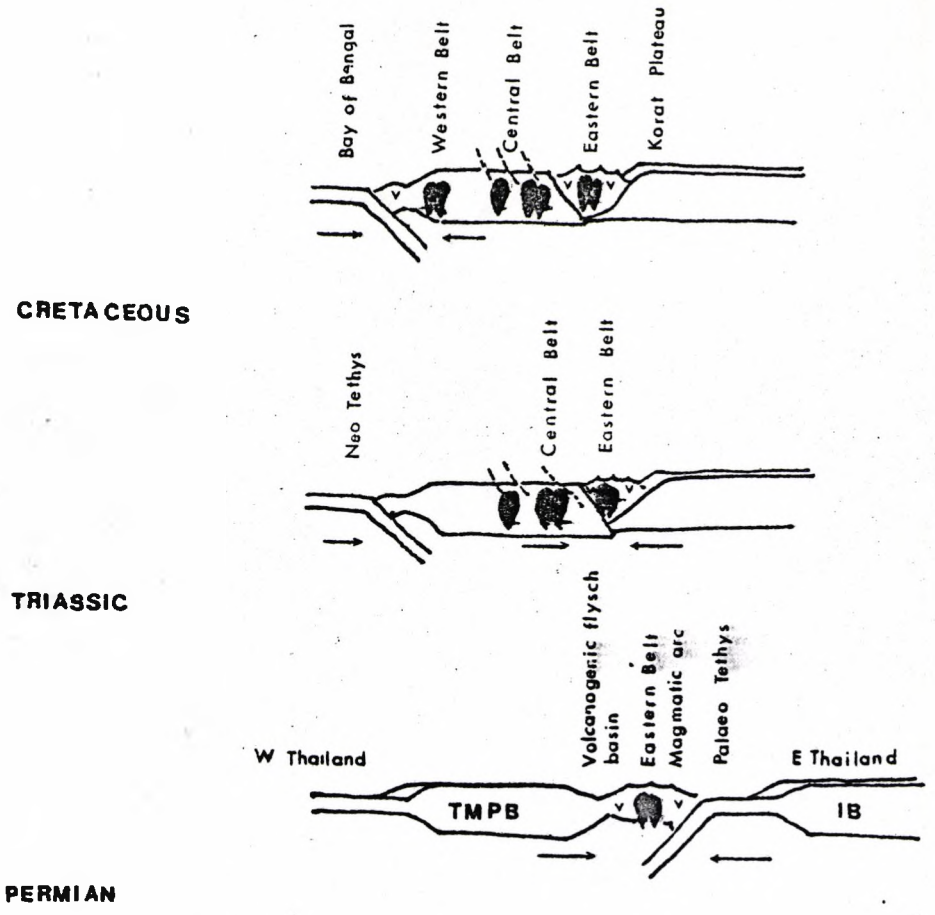

Figure 8.2.2 Schematic W-E sections across Thailand showing plate tectonic reconstruction and the granitic belts (modified from Ridd, 1980 and Beckinsale, 1979). TMPB = Thai-Malay Peninsula Block, IB = Indo-China Block; Granites shown in solid black; v indicates associated volcanics.

8.3 Granite Typology of the Tak Batholith

Pitcher (in press), in the recent review referred to above, suggested that at least five types of granites exist, namely (i) a M-type which includes the plagio-granite of the oceanic island-arcs; (ii) an I (Cordilleran) - type representing the voluminous gabbro-quartz diorite-tonalite assemblages of active continental plate edges; (iii) an I-(Caledonian) - type which represents the granodiorite and granite of the immediate post-orogenic uplift regimes; (iv) a S-type which is the peraluminous granite assemblage of encratonic and continental-collision fold belts; (v) an A-type which includes the alkaline granites of both the stabilised fold belts and the swells and rifts of the cratons.

The detailed characteristics of these five types of granite are summarised in Table 8.1.2. and these criteria will now be discussed in relation to the granites of the Tak Batholith.

8.3.1 The Tak and the Mae-Salit plutons have a high and narrow range of SiO_2. In these two plutons monzogranite predominates. The Western Main Range has a somewhat wider range of SiO_2 contents with monzonite predominating. There are minor associated bodies of hornblende-diorite (appinite). The Eastern Pluton has an even wider range of SiO_2 values with granodiorite predominating, plus some tonalite and hornblende-diorite (appinite). This suggests that if all four plutons are of the same type, they can only be designated as I-(Caledonian) type.

8.3.2. The common mafic minerals in all four plutons are hornblende and biotite. Alkali amphiboles and pyroxenes are absent as are muscovite, and biotite, monazite, garnet and cordierite. All four plutons contain magnetite, rather than ilmenite, as the ore phase. Sphene and allanite occur in all except the Eastern Pluton. The K-feldspar occurs as interstitial and xenomorphic grains in the Eastern Pluton, but in the other three plutons, K-feldspar often occurs as

megacrysts. Most of the xenoliths are dioritic although occasional metasedimentary xenoliths are seen.

8.3.3. All of the plutons normally show small amounts of normative corundum, usually less than 1%. The only values of initial $^{87}Sr/^{86}Sr$ ratios available for the rocks of the Tak Batholith are given by Teggin (1975). He gives values for the "pink" and "white" granite of the Tak Pluton of 0.7104 and 0.7158 respectively. The Tak Batholith is little mineralized. There are minor amounts of Cu mineralisation, but in contrast to other Thai granites and of course the Malay granites there is no evidence of Sn and W deposits.

8.3.4. The chemical and mineralogical characteristics above lead to the conclusion that the granitic rocks of the Tak Batholith should be considered as I-(Caledonian) types. The rather high initial $^{87}Sr/^{86}Sr$ ratios conflict with this, unless one accepts the suggestion of Beckinsale (1979) that such values can be observed in I-type granites, due to contamination by crustal Sr.

8.3.5 Pitcher's (in press) typology gives a number of criteria which define the environment and likely mechanism of emplacement of the various types of granite.

The Tak Batholith is an isolated complex of multiple plutons, rather than the great multiple linear batholiths, as exemplified by the Peruvian Coastal Batholith in South America, described by Pitcher (1979). It is sometimes associated with small volumes of volcanics, mainly of a pyroclastic nature. The Tak Batholith is thought to be related to short, sustained plutonism rather than a long-duration episodic plutonism, and shows no relation to regional metamorphism, as do the synkinematic granites described by Marmo (1971). Since the Tak Batholith consists of high-level granites this suggests that they are post-kinematic. They are locally associated with small

outcrops of red-bed (Khao Daeng formation) as defined on Bunopas' map (1974), thus indicating a relationship with a post-orogenic uplift regime. The Tak Batholith is associated with coeval faulting rather than with strong folding. Two major fault zones, namely the NW-SE trending Ping Fault Zone and the NE-SW trending Thoen Fault Zone are recognised in this area (Campbell and Nutalaya, 1974).

According to Pitcher (in press) those I-type granites with restricted compositional ranges and having no clear association in space and time with an identifiable plate-edge are to be regarded as the normal type of plutonic intrusion occurring within a narrow time interval during a phase of rapid uplift and red-bed molasse formation. They represent a post-closure, tensional regime. He also empahsises that the occurrence of the "intermediate" I-type granite or I-(Caledonian) type is not necessarily directly related to the subduction zone, as is commonly the case with I-type proper - i.e. the I-(Cordilleran) type.

In the case of the Tak Batholith, it is more likely that these rocks could well be classified as I-(Caledonian) type or "intermediate" I-type and should be included with the Eastern Belt granites of the Thai-Malay Peninsula (Pitcher, pers. comm.).

From all the evidence above it is apparent that if all the granites of the various plutons making up the Tak Batholith are to be considered in only one category, then they have to be I-(Caledonian) types. It should be borne in mind that some of the granites do show features of both I-(Cordilleran) and S-types.

8.4 Mode of emplacement of the Tak Batholith

While there are several mechanisms that could be considered for the mode of emplacement of granitic bodies, some have been rejected, eg. diapiric or salt-dome-like intrusion. Reasons for this are the presence of vertical or sub-vertical contacts between the plutons

and the country rock, the existence of flat roofs to the plutons, the lack of synclinorium folding in the country rock and the absence of migmatite development.

Two mechanisms considered likely for emplacement of the Tak Batholith are (a) piece-meal magmatic stoping and (b) high-level block-like intrusion.

8.4.1 Piece-meal magmatic stoping.

According to Daly (1914), the mechanism of magmatic stoping includes the following essential features:

a) There would be marginal shattering of the solid rocks, which form the roof and walls of the magma chambers.

b) Blocks and xenoliths produced by this shattering would sink in the magmatic liquid.

c) These processes would be repeated until the magma chamber is full of liquid magma.

8.4.2 High-level block-like intrusion

This mechanism was put forward by Rast (1969); he suggests the magma is pushed up under a faulted sedimentary block and then rises passively to a high-level in the crust. There would be little escape of magma along the fault planes. The envelope or wall rocks will not be strongly deformed or metamorphosed by the intrusion. Stoping plays a much less important part in this type of intrusive process. It is possible that a chilled margin would be formed along the roof contact zone, especially if the magma is in contact with a rather thin roof cover at a high level. There is likely to be little mineral orientation in the rocks of the pluton as the crystals have relatively free movement, since there is insufficient external pressure to cause any orientation.

8.4.3 Features of the Tak Batholith

The features which might help to indicate the mode of emplacement are as follows:

a) The Tak Batholith is a composite pluton, consisting of one calcic pluton on the eastern flank, and three potassic plutons on the western flank.

b) Each of these plutons is an elongated block-like shape, orientated along the general NE-SW direction of the regional tectonic trend in this area.

c) The roof cover and wall rocks are Palaeozoic and Mesozoic metasediments and volcanics. They are only slightly deformed, show weak metamorphism and there is no evidence of migmatite development.

d) Most of the contacts, both between the individual plutons and between the plutons and the wall rocks are sharp and are steep or vertical.

Minor acidic and basic intrusives usually occur along the contact zones.

e) There is no distinctive mineral orientation or any structural fabric in the granites.

f) One of the plutons on the eastern flank - the Eastern Pluton has a chilled margin on the roof contact. The other three plutons do not show chilled margins, but are commonly associated with minor acidic intrusives along the contacts.

The evidence of the various features above leads to the conclusion that forceful intrusion did not play a significant part in the emplacement of the Tak Batholith. Thus the mechanism of a high-level block-like intrusion is considered to be most likely. This proposed mode of emplacement of the plutons of the Tak Batholith is shown in Figure 8.4.3.

As indicated in earlier chapters, the sequence of intrusion of the four plutons making up the Tak Batholith appears to be, firstly, the Eastern Pluton, followed by the Western Main Range Pluton. Subsequently both the Tak and Mae-Salit Plutons were intruded into the complex.

The first stage (a) is shown in Figure 8.4.3, where the Eastern Pluton can be seen intruding the country rock, by upward movement under a faulted sedimentary block. Little deformation of the wall rock occurs, and the cover remains as a flat roof to the pluton. No stoping of the sediment occurs on the roof contact, but the chilled margin formed at the roof contact, does fracture and xenoliths of chilled margin fall into the magma. The next stage, the emplacement of the Western Main Range occurs in a similar manner of upward movement along vertical fault planes, some of which have developed within the Eastern Pluton itself. The same features of undisturbed wall rocks and roof are apparent. Late-stage acidic intrusives (leucogranites) develop along the contact planes. Again no stoping occurs, but in contrast to the Eastern Pluton, there is no development of a chilled margin. The Mae-Salit pluton was emplaced by the same process of high-level block-like intrusion into the western flank of the Western Main Range, with only minor amounts of late stage intrusives along the contacts. The Tak Pluton intrudes both the Western Main-Range and the Eastern Pluton, again by block-like intrusion along fault planes. There is extensive development of pegmatites around the border of the Tak Pluton.

Pitcher's (in press) classification of granite types shows that the I-(Caledonian) type granites would be intruded fairly rapidly into a faulted regime. Emplacement of such granites would not be sustained over a long period.

The model of emplacement of the Tak Batholith therefore agrees with the previous evidence, which suggested that these granites are indeed I-(Caledonian) type.

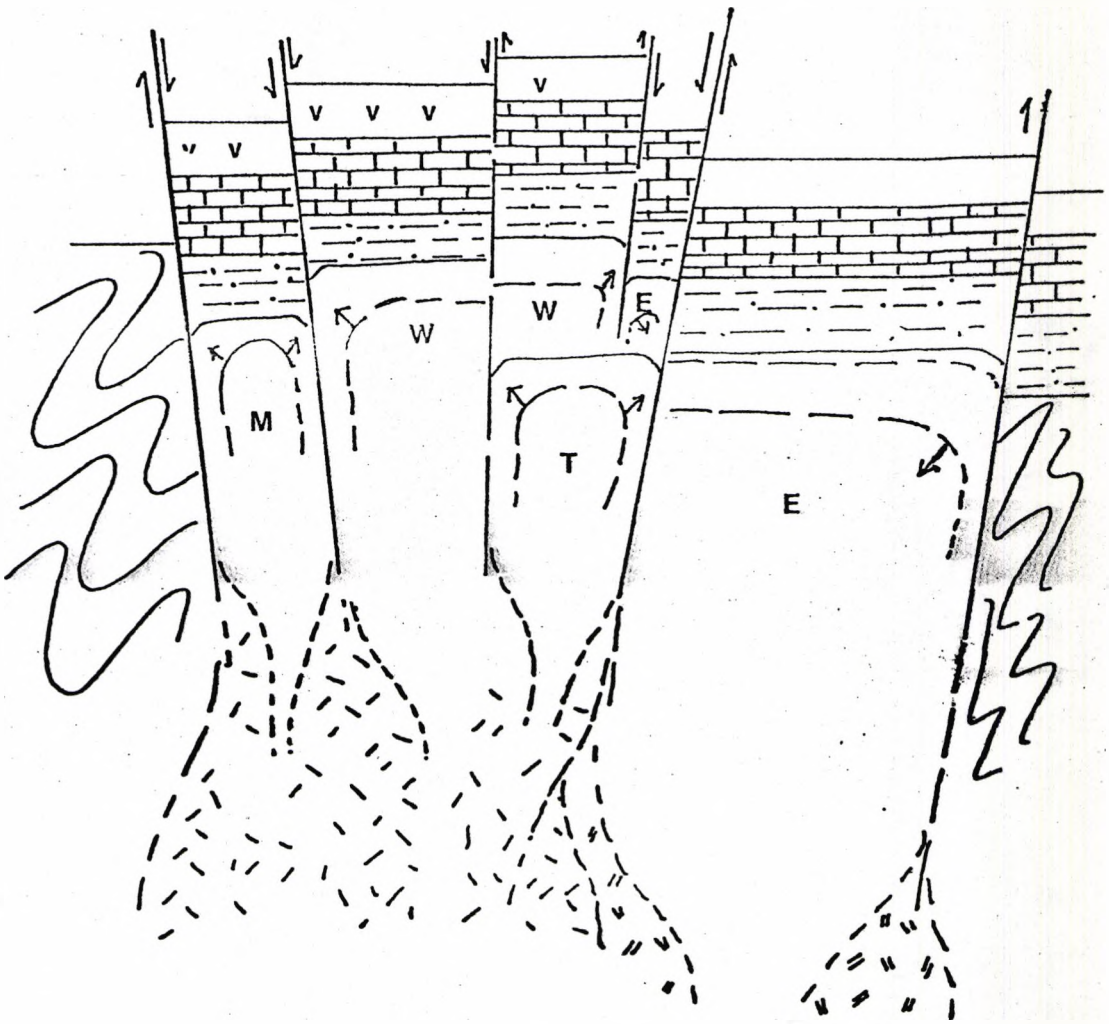

T Tak Pluton

M Mae-Salit Pluton

W Western Main Range Pluton

E Eastern Pluton

Dioritic magma ? (appinite)

Andesitic magma ?

V V Permo-Triassic volcanics

Permian limestone

Palaeozoic metasediments

Pre-Cambrian gneiss

Fault

Outward zoning pluton

Inward zoning pluton

Figure 8.4.3 Schematic model for the mode of emplacement of the Tak Batholith.

CHAPTER 9

CONCLUSIONS

9.1 Concluding discussion

Before summarising the major conclusions of this work, some discussion is necessary of some U, Th, Hf and Ta data, obtained by instrumental neutron activation analysis (see Tables 9.1 for U and Th and Appendix III for Hf and Ta). The most important features of these results are the strikingly high values for the Tak, Mae-Salit and Western Main Range Plutons; the average value of 15 analyses gives ca. 16 ppm U and ca. 77 ppm Th. Comparison of these values with U and Th contents from other granites, shows that such high values are rare. For instance, Killeen and Heier (1975) indicate averages of ca. 6 ppm for U and ca. 26 ppm for Th in the Precambrian granitic rocks of the Telemark area, Norway, while Hennessy (1981), in a survey of British granites, which Pitcher (in press), classifies as I-(Caledonian)-type, gives mean values of 4.7 ppm U and 14.6 ppm Th, which compare with the average values of the Eastern Pluton of 4.0 and 18.5 ppm respectively. O'Connor (1981) gives mean values for the British and Irish Caledonian granitic plutons of 4.0 ppm U and 14.1 ppm Th, these averages including the results of Hennessy (1981).

In contrast, after a comprehensive study of an uraniferous granite in Wyoming, U.S.A., Stuckless et al., (1977) quote values of ca. 10 ppm U and ca. 50 ppm Th in what they describe as the biotite phase. Much higher U values (around 75 ppm) were found in the fracture zones, where hydrothermal alteration was apparent. This might well be expected, due to the well-documented mobility of U compared to Th. In the Tertiary granites of the Mourne Mountains, Ireland, O'Connor

Table 9.1 Selected analytical data for the granitic rocks of the Tak Batholith (K as %; others in ppm)

	Eastern Pluton					
	T29	CTK28	T73	CTK62-1	T33	T25
Th	15	22	12	18	13	31
U	4	4	2	4	2	8
Pb	16	21	21	24	26	29
K	2.18	1.96	2.40	2.59	3.34	3.43

	Western Main Range Pluton							
	T84	T50	T90	CTK10	T14	T16	T49	T65
Th	77	98	74	95	77	83	61	53
U	12	15	13	12	30	20	20	8
Pb	64	59	59	60	83	76	57	67
K	3.95	3.84	3.83	3.93	4.37	4.45	4.51	5.22

	Mae-Salit Pluton		Tak Pluton				
	CTK26	CTK22	T01	T1	CTK48B	T02B	T02
Th	74	102	76	93	77	65	52
U	16	15	16	16	19	14	11
Pb	198	61	86	246	63	53	97
K	3.61	4.33	4.89	4.71	4.36	4.27	4.18

(1981) gives values of ca. 28 ppm U and ca. 91 ppm Th; these values are considerably higher than the values given for all the other Irish granites. The Mourne granite is emplaced into Lower Palaeozoic meta-sediments at a high crustal level in ring fractures. The pluton is thought to be a small batch of highly fractionated magma, possibly containing a substantial crustal component (O'Connor, 1981 (and others)). These Tertiary samples have a restricted compositional range and O'Connor (1981) suggests that, while in the main U occurs in primary apatite, zircon and monazite, there may be a discrete U phase in the Mourne granites. He also takes the view that the high $^{87}Sr/^{86}Sr$ ratios observed for the Irish tertiary granites (> .710) must be due to crustal contamination, and contrasts the low radioelement values of granites emplaced into depleted Lewisian basement, with the high values of granites emplaced into Lower Palaeozoic sediments. This fits fairly well with the evidence of these three plutons from the Tak Batholith, although the radioactive accessory minerals here are sphene and allanite (cf. Ragland et al., 1967). Thorium is also likely to be present in zircon, as radiogenic haloes are seen in the biotites from all four plutons, but as noted earlier, sphene and allanite are not present in the Eastern Pluton.

Turning to the contents of U and Th in the Eastern Pluton (Table 9.1) it can be seen that these values are much lower, and are very similar to those given in Killeen and Heier (1975), who quote several other authors. Thus the average for continental crust is given as ca. 2 ppm U and ca. 10 ppm Th (see also Hennessy, 1981 and O'Connor, 1981). The U and Th contents of the Eastern Pluton can be seen to be similar to values for other granodiorites, e.g. 2.0, 2.4 and 5.2 ppm U and 7.8, 10.3 and 19.2 ppm Th in the rocks of the eastern United States (Larsen and Gottfried, 1960).

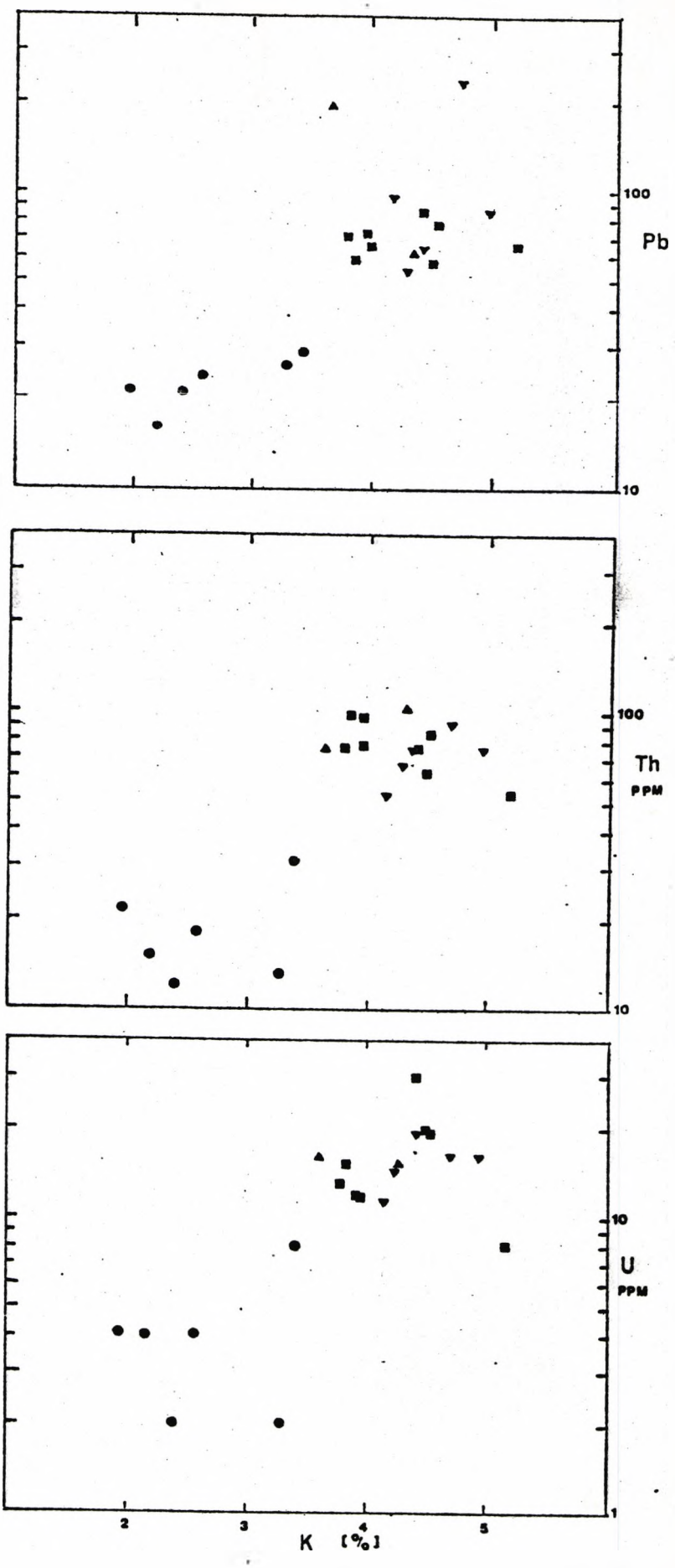

Figure 9.1 Plots of Th, U and Pb vs. K for the granitic rocks of the Tak Batholith

solid circle - Eastern pluton; solid square - Western Main Range Pluton; solid triangle, point up - Mae Salit Pluton; solid triangle, point down - Tak Pluton.

Figure 9.1 shows plots of U and Th vs. K for the four plutons and indicates the low values in the Eastern Pluton are associated with lower K contents. The values for Pb follow a similar pattern, being significantly higher in the Tak, Mae-Salit and Western Main Range plutons. The average value for those three plutons is ca. 82 ppm, which is somewhat higher than the 48 ppm given for uraniferous Wyoming granite (Stuckless et al., 1977). They suggest that the Pb, along with the U and Th is contained in the accessory minerals. The likely source of this Pb would seem to be as the end-product of the classic radioactive decay chains.

9.2 Conclusions

9.2.1 The Tak Batholith, formerly considered to be a single intrusion, has been shown to consist of four separate plutons, each exhibiting distinctive trends in chemistry.

9.2.2 One of the most intriguing aspects of the Tak Batholith is the outward zoning of three of the four plutons. The earliest pluton, i.e. the Eastern Pluton, shows normal zoning, which has been fairly well explained by Vance (1961). He described how the minerals which would crystallise initially, plagioclase and hornblende, possibly with biotite, will do so inthe colder border regions of the pluton. This would seal off the central parts and the composition would become more acidic, either by gravity settling or by filter pressing or some other mechanism, leaving an acidic residual liquid, which crystallised in the centre of the pluton.

9.2.3 The other three plutons, as shown in the earlier chapters, show an unusual outward zonation. They tend to be associated with late-stage acidic intrusives, which may be derived from the magma itself. Kennedy (1955) pointed out that volatile-rich magmas may

differentiate by movement of Si, Na and K in the volatile phase to the lower temperature and pressure regions along the roof and at the sides of the pluton. This would result in the chemical composition of the central zone being more basic and permit the crystallisation of mafic and calcic minerals i.e. plagioclase and hornblende. This is a possible explanation of the zonation in the case of the Tak and Western Main Range Plutons (see Chapter 7).

Alternatively, Hildreth (1981, p. 10153), when discussing gradients in silicic magma chambers pointed out that "some dacite and rhyolitic liquid may separate from less silicic parents by means of ascending boundary layers along the walls of convecting magma chambers". He also stated that zonations in magma chambers may be accomplished by liquid state thermodiffusion and volatile complexing. In this case thermal gradients across the magma chamber are critical. The high concentrations of U, Th, Sr, Ba, Rb and high field strength elements (HFS) such as Ta and Hf in the acid rocks of these plutons suggest that silicic zonation and possible liquid separation are responsible for the zonations seen. Indeed in the modelling (Chapter 7) it was postulated for the Tak and the Western Main Range plutons that a silica rich liquid separated from the original liquid, in part at least.

9.2.4 The sharp contacts seen between the intrusives and the main body of the pluton are thought to be caused by vertical movement of the pluton, while the acidic margin was still molten.

As there are no such acidic intrusions around the Mae-Salit pluton, this explanation may not be valid and a fractionation model seemed more likely (Chapter 7). This poses an interesting question, namely how can the more basic minerals crystallise in the central part first,

when presumably the border region is colder, since it is of course in contact with a cold environment. This could be possible in a magma with a high water content, because the liquidus temperature of plagioclase and hornblende will occur at a higher temperature in the drier central part of the pluton.

9.2.5 On turning to some of the trace element contents, perhaps the REE contain the most important information. It was seen in Chapter 6 that accessory minerals - notably sphene and allanite - have a marked effect on LREE distributions. The appearance or non-appearance of a negative Eu anomaly usually indicates plagioclase or plagioclase plus hornblende fractionation extraction respectively occurred. The evidence on the Tak pluton for example, indicates some plagioclase fractionation may have been involved, but extraction of a "pegmatite" phase was necessary to produce the observed trends. A similar extraction mechanism is advocated for the Western Main Range Pluton.

9.2.6 Consideration of the Rb, Sr and Ba variations within the plutons on a composite diagram (Figure 9.2.6.1) shows some distinctive features. The Ba/Sr and Ba/Rb plots show that the three outward zoned plutons fall into very similar trends, indicating that either a combination of plagioclase and biotite, or mainly K-feldspar may account for the observed changes in these elements. On these two diagrams the Eastern Pluton clearly enforces the previous evidence that conventional plagioclase/hornblende fractionation is the dominant process. On the Rb/Sr plot, the Eastern Pluton appears similar to two of the other plutons, but here it is the Tak Pluton which is somewhat different, this time re-inforcing the suggestion that removal of K-feldspar and plagioclase (in the form of a pegmatite perhaps) is important in causing the observed differentiation.

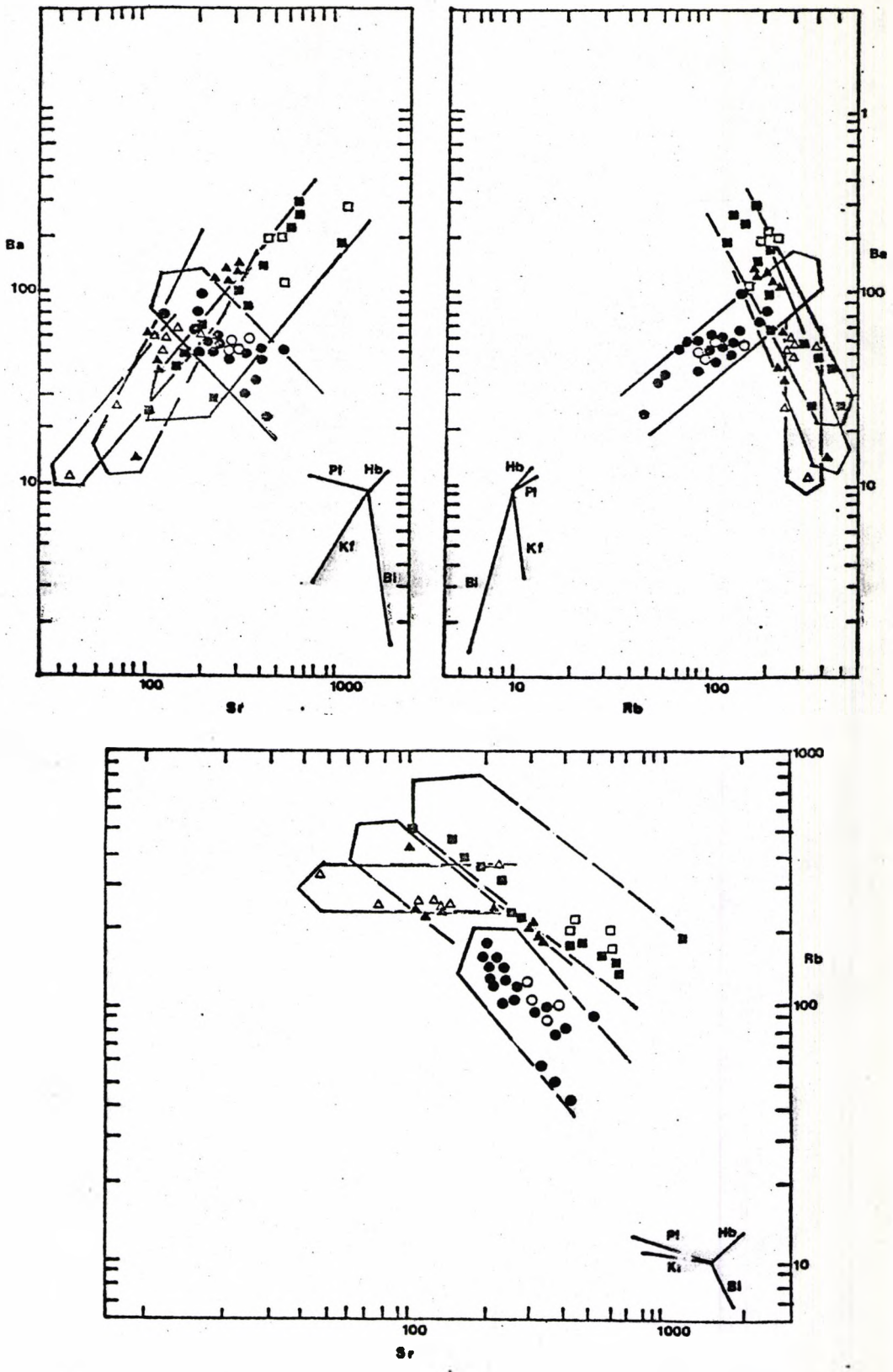

Figure 9.2.6.1 Plots of Ba vs. Sr; Ba vs. Rb; Rb vs. Sr for the granitic rocks of the Tak Batholith.

solid circle - Eastern Pluton; solid square - Western Main Range Pluton; solid triangle - Mae Salit Pluton; open triangle - Tak Pluton; open square - appinite associated with Western Main Range Pluton; open circle - porphyry (chilled margin of Eastern Pluton). Arrows enclose samples from each pluton and point in direction of increasing acidity.

The U, Th rich plutons are similar to other radioactive element enriched granites, such as the granites of the Olden Window, Sweden (Troeng, 1982) which has U averages of 12 and 19 ppm and Th averages of 41 and 45 ppm. These granites show marked LREE enrichment and contain allanite and monazite. Similar granites from Sweden (Wilson and Akerblom, 1982) have U > 10 ppm and are highly differentiated alkali granites with $^{87}Sr/^{86}Sr$ values > 0.708. In the Hercynian of Europe (Pagel, 1982) there are amphibole-biotite uraniferous granites - in fact subalkaline potassic granites - characterised by sphene, allanite and thorite as accessory minerals and magnetite. The presence of magnetite plus magnesium biotite suggests a higher temperature of formation and higher fO_2 conditions than the more usual muscovite-biotite type of granite. These rocks show characteristic LREE enrichment and La/Yb ratios of 22-36. Typically the subalkaline granitoid association shows high U, Th, LREE, Ba, Rb and Sr similar to shoshonite compositions (Pagel, 1982).

All these characteristics are well seen in the three U-enriched granites (Table 9.1), in contrast to the more normal Eastern Pluton. The Rb values vary from a range of 139-459 ppm in the uraniferous granites to a range of 52-167 ppm in the Eastern Pluton. The Sr values likewise vary from 23-1137 to 100-577 ppm and the Ba values from 35 - 3102 to 318 - 1138 ppm between the uraniferous plutons and the Eastern Pluton respectively. The Hf and Ta contents are also enriched with these LILS as are the LREE (e.g. total REE in the uraniferous granites ca. 302; in the Eastern Pluton 103 ppm). The uraniferous granites have La/Yb ratios of 30, 28 and 23 for the three plutons, compared to a value of 12 for the Eastern Pluton. The alkalic character of the rocks is seen in Figure 9.2.6.2 where on a K_2O vs. SiO_2 diagram they plot above the area of calc-alkaline

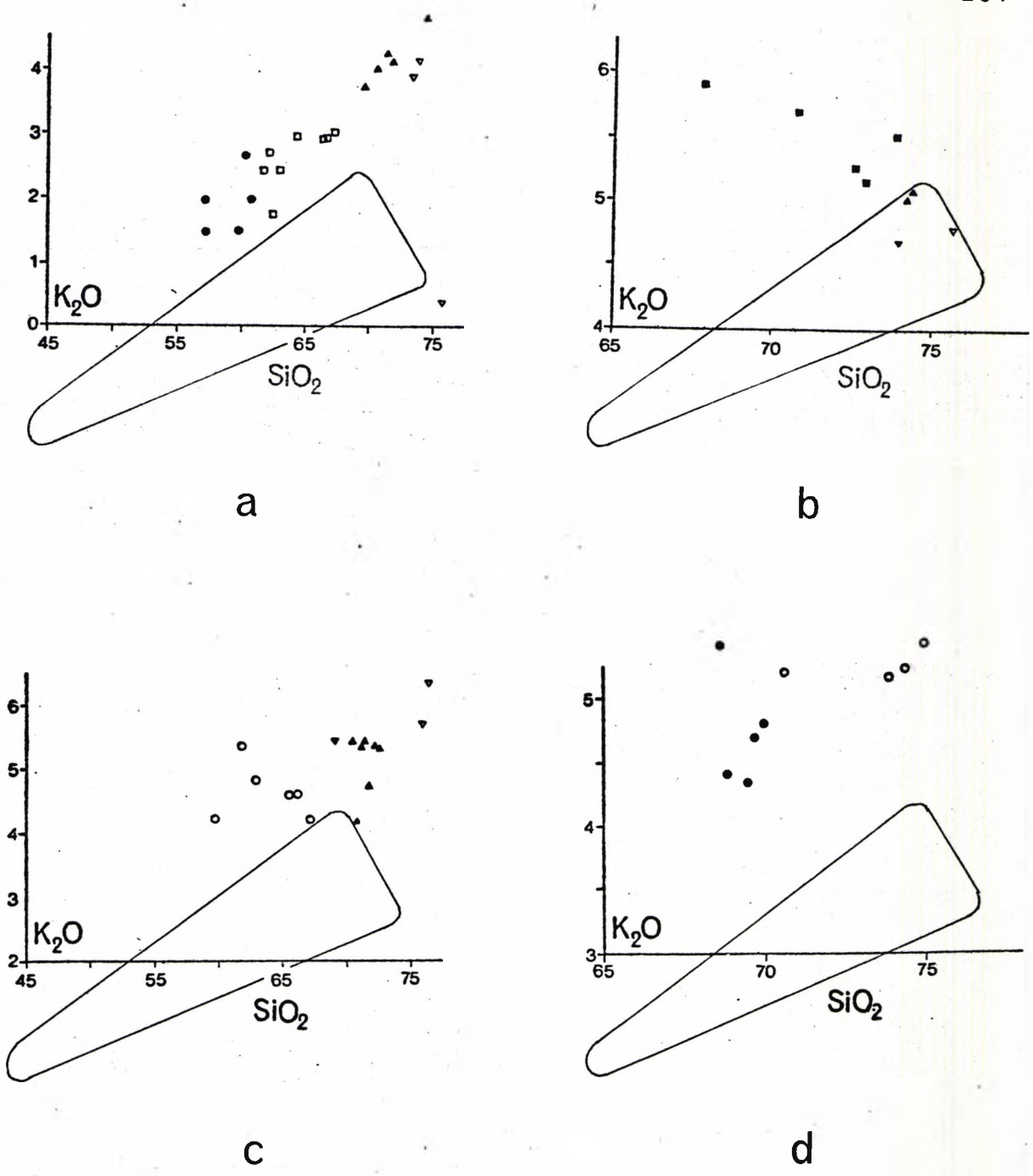

Figure 9.2.6.2 Harker diagrams for K_2O vs. SiO_2 for (a) Eastern Pluton; (b) Tak Pluton; (c) Western Main Range Pluton; (d) Mae-Salit Pluton, symbols as figure 7.1.1 to 7.1.4. Solid line enclose field of calc-alkaline series of island arcs (Morrison, 1980).

series.

These characteristics are not dissimilar either to the metalliferous granites of the Scottish Caledonides (Plant, et al., 1980) and indeed this would fit in with the typology (I-Caledonian type) derived earlier. The tectonic setting is also similar as far as can be determined:- i.e. post-tectonic, a high structural level, a low pressure thermal aureole and an isotopic composition indicative of a mainly mantle origin. In Scotland intrusion took place rapidly along deep fractures on uplift, following collision of the Scottish and the English-Welsh plates, a situation not at all dissimilar from the Thai granites discussed here. Mineralisation is absent, as these Thai plutons did not apparently interact with epizonal water during or after emplacement (cf. Plant et al., 1980).

In the three uraniferous plutons of the Tak Batholith the accessory minerals (sphene, allanite) appear to have crystallised early as indicated by the REE decrease with increasing D.I.

It is important to emphasise the problems common to modelling granites - namely that the major and trace elements may not behave coherently, decoupling may be common and major element modelling in particular may not be valid. This is specifically the case where minor phases with very large K_Ds are concerned. These minerals may often show very pronounced zoning, which will further complicate any attempts at modelling.

9.2.7 Consideration of typology (Pitcher, in press) indicates the three uraniferous granites are I-Caledonian type, while the earlier Eastern pluton is closer to I-Cordilleran type.

A similar relationship exists in the British Caledonides where the earlier intrusions are not uraniferous, while the later ones are (Plant, et al., 1980).

The uraniferous plutons are not mineralised as presumably they did not react with epizonal water on emplacement.

9.2.8 The tectonic setting of the granites, which show shonshonitic affinities, is similar to that of the Caledonian granites viz. intrusion post-subduction into an uplift regime.

9.2.9 The high contents of U, Th, Ba, Sr, Rb and HFS elements is compatible with the tectonic setting indicated above and together with the petrologic data suggests a sub-crustal derivation. However, the $^{87}Sr/^{86}Sr$ ratios of 0.710 and 0.716 for the different facies of the Tak pluton (Teggin, 1975) indicates that some crustal component must be involved.

9.3 Further Investigations

It is clear from the foregoing conclusions that there are important aspects of the work that require further study.

9.3.1 The site of the U and Th should be established, preferably using lexan print, indicating fission track distribution. It seems possible that specific uranium/thorium minerals may be present.

9.3.2 The late acidic intrusions should be studied in greater detail, specifically to relate to the modelling of the zonations.

9.3.3 Initial $^{87}Sr/^{86}Sr$ ratios using whole rock isochrons should be determined for all the plutons, especially the Eastern pluton.

9.3.4 Stable isotope studies should indicate the interaction or lack of interaction with epizonal waters and the extent of weathering.

9.3.5 To establish the zonal patterns more exactly consideration might be given to the use of trend surface analyses, although it is appreciated that the lack of exposure might be a limiting factor.

REFERENCES

Adams, J.A.S., Osmond, J.K. and Rogers, J.J.W., 1959. The geochemistry of thorium and uranium. In: Physics and Chemistry of the Earth (eds) Ahrens L.H., Press, F., Rankema, K. and Runcorn, S.K. Pergamon, London, 3, pp. 298-348.

Atherton, M.P., 1981. Horizontal and vertical zoning in the Peruvian Coastal Batholith. J. Geol. Soc. Lond., 138, 343-349.

Bateman, P.C. and Chappell, B.W., 1979. Crystallization, fractionation and solidification of the Tuolumne Intrusive series, Yosemite National Park, California. Geol. Soc. Am. Bull., 90, 465-482.

Baum, F., Braun, E. von, Hahn, L., Hess, A., Koch, K.E. Krause, G., Quarch, H. and Siebenhuner, M., 1970. On the geology of Northern Thailand. Beih. Geol. Jahrb., 102, 1-24.

Beckinsale, R.D. 1979. Granite Magmatism in the Tin Belt of South-East Asia. In: Origin of Granite Batholiths : Geochemical Evidence. (eds) Atherton, M.P. and Tarney, J. Shiva, Orpington, U.K., 148 pp.

Blake, D.H., Elwell, R.W.D., Gibson, I.L., Skelhorn, R.R. and Walker, G.P.L., 1965. Some relationships resulting from the intimate association of acid and basic magmas. J. Geol. Soc. Lond., 121, 31-49.

Brown, G.F., Buravas, S., Charaljavunophet, J., Jalichandru, N., Johnson, W., Strethaputra, V. and Taylor, G.C. Jr., 1951. Geological reconnaissance of the mineral deposits of Thailand. U.S. Geol. Surv. Bull., 984.

Brown, G.C., Hughes, D.J. and Esson, J., 1973. New X-ray fluorescence data retrieval techniques and their application to U.S.G.S. standard rocks. Chem. Geol., II, 223-229.

Bunopas, S., 1974. Geological map of Thailand : Changwat Phitoanulok, 1:250,000 Thailand. Geological Survey Division, Bangkok.

Bunopas, S., 1976. Stratigraphic succession in Thailand : a preliminary summary. J. Geol. Soc. Thailand, 2, 31-58.

Burton, C.K., 1973. Mesozoic. In: Geology of the Malay Peninsula (eds. Gobbett, D.J. and Hutchinson, C.S.), Wiley-Interscience, New York, pp. 97-141.

Campbell, K.V., 1974. Basement complexes (of Thailand). Dept. Geol. Sci., Chieng Mai Univ. Spec. Pub. no. 1, pp. 3-12.

Campbell, K.V. and Nutalaya, P., 1974. Structural elements and deformation events (of Thailand). Geol. Soc. Thai. Newsletter, 6, no. 2.

Chao, E.C.T. and Fleischer, M., 1960. Abundance of zirconium in igneous rocks. Rep. 21st Internat. Geol. Cong., Norden, pt. 1, 106-131.

Chappell, B.W. and White, A.J.R., 1974. Two constrasting granite types. Pacific Geology, 8, 173-174.

Clark, S.P., Peterman, Z.E. and Heier, K.S., 1966. Abundance of uranium, thorium and potassium. In : Handbook of physical constants (rev. ed.). Geol. Soc. Am. Memoir, 97, 523-39.

Condie, K.C., 1978. Geochemistry of proterozoic granitic plutons from New Mexico, U.S.A. Chem. Geol. 21, 131-49.

Curtis, C.D., 1964. Applications of the crystal-field theory to the inclusion of trace transition elements in minerals during magmatic differentiation. Geochim, Cosmochim. Acta, 28, 389-403.

Daly, R.A., 1914. Igneous rocks and their origin. McGraw Hill, New York, 563 pp.

Deer, W.A., Howie, R.A. and Zussman, J., 1963. Rock-forming minerals. Vol. 4, Longmans, London.

Dier, J., 1973. Granites and their enclaves : the bearing of enclaves on the origin of granites. Elsevier, Amsterdam. 293 pp.

Duffield, J. and Gilmore, G.R., 1979. An optimum method for the determination of rare earth elements by neutron activation analysis. J. Radioanal. Chem., 48, 135-145.

Ewart, A. and Taylor, S.R., 1969. Trace element geochemistry of the Rhyolitic volcanic rocks, Central North Island, New Zealand. Phenocryst data. Contrib. Mineral. Petrol., 22, 127-46.

Fourcade, S., and Allegre, C.J., 1981. Trace element behaviour in granite genesis. A case study : the calc-alkaline plutonic association from the Querigut complex, C. Pyrenees, France. Contrib. Mineral. Petrol., 76, 177-195.

Garson, M.S., Young, B., Mitchell, A.H.G. and Tait, B.A.R., 1975. The geology of the tin belt in peninsular Thailand around Phuket, Phangnga and Takua Pa. Overseas. Mem. Inst. Geol. Sci. London, 1.

Gordon, G.E., Randle, K., Goles, G.G., Corliss, J.B., Beeson, M.H. and Oxley, S.S., 1968. Instrumental activation analysis of standard rocks with high-resolution -ray detectors. Geochim, Cosmochim. Acta., 32, 369-396.

Gubler, J., 1935. Etudes geologiques au Cambodge. Occidental. Bull. Serv. Geol. Indo-Chine, 23, Fasc. 2.

Hanson, G.N., 1980. Rare earth elements in petrogenetic studies of igneous systems. Ann. Rev. Earth Planet Sci., 8, 371-406.

Heier, K.S. and Rogers, J.J.W., 1963. Radiometric determination of thorium, uranium and potassium in basalts and in two magmatic differentiation series. Geochim. Cosmochim. Acta, 27, 137-54.

Hennessy, J., 1981. A classification of British Caledonian granites based on uranium and thorium contents. Mineral. Mag., 44, 449-454.

Hildreth, W., 1979. The Bishop tuff : evidence for the origin of compositional zonation in silicic magma chambers. Geol. Soc. Am. Spec. Pap., 180, 43-75.

Hildreth, W., 1981. Gradients in Silicic Magma Chambers : implications for lithospheric magmatism. J. Geophys. Res., 86, no. B11, 10153-92.

Hon, R. and Noyes, H.J., 1977. REE and other trace elements during fractionation of granitic aplites of Sierra Nevada Batholith, CA and Katahdin pluton ME. Geol. Soc. Am. Abstr. with Programs, 9, p. 1023.

Hutchison, C.S., 1973. Tectonic evolution of Sundaland : a Phanerozoic synthesis. Bull. Geol. Soc. Malaysia, 6, 61-86.

Hutchinson, C.S., 1975. Ophiolite in Southeast Asia. Bull. Geol. Soc. Am., 86, 797-806.

Kennedy, G.C., 1955. Some aspects of the role of water in rock melt. Geol. Soc. Am. Spec. Pap., 62, 489-504.

Killeen, P.G. and Heier, K.S., 1975. Th, U, K and Heat Production Measurements in Ten Precambrian Granites of the Telemark Area, Norway. Norges geol. Unders. 319, 59-83.

Klompe, H.F.Th., 1962. Igneous and structural features of Thailand. Geol. en Mijn., 41, 290-302.

Kobayashi, T., 1960. Notes on the geological history of Thailand and adjacent territories. Jap. J. Geol. and Geog., 31, 129-48.

Lambert, R.S.J. and Holland, J.G., 1974. Yttrium geochemistry applied to petrogenesis utilizing calcium-yttrium relationships in minerals and rocks. Geochim. Cosmochim. Acta, 38, 1393-1414.

Lambert, I.B. and Heier, K.S., 1967. The vertical distribution of uranium, thorium and potassium in the continental crust. Geochim. Cosmochim, Acta, 31, 377-390.

McCarthy, T.S. and Kable, E.J.D., 1978. On the behaviour of rare-earth elements during partial melting of granitic rock. Chem. geol., 22, 21-29.

Larsen, E.S. and Gottfried, D., 1960. Uranium and thorium in selected suites of igneous rocks. Amer. J. Sci., 258A, 151-169.

Mahawat, C. and Joungusook, N., 1971. Geology of the Tak area (unpublished report In Thai) Geological Survey, Department of Mineral Resources, Thailand.

Marmo, V., 1971. Granite Petrology and the granite problem. Elsevier, Amsterdam, 244 pp.

Miller, C.F. and Mittlefehldt, D.W., 1982. Depletion of light rare-earth elements in felsic magma. Geol., 10, 129-133.

Mitchell, A.H.G., 1977. Tectonic settings for emplacement of South-east Asian tin granites. Bull. Geol. Soc. Malaysia, 9, 123-40.

Mitchell, A.H.G., Young, B. and Jantararipa, W., 1970. The Phuket group in peninsula Thailand: a Palaeozoic (?) geosynclinal deposit. Geol. Mag. 108, 411-27.

Nagasawa, H., 1970. Rare earth concenration in zircon and apatite and their host dacites and granites. Earth Plant. Sci. Lett., 9, 359-364.

Nagasawa, H. and Schnetzler, C.C., 1971. Partitioning of rare-earth alkali, and alkali-earth elements between phenocrysts and acidic igneous magma. Geochim. Cosmochim. Acta, 35, 953-968.

Pearce, J.A. and Norry, M.J., 1979. Petrogenetic implications of Ti, Zr, Y and Nb variations in volcanic rocks. Contr. Mineral. Petrol., 69, 33-47.

Pegram, W.J., Sands, T.W., and Hodges, K.V., 1980. Rare-earth element geochemistry and Nd isotopic composition of some Egyptian Younger Granites. Geol. Soc. Am. Abstr. with Programs, 12, p.497.

Philpotts, J.A. and Schnetzler, C.C., 1968. Europium anomalies and genesis of Basalt. Chem. Geol., 3, 5-13.

Piyasin, S., 1974. Geological map of Thailand: Changwat Uttaradit. 1:250,000. Thailand. Geological Survey Division, Bangkok.

Pitcher, W.S., 1979. The nature, ascent and emplacement of granite magmas. J. Geol. Soc. Lond, 136, 627-62.

Pitcher, W.S., (in press). Granite Type and tectonic Environment.

Pongsapich, W. and Mahawat, C., 1977. Some aspect of Tak granites, Northern Thailand. Bull. Geol. Soc. Malaysia, 9, 175-186.

Ragland, P.C., Billings, G.K. and Adams, J.A.S; 1967. Chemical fractionation and its relationship to the distribution of thorium and uranium in a zoned granite batholith. Geochim. Cosmechim. Acta, 31, 17-33.

Rast, N., 1969. The initiation, ascent and emplacement of magma: In The Mechanism of Igneous Intrusion (eds. Newall, G. and Rast, N.) Gallery Press, Liverpool, U.K.

Ridd, M.F., 1971a. Southeast Asia as a part of Gondwanaland. Nature, 234, 531-33.

Ridd, M.F., 1971b. The Phuket group of peninsular Thailand. Geol. Mag., 108, 445-46.

Ridd, M.F., 1971c. Faults in Southeast Asia and the Andoman Rhombochasm. Nature, 229, 51-52.

Ridd, M.F., 1978. Thailand. In: The Phanerozoic Geology of the World, vol. II, The Mesozoic (eds. Moullade, M. and Nairn, A.E.M.)., Elsevier, Amsterdam. pp. 145-63.

Ridd, M.F., 1980. Possible Palaeozoic drift of S.E.Asia and Triassic collision with China. J. Geol. Soc. Lond. 137/5, 635-640.

Ringwood, A.E., 1955a. The principles governing trace element distribution during magmatic crystallization. Part I: The influence of electronegativity. Geochim. Cosmochim. Acta, 7, 189-202.

Ringwood, A.B., 1955b. The principles goberning trace-element behaviour during magmatic crystallization Part II: The role of complex formation Geochim. Cosmochim.Acta, 7, 242-254.

Rodolfo, K.S., 1969. Bathymetry and marine geology of the Andaman Basin, and tectonic implications for Southeast Asia. Geol. Soc. Am. Bull., 80, 1203-30.

Rogers, J.J.W. and Ragland, P.C., 1961. Variation of thorium and uranium in selected granitic rocks. Geochim. Cosmochim. Acta, 25, 99-109.

Shaw, D.M., 1977. Trace element behavior during anatexis. In: Magma Genesis (ed. Dick, H.T.B.) Bull. Oregon Dept. Geol. Min. Industr., 96, 189-213.

Siedener, G., 1965. Geochemical features of a strongly fractionated alkali igneous suite. Geochim. Cosmochim. Acta, 29, 113-137.

Smith, W.L., 1957. Uranium and Thorium in the accessory allanite of igneous rocks. Am. Mineral., 42, 367-78.

Snelling, N.T., Hart, R. and Hardington, R.R., 1970. Age determination on samples from the Phuket region of Thailand. Rep. Inst. Geol. Sci. London. IGU. 70.19 (Unpublished).

Spark, R.S.J., Pinkerton, H. and Macdonald, R., 1977. The transport of xenoliths in magmas. Earth Planet. Sci. Lett., 35, 234-38.

Stauffer, P.H., 1974. Malaya and Southeast Asia in the pattern of continental drift. Geol. Soc. Malaysia Bull., 7, 89-138.

Streckeisen, A., 1976. To each plutonic rock its proper name. Earth Sci. Rev., 12, 1-33.

Stuckless, J.A., Bunker, C.M., Buch, C.A., Doering, W.P. and Scott, J.H. 1977. Geochemical and Petrological Studies of a Uraniferrous granite from The Granite Mountain, Wyoming. Jour. Research U.S. geol. Sur. 5, No.1. 61-81.

Suensipong, S., Burton, C.K., Mantagit, N. and Workman, D.R.,(1978) Geological evolution and igneous activity of Thailand and adjacent areas. EPISODES Geol. Newsletter IUGS. 178, No.3. 12-18.

Taylor, H.P. and Silver, L., 1978. Oxygen isotope relationships in plutonic igneous rocks of the Peninsular Ranges Batholith, Southern and Baja California. 4th Conf. Geochronology, Cosmochronology and Isotope geology. Snowmass-at-Aspen.

Teggin, D.E., 1975. The granites of northern Thailand. Ph.D. Thesis University of Manchester, U.K. (unpublished).

Turekian, K.K. and Wedepohl, K.H., 1961. Distribution of the elements in some major units of the earth's crust. Bull. Geol. Soc. Am., 72, 175-92.

Vance, J. A., 1961. Zoned granitic intrusions - an alternative hypothesis of origin. Bull. Geol. Soc. Am., 72, 1723-7.

Von Braun, E., Besang, C., Eberle, W., Harre, W., Kreuzer, H., Len, H., Muller, P. and Wendt, I., 1976. Radiometric Age Determinations of Granites in Northern Thailand. Geol. Jahrb., Hannover, B21, 171-204.

Wager, L.R. and Mitchell, R.L., 1951. The distribution of Trace elements during strong fractionation of basic magma - a further study of the Skaergaard intrusion, East Greenland. Geochim. Cosmochim. Acta. 1, 129-208.

Wedepohl, K.H. 1956. Untersuchungen zur Geochemic des Bleis. Geochemie Cosmochim. Acta, 10, 69-148.

White, A.T.R., 1979. Sources of granite magmas. Abstr. with Programs. Geol. Soc. Am. An. Gen. Met. p.539.

ADDITIONAL REFERENCES

Cox, K.G., Bell, J.D. and Pankhurst, R.J., 1979. The Interpretation of Igneous rocks. George Allen and Unwin Ltd., London, 449 pp.

Ludington, S., 1981. The Redskin Granite - evidence for thermo-gravitational diffusion in a Precambrian granite batholith. J. geophys. Res., 86, no. B11, 10423-10430.

Moll, E.J., 1981. Geochemistry and Petrology of Mid-Tertiary ash flow tuffs from the Sierra el Vinalento area, Eastern Chihuahua, Mexico. J. Geophys. Res., 86, no. B11, 10321-10334.

Morrison, G.S., 1980. Characteristics and tectonic setting of the Shonshonite rock association. Lithos 13, 97-108.

O'Connor, P.J., 1981. Radioelement geochemistry of Irish granites. Mineral. Mag., 44, 485-95.

Pagel, M., 1982. The mineralogy and geochemistry of uranium, thorium and rare-earth elements in two radioactive granites of the Vosges, France. Mineral. Mag., 46, 149-161.

Plant, J.A., Brown, G.C., Simpson, P.R. and Smith, R.T., 1980. Signatures of metalliferous granites in the Scottish Caledonides. Tran. Inst. Min. Mettall., 89B, 198-210.

Troeng, B., 1982. Uranium-rich granites in the Olden window, Sweden. Mineral. Mag., 46, 217-26.

Wilson, M.R. and Akerblom, G.V., 1982. Geological setting and geochemistry of uranium-rich granites in the Proterozoic of Sweden. Mineral. Mag., 46, 233-45.

APPENDIX 1 Analytical Methods

(1) Rock crushing

The rock sample of approximately 5 kg was coarse-crushed by a jaw crusher to chips 1-2 cm in diameter. This coarse, crushed sample was then washed by deionized water, to remove dust, and dried. This material was then crushed to approximately 120 μ (100 mesh) by a Tungsten-Carbide barrel on a Tema rotary crusher. The fine crushed sample was homogenized by mixing on glazed paper. About 10 gm of this sample was ground by hand in an agate mortar until all the powder was less than 53 μ (300 mesh). This powder was used for the determination of major and trace elements by X-ray fluorescence, ferrous iron by the classical method and the Rare Earth Elements and Th and U by neutron activation analysis.

(2) X-Ray Fluorescence Method

Introduction:

X-ray fluorescence analysis provides a rapid, convenient and accurate method of determining the elements present in a sample.

The principle of the method is that when an element in a multi-component sample is bombarded with primary X-ray photons, secondary X-ray photons characteristic of this element are produced. These secondary or fluorescent X-rays are then dispersed according to their wave lengths. This is achieved by using a crystal of known d-spacing where diffraction takes place according to Bragg's relationship $n\lambda = 2d \sin\theta$, where λ is the wavelength, d is the spacing between the planes of the crystal, θ is the angle of incidence of the X-ray on the crystal. The intensity of the diffracted fluorescent radiation is then measured, and the concentration of the element producing this radiation can be found, since the intensity is proportional to concentration.

Sample preparation:

The sample for presentation for X-ray fluorescence analysis should be completely homogeneous and form a disc or layer with a perfectly planar surface. The technique used in the present work is the pressed powder pellet.

The pellets are made by mixing 7 g of homogeneous sample powder (grain size less than 53 μ) with 10-15 drops of polyvinyl alchol (Moviol). The mixture is then compressed against a glass disc, using a hydrolic press to a pressure of 4-6 tons in a die 40 mm diameter. Then the pressed powder pellet is removed, without touching the smooth planar surface, and allowed to dry. The powder pellet method was chosen because of the following advantages:

1. Easy of preparation of sample.
2. Analyses of the trace element were required.
3. Although it is recognised that matrix effects are pronounced in powder pellets, this was overcome by using a limited calibration technique and applying matrix correction procedures using a standard computer program.

A Siemen's X-ray spectrometer (Siemens SRS1) in conjunction with a counting console was used. The condition of the analysis are shown in Table A.I.1 and A.I.2.

Major Element Calibration:

The method of calibration involves the use of a series of external standards in which the concentration of the required element varies over a limited range in a matrix, whose composition is chosen such that the overall absorption is very close to that of the samples.

The method used in the present work is that outlined by Brown et al., (1973) in which a computer program corrects for the matrix effects. The program also corrects the count data for drift, assuming linear variation with time and for background effects. The corrected counts are then normalised by developing a ratio for each standard and unknown against the drift monitor counts. The three steps involved are as follows:

1. The intensity ratios for the standards are regressed against their known chemical analyses and the resulting quadratic equation is applied to the intensity ratios for all standards and unknowns to obtain results to a first approximation. These results are used to calculate approximate mass absorption coefficients.

A series of ratios, crudely corrected for mass absorption is then derived for the standards and unknowns.

	Radiation	KV	mA	Crystal	Collimeter	2θ Peak	2θ Background	Base Line	Channel Width	Detector Voltage	Counting time Peak	Counting time Background	Precision C*
SiO_2	Cr	35	30	PET	0.41	109.13	110.10	0.625	0.75	1600	20	20	0.0045
TiO_2	Cr	35	30	LiF(100)	0.15	86.17	86.89	0.85	0.55	1600	20	20	0.1010
Al_2O_3	Cr	50	40	PET	0.4	146.19	144.00	0.59	0.80	1600	20	20	0.010
Fe_2O_3	Cr	30	20	LiF(100)	0.15	57.54	56.90	0.76	0.62	1610	20	20	0.0665
MnO	Cr	50	40	LiF(100)	0.15	63.00	63.52	1.05	0.74	1620	20	20	0.1059
MgO	Cr	50	40	RAP	0.4	44.44	43.37	0.90	0.90	1620	40	20	0.1437
CaO	Cr	35	30	LiF(100)	0.15	113.16	114.20	0.64	0.72	1630	20	20	0.0294
Na_2O	Cr	50	40	RAP	0.4	54.26	55.10	1.05	0.86	1620	40	40	0.0203
K_2O	Cr	30	24	LiF(100)	0.15	136.73	135.73	0.54	0.75	1620	20	20	0.0140
P_2O_5	Cr	30	40	PET	0.14	89.45	88.70	0.84	0.66	1625	40	40	0.1195

Table A.I.1. Conditions for X-ray Fluorescence Analysis for major elements, using pressed powder pellets.

(2) These corrected intensity ratios are fitted against the known chemical analysis and the new set of quadratic regression line coefficients are applied to the crudely corrected ratios for both standards and unknown obtained in (1).

(3) The final mass absorption corrected analyses derived from analytical data for the standard using (1) and (2) are regressed against their known chemical analyses. This fit should give a straight line for each element. However, minor deviations often occur and therefore the final analytical results for the unknowns are generated by applying the quadratic functions of regression (3) to the analyses from (2).

Trace Element Calibration:

The method is based on that of Brown et al. (1973) and uses their computer program which has been slightly modified.

Synthetic primary standards are employed: pure SiO_2 (BLK), pure SiO_2 "spiked" with known concentrations of trace element (MESS 1 and MESS 2), and a synthetic pellet of andesitic composition (SPA) containing only major elements but no trace elements (other than Ti). These monitor instrument shift.

Each time the XRF is switched on these standards are run before any unknowns. The resulting counts are used to calibrate the peak and to determine the background slope for correction of the sample counts. Subsequently, a given number of secondary standards (either SiO_2-based synthetics (for Sc) or of known major and trace elements composition (USGS : for all elements)) followed by the unknowns are counted at all peak and background positions. Drift monitor measurements are made on the primary synthetic standard (MESS 1 or MESS 2) between counts for successive samples. Within the program the sample counts are corrected for drift, background and the interference effects and expressed as ratios to the primary standard net counts. These ratios are corrected for mass

absorption by all the previously determined major elements at the measured trace element wavelengths.

Thus the first analytical result is obtained using the trace element concentration of one synthetic standard (viz. uncorrected value). A more refined analysis is produced by computing a least squares fit regression line of these results versus unknown concentrations for the secondary standards and obtaining final values for the unknowns from this line (viz. corrected values).

	Radiation	KV	mA	Crystal	Collimotor	2θ Peak	2θ Background	Base Line (V)	Channel Width (V)	Detector Voltage (V)	Counting time Peak	Counting time Background	Precision
Ba	Cr	50	40	LiF(100)	0.15	79.24	80.40	0.73	0.50	1600	100	40	0.0436
Ce	W	45	60	LiF(100)	0.15	71.65	70.90 72.92	0.95	0.52	1600	100	40	0.0372
Co	W	45	50	LiF(100)	0.15	78.00	77.40 78.60	1.00	0.82	1165	100	40	0.1081
Cr	W	45	50	LiF(100)	0.15	69.37	68.25 70.50	0.95	0.92	1160	40	20	0.1562
La	W	45	50	LiF(100)	0.15	82.96	80.20	0.61	0.56	1580	100	40	0.0732
Nd	W	45	60	LiF(100)	0.15	72.16	70.90 72.92	0.95	0.52	1600	100	40	0.045
Ni	W	45	50	LiF(100)	0.15	48.68	47.90 49.60	1.00	0.80	1145	40	20	0.1617
Pb	W	45	50	LiF(100)	0.15	40.47	38.80 41.00	1.00	0.60	1135	100	40	0.1132
Rb	W	35	40	LiF(100)	0.15	38.05	33.10 34.85 38.80	0.86	0.52	1110	100	40	0.1005
Sc	Cr	45	50	Lif(100)	0.15	96.50	97.72	0.82	0.66	1610	40	20	0.0583
Sr	W	45	50	LiF(100)	0.15	32.17	31.00 33.10 37.00	0.85	0.52	1105	100	40	0.0192
Th	W	45	50	LiF(100)	0.15	39.33	38.80 41.00	1.00	0.60	1135	100	40	0.0685
Ti	W	45	60	LiF(100)	0.15	77.28	76.00 78.00	0.85	0.80	1140	100	40	0.0217
V	W	45	60	LiF(100)	0.15	76.94	76.00 78.00	0.85	0.80	1140	100	40	0.01227
Y	W	35	40	LiF(100)	0.15	33.96	33.10 34.85 38.80	0.86	0.52	1110	100	40	0.0083
Zn	W	35	40	LiF(100)	0.15	60.66	59.70 61.60	0.79	0.74	1125	40	20	0.0907
Zr	W	45	50	LiF(100)	0.15	32.17	31.00 33.10 37.00	0.85	0.52	1105	100	40	0.1233

Table A.I.2 Conditions for X-Ray Fluorescence Analysis for minor and trace elements, using pressed powder pellets.

3) Determination of Ferrous Iron

Ferrous iron was determined by the well-known 'classical' technique. The sample powder is treated with hot hydrofluoric and sulphuric acids. The contents of the Pt crucible are then transferred to a beaker containing a mixture of sulphuric, phosphoric and boric acids. The mixture is then titrated with potassium dichromate, until the indicator, sodium diphenylamine sulphonate assumes a permanent purple colour. This method is fast and direct, no comparisons are made with other rocks. The presence of sulphides or organic matter renders an accurate determination of ferrous iron impossible. Carbonate and graphite will not normally interfere. None of these components present any serious problem in any of the rocks analysed.

(4) Neutron activation analysis

(4a) Rare Earth Elements:

While it is possible to determine some of the rare earth elements (REE) by neutron activation, followed by gamma ray spectroscopy (e.g. Gordon et al. 1968), some of the short-lived isotopes, or those having weak gamma rays, are difficult or impossible to determine. This applies particularly to Pr, Gd, Er and Tm, and in some respects to Nd and Ho. The main problem is the high Compton background arising from the decay of ^{24}Na, which produces a strong gamma ray at 1369 KeV and has a 15 hour half-life. A chemical separation is considered essential if reliable results are to obtained for the whole suite of 14 REE. The technique is also more likely to produce accurate results for Gd, which is crucial in interpreting any Eu anomaly.

The method used is that developed by Duffield and Gilmore (1979), and the facilities used were those of the Universities of Manchester and Liverpool's Research Reactor at Risley, Warrington (URR). Briefly, the samples (around 300 mg) are irradiated for 7½ hours at a neutron flux of $3 * 10^{12}$ cm^{-2} sec^{-1}, together with liquid REE standards. For certain interference reasons, the 14 REE are divided into two groups of seven. The following day the samples are transferred to Pt crucibles and attacked with HF and $HClO_4$ acids. An aliquot of a solution of inactive La is added to each as carrier. The hydroxides are precipitated with ammonia at pH 9, leaving the Na, K, Mg and Ca in the supernatant. A precipitation with fluoride leaves Sc in the supernatant, and a final precipitation with oxalate enables the REE to be transferred to polythene vials for counting. This separation must be completed within a normal working day, as the samples must be counted overnight, if the short-lived isotopes are to be observed. Two counts are performed; one short enough (say 8-10 minutes) to ensure that the very active gamma ray peaks from ^{153}Sm, ^{152m}Eu and

^{166}Ho do not overflow. The 4096 channel analyser used has a maximum capacity in any one channel of 65535 counts. A second and longer count (say 1 hour) enables reliable values to be obtained from the gamma ray peaks of ^{142}Pr, ^{159}Gd and ^{171}Er; ^{140}La can be observed in both counts. After a decay of about 10 days a third count of around 1 hour is recorded. This enables sensible peaks to be observed for the longer-lived isotopes; ^{141}Ce, ^{147}Nd, ^{160}Tb, ^{169}Yb, ^{175}Yb and ^{177}Lu. Although results for ^{170}Tm can sometimes be obtained by examining the spectra from this third count by least squares analysis, this has not been done on these samples. The only rare earth missing, apart from Pm which does not occur in nature, having no stable isotopes, is Dy; the isotope involved, ^{165m}Dy, has a half-life of 1.26 minutes, so it has decayed to a negligible level, even before the chemical separation started.

The oxalate precipitates are now irradiated in the rabbit facility. This enables an irradiation of 20 seconds and a count of 200 seconds to be started within 1½ minutes of the start of the irradiation. Not only does one obtain results for Dy, but since all the La present is activated, one has a measure of the chemical yield during the separation. The two liquid standards are treated with oxalate only, and a yield of 100% is assumed.

A computer program, devised by Dr. G.R. Gilmore, URR, searches for gamma ray peaks, calculates the energy and area of any peak found. A second computer program devised by M.S. Brotherton, Department of Geology, University of Liverpool, calculates the decay and other corrections, and the final values. Results using these methods have shown good agreement with published values on certain standard rocks.

A tabulation of the isotopes, half-lives and gamma ray energies used is given below.

ISOTOPE	HALF-LIFE (Mins)	GAMMA RAY ENERGIES KeV
^{140}La	2416	329, 487, 816, 1596
^{141}Ce	46627	145
^{142}Pr	1152	1576
^{147}Nd	15926	91, 531
^{153}Sm	2808	69, 103
^{152m}Eu	588	122, 344, 842, (964)
^{159}Gd	1080	364
^{160}Tb	103824	299, 879, (966)
^{165m}Dy	1.26	108
^{166}Ho	1614	81
^{171}Er	451	308
^{170}Tm	182880	(84)
^{169}Yb	45792	177
^{175}Yb	6062	283, 396
^{177}Lu	9706	208

(4b) Ta, Hf, U and Th:

Direct instrumental neutron activation analysis, i.e. irradiation followed by gamma ray spectroscopy, can be used to analyse for these four elements. Enhancement, particularly for Ta and U, can be achieved by using epithermal neutron activation. The epithermal region of a reactor neutron spectrum is that between the thermal region (around 0.01 eV) and the fast neutron peak (say 1 MeV). The neutrons involved therefore have energies ranging from 0.1 to 10^5 eV. This is achieved by lining the sample can with Cd sheet. Cadmium has a very high cross-section to thermal neutrons and hence is a very good absorber of such neutrons.

The samples (around 250 mg) and a combined liquid standard are irradiated for 7½ hours at a neutron flux of around $3 * 10^{12}$ cm^{-2}/sec^{-1}. After a decay of 7 - 10 days, the vials are counted for around 600 seconds on a Ge(Li) detector and the information stored in a 4096 channel analyser. From these spectra, results are calculated for U and Th. After a decay of around 30 days the vials are counted again, this time for around 10,000 seconds, and the spectra yield results for Th, Ta and Hf. Results obtained by this method give reasonable agreement with published values.

The isotopes involved, their half-lives and the gamma ray energies used are given below:

ISOTOPE	HALF-LIFE (Days)	GAMMA RAY ENERGIES (KeV)
^{239}Np (from ^{239}U)	2.35	(228), 277
^{233}Pa (from ^{233}Th)	27	(299), 312
^{181}Hf	44.6	346, 482
^{182}Ta	115.1	152, 222, 1189, 1222, 1231

APPENDIX II Sample Location

Sample Number	Rock Unit	Rock Type	Grid Reference
T01	Tak Pluton	monzogranite	5145, 18685
T1	"	"	5194, 18598
CTK48B	"	"	5129, 18701
T43	"	"	5160, 18782
T02B	"	"	5186, 18685
T10B	"	"	5189, 18653
T02	"	"	5192, 18682
T12	"	microgranite	5208, 18620
CTK8	"	granite porphyry	5177, 18790
T11	Mae-Salit Pluton	monzogranite	5145, 18959
CTK7	"	"	5160, 19001
T48B	"	"	5151, 18989
CTK25	"	"	5142, 18935
CTK26	"	"	5149, 18985
CTK22	"	"	5165, 18929
CTK63-1	"	"	5172, 18974
CTK2	"	"	5176, 18992

APPENDIX II (continued)

Sample Number	Rock Unit	Rock Type	Grid Reference
CTK44	Mae-Salit Pluton	monzogranite	5169, 18954
CTK45	Western Main Range Pluton	monzonite	5170, 18956
CTK60-1	"	"	5226, 19004
T84	"	"	5202, 19183
T50	"	"	5175, 19186
T90	"	"	5186, 18971
CTK56X	"	"	5258, 19089
CTK31	"	granite porphyry	5199, 19114
CTK62	"	monzogranite	5207, 18769
CTK10	"	"	5201, 18878
T14	"	"	5167, 18780
T15	"	"	5169, 18862
T16	"	"	5171, 18855
CTK33	"	"	5223, 19252
T49	"	"	5186, 19255

APPENDIX II (continued)

Sample Number	Rock Unit	Rock Type	Grid Reference
T65	Western Main Range Pluton	microgranite	5301, 18979
T13	"	"	5159, 18860
T18B	"	Appinite	5229, 19022
T98	"	"	5145, 19013
T78	"	"	5216, 19033
T4	"	"	5152, 18927
T76	Eastern Pluton	Granodiorite porphyry	5315, 18670
T23	"	"	5291, 18703
CTK46	"	"	5282, 18669
CTK47-2	"	"	5311, 18644
CTK4	"	quartz-diorite	5205, 18683
T38B	"	"	5305, 18945
CTK5	"	"	5201, 18702
CTK65-1	"	"	5207, 18712
CTK58	"	"	5205, 18674
CTK64	"	"	5202, 18708
T48	"	"	5327, 18975

APPENDIX II (continued)

Sample Number	Rock Unit	Rock Type	Grid References
CTK57	Eastern Pluton	granodiorite	5301, 19025
T28	"	"	5349, 18835
T29	"	"	5346, 18853
CTK1	"	"	5272, 18665
CTK62-1	"	"	5285, 18662
CTK47	"	"	5270, 18660
T73	"	"	5300, 18652
CTK40	"	monzogranite	5305, 19155
T30	"	"	5286, 19055
T31	"	"	5305, 19081
T32	"	"	5328, 19057
T33	"	"	5302, 19060
CTK34	"	microgranite	5301, 19228
T25	"	"	5241, 18669
T86	"	aplite	5290, 19007

APPENDIX III: Neutron activation results

(i) Rare earth elements

	Tak Pluton		
	T01	T10B	T02
La	132	55.7	33
Ce	374	224	71
Pr	28	13	8.2
Nd	102	47	36
Sm	13.2	7	6
Eu	1.54	0.57	0.32
Gd	9	5.7	5
Tb	1.1	0.62	0.62
Dy	6	3.7	3.8
Ho	1.3	0.51	0.46
Er	-	1.7	2.2
Tm	-	-	-
Yb	2.7	2.02	2.4
Lu	0.52	0.34	0.37
La/Yb	49	28	14

	Mae-Salit Pluton			
	T48B	CTK7	CTK22	CTK44
La	60	39.3	63.5	27.6
Ce	223	137	239	112
Pr	13.9	8	13.1	5
Nd	54	30	48	23
Sm	8.6	5.5	6.3	2.03
Eu	2.18	1.22	0.78	0.35
Gd	7.4	6.2	4.7	-
Tb	0.81	0.78	0.55	0.21
Dy	5.0	5.1	3.3	1.3
Ho	o.82	o.76	0.34	0.21
Er	2.4	2.3	1.4	1.2
Tm	-	-	-	-
Yb	2.03	2.67	1.48	1.1
Lu	0.31	0.39	0.24	0.32
La/Yb	30	15	43	25

Western Main Range Pluton

	T50	CTK62	CTK33	T16
La	33	63	87	64
Ce	71	103	145	83
Pr	8.2	10	14	8
Nd	36	41	55	40
Sm	6	6.4	7.6	4
Eu	0.32	0.97	1.03	0.91
Gd	5	6	6	3.2
Tb	0.62	0.67	0.68	0.42
Dy	3.8	5.3	5.5	4.4
Ho	0.46	0.7	0.6	1
Er	2.2	2.1	1.3	1.1
Tm	-	-	-	-
Yb	2.4	2.49	3.1	2.4
Lu	0.37	0.45	0.51	0.36
La/Yb	14	25	28	27

Eastern Pluton

	T48	T73	T29	T33	T23	T25	CTK34
La	43	36	27	27	31	35	11.7
Ce	57	102	45	49	86	46	19.7
Pr	7.3	7.3	5	5.5	6.1	5.2	3.9
Nd	45	32	22	24	26	30	15.2
Sm	5.1	5.9	4.2	4.4	4.7	4.4	3.93
Eu	1.73	1.31	1.07	1	1.22	0.52	1
Gd	3.4	6	3	5	5	4.6	5
Tb	0.51	0.88	0.57	0.62	0.72	0.82	0.82
Dy	4.4	6	3.4	3.2	4.8	8.8	8.5
Ho	0.81	1.3	0.58	0.46	1.1	2.7	1.2
Er	1.6	4.4	2.70	2.8	3.0	3.5	4.4
Tm	-	-	-	-	-	-	-
Yb	1.7	3.1	2.1	2	2.6	5.4	5.2
Lu	0.29	0.48	0.30	0.29	0.39	0.82	0.81
La/Yb	25	12	13	14	11.9	7	2

Appinites

	T98	T18B	T78	T4
La	103	107	33.5	17
Ce	282	127	171	68
Pr	21	12	13	4.6
Nd	82	55	54	18.9
Sm	13.3	5.4	10.9	4.3
Eu	2.29	1.2	2.23	1.09
Gd	10	3.3	7.4	4.7
Tb	1.09	0.57	1.17	0.59
Dy	6.30	5.2	7.7	4.1
Ho	1.10	1.1	1.25	0.61
Er	6	1.4	4.3	2.4
Tm	-	-	-	-
Yb	2.0	2.9	4.27	1.87
Lu	0.32	0.49	0.61	0.27
La/Yb	52	37	8	10

(ii) miscellaneous neutron activation results
(rock type, and location see appendix II)

	T1	T12	CTK7	CTK26	CTK22	CTK2	T65	CTK10
Hf	8.3	4.2	3.2	6.8	8.3	4.0	2.9	8.2
Ta	2.1	4.4	1.1	2.4	2.1	1.3	1.5	2.3

APPENDIX IV: Analyses of minerals

(i) Analyses of hornblende

	Western Main Range Pluton			Eastern Pluton		
	T4	CTK45	CTK50	CTK4	CTK47	CTK47-2
SiO_2	46.67	46.88	46.70	50.31	49.32	49.62
TiO_2	1.24	1.41	1.53	0.25	0.67	1.37
Al_2O_3	7.52	6.96	6.67	4.24	6.51	8.24
Fe_2O_3	14.88	15.76	14.61	19.00	09.48	17.75
MnO	0.39	0.83	0.94	0.62	0.53	0.48
MgO	12.55	12.01	13.08	11.64	11.43	11.49
CaO	12.42	12.00	11.32	10.28	10.07	10.32
Na_2O	1.28	1.33	1.63	0.55	1.45	1.37
K_2O	0.86	0.77	0.64	0.27	0.77	0.51
P_2O_5	0.00	0.20	0.00	0.00	0.00	0.11
TOTAL	98.05	98.17	97.11	97.93	98.78	98.27

(ii) Analyses of biotite

	Western Main Range Pluton			Eastern Pluton	
	T4	CTK45	CTK50	CTK4	CTK47
SiO_2	37.83	37.47	38.27	36.42	36.44
TiO_2	3.94	2.88	3.24	4.11	4.14
Al_2O_3	13.88	14.67	14.11	14.83	14.46
Fe_2O_3	19.15	21.94	17.81	22.57	23.01
MnO	0.25	0.32	0.62	0.44	0.44
MgO	11.73	9.52	13.81	9.94	8.50
CaO	0.00	0.00	0.00	0.00	0.21
Na_2O	0.00	0.00	0.00	0.37	0.49
K_2O	10.01	9.80	9.52	9.16	8.69
P_2O_5	0.00	0.21	0.00	0.00	0.00
TOTAL	96.73	96.82	97.38	97.85	96.38

(iii) Analyses of plagioclase

	Western Main Range Pluton			Eastern Pluton	
	T4	CTK45	CTK50	CTK4	CTK47
SiO_2	59.08	60.95	61.14	56.28	57.23
TiO_2	0.00	0.00	0.00	0.00	0.00
Al_2O_3	25.68	24.29	23.91	28.43	27.26
Fe_2O_3	0.00	0.24	0.00	0.00	0.00
MnO	0.00	0.00	0.00	0.00	0.00
MaO	0.00	0.00	0.28	0.00	0.00
CaO	8.27	6.72	5.75	9.82	9.46
Na_2O	6.45	6.94	8.31	5.55	5.99
K_2O	0.26	0.22	0.17	0.48	0.34
P_2O_5	0.30	0.00	0.22	0.00	0.00
TOTAL	100.05	99.36	99.76	100.50	100.20

APPENDIX V

Classification of plutonic rocks (from Streckeisen, 1976)

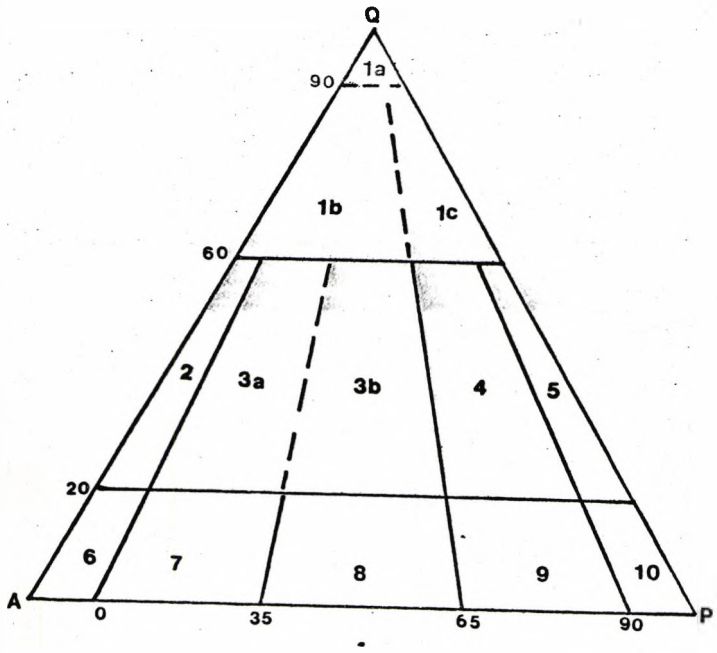

Field	Plutonic rocks
1a	quartz rocks *sensu stricto*
1b	quartz-granite
1c	quartz-granodiorite
2	alkali granite
3	granite
3a	syenogranite
3b	monzogranite
4	granodiorite
5	quartz-diorite
6	alkali syenite
7	syenite
8	monzonite (syenodiorite)
9	Monzodiorite and monzogabbro (syenodiorite and syenogabbro)
10	diorite, gabbro, anorthosite